



HAL
open science

Control of the rheological properties of hydrogels made by self-association of amphiphilic copolymers, blocks and grafts, anionics or cationics

Lionel Lauber

► **To cite this version:**

Lionel Lauber. Control of the rheological properties of hydrogels made by self-association of amphiphilic copolymers, blocks and grafts, anionics or cationics. Material chemistry. Le Mans Université, 2016. English. NNT : 2016LEMA1010 . tel-01495957

HAL Id: tel-01495957

<https://theses.hal.science/tel-01495957>

Submitted on 27 Mar 2017

HAL is a multi-disciplinary open access archive for the deposit and dissemination of scientific research documents, whether they are published or not. The documents may come from teaching and research institutions in France or abroad, or from public or private research centers.

L'archive ouverte pluridisciplinaire **HAL**, est destinée au dépôt et à la diffusion de documents scientifiques de niveau recherche, publiés ou non, émanant des établissements d'enseignement et de recherche français ou étrangers, des laboratoires publics ou privés.

Thèse de Doctorat

Lionel LAUBER

*Mémoire présenté en vue de l'obtention du
grade de Docteur de l'Université du Maine
sous le sceau de l'Université Bretagne Loire*

École doctorale : 3MPL

Discipline : *Chimie des matériaux*

Spécialité : *Chimie et physico-chimie des polymères*

Unité de recherche : IMMM, UMR CRNS 6283

Soutenue le 19/09/2016

Control of the rheological properties of hydrogels made by self-association of amphiphilic copolymers, blocks and grafts, anionics or cationics

JURY

Rapporteurs :	Catherine AMIEL , Professeur des universités, ICMPE Université Paris-Est Thierry AUBRY , Professeur des universités, Université de Bretagne Occidentale
Examineurs :	Jean-François ARGILLIER , Ingénieur de recherche, IFP Energies Nouvelles Gaëlle MORANDI , Maître de Conférences, INSA Rouen
Directeur de Thèse :	Olivier COLOMBANI , Maître de Conférences, Université du Maine
Co-Directeur de Thèse :	Christophe CHASSENIEUX , Professeur des universités, Université du Maine (absent lors du jury)
Co-encadrant de Thèse :	Taco NICOLAI , Directeur de recherche CNRS, Université du Maine

Remerciements

Je souhaite tout d'abord remercier mon directeur de thèse Olivier Colombani, mon co-directeur de thèse Christophe Chassenieux ainsi que mon co-encadrant de thèse Taco Nicolai. Je les remercie pour les discussions scientifiques qui furent toujours intéressantes et stimulantes. Grâce à vous j'ai aussi grandement appris sur moi-même. Je suis particulièrement reconnaissant à Olivier Colombani pour m'avoir guidé et soutenu dans les moments difficiles de la thèse.

Je remercie Thierry Aubry et Catherine Amiel pour avoir accepté de rapporter ce manuscrit de thèse et pour M. Aubry d'avoir présidé le jury. Je remercie Gaëlle Morandi d'avoir accepté d'examiner ce travail au bout de trois années en tant que membre du comité de suivi de thèse avec Catherine Amiel. Je remercie aussi Jean-François Argillier d'avoir été membre de jury et pour les échanges intéressants que nous avons eu.

Je souhaite remercier Élise Deniau et ses stagiaires pour la synthèse des polymères gradients THgx. Je tiens à exprimer ma reconnaissance à Olivier Boyron, Cédric Gaillard, Patricia Gangnery et Emmanuelle Mebold pour les analyses qu'ils ont effectuées en SEC DMF, Cryo-TEM/AFM et Chromatographie respectivement.

Je remercie Jérémy Depoorter et Julien Santarelli pour leurs sympathies et pour avoir respectivement élagué la synthèse des polymères greffés et synthétisé le TH50c.

Je tiens à remercier Erwan Nicol pour son aide dans l'interprétation de certaines RMN et les discussions en salle café. Un grand merci à Daniel Choplin pour ses discussions et son aide dans les méandres des démarches administratives. Je remercie Cyrille Dechancé et Boris Jacquette pour leurs sympathies, leurs aides devant les appareils récalcitrants et pour les analyses qu'ils ont effectuées. Je tiens également à remercier Frederick Niepceron pour sa sympathie et sa maîtrise de la force.

Je tiens à remercier des doctorants « anciens », maintenant docteurs !, pour leurs accueils au Mans : René, Fabien, Sylvain, Flavien, Anna et Andrei. Je remercie tout particulièrement

Fabien, pour m'avoir aidé à m'intégrer, et René pour les discussions toujours très « sérieuses » que nous avons eues.

Ensuite, que serait un laboratoire sans post-doctorants sympathiques et toujours ouverts à la discussion comme Khalid et Bach (M. étoiNe !), merci.

Cécile, je te remercie chaleureusement pour les discussions toujours intéressantes et nombreuses que nous avons eues, dommage que tu sois en cotutelle avec Toulouse et que tu ne profites pas suffisamment du Mans.

Malika, je te remercie profondément pour ton écoute, nos discussions et ta gentillesse pour ces deux dernières années de thèse. On est d'accord la première ne compte pas ! Je te souhaite bon courage pour la rédaction, la fin de ta thèse et la suite. N'oublie jamais que j'ai dû remplacer une application sur mon téléphone en Juillet 2016 !

Walailuk, merci pour ta sympathie, nos discussions et m'avoir expliqué la prononciation en thaïlandais (mou, moü, moü ...).

Je tiens à remercier une stagiaire récurrente de PCI qui doit connaître plus de personnes dans l'institut que n'importe qui d'autre, Inès.

Les repas au RU ont eu une saveur particulière grâce aux « doctorants du 4ème », Maud et Mael, qui ont du vernis à ongle ou un humour décoiffant !

Enfin je tiens à remercier tous les doctorants, post-doctorants, stagiaires ou intérimaires de PCI, je pense bien sûr à : Anna Kharlamova, Justine, Frédérico, Alex, Alberto, Nannan, Gireesh, Lucie, Thomas, Romain, Asma, Maeliss et Bruna.

Pour finir, je tiens à remercier ma famille. Mes parents, Philippe et Édith, qui ont toujours soutenu mes choix y compris lorsqu'ils étaient imprécis. Maman, finalement, à ma grande surprise en fin de seconde, j'ai fait des études scientifiques, je te dois donc une calculatrice ! Je remercie aussi ma sœur, Laetitia, mon beau-frère, Florian, et ma nièce, Léna, pour tant de raisons que leurs énumérations seraient fastidieuses.

Je dédie l'ensemble de cette thèse à ma famille.

Table of Content

INTRODUCTION	1
CHAPTER 1: BIBLIOGRAPHY.....	5
I. Rheology of self-assembled dynamic amphiphilic copolymers.....	6
I.1. Rheology of dynamic triblock copolymers	6
I.2. Rheology of multi-stickers	9
I.3. Definition of dynamic amphiphilic copolymers	12
II. Block-random copolymers.....	14
II.1. Structure and rheological properties of block-random copolymers.....	14
II.2. Random copolymer structure	19
III. Mixtures of dynamic amphiphilic polymers: structure and rheology.....	20
III.1. Structure of mixtures of dynamic amphiphilic copolymers	20
III.2. Rheological properties of mixtures of amphiphilic triblock copolymers	22
IV. Conclusion of the literature review	24
V. References.....	27
CHAPTER 2 : MATERIALS AND METHODS	33
I. Experimental techniques	33
I.1. Differential refractometry	33
I.2. Light scattering.....	33
I.3. Rheology	40
I.4. Size exclusion chromatography	42
I.5. Gas Chromatography	43
I.6. NMR.....	43
II. Polymer based on acrylic acid (AA) and <i>n</i> -butyl acrylate (<i>n</i> BA).....	43
II.1. Synthesis of linear copolymers	43
II.2. Synthesis of graft copolymers.....	47
II.3. Sample preparation	54
II.4. Potentiometric titration	56
II.5. Refractometry	59
III. Polymer based on DMAEMA and <i>n</i> BMA	60
III.1. Synthesis.....	60
III.2. Sample preparation.....	65

III.3. Titration.....	66
IV. References.....	68
CHAPTER 3: PRINCIPAL RESULTS.....	70
I. Highlighting the Role of the Random Associating Block in the Self- Assembly of Amphiphilic Block–Random Copolymers	70
II. pH-Controlled Rheological Properties of Mixed Amphiphilic Triblock Copolymers....	74
II.1. Self-Assembly of mixtures of diblock copolymers.....	75
II.2. Rheological Properties of Mixed Amphiphilic Triblock Copolymers	76
III. pH-Responsive Transient Networks Formed By Amphiphilic Graft Copolymers	80
IV. pH and thermo-responsive self-assembly of cationic triblock copolymers with controlled dynamics	84
V. Block-random copolymers: a universal way to control exchange dynamics.....	88
VI. References.....	92
CONCLUSIONS AND PERSPECTIVES	94
CHAPTER 4 : ARTICLE 1	98
Supporting information of article 1.....	116
CHAPTER 5 : ARTICLE 2	126
Supporting information of article 2.....	146
CHAPTER 6 : ARTICLE 3	150
Supporting information of article 3.....	168
CHAPTER 7 : ARTICLE 4	182
Supporting information of article 4.....	204
CHAPTER 8 : APPENDIX 1	214
I. Synthesis and titration of the gradient triblock copolymers	214
I.1. Synthesis of the gradient triblock copolymers.....	214
I.2. Titration of the gradient triblock copolymers.....	216
II. Self-association of THgx.....	217
III. Rheological properties	218
IV. Conclusion	221
V. References	222
CHAPTER 9 : APPENDIX 2	224

Introduction

Amphiphilic copolymers are macromolecules able to self-assemble in water and form aggregates or micelles of different morphologies. These systems, especially amphiphilic block copolymers, were widely studied in the literature and are often cited for potential applications such as drug delivery, enhanced oil recovery and viscosifying agent.

Actually, only few self-assembling amphiphilic (co)polymers are really used at an industrial scale. Among them can be found pluronics, Hydrophobically modified Ethylene oxide Urethane (HEUR) or Hydrophobically Alkali-Soluble Emulsions (HASE). Two major limitations inhibit the use of self-assembling amphiphilic (co)polymers at large-scale: their synthesis difficulties/costs and/or their out-of-equilibrium states.

Indeed, contrary to molecular surfactants, most amphiphilic copolymers form frozen aggregates i.e. without dynamic exchange of single polymer chains between aggregates.¹ This out-of-equilibrium state limits their applications. For example, in the case of self-healing materials, physical hydrogels made of amphiphilic (co)polymers can “heal” i.e. recover their initial rheological properties, only if dynamic exchange occurs allowing the system to re-equilibrate. This was illustrated by Okay et al. with polymers made of poly(N,N-dimethylacrylamide) modified with 2 mol% of stearyl methacrylate in aqueous sodium dodecyl sulfate–NaCl solutions.² The exchange dynamics of the hydrophobic moieties depended on the amount of surfactant thereby controlling the mechanical properties and the self-healing process. The dynamic exchange is one of the key parameters to control in order to modify the rheological properties of self-assembling amphiphilic (co)polymers.

One of the recently proposed strategies to control dynamic exchange is to add pH-sensitive hydrophilic units inside the hydrophobic block(s) of amphiphilic copolymers. This strategy allowed controlling the structure of several types of di/triblock copolymers³⁻⁹ and it has been proven for triblock copolymers that the exchange dynamics were also controlled.^{10, 11} The triblock copolymers (THx) were composed of a poly(acrylic acid) (PAA) central block and two statistical copolymers made of AA and *n*-butyl acrylate (*n*BA) $P(nBA_{1-x}\text{-stat-AA}_x)_{100}$ end blocks. The dynamic exchange was controlled by the pH and the AA content in the hydrophobic blocks. The general purpose of this work is to determine the most relevant parameters to control the rheological properties of amphiphilic copolymers.

The origin of the self-association of diblocks and triblocks coming from their random associating block(s) $P(nBA_{1-x}\text{-stat-AA}_x)_{100}$, we chose to study the self-association of this neat

INTRODUCTION

block and to correlate it to the one of the diblocks $P(AA)_{100}$ - b - $P(nBA_{1-x}$ - $stat$ - $AA_x)_{100}$ (DHx). Thereafter, in order to control the rheological properties by simple polymer formulation, instead of doing new polymer synthesis, mixtures of triblock copolymers THx were investigated. In this context, mixtures of DHx were performed to better understand the co-micellisation of THx. Then, the role of the architecture was investigated by studying polymers more relevant for industrial applications: graft copolymers $P(AA)_{500}$ - g - $[P(nBA_{1-x}$ - $stat$ - $AA_x)_{100}]_y$. Finally, cationic triblock copolymers were investigated to try to extend our concept and bring thermo-sensitivity to the transient networks.

This manuscript is divided into seven chapters and two appendices:

- Chapter one gives an overview of the literature on the self-association of amphiphilic copolymers and especially on the rheological properties of triblock and multi-sticker copolymers. Thereafter, the interest of using block-random copolymers as hydrophobic blocks to control their structure and rheological properties in aqueous medium is shown. To finish, the behavior of mixtures of amphiphilic copolymers is reviewed.
- Chapter two presents the materials and methods used during this PhD.
- Chapter three summarizes the results of this work, highlighting the most relevant ones. These results are presented in more details in the following four chapters (chapters 4-7), each corresponding to an article published or to be submitted.
- Chapter four deals with the light scattering study of the self-association of the neat $P(nBA_{1-x}$ - $stat$ - $AA_x)_{100}$ random blocks related to that of the $P(AA)_{100}$ - b - $P(nBA_{1-x}$ - $stat$ - $AA_x)_{100}$ diblocks.
- Chapter five focuses on the mixtures of $P(nBA_{1-x}$ - $stat$ - $AA_x)_{100}$ - b - $P(AA)_{100}$ diblocks and the rheological properties of mixtures of $P(nBA_{1-x}$ - $stat$ - $AA_x)_{100}$ - b - $P(AA)_{200}$ - b - $P(nBA_{1-x}$ - $stat$ - $AA_x)_{100}$ triblocks.
- Chapter six presents the results obtained on $P(AA)_{500}$ - g - $[P(nBA_{1-x}$ - $stat$ - $AA_x)_{100}]_y$ graft copolymers. The latter were studied to evaluate the impact of the architecture and were compared with the triblock copolymers.
- Chapter seven is related to $P(nBMA_{1-x}$ - $stat$ - $DMAEMA_x)_{100}$ - b - $P(DMAEMA)_{200}$ - b - $P(nBMA_{1-x}$ - $stat$ - $DMAEMA_x)_{100}$ cationic triblock copolymers, studied to extend the pH range in which complex fluids can be obtained, bring new thermo-sensitive properties and extend our concept.

- The last part of this manuscript contains two appendices, one on gradient-triblock copolymers $P(nBA_{1-x}\text{-grad-AA}_x)_{50}\text{-}b\text{-}P(AA)_{100}\text{-}b\text{-}P(nBA_{1-x}\text{-grad-AA}_x)_{50}$ and one on light scattering experiments performed on graft copolymers.

Finally, conclusions and perspectives of this work are available at the end of chapter three of the manuscript.

References

1. Nicolai, T.; Colombani, O.; Chassenieux, C. *Soft Matter* **2010**, 6, (14), 3111-3118.
2. Okay, O., Self-Healing Hydrogels Formed via Hydrophobic Interactions. In *Supramolecular Polymer Networks and Gels*, Seiffert, S., Ed. Springer International Publishing: Cham, 2015; pp 101-142.
3. Dutertre, F.; Boyron, O.; Charleux, B.; Chassenieux, C.; Colombani, O. *Macromol. Rapid Commun.* **2012**, 33, (9), 753-759.
4. Wright, D. B.; Patterson, J. P.; Gianneschi, N. C.; Chassenieux, C.; Colombani, O.; O'Reilly, R. K. *Polym. Chem.* **2016**.
5. Wright, D. B.; Patterson, J. P.; Pitto-Barry, A.; Lu, A.; Kirby, N.; Gianneschi, N. C.; Chassenieux, C.; Colombani, O.; O'Reilly, R. K. *Macromolecules* **2015**, 48, (18), 6516-6522.
6. Wright, D. B.; Patterson, J. P.; Pitto-Barry, A.; Cotanda, P.; Chassenieux, C.; Colombani, O.; O'Reilly, R. K. *Polym. Chem.* **2015**, (6), 2761-2768.
7. Borisova, O.; Billon, L.; Zaremski, M.; Grassl, B.; Bakaeva, Z.; Lapp, A.; Stepanek, P.; Borisov, O. *Soft Matter* **2012**, 8, (29), 7649-7659.
8. Borisova, O.; Billon, L.; Zaremski, M.; Grassl, B.; Bakaeva, Z.; Lapp, A.; Stepanek, P.; Borisov, O. *Soft Matter* **2011**, 7, (22), 10824-10833.
9. Bendejacq, D. D.; Ponsinet, V.; Joanicot, M. *Langmuir* **2005**, 21, (5), 1712-1718.
10. Charbonneau, C.; Chassenieux, C.; Colombani, O.; Nicolai, T. *Macromolecules* **2011**, 44, (11), 4487-4495.
11. Shedge, A.; Colombani, O.; Nicolai, T.; Chassenieux, C. *Macromolecules* **2013**, 47, (7), 2439-2444.

INTRODUCTION

CHAPTER 1: BIBLIOGRAPHY

Hydrogels are materials consisting of a three dimensional polymer network typically containing more than 90 % water. They can be transient or permanent depending on whether the cross-links forming the network have a finite lifetime allowing the material to flow or are permanent. Moreover, reversible hydrogels are obtained when the crosslinks can be broken and reformed using a stimulus (pH, temperature...). A classical way to produce reversible and/or transient hydrogels is to use self-assembling amphiphilic copolymers. With the next two examples, the potential of such hydrogels is shown.

In the field of polymers for enhanced oil recovery, hydrophobically modified polyacrylamides (HMPAM) are widely studied and, to some extent, already used to increase oil extraction from oil wells. Indeed, high molecular weight polyacrylamides bearing small alkyl grafts consisting of ~12-18 carbons self-assemble in aqueous medium into transient physical networks drastically increasing the solution viscosity.¹ This helps pushing the oil out of the oil well. However, the size of the alkyl chains must remain rather short to keep the polymer soluble so that the network remains transient with a finite viscosity.

Self-healing properties of hydrogels were demonstrated using similar polymers. As emphasized by Okay *et al.*, self-healing materials can be obtained using self-assembled polymers with adjustable exchange dynamics of the hydrophobic moieties from the hydrophobic microdomains.² For instance, poly(N,N-dimethylacrylamide) modified with 2 mol% stearyl methacrylate in aqueous sodium dodecyl sulfate–NaCl solutions leads to self-healing hydrogels. The exchange dynamics of the hydrophobic moieties depended on the amount of surfactant thereby controlling the mechanical properties and the self-healing process.

Tuning the exchange dynamics is thus key to controlling the rheological properties of self-assembled polymers. However, it can be hard to tune the exchange dynamics to reach the desired rheological properties for a given application. In the following the most relevant parameters to control the rheological properties of amphiphilic polymers will be discussed. First, BAB amphiphilic triblock copolymers consisting of a central hydrophilic A block and lateral hydrophobic B blocks will be discussed since they are « simple » systems that can be used as models. Then, polymers bearing many associative groups will be described. Since the exchange of hydrophobic moieties between hydrophobic cores has a strong influence on the rheological properties, its mechanism and the parameters affecting it will be explained.

CHAPTER 1: BIBLIOGRAPHY

To control the exchange dynamics several strategies can be used. Among them, addition of hydrophilic units inside the hydrophobic blocks of the copolymers leading to so-called “block-random copolymers” is of special interest and will be emphasized. Rheological properties of block-random copolymers will be reviewed and details of their self-assembly will be given.

Finally, another approach to control the rheological properties of amphiphilic copolymers by mixing different polymers will be discussed. Indeed, it would be useful to be able to change the rheological properties by formulation instead of synthesizing new copolymers for each application.

I. Rheology of self-assembled dynamic amphiphilic copolymers

I.1. Rheology of dynamic triblock copolymers

In this section, the focus is on systems in thermodynamic equilibrium where exchange of hydrophobic blocks occurs within the experimental time-window. Despite its interest, the rheology of out-of-equilibrium (or frozen) self-assembled networks will not be described in details here.

When dissolved in a selective solvent for the A-block, amphiphilic triblock copolymers of BAB type self-assemble as described in Figure 1.1. When the polymer concentration is above the critical association concentration (c.a.c.), BAB triblocks form flower-like micelles with the B blocks forming their cores. Provided that the B blocks can exchange within the experimental time scale, the systems reach thermodynamic equilibrium.

If the polymer concentration is increased, the flower-like micelles can bridge and form aggregates by locating the two B blocks of one chain into two different micellar cores. If the concentration is further increased, a three-dimensional network forms above the critical percolation concentration (C_p).³⁻¹⁴

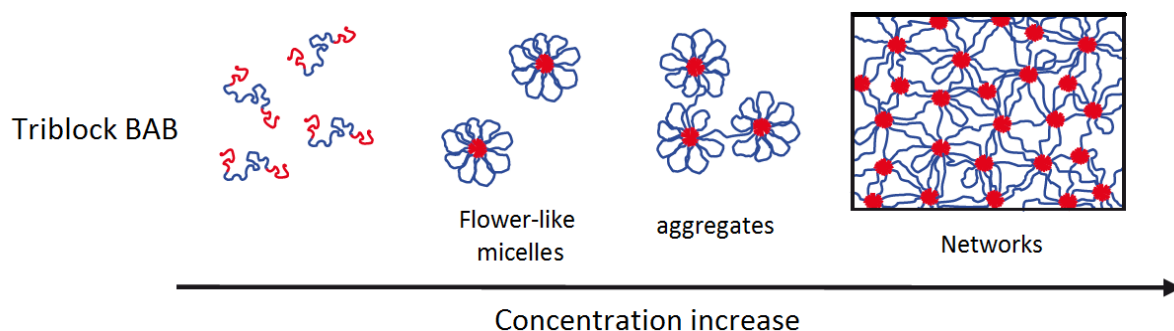


Figure 1.1. Self-assembly of dynamic BAB triblocks with increasing polymer concentration, adapted from ref⁸⁴.

By measuring the evolution of the viscosity with the polymer concentration, percolation of the aggregates can be observed. For example, let us consider two types of hydrophobically modified poly(ethylene oxide)s, one functionalized only on one side by a fluoro-alkyl and the other functionalized on both sides.¹² With only one fluoro-alkyl end, the BA diblock copolymer does not form a 3D network and its viscosity remains low as shown in Figure 1.2 for concentrations below the concentration at which the polymeric micelles jam. However, with two fluoro-alkyls per PEO chain the viscosity increases dramatically by 6 decades at the percolation concentration. The fact that the viscosity is still measurable after C_p implies that the B blocks can exchange, leading to a transient network. For a (quasi-)permanent network with infinite relaxation time, the viscosity would diverge at C_p .

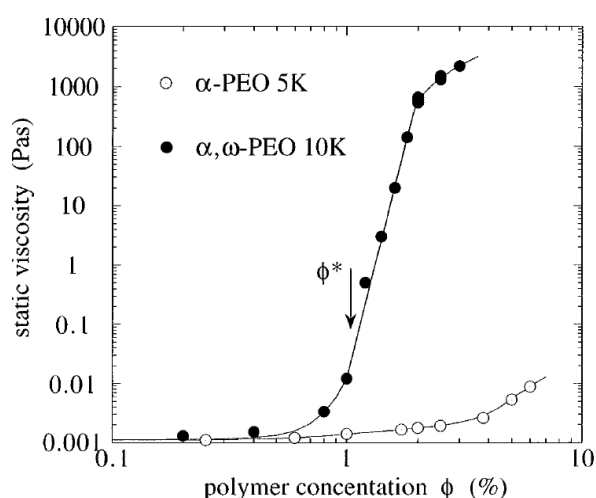


Figure 1.2. Static viscosity as function of the polymer concentration (ϕ) for poly(ethylene oxide) hydrophobically modified with fluoro-alkyls at one (α -PEO 5K) and two (α,ω -PEO 10K) extremities.¹² ϕ^* represents the percolation concentration of the latter, the solid lines are guides to the eye.

CHAPTER 1: BIBLIOGRAPHY

To probe the rheological properties in more detail, dynamic oscillatory shear measurements in the linear regime can be done to determine the high frequency elastic modulus (G_e) and the relaxation time (τ) of the transient network. The solution viscosity (η) is equal to the product of these two parameters:

$$\eta = G_e \cdot \tau$$

Annable *et al.* studied the viscoelastic response of Hydrophobically Modified Urethane-Ethoxylate (HEUR) end-capped with hexadecanol on both sides. Oscillatory deformation was applied as illustrated in Figure 1.3 at C above C_p .¹⁵ At low frequencies the system is liquid-like: the storage modulus (G') has a slope of two and the loss modulus (G'') has a slope of one when plotted vs the frequency on a log-log scale. However, at high frequencies G' becomes independent of the frequency and is equal to G_e , whereas G'' decreases and is much smaller than G' . This is typical behaviour for a solid. The relaxation time may be defined as the inverse of the angular frequency at which G' and G'' intersect ($\tau=1/\omega$).

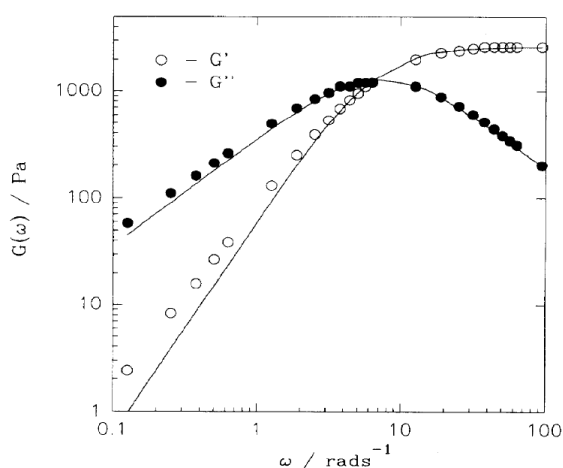


Figure 1.3. Evolution of the storage (G') and loss (G'') moduli as a function of the angular frequency for a solution of hexadecanol end-capped HEUR of 20 kg/mol at 7% w/v and $T=298$ K. The solid lines correspond to the a single exponential relaxation process.¹⁵

The lifetime and the amount of bridges define the visco-elastic properties. The elastic modulus G_e varies with the concentration since the fraction of chains involved in the network increases with the polymer concentration until all of them are elastically active. For a perfect network without defects, the value of the elastic modulus can be estimated using the rubber elasticity theory.¹⁶ By assuming an extensional deformation of an incompressible rubber network, the elastic modulus is as follows:

$$G_e \approx \nu \cdot k_B \cdot T \quad \text{with } \nu = N_a \cdot C / M_n$$

with ν the total number of elastically active chains, k_B the Boltzman constant, C the polymer concentration, N_a the Avogadro constant, M_n the number-average molar mass of the polymer and T the absolute temperature.

Before the formation of a perfect network, the elastic modulus is lower than predicted by the model due to different types of defects as illustrated in Figure 1.4. Such defects can also affect the value of the relaxation time¹⁷ and therefore measurements must be made at $C \gg C_p$ where the relaxation time does not depend anymore on the polymer concentration and is directly related to the exchange time of the B blocks.

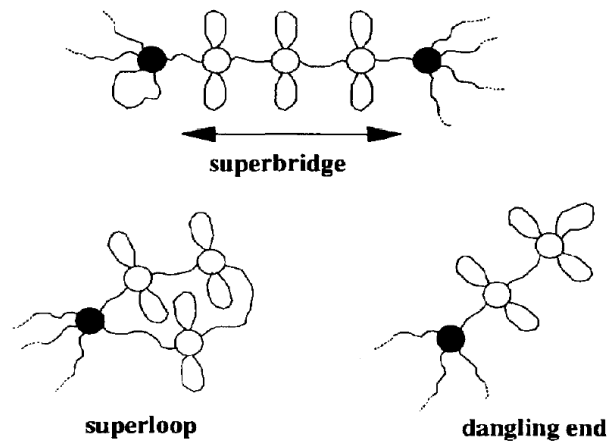


Figure 1.4. Schematic illustration of various possible network defects.¹⁵

I.2. Rheology of multi-stickers

Polymers bearing many associative groups are often called multi-stickers and their self-association can lead to dynamic networks for the same reasons as triblock copolymers discussed in the previous section. Varying the size of the stickers, their hydrophobicity and their amount results in a wide range of systems with bottle-brush¹⁸ and triblock copolymers as extreme cases. Since several stickers are bound to the same polymer chain, intramolecular aggregation can occur i.e. stickers from the same chain can form a hydrophobic microdomain. There is a balance between intra and inter molecular aggregation with multi-sticker polymers. For neutral multi-sticker polymers, Rubinstein and Semenov proposed a theory to explain their rheological response assuming pair-wise interaction between hydrophobic groups: the sticky reptation.^{19, 20} At low concentration, the intramolecular association governs the

CHAPTER 1: BIBLIOGRAPHY

properties i.e. the viscosity remains low. At a specific concentration, the intermolecular association starts to play an important role and a sharp increase in viscosity occurs. In the semi-dilute non-entangled regime, a single relaxation time and a constant elastic modulus at high frequency are expected. Even if the assumption of the model of a pair-wise association is rarely true,²¹⁻²³ it gives an overall idea of the expected rheological behaviour.

I.2.1. Hydrophobically modified polymers with alkyl chains

In this section, the rheological properties of systems with a hydrophilic backbone and hydrophobic alkyl stickers are discussed. As will be explained in detail in section II.2, addition of hydrophobic stickers can lead to complex structures and even to phase separation if the system becomes too hydrophobic.²⁴⁻³¹

To date, most of the studies were conducted on Hydrophobically Modified PolyAcrylamide (HMPAM).^{13, 21-23, 32-41} The sticker is usually an alkyl chain with a length ranging from 6 to 18 carbons.^{22, 23, 32-35, 37-43} HMPAM are often obtained by micellar copolymerization, therefore the distribution of the hydrophobic monomers is usually not random.^{21, 37, 41} Different HMPAM usually have the same qualitative behaviour. The relaxation time of the transient network increases with increasing alkyl length. The viscosity strongly increases with the concentration, the alkyl size and the grafting density.^{13, 21-23, 32-41} The oscillatory measurements indicate a broad distribution of relaxation times and a constant elastic modulus at high frequency.^{21, 22, 37, 40}

So far we only focused on linear responses of such systems but we wish to highlight interesting work on non-linear rheology made by Cadix⁴⁴ and Wang^{34, 42}. They studied poly(N,N-dimethylacrylamide) modified by C12 to C18 alkyl stickers and containing some acrylic acid units within the backbone due to partial hydrolysis of some N,N-dimethylacrylamide units. Most self-assembled amphiphilic copolymers exhibit a weak shear-thickening effect with increasing shear rate followed by a strong shear-thinning behaviour. By contrast, the systems studied by Cadix and Wang underwent shear induced gelation, i.e. the viscosity of the system diverged at a threshold shear rate value (Figure 1.5). The authors attributed this spectacular phenomenon to the formation of inter rather than intra chain cross-links induced by shear as illustrated in Figure 1.6.

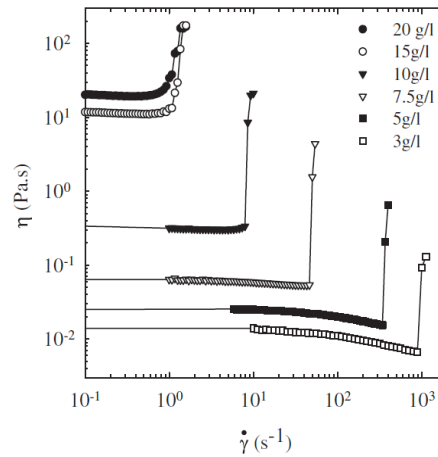


Figure 1.5. Viscosity of aqueous solution of a Copolymer of *N,N*-dimethylacrylamide and acrylic acid at $T=20^{\circ}\text{C}$ as function of the shear rate at several polymer concentrations.³⁴

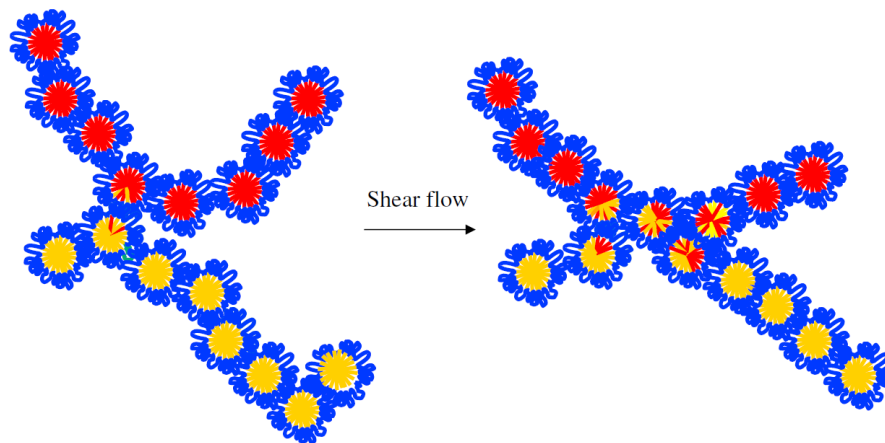


Figure 1.6. Schematic drawing of two, chemically similar, polymer chains at rest and under shear. The copolymers are made of *N,N*-dimethylacrylamide (DMA) and acrylic acid (AA) (both in blue) functionalised with alkyls groups (in yellow and red), from ref.³⁴

Hydrophobically modified polymers with alkyl chains already give access to interesting materials capable of enhancing the viscosity of aqueous solutions. However, they usually offer limited stimuli-responsiveness.^{23, 41} Graft copolymers are interesting to develop new smart materials since they can bear different types of stimuli-responsive grafts.

I.2.2. Graft copolymers

Graft copolymers are hydrophobically modified polymers with stickers different from simple alkyl chains. Thermosensitive groups may be grafted to the hydrophilic backbone to impart them with interesting rheological properties. Due to its Lower Critical Solution Temperature

CHAPTER 1: BIBLIOGRAPHY

(LCST) around 33 °C close to the human body temperature, poly(N-isopropylacrylamide) (PNIPAM) has been used as an associative sticker by several research groups.^{36, 45-48} For instance, Hourdet *et al.* grafted PNIPAM on a PAA backbone (PAA-g-PNIPAM). Viscosities of PAA-g-PNIPAM aqueous solutions are the same as those of the PAA homopolymer no matter the polymer concentration at 25 °C, but the viscosity increased by 2-3 decades around 40 °C at 0.42 mol/kg. The relaxation time was still measurable (~ 1 sec) at 60 °C. The network formed by PAA-g-PNIPAM was therefore reversible and dynamic. Petit *et al.* obtained similar results using PAM as hydrophilic backbone even at higher grafting density (up to 70 wt%). The same thermothickening behavior was found using for the associative blocks POE,⁴⁹ PPO,⁵⁰ poloxamers⁵¹ or statistical copolymers made of thermosensitive and acrylamide monomers.^{52, 53} For all these systems the networks were reversible and dynamic. More hydrophobic poly(*n*-butyl acrylate) (*Pn*BA) grafts were attached on a PAA hydrophilic backbone by Podhajecka *et al.*⁵⁴ PAA-g-*Pn*BA displayed a sol-gel transition at very low concentrations compared to PAA-C12 for instance. The sol-gel concentration decreased as the hydrophobicity or the number of stickers increased. The network formed was however irreversible and frozen due to the high hydrophobicity of the *Pn*BA grafts.

From these examples it appears that polymers with grafted hydrophobic groups may be used to form stimuli-responsive materials. However, the hydrophobicity of the grafts must remain moderate to obtain dynamic networks.

I.3. Definition of dynamic amphiphilic copolymers

Surfactants are molecules bearing a hydrophilic head group and a hydrophobic tail group. Above their critical micellar concentration (c.m.c.), they self-assemble into micelles to reduce contact between the tail and water. Surfactant micelles are at equilibrium and surfactant molecules always exchange more or less rapidly between micelles.⁵⁵

Like molecular surfactants, amphiphilic copolymers contain both hydrophilic and hydrophobic parts and self-assemble in selective solvents. Unlike surfactants however, amphiphilic copolymers are not always able to exchange between micelles and may therefore form out-of-equilibrium structures.⁵⁶ This difference comes from the mechanism of extraction of unimers, i.e. amphiphilic molecules, from micelles. To extract a unimer, several steps are needed as illustrated in Figure 1.7.⁵⁶⁻⁵⁸

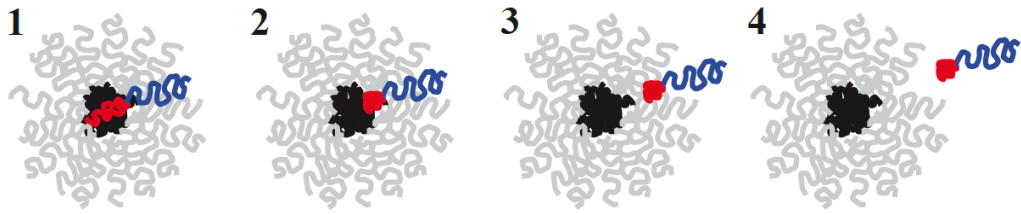


Figure 1.7. Expulsion mechanism of a polymer chain from a micellar core 1) movement of the hydrophobic block inside the micellar core 2) creation of an interface between the hydrophobic block and the solvent by retraction of the hydrophobic block at the core/shell interface 3) diffusion of the polymer chain through the shell 4) release from the micelle.⁵⁶⁻⁵⁸

Two major steps are usually rate limiting. Movement of the hydrophobic block inside the micellar core (step 1) is unfavorable for glassy polymers i.e. when the hydrophobic block has a high glass transition. The creation of an interface between the hydrophobic block and the solvent and migration of the hydrophobic bud to the aqueous medium (steps 2-4) have an energy cost that can be much higher than the thermal energy.

Halperin *et al.* demonstrated that the energy required to create an interface in step 2 is:

$$E_a \propto \gamma_{B/solvent} N_B^{2/3}$$

with $\gamma_{B/solvent}$ the interfacial tension between the hydrophobic block and the solvent and N_B the size of the hydrophobic block. Even if the coefficient 2/3 is a matter of theoretical debate the importance of the block size and of its hydrophobicity is clear.⁵⁹⁻⁶¹

The importance of the hydrophobicity of the hydrophobic polymers has been well demonstrated experimentally by Jacquin *et al.*⁶² They considered three diblocks with poly(acrylic acid) as hydrophilic block and poly(styrene) (PS), poly(*n*-butyl acrylate) (PnBA) or poly(diethyleneglycol ethylether acrylate) (PDEGA) as hydrophobic blocks. PS has a glass transition (T_g) around 100 °C, PnBA around -55 °C and the glass transition of PDEGA is below -50 °C. They demonstrated that both PS ($\gamma=35$ mN/m) and PnBA ($\gamma=20$ mN/m) formed frozen micelles but PDEGA formed dynamic system because the interfacial tension was much lower (4 mN/m). It shows that even polymers with low T_g need low γ to be dynamic.

To measure the exchange dynamics, many different strategies were proposed in the literature. The exchange dynamics can be computed indirectly by measuring the restructuring time of micelles after abrupt change of their environmental conditions. This can be achieved with

CHAPTER 1: BIBLIOGRAPHY

several time-resolved techniques using fluorescence^{63, 64}, light scattering⁶⁵⁻⁶⁹ or NMR⁷⁰ for detection.

To measure directly the exchange dynamics, many authors used TR-SANS^{67, 71-76} or TR-fluorescence.^{63, 77-79} These methods measure directly the exchange time. However, they usually require either deuterated polymers (TR-SANS) or molecular probes (TR-fluorescence) which might affect the system. To avoid perturbation of the system, exchange dynamics can also be measured by visco-elastic relaxation time of networks which is related to the exchange time as discussed in part I.¹⁷

As explained previously, transient networks are formed only if the self-assembled polymers are dynamic. One strategy of particular interest to reach dynamic systems is to incorporate hydrophilic units inside the hydrophobic blocks. Tsitsilianis *et al.* suggested to call such copolymers “block-random” and highlighted their great potential.⁸⁰ In the next section, the interest of this strategy will be discussed.

II. Block-random copolymers

The incorporation of hydrophilic units inside hydrophobic blocks may allow the formation of dynamic systems. This block-random strategy was first described by Bendejacq *et al.* for P(S-*stat*-AA)-*b*-PAA.^{81, 82} It not only allows control of the exchange dynamics but also of the structure of the self-assembly as recently highlighted by Tsitsilianis *et al.*⁸⁰ The physico-chemical properties of associative blocks such as thermo-sensitivity^{80, 83} and hydrophobicity,^{17, 80-82, 84-88} for instance, may be tuned depending on the ratio of the comonomers in the random block. This is first highlighted by discussing the structure and rheological properties of self-assembled block-random copolymers. Then, details of the structure of neat random copolymers are provided, because the behaviour of these blocks alone explains to some extent that of the block-random copolymers.

II.1. Structure and rheological properties of block-random copolymers

II.1.1. Copolymers based on acrylic acid and *n*-butyl acrylate

In recent years, our research group focused its attention on block-random copolymers based on acrylic acid (AA) and *n*-butyl acrylate (*n*BA) to design polymers with pH-controlled exchange dynamics. Several systems were studied and are depicted in Figure 1.8.

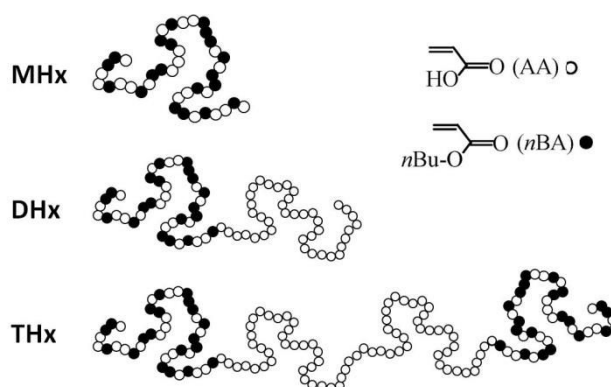


Figure 1.8. Schematic representation of the monoblock (MHx), diblock (DHx) and triblock (THx) copolymers with x the %AA in the hydrophobic blocks.

Lejeune *et al.* synthesized a block-random diblock copolymer, $P(nBA_{50\%}\text{-stat-AA}_{50\%})_{100}\text{-}b\text{-}P(AA)_{100}$, consisting of a hydrophobic random block containing 50% AA and 50% nBA units and a pure PAA hydrophilic block.⁸⁶ This polymer, called DH50, self-assembles in aqueous medium into micelles exhibiting an aggregation number reversibly controlled by the pH as illustrated in Figure 1.9.^{85, 86} The AA units in the hydrophobic block of DH50 provide the pH-sensitivity, their ionization degree (α , percentage of ionized AA units) increasing with the pH from $\alpha = 0$ (pH ~ 3) to $\alpha = 1$ (pH ~ 9).⁸⁹

Charbonneau *et al.* designed TH50, a BAB triblock copolymer with two $P(nBA_{50\%}\text{-stat-AA}_{50\%})_{100}$ random blocks as B blocks and a PAA_{200} central A block.¹⁷ This polymer is equivalent to two DH50 diblocks connected together by their PAA blocks. It was demonstrated that the aggregation number evolves similarly for TH50 and DH50 as a function of α in dilute solution (Figure 1.9).^{17, 84} However, since TH50 chains contain two hydrophobic blocks, they form flower-like micelles at low concentration with the two B blocks incorporated in the same hydrophobic core. With increasing concentration, two B blocks can enter two different cores thus bridging the flower-like micelles. Eventually, the percolation concentration is reached where the bridged micelles form a percolated 3D network. The percolation concentration increased as the ionization degree increased.

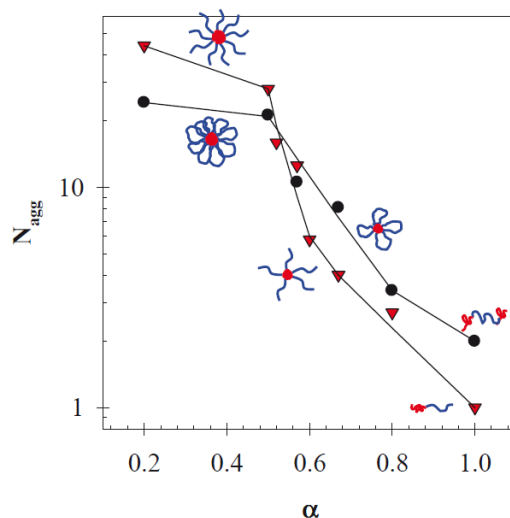


Figure 1.9. Evolution of the aggregation number as a function of the ionization degree for solutions of DH50 and TH50. The solid lines are guides to the eye.^{84, 85}

The rheological properties of the network were probed by Charbonneau *et al.* at several ionization degrees, temperatures and concentrations.¹⁷ Below $\alpha = 0.7$, the system forms transient hydrogels with relaxation time directly related to the exchange rate of the hydrophobic blocks and increasing with decreasing α . Master curves could be obtained both as a function of temperature and α (Figure 1.10). The temperature dependence of the relaxation time could be described in terms of an activation energy $E_a \approx 120$ kJ/mol. The relaxation time distribution was broad probably due to the dispersity in length and chemical composition of the hydrophobic blocks.

Shedge *et al.* designed two other triblock copolymers with different AA contents in the hydrophobic blocks, $x = 40$ and 60% respectively.⁸⁷ The rheological response of the three triblocks was qualitatively similar to those depicted in Figure 1.10. A unique master curve was obtained for all triblock copolymers with the same activation energy and the same broad relaxation time distribution. Quantitatively, the relaxation time, defined as the inverse of the angular frequency (ω) for which G' and G'' cross, strongly increases for a given α with decreasing AA content in the hydrophobic block, see Figure 1.11a. Interestingly, the amount of charges in the hydrophobic blocks, called the fraction of charged units, appeared as the major parameter influencing both the relaxation time and the percolation concentration of THx as illustrated in Figure 1.11b. The fraction of charged units was defined as follows: $f = [AA^-]_{MHx} / ([AA^-] + [AAH] + [nBA])_{MHx}$ with MHx the hydrophobic blocks.

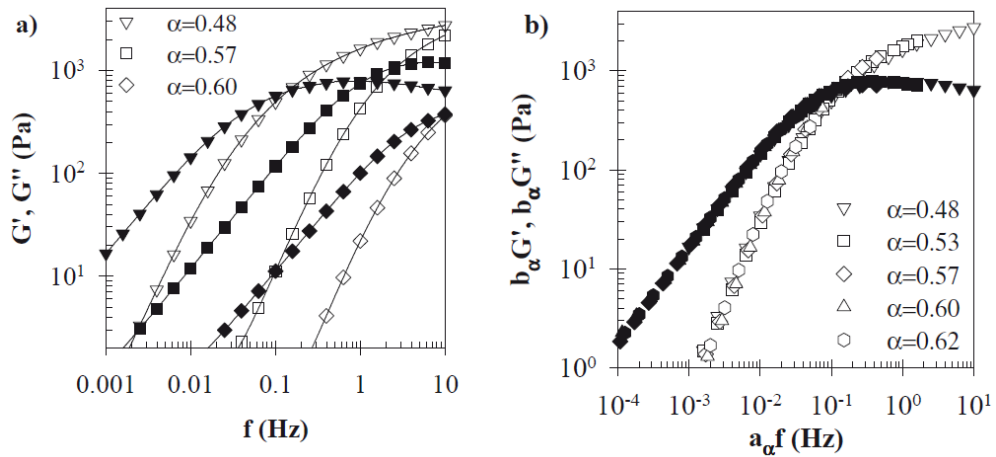


Figure 1.10. a) Evolution of the storage modulus (G' , open symbols) and loss modulus (G'' , closed symbols) as a function of the frequency for TH50 solutions at $C=67$ g/L and several ionization degrees. b) Master curves obtained by vertical and horizontal shifts of the data in a) with $\alpha_{ref}=0.48$.¹⁷

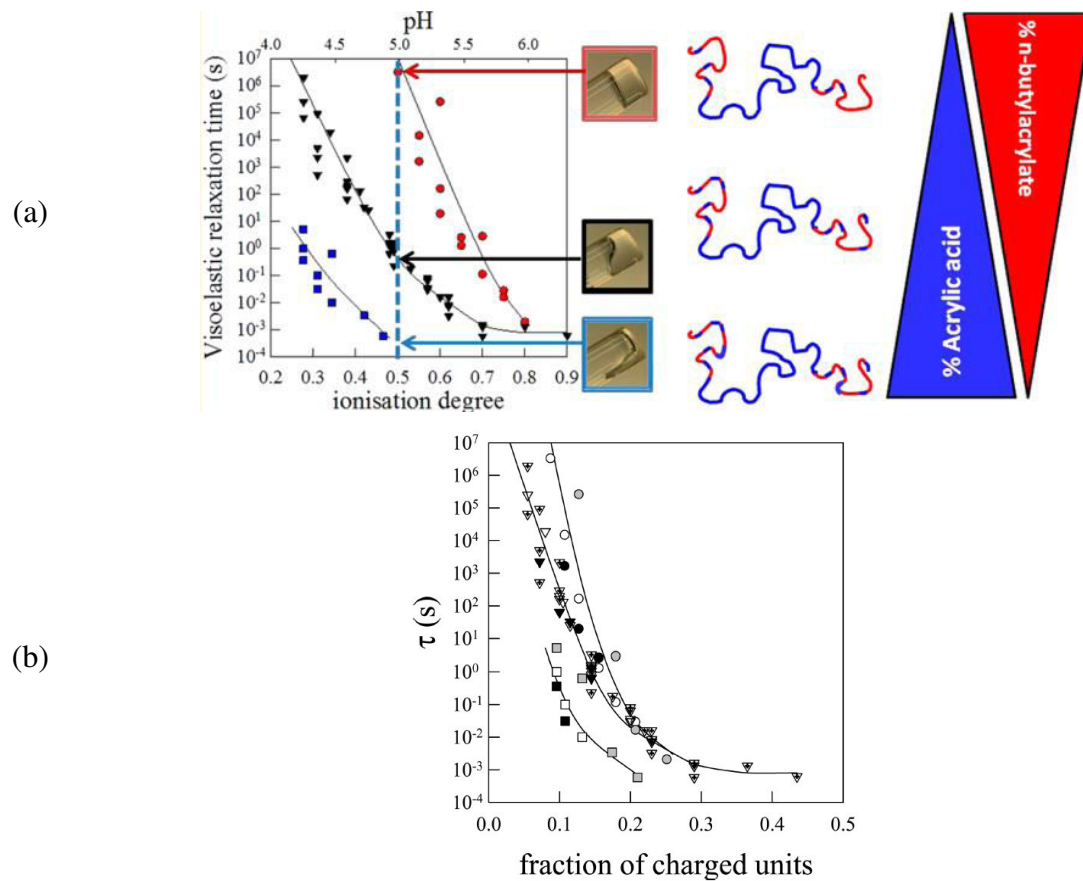


Figure 1.11. Evolution of the relaxation time of the three copolymers as a function of the ionisation degree (a) or of the fraction of charged units (b) at several concentrations. $T_{ref} = 20$ °C, solid lines are guides to the eye.⁸⁷

II.1.2. Other copolymers

Even if the exchange dynamics were not systematically measured on other systems, some studies indicate that incorporating hydrophilic units within the hydrophobic block of block-random copolymers may be a universal strategy to obtain dynamic systems. For instance, our group applied this strategy with a copolymer based on dimethylaminoethyl methacrylate (DMAEMA) and *n*-butyl methacrylate (*n*BMA).⁹⁰ P(*n*BMA_{50%}-*stat*-DMAMEA_{50%})-*b*-PDMAEMA diblock copolymers formed aggregates with a pH-dependent aggregation number, see Figure 1.12. In a similar manner, Wright *et al.* used this approach to tune the aggregation number as function of α of P(DEAEMA-*co*-DMAEMA)-*b*-PDMAEMA diblocks with different diethylaminoethyl methacrylate (DEAEMA) contents.⁸⁸ They also used block-random blocks to obtain micelles in thermodynamic equilibrium.^{88, 91, 92}

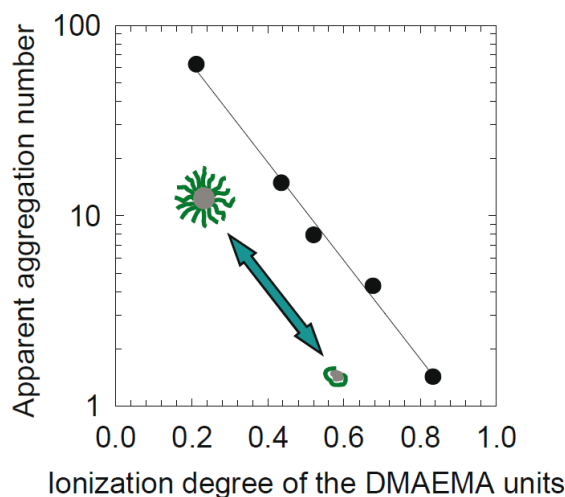


Figure 1.12. Evolution of the apparent aggregation number as a function of the ionization degree for a cationic diblock copolymer P(*n*BMA_{50%}-*stat*-*n*BMA_{50%})-*b*-PDMAEMA at $[Na^+] = 0.5 \text{ mol/L}$.⁹⁰

It is interesting to note that gradient copolymers can be used as hydrophobic blocks in a similar way. Borisova *et al.* synthesised a diblock PAA-*b*-P(AA-*grad*-S) and a triblock P(AA-*grad*-S)-PAA-*b*-P(AA-*grad*-S) that could self-assemble reversibly.^{93, 94} However, it is not clear whether gradient copolymers can form dynamic systems since P(AA-*grad*-S)-PAA-*b*-P(AA-*grad*-S) did not exhibit any visco-elastic behaviour with a measurable relaxation time for the pH and temperatures investigated; either viscous liquids or gels were observed.⁹⁴

II.2. Random copolymer structure

The chemical structure of copolymers made of at least two monomers can vary from the two limiting cases of random and diblock copolymers affecting the polymer properties. Here only random copolymers are considered. As recently reviewed by Li *et al.*, amphiphilic random copolymers can self-assemble into various morphologies due to the random distribution of hydrophilic and hydrophobic units.⁹⁵ As explained for multi-sticker polymers, amphiphilic random copolymers can form hydrophobic micro-domains either with themselves (intramolecular aggregation) or with other copolymers (intermolecular aggregation).

Important theoretical works were conducted within the last two decades to determine the phase diagrams of such copolymers. When intramolecular aggregation is dominant different morphologies such as “pearl-necklace” or “globule” were predicted at low concentration and low ionic strength.^{25, 27, 28, 96, 97} The presence of salt was shown to drastically affect the phase diagram usually decreasing the extent of intramolecular aggregation.⁹⁸ Intramolecular aggregation was experimentally observed with poly(styrene-*co*-styrene sodium sulfonate) (PSSNa) at low concentration and without added salt.⁹⁹⁻¹⁰² Intermolecular aggregation was also observed for hydrophobically modified copolymers.^{95, 103-107} Riemer *et al.* studied hydrophobically modified polyacrylates with different alkyl chain lengths which aggregate either intra or intermolecularly, see Figure 1.13.¹⁰⁷ It appeared that when the PAA backbone is studied at high pH and is decorated with short alkyl grafts, corresponding to less hydrophobic conditions, hydrophobic microdomains were not formed. However, with longer alkyl chains and at lower pH the electrostatic repulsion of the backbone could be overcome resulting in the formation of hydrophobic microdomains.

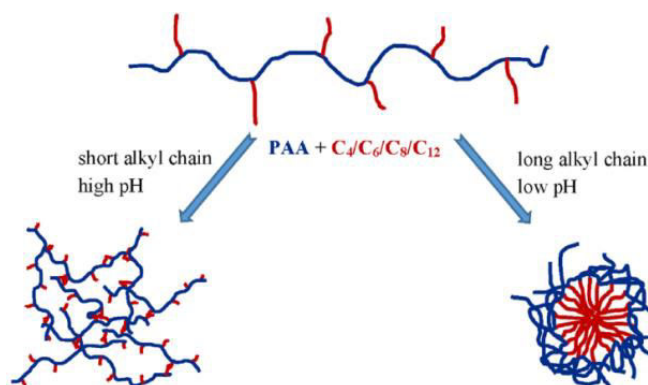


Figure 1.13. Schematic illustration of the different aggregations behaviours for hydrophobically modified PAA at different pH.¹⁰⁷

CHAPTER 1: BIBLIOGRAPHY

Gotzamanis *et al.* investigated the relationship between the self-assembly of random blocks and that of block-random diblocks made with these random blocks.⁸³ They studied the random block P(EGMA-*co*-MMA) and the diblock P(EGMA-*co*-MMA)-*b*-PDEAEMA based on oligo(ethylene glycol) methacrylate (EGMA), methyl methacrylate (MMA) and 2-(diethylamino)ethyl methacrylate (DEAEMA). The amount of MMA affected the thermosensitivity of P(EGMA-*co*-MMA) and therefore the aggregation number of the amphiphilic block copolymers. The LCST of P(EGMA-*co*-MMA) varied from 65 to 45 °C for MMA contents between 0 and 23.

III. Mixtures of dynamic amphiphilic polymers: structure and rheology

As previously shown, block-random copolymers can be used to produce dynamic copolymers and transient networks. The rheological properties of triblock copolymer solutions can be modified for given conditions of pH, temperature or ionic strength by synthesizing polymers containing different amounts of hydrophilic units within the hydrophobic blocks. Another interesting approach is to change the rheological properties by mixing different copolymers rather than doing extensive synthetic work for each application.

III.1. Structure of mixtures of dynamic amphiphilic copolymers

Theoretical studies on mixtures of neutral copolymers revealed some important criterions to obtain comicelles.¹⁰⁸⁻¹¹⁰ As first explained by Shim *et al.*, the relative concentrations of each copolymer affects the comicellisation.¹⁰⁸ Usually, comicellisation occurs when both copolymers are above their critical association concentration and critical association temperature as illustrated in Figure 1.14.^{108, 111}

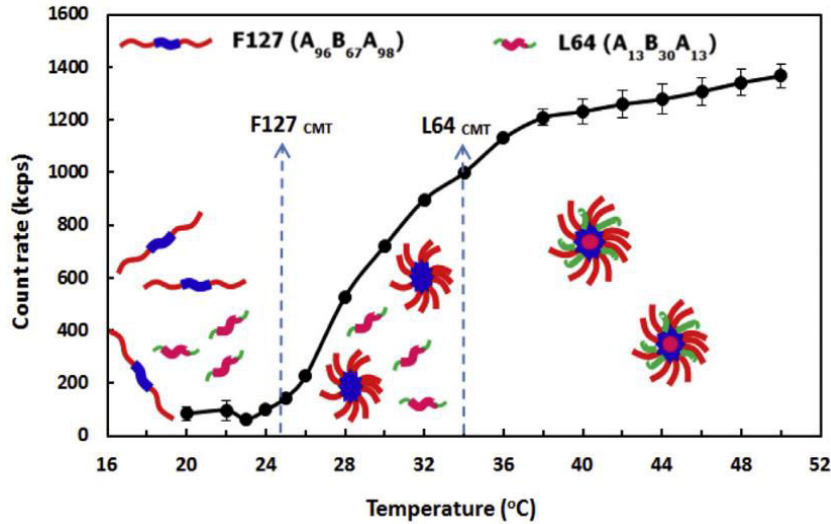


Figure 1.14. Evolution of the count rate as a function of the temperature for 50:50 mixtures of pluronics F127 and L64.¹¹¹

When comicellization occurs, the distribution of micelles is still an open debate. According to Sens *et al.*¹⁰⁹, comicelles can be in equilibrium with micelles of pure copolymers if the difference of curvature is not too large. These theoretical predictions were supported by experimental work on pluronics¹¹² and gangliosides,¹¹³ the latter being biological amphiphiles. Ricardo *et al.* demonstrated the importance of the size and the hydrophobicity of the hydrophobic blocks on the comicellisation.¹¹⁴ By studying with light scattering the comicellisation of pluronics with either butyl or styrene oxide as hydrophobic block ($E_mB_nE_m$ and $E_mS_nE_m$), they demonstrated that only comicelles were formed as long as the mixed polymers had a similar hydrophobicity, independently of the hydrophobic block length. Recently, Renou *et al.* demonstrated that co-micelles were formed for mixtures of PEO-alkyl bearing either short or long alkyl chains.¹¹⁵ Hydrodynamic radii were always larger for the comicelles than the average value of non hybridized pure micelles of each diblock since one of the polymer has a hydrophilic block longer than the other polymer, as illustrated in Figure 1.15. Recent dissipative particle dynamics simulations on different mixtures of pluronics indicated that there is always a bimodal distribution of micelles even if it is not always measurable.¹¹⁶

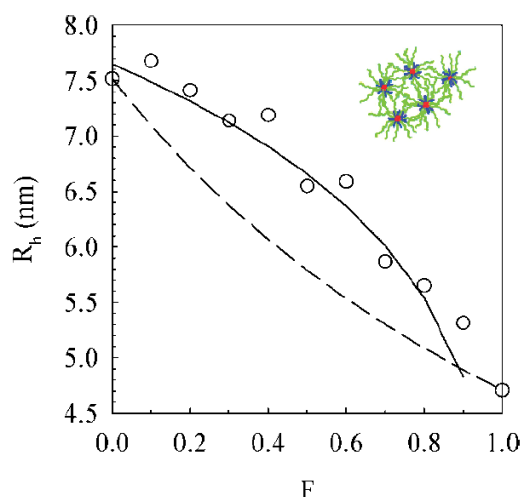


Figure 1.15. Evolution of the hydrodynamic radius of mixtures of PEO-alkyl with different alkyl lengths as a function of the fraction of long PEO-alkyl in the mixture (F). The solid line is a guide to the eye. The dashed line represents the prediction of the average R_h for binary mixtures of pure micelles with two different sizes. Adapted from ref. ¹¹⁵

Mixtures of charged amphiphilic copolymers have barely been studied in the literature but we wish to highlight the work of Wright *et al.* who studied mixtures of polymers with block-random copolymers as associative block.^{91, 92} They used diblock copolymers consisting of random associative blocks of dimethylaminoethyl methacrylate (DMAEMA) and diethylaminoethyl methacrylate (DEAEMA) with different DMAEMA contents, and of a hydrophilic PDMAEMA block: P(DMAEMA-co-DEAEMA)-b-PDMAEMA.⁸⁸ The study was performed at an ionization degree of the monomer units close to zero. Interestingly, the structure of hybrid micelles formed by mixing P(DMAEMA-co-DEAEMA)-b-PDMAEMA diblocks mimicked that of pure diblocks with the same overall chemical composition, similarly to what was observed by Renou *et al.*¹¹⁷ for neutral PEO-alkyl diblocks.

III.2. Rheological properties of mixtures of amphiphilic triblock copolymers

Despite their interest, studies focusing on the rheological properties of mixtures of dynamic amphiphilic polymers are rare. Mixtures of amphiphilic triblock copolymers are more often done to tune the sol-gel phase diagram or to change the micelle morphology as in the case of pluronics for instance.^{111, 114, 118-121}

Annable *et al.* studied transient networks formed by mixtures of PEO chains end capped with alkyls of different lengths (C12 to C20).¹⁵ The average length of the alkyl chain was 16 for all

mixtures. The authors demonstrated that polymer chains relax independently for all mixtures. For instance, a 50:50 mixture of C12 and C20 leads to a co-network with two relaxation times corresponding to those of the corresponding pure network of C12 and C20 respectively, see Figure 1.16. Similar results were obtained by Ruffier *et al.* on mixtures of PEO end capped with alkyl or fluorinated alkyl chains.⁸ For a 50:50 ratio, two relaxation times were observed as depicted in Figure 1.17. Since Renou *et al.* showed that PEO-alkyl of different sizes of the alkyl chain co-micellises, it is interesting to remark that polymers that co-micellise do not lead to a network with one single average relaxation time.

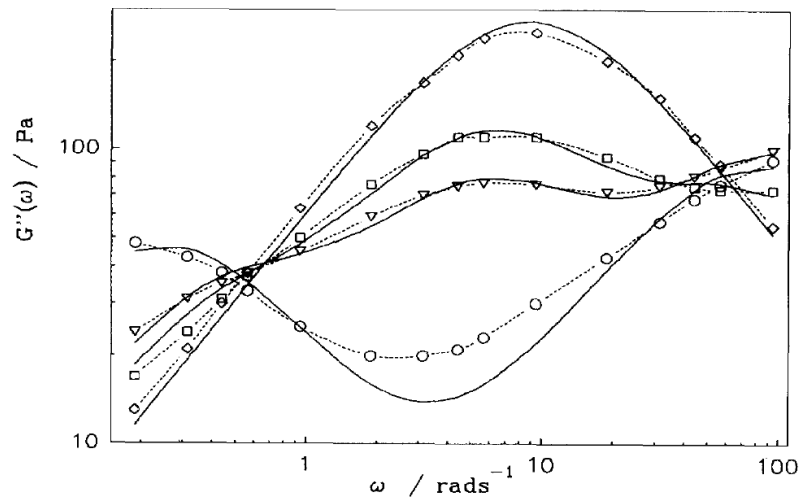


Figure 1.16. Loss modulus against angular frequency for mixtures of HEUR with C12, C16 and C20 end caps.¹⁵ The ratios are (\diamond) 0:100:0 (\square) 25:50:25 (∇) 40:20:40 (\circ) 50:0:50, the weight average of the cap length is always C16.

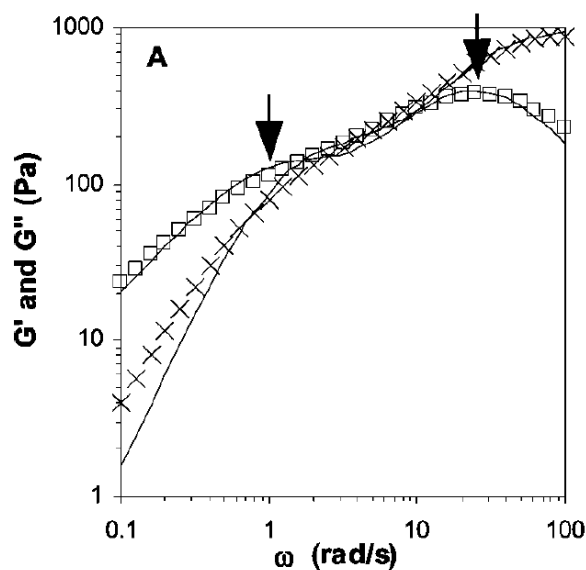


Figure 1.17. Evolution of the elastic (\square) and viscous (\times) moduli as a function of the angular frequency for mixtures at 3%(w/v) and 50:50 of $C_{18}H_{37}$ -PEO- $C_{10}H_{20}$ - C_8F_{17} / $C_{18}H_{37}$ -PEO- C_2H_4 - C_8F_{17} in the presence of SDS (8 mmol/L), at 25 °C.⁸

IV. Conclusion of the literature review

The exchange dynamics of self-assembled amphiphilic copolymers bearing at least two hydrophobic parts per chain appear as a key parameter to control the rheological properties of aqueous solutions of these polymers. Within this PhD work, we aimed at rationalizing the parameters allowing a control of these exchange dynamics and of the resulting rheological properties so that such smart materials may be relevant for industrial applications.

The starting point of this work was three triblocks copolymers, TH x , consisting of a poly(acrylic acid) P(AA) central block connected on each side to two random copolymers containing x mol% of AA and $(1-x)$ mol% of n -butyl acrylate (n BA).^{17, 87} It was shown that using random copolymers as hydrophobic blocks allowed controlling the exchange dynamics based on the content x of AA units within the hydrophobic blocks. But the impact of x on the structure of the self-assembled aggregates was not clearly identified. It was shown that DH50 diblocks and TH50 triblocks self-assembled progressively with decreasing ionization degree of the AA units. However, the relationship between the self-assembly of the neat hydrophobic block and that of the di/triblocks remains unclear. To the best of our knowledge, only Gotzamanis *et al.* reported preliminary studies linking the self-association of diblock copolymers with that of their neat hydrophobic block.⁸³ One objective of this work was

therefore to understand whether there is a relationship between the self-assembly of DHx diblock copolymers and that of their neat $P(nBA_{1-x}\text{-stat-AA}_x)_{100}$ hydrophobic blocks noted MHx. This study will help determining whether the factors affecting the exchange dynamics (pH, ionic strength and %AA) also impact the structure of the self-assembled aggregates.

The rheological properties of aqueous solutions of THx triblock copolymers are mainly controlled by the fraction of charged units within their hydrophobic block, the latter depending on the AA content x within these blocks and on the pH. However, for applications, THx have two major drawbacks: a) new syntheses are needed to change the rheological properties of THx solutions at constant pH and b) triblocks are difficult to produce industrially.

To solve the first problem, mixtures of triblocks would be interesting. The literature contains few examples of mixtures of dynamic copolymers used to design materials with controlled rheological properties and all of them are based on neutral polymers. Usually, mixtures of two dynamic triblocks lead to visco-elastic fluids with two relaxation times. However, to the best of our knowledge mixtures of amphiphilic copolyelectrolytes have never been studied. The study of mixtures of THx with different %AA in the hydrophobic blocks may also help to better understand how the distribution of relaxation times measured by rheology is affected by the dispersity of the THx copolymers since copolymer blending is a way to change the dispersity of the hydrophobic blocks composition in a controlled manner.

The second problem may be solved by using graft copolymers rather than triblock copolymers. The use of graft copolymers is of special interest for large-scale applications of amphiphilic copolymers as more resilient in industrial formulation due to the large amount of stickers. In addition, a comparison between the rheological properties of triblocks and multi stickers (or graft) copolymers will show the importance of the topology of the copolymers. Graft copolymers bearing thermo-sensitive associative grafts have been studied extensively, but graft copolymers with pH sensitive grafts leading to pH-controlled dynamics have not yet been reported.

Finally, the literature clearly shows that the incorporation of hydrophilic pH-sensitive units within the hydrophobic blocks of amphiphilic copolymers usually leads to smart materials exhibiting reversible self-assembly or sol-gel transition. Many systems have already been studied using different types of chemical groups with low or high glass transition, anionic or

CHAPTER 1: BIBLIOGRAPHY

cationic monomers, statistical or gradient unit repartition. However, to date, it was clearly proven only in the case of the THx triblocks that the exchange dynamics could also be controlled by this strategy. Therefore, the last objective of this work was to extend the concept by determining whether the exchange dynamics could also be controlled similarly with other comonomers. DMAEMA, a monomer exhibiting both pH and temperature responsiveness, was used in order to impart pH and thermo-sensitivity to the systems.

V. References

1. Wever, D. A. Z.; Picchioni, F.; Broekhuis, A. A. *Prog. Polym. Sci.* **2011**, 36, (11), 1558-1628.
2. Okay, O., Self-Healing Hydrogels Formed via Hydrophobic Interactions. In *Supramolecular Polymer Networks and Gels*, Seiffert, S., Ed. Springer International Publishing: Cham, 2015; pp 101-142.
3. Hietala, S.; Mononen, P.; Strandman, S.; Jarvi, P.; Torkkeli, M.; Jankova, K.; Hvilsted, S.; Tenhu, H. *Polymer* **2007**, 48, (14), 4087-4096.
4. Stavrouli, N.; Aubry, T.; Tsitsilianis, C. *Polymer* **2008**, 49, (5), 1249-1256.
5. Sfika, V.; Tsitsilianis, C. *Macromolecules* **2003**, 36, (13), 4983-4988.
6. Bossard, F.; Sfika, V.; Tsitsilianis, C. *Macromolecules* **2004**, 37, (10), 3899-3904.
7. Bossard, F.; Tsitsilianis, C.; Yannopoulos, S. N.; Petekidis, G.; Sfika, V. *Macromolecules* **2005**, 38, (7), 2883-2888.
8. Rufier, C.; Collet, A.; Viguiet, M.; Oberdisse, J.; Mora, S. *Macromolecules* **2008**, 41, (15), 5854-5862.
9. Calvet, D.; Collet, A.; Viguiet, M.; Berret, J. F.; Serero, Y. *Macromolecules* **2003**, 36, (2), 449-457.
10. Lafleche, F.; Durand, D.; Nicolai, T. *Macromolecules* **2003**, 36, (4), 1331-1340.
11. Lafleche, F.; Nicolai, T.; Durand, D.; Gnanou, Y.; Taton, D. *Macromolecules* **2003**, 36, (4), 1341-1348.
12. Serero, Y.; Aznar, R.; Porte, G.; Berret, J. F.; Calvet, D.; Collet, A.; Viguiet, M. *Phys. Rev. Lett.* **1998**, 81, (25), 5584-5587.
13. Grassl, B.; Billon, L.; Borisov, O.; Francois, J. *Polymer International* **2006**, 55, (10), 1169-1176.
14. Alami, E.; Almgren, M.; Brown, W.; Francois, J. *Macromolecules* **1996**, 29, (6), 2229-2243.
15. Annable, T.; Buscall, R.; Ettelaie, R.; Whittlestone, D. *J. Rheol.* **1993**, 37, (4), 695-726.
16. Green, M. S.; Tobolsky, A. V. *J. Chem. Phys.* **1946**, 14, (2), 80-92.
17. Charbonneau, C.; Chassenieux, C.; Colombani, O.; Nicolai, T. *Macromolecules* **2011**, 44, (11), 4487-4495.
18. Lee, H. I.; Pietrasik, J.; Sheiko, S. S.; Matyjaszewski, K. *Prog. Polym. Sci.* **2010**, 35, (1-2), 24-44.
19. Rubinstein, M.; Semenov, A. N. *Macromolecules* **2001**, 34, (4), 1058-1068.
20. Doyle, P. S.; Shaqfeh, E. S. G.; Gast, A. P. *Macromolecules* **1998**, 31, (16), 5474-5486.
21. Regalado, E. J. n.; Selb, J.; Candau, F. o. *Macromolecules* **1999**, 32, (25), 8580-8588.
22. Cram, S. L.; Brown, H. R.; Spinks, G. M.; Hourdet, D.; Creton, C. *Macromolecules* **2005**, 38, (7), 2981-2989.
23. Kujawa, P.; Audibert-Hayet, A.; Selb, J.; Candau, F. o. *Macromolecules* **2006**, 39, (1), 384-392.
24. Dobrynin, A. V. *Curr. Opin. Colloid Interface Sci.* **2008**, 13, (6), 376-388.
25. Dobrynin, A. V.; Rubinstein, M. *Macromolecules* **1999**, 32, (3), 915-922.
26. Ulrich, S.; Laguerre, A.; Stoll, S. *J. Chem. Phys.* **2005**, 122, (9), 094911.
27. Dobrynin, A. V.; Rubinstein, M. *Macromolecules* **2001**, 34, (6), 1964-1972.
28. Dobrynin, A. V.; Rubinstein, M. *Macromolecules* **2000**, 33, (21), 8097-8105.

CHAPTER 1: BIBLIOGRAPHY

29. Vasilevskaya, V. V.; Klochkov, A. A.; Lazutin, A. A.; Khalatur, P. G.; Khokhlov, A. R. *Macromolecules* **2004**, 37, (14), 5444-5460.
30. Chepelianskii, A.; Mohammad-Rafiee, F.; Trizac, E.; Raphael, E. *J. Phys. Chem. B* **2008**, 113, (12), 3743-3749.
31. Vasilevskaya, V. V.; Potemkin, I. I.; Khokhlov, A. R. *Langmuir* **1999**, 15, (23), 7918-7924.
32. Zhu, Z.; Jian, O.; Paillet, S.; Desbrières, J.; Grassl, B. *Eur. Polym. J.* **2007**, 43, (3), 824-834.
33. Yang, Q.; Song, C.; Chen, Q.; Zhang, P.; Wang, P. *J. Polym. Sci., Part B: Polym. Phys.* **2008**, 46, (22), 2465-2474.
34. Wang, J.; Benyahia, L.; Chassenieux, C.; Tassin, J.-F.; Nicolai, T. *Polymer* **2010**, 51, (9), 1964-1971.
35. Tomatsu, I.; Hashidzume, A.; Yusa, S.-i.; Morishima, Y. *Macromolecules* **2005**, 38, (18), 7837-7844.
36. Petit, L.; Karakasyan, C.; Pantoustier, N. g.; Hourdet, D. *Polymer* **2007**, 48, (24), 7098-7112.
37. Feng, Y.; Billon, L.; Grassl, B.; Bastiat, G.; Borisov, O.; François, J. *Polymer* **2005**, 46, (22), 9283-9295.
38. Caputo, M. R.; Selb, J.; Candau, F. *Polymer* **2004**, 45, (1), 231-240.
39. Castelletto, V.; Hamley, I. W.; Xue, W.; Sommer, C.; Pedersen, J. S.; Olmsted, P. D. *Macromolecules* **2004**, 37, (4), 1492-1501.
40. Hourdet, D.; Ducouret, G.; Varghese, S.; Badiger, M. V.; Wadgaonkar, P. P. *Polymer* **2013**, 54, (11), 2676-2689.
41. Kujawa, P.; Audibert-Hayet, A.; Selb, J.; Candau, F. *Journal of Polymer Science Part B-Polymer Physics* **2004**, 42, (9), 1640-1655.
42. Lele, A.; Shedje, A.; Badiger, M.; Wadgaonkar, P.; Chassenieux, C. *Macromolecules* **2010**, 43, (23), 10055-10063.
43. Maia, A. M. S.; Villetti, M. A.; Borsali, R.; Balaban, R. C. *Journal of the Brazilian Chemical Society* **2013**, 24, (11), 1871-1879.
44. Cadix, A.; Chassenieux, C.; Lafuma, F. o.; Lequeux, F. o. *Macromolecules* **2005**, 38, (2), 527-536.
45. Hourdet, D.; Gadgil, J.; Podhajecka, K.; Badiger, M. V.; Brûlet, A.; Wadgaonkar, P. P. *Macromolecules* **2005**, 38, (20), 8512-8521.
46. Iatridi, Z.; Bokias, G. *Langmuir* **2009**, 25, (13), 7695-7703.
47. Durand, A.; Hourdet, D. *Polymer* **1999**, 40, (17), 4941-4951.
48. Durand, A.; Hourdet, D. *Polymer* **2000**, 41, (2), 545-557.
49. Hourdet, D.; Lalloret, F.; Audebert, R. *Polymer* **1994**, 35, (12), 2624-2630.
50. Gouveia, L. M.; Grassl, B.; Müller, A. J. *J. Colloid Interface Sci.* **2009**, 333, (1), 152-163.
51. Bromberg, L. *Langmuir* **1998**, 14, (20), 5806-5812.
52. Wever, D. A. Z.; Riemsma, E.; Picchioni, F.; Broekhuis, A. A. *Polymer* **2013**, 54, (21), 5456-5466.
53. Wang, Y.; Feng, Y. J.; Wang, B. Q.; Lu, Z. Y. *J. Appl. Polym. Sci.* **2010**, 116, (6), 3516-3524.
54. Podhajecka, K.; Prochazka, K.; Hourdet, D. *Polymer* **2007**, 48, (6), 1586-1595.
55. Holmberg, K.; Jönsson, B.; Kronberg, B.; Lindman, B., *Surfactants and Polymers in Aqueous Solution*. 2006.
56. Nicolai, T.; Colombani, O.; Chassenieux, C. *Soft Matter* **2010**, 6, (14), 3111-3118.
57. Tian, M. M.; Qin, A. W.; Ramireddy, C.; Webber, S. E.; Munk, P.; Tuzar, Z.; Prochazka, K. *Langmuir* **1993**, 9, (7), 1741-1748.

58. Halperin, A.; Alexander, S. *Macromolecules* **1989**, 22, (5), 2403-2412.
59. Choi, S. H.; Lodge, T. P.; Bates, F. S. *Phys. Rev. Lett.* **2010**, 104, (4), 047802-047806.
60. Choi, S. H.; Bates, F. S.; Lodge, T. P. *Macromolecules* **2011**, 44, (9), 3594-3604.
61. Halperin, A. *Macromolecules* **2011**, 44, (13), 5072-5074.
62. Jacquin, M.; Muller, P.; Cottet, H.; Theodoly, O. *Langmuir* **2010**, 26, (24), 18681-18693.
63. Hurtrez, G.; Dumas, P.; Riess, G. *Polym. Bull.* **1998**, 40, (2-3), 203-210.
64. Wang, Y. M.; Balaji, R.; Quirk, R. P.; Mattice, W. L. *Polym. Bull.* **1992**, 28, (3), 333-338.
65. Simone, P. M.; Lodge, T. P. *Macromolecular Chemistry and Physics* **2007**, 208, (4), 339-348.
66. Meli, L.; Lodge, T. P. *Macromolecules* **2009**, 42, (3), 580-583.
67. Meli, L.; Santiago, J. M.; Lodge, T. P. *Macromolecules* **2010**, 43, (4), 2018-2027.
68. Wang, D.; Yin, J.; Zhu, Z. Y.; Ge, Z. S.; Liu, H. W.; Armes, S. P.; Liu, S. Y. *Macromolecules* **2006**, 39, (21), 7378-7385.
69. Ge, Z. S.; Cai, Y. L.; Yin, J.; Zhu, Z. Y.; Rao, J. Y.; Liu, S. Y. *Langmuir* **2007**, 23, (3), 1114-1122.
70. Kriz, J.; Masar, B.; Pospisil, H.; Plestil, J.; Tuzar, Z.; Kiselev, M. A. *Macromolecules* **1996**, 29, (24), 7853-7858.
71. Lund, R.; Willner, L.; Richter, D.; Iatrou, H.; Hadjichristidis, N.; Lindner, P. *Journal of Applied Crystallography* **2007**, 40, S327-S331.
72. Lund, R.; Willner, L.; Richter, D.; Dormidontova, E. E. *Macromolecules* **2006**, 39, (13), 4566-4575.
73. Lund, R.; Willner, L.; Stellbrink, J.; Richter, D. *Physica B-Condensed Matter* **2006**, 385, 735-737.
74. Lund, R.; Willner, L.; Stellbrink, J.; Lindner, P.; Richter, D. *Phys. Rev. Lett.* **2006**, 96, (6), 068302-068306.
75. Jacquin, M.; Muller, P.; Talingting-Pabalan, R.; Cottet, H.; Berret, J. F.; Futterer, T.; Theodoly, O. *Journal of Colloid and Interface Science* **2007**, 316, (2), 897-911.
76. Willner, L.; Poppe, A.; Allgaier, J.; Monkenbusch, M.; Richter, D. *Europhysics Letters* **2001**, 55, (5), 667-673.
77. Rager, T.; Meyer, W. H.; Wegner, G.; Winnik, M. A. *Macromolecules* **1997**, 30, (17), 4911-4919.
78. Wang, Y. M.; Kausch, C. M.; Chun, M. S.; Quirk, R. P.; Mattice, W. L. *Macromolecules* **1995**, 28, (4), 904-911.
79. Rager, T.; Meyer, W. H.; Wegner, G. *Macromolecular Chemistry and Physics* **1999**, 200, (7), 1672-1680.
80. Tsitsilianis, C.; Gotzamanis, G.; Iatridi, Z. *Eur. Polym. J.* **2011**, 47, (4), 497-510.
81. Bendejacq, D.; Ponsinet, V.; Joanicot, M.; Vacher, A.; Airiau, M. *Macromolecules* **2003**, 36, (19), 7289-7295.
82. Bendejacq, D. D.; Ponsinet, V.; Joanicot, M. *Langmuir* **2005**, 21, (5), 1712-1718.
83. Gotzamanis, G.; Tsitsilianis, C. *Polymer* **2007**, 48, (21), 6226-6233.
84. Charbonneau, C.; Lima, M. M. D.; Chassenieux, C.; Colombani, O.; Nicolai, T. *Phys. Chem. Chem. Phys.* **2013**, 15, (11), 3955-3964.
85. Lejeune, E.; Chassenieux, C.; Colombani, O., pH Induced Desaggregation Of Highly Hydrophilic Amphiphilic Diblock Copolymers. In *Trends in Colloid and Interface Science Xxiv*, Starov, V.; Prochazka, K., Eds. 2011; Vol. 138, pp 7-16.
86. Lejeune, E.; Drechsler, M.; Jestin, J.; Muller, A. H. E.; Chassenieux, C.; Colombani, O. *Macromolecules* **2010**, 43, (6), 2667-2671.

CHAPTER 1: BIBLIOGRAPHY

87. Shedge, A.; Colombani, O.; Nicolai, T.; Chassenieux, C. *Macromolecules* **2013**, 47, (7), 2439-2444.
88. Wright, D. B.; Patterson, J. P.; Pitto-Barry, A.; Cotanda, P.; Chassenieux, C.; Colombani, O.; O'Reilly, R. K. *Polym. Chem.* **2015**, (6), 2761-2768.
89. Colombani, O.; Lejeune, E.; Charbonneau, C.; Chassenieux, C.; Nicolai, T. *J. Phys. Chem. B* **2012**, 116, (25), 7560-7565.
90. Dutertre, F.; Boyron, O.; Charleux, B.; Chassenieux, C.; Colombani, O. *Macromol. Rapid Commun.* **2012**, 33, (9), 753-759.
91. Wright, D. B.; Patterson, J. P.; Gianneschi, N. C.; Chassenieux, C.; Colombani, O.; O'Reilly, R. K. *Polym. Chem.* **2016**.
92. Wright, D. B.; Patterson, J. P.; Pitto-Barry, A.; Lu, A.; Kirby, N.; Gianneschi, N. C.; Chassenieux, C.; Colombani, O.; O'Reilly, R. K. *Macromolecules* **2015**, 48, (18), 6516-6522.
93. Borisova, O.; Billon, L.; Zaremski, M.; Grassl, B.; Bakaeva, Z.; Lapp, A.; Stepanek, P.; Borisov, O. *Soft Matter* **2012**, 8, (29), 7649-7659.
94. Borisova, O.; Billon, L.; Zaremski, M.; Grassl, B.; Bakaeva, Z.; Lapp, A.; Stepanek, P.; Borisov, O. *Soft Matter* **2011**, 7, (22), 10824-10833.
95. Li, L.; Raghupathi, K.; Song, C.; Prasad, P.; Thayumanavan, S. *Chem. Commun.* **2014**, 50, (88), 13417-13432.
96. Faraudo, J.; Martin-Molina, A. *Curr. Opin. Colloid Interface Sci.* **2013**, 18, (6), 517-523.
97. Khokhlov, A. R.; Khalatur, P. G. *Curr. Opin. Colloid Interface Sci.* **2005**, 10, (1-2), 22-29.
98. Vasilevskaya, V. V.; Khokhlov, A. R.; Yoshikawa, K. *Macromol. Theory Simul.* **2000**, 9, (8), 600-607.
99. Baigl, D. Etude expérimentale de polyélectrolytes hydrophobes modèles. Université Paris VI, 2003.
100. Baigl, D.; Ober, R.; Qu, D.; Fery, A.; Williams, C. E. *Europhys. Lett.* **2003**, 62, (4), 588.
101. Baigl, D.; Sferrazza, M.; Williams, C. E. *Europhys. Lett.* **2003**, 62, (1), 110.
102. Dasmahapatra, A. K.; Kumaraswamy, G.; Nanavati, H. *Macromolecules* **2006**, 39, (26), 9621-9629.
103. Dutta, P.; Dey, J.; Ghosh, G.; Nayak, R. R. *Polymer* **2009**, 50, (6), 1516-1525.
104. Petit-Agnely, F.; Iliopoulos, I.; Zana, R. *Langmuir* **2000**, 16, (25), 9921-9927.
105. Sato, Y.; Hashidzume, A.; Morishima, Y. *Macromolecules* **2001**, 34, (17), 6121-6130.
106. Wu, X.; Qiao, Y.; Yang, H.; Wang, J. *J. Colloid Interface Sci.* **2010**, 349, (2), 560-564.
107. Riemer, S.; Prévost, S.; Dzionara, M.; Appavou, M.-S.; Schweins, R.; Gradzielski, M. *Polymer* **2015**, 70, 194-206.
108. Shim, D. F. K.; Marques, C.; Cates, M. E. *Macromolecules* **1991**, 24, (19), 5309-5314.
109. Sens, P.; Marques, C. M.; Joanny, J. F. *Macromolecules* **1996**, 29, (14), 4880-4890.
110. Borovinskii, A. L.; Khokhlov, A. R. *Macromolecules* **1998**, 31, (22), 7636-7640.
111. Pragatheeswaran, A. M.; Chen, S. B.; Chen, C.-F.; Chen, B.-H. *Polymer* **2014**, 55, (20), 5284-5291.
112. Alexandridis, P.; Holzwarth, J. F.; Hatton, T. A. *Macromolecules* **1994**, 27, (9), 2414-2425.
113. Cantu, L.; Corti, M.; Salina, P. *The Journal of Physical Chemistry* **1991**, 95, (15), 5981-5983.
114. Ricardo, N. g. M. P. S.; Chaibundit, C.; Yang, Z.; Attwood, D.; Booth, C. *Langmuir* **2006**, 22, (3), 1301-1306.

115. Renou, F. d. r.; Benyahia, L.; Nicolai, T.; Glatter, O. *Macromolecules* **2008**, 41, (17), 6523-6530.
116. Prhashanna, A.; Khan, S. A.; Chen, S. B. *J. Phys. Chem. B* **2015**, 119, (2), 572-582.
117. Renou, F.; Nicolai, T.; Nicol, E.; Benyahia, L. *Langmuir* **2009**, 25, (1), 515-521.
118. Harrison, W. J.; Aboulgasem, G. J.; Elathrem, F. A. I.; Nixon, S. K.; Attwood, D.; Price, C.; Booth, C. *Langmuir* **2005**, 21, (14), 6170-6178.
119. Hamley, I. W., Neutral Block Copolymers in Dilute Solution. In *Block Copolymers in Solution: Fundamentals and Applications*, Wiley, Ed. 2005.
120. Chaibundit, C.; Ricardo, N. g. M. P. S.; Costa, F. v. d. M. L. L.; Yeates, S. G.; Booth, C. *Langmuir* **2007**, 23, (18), 9229-9236.
121. Newby, G. E.; Hamley, I. W.; King, S. M.; Martin, C. M.; Terrill, N. J. *J. Colloid Interface Sci.* **2009**, 329, (1), 54-61.

CHAPTER 2: MATERIALS AND METHODS

CHAPTER 2 : MATERIALS AND METHODS

I. Experimental techniques

I.1. Differential refractometry

A differential refractometer, Optilab rEX Wyatt-822, from Wyatt Technology Corporation using a laser beam with a wavelength of 633 nm was used to measure the refractive index increments, dn/dc .

Aqueous polymer solutions with concentrations ranging from 1 to 5 g/L were injected and the refractive index differences with the solvent were measured as a function of the polymer concentration, see Figure 2.1. The dn/dc is defined as the slope of the refractive index difference as a function of the polymer concentration as shown in Figure 2.1.

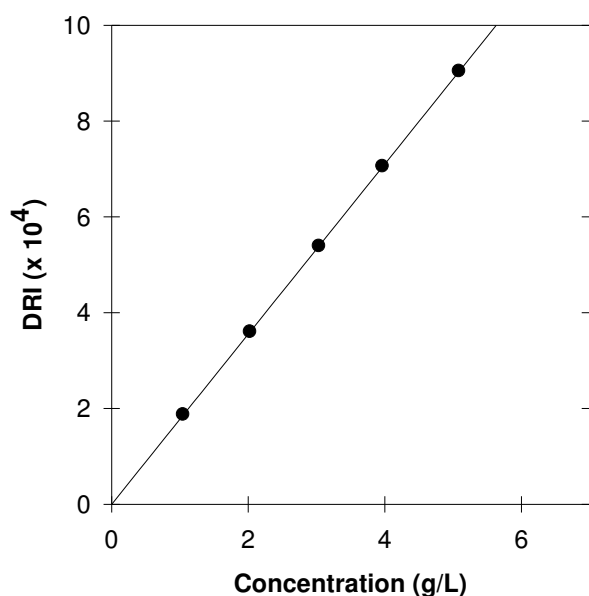


Figure 2.1. Evolution of the refractive index difference between the polymer solution and the pure solvent as a function of the polymer concentration for DH50 solutions at $\alpha=0.68$ and $[Na^+]=0.1$ mol/L.

I.2. Light scattering

Light scattering experiments were used to characterise the self-assembled polymers in solution at the nanoscale. Two types of light scattering experiments were used: static and dynamic.

Static light scattering gives access to the weight average molar mass (M_w) and the z-average radius of gyration (R_g) of the scatterers. Dynamic light scattering measures the self-diffusion coefficient (D_0) of the scatterers and hence their hydrodynamic radius. In both cases, interactions between the scatterers can affect the measurements giving only apparent values of the molar mass and hydrodynamic radius as explained in section I.2.4c) of this chapter.

I.2.1. Apparatus

Light scattering measurements were done using an ALV-CGS-8F system operating with a vertically polarized He-Ne laser with wavelength $\lambda_0 = 632.8$ nm (ALV-GmbH, Germany) coupled with an ALV-5003 multi tau correlator system (ALV-GmbH, Germany). Samples were placed in a thermostated decalin bath that is quasi isorefractive with glass in order to lower reflections of light at the surface of the light scattering cells.

The measurements were done at several angles of observation ranging from 12 to 150° giving access to about one decade of scattering wave vectors (from 2.77×10^6 m⁻¹ to 2.55×10^7 m⁻¹ in water) since $q = \frac{4\pi n}{\lambda_0} \sin\left(\frac{\theta}{2}\right)$ (with θ the angle of observation and $n = 1.33$ the refractive index of the solvent that is water in the present investigation).

I.2.2. Principle

In a light scattering experiment, a monochromatic plane-polarized light wave of intensity I_0 and wavelength λ_0 illuminates a sample of volume V . With a detector at a distance B , the scattered light intensity I_θ is measured at θ angle (Figure 2.2).

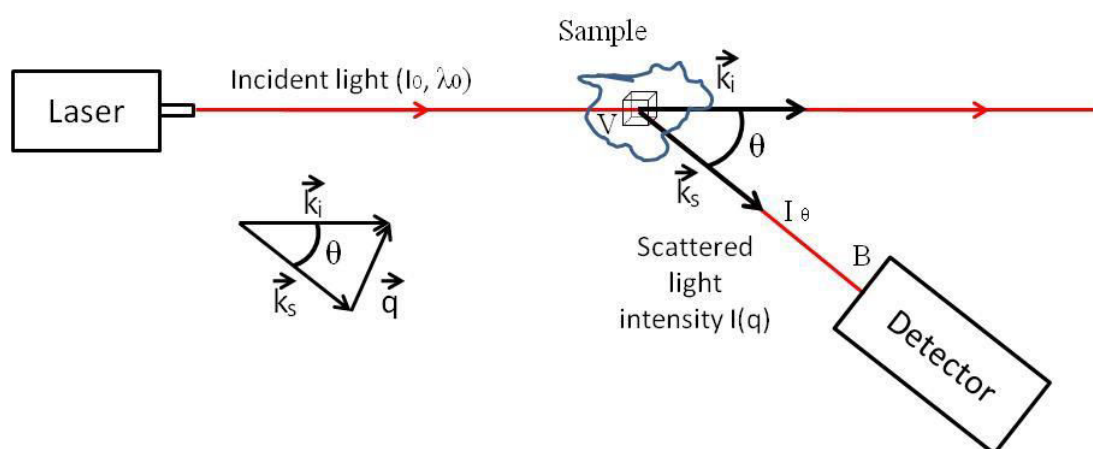


Figure 2.2. Schematic drawing of a light scattering experiment.

The scattered light intensity I_θ depends on the angle θ between the wave vector of the incident light (\vec{k}_i) and the wave vector of the scattered light (\vec{k}_s). These wave vectors define the scattering wave vectors \vec{q} with the following norm:

$$q = \frac{4\pi n}{\lambda_0} \sin\left(\frac{\theta}{2}\right) \quad (2.1)$$

with n the refractive index of the solvent.

Light scattering originates from the spatial density fluctuations of the solvent and concentration fluctuations of the scattering particles. The scattered intensity fluctuates with time as shown on Figure 2.3 because of Brownian motion. Static light scattering focuses on the time-average scattered intensity $\langle I \rangle$ to determine the molar mass (M_w), the radius of gyration (R_g) and the interactions between the particles. Dynamic light scattering relies on the fluctuations of the scattered intensity with time to calculate the self-diffusion coefficient and therefore the hydrodynamic radius (R_h) of the particles.

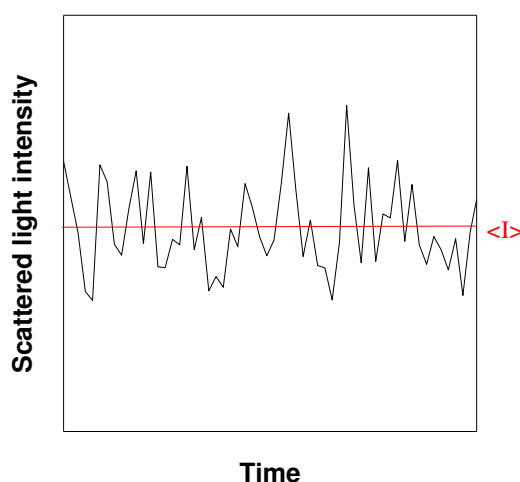


Figure 2.3. Evolution of the scattered light intensity as a function of time for a solution of scattering particles.

I.2.3. Static light scattering (SLS)

In static light scattering, the scattered light intensity at one or several angles (θ) is studied. The total scattered light intensity is the sum of the light scattered by the solvent (I_{sol}) and by the particles in solution (I_θ). Because the volume V and the distance R to the detector are difficult to measure easily, a reference is generally used. In our case, toluene was used as

CHAPTER 2: MATERIALS AND METHODS

reference since its Rayleigh ratio is well known ($R_{\theta\text{-tol}} = 1.36 \times 10^{-5} \text{ cm}^{-1}$ at $\lambda_0 = 633 \text{ nm}$). The Rayleigh ratio of the system is calculated with equation (2.2).

$$R_{\theta} = \frac{I_{\theta} - I_{sol}}{I_{tol}} R_{\theta\text{-tol}} \left(\frac{n_{tol}}{n} \right)^2 \quad (2.2)$$

with I_{tol} the scattered light intensity of toluene, n_{tol} the refractive index of toluene (1.498).

The Rayleigh ratio depends on the weight concentration of the scattering particles (C), their weight-average apparent molar mass (M_{app}), a structure factor ($S(q)$) and a constant K :

$$R_{\theta} = K \cdot C \cdot M_{app} \cdot S(q) \quad (2.3)$$

K is defined by equation (2.4) where N_a is the Avogadro number ($6.02 \times 10^{23} \text{ mol}^{-1}$) and dn/dc is the refractive index increment of the solute.

$$K = \frac{4\pi^2 n_{sol}^2 \left(\frac{dn}{dc} \right)^2}{\lambda_0^4 \cdot N_a} \quad (2.4)$$

In this work, most structure factors were close to unity indicating that the scatterers were small ($q \cdot R_g \ll 1$ with R_g the radius of gyration):

$$S(q) = 1 - \frac{q^2 R_g^2}{3} \quad (2.5)$$

Since $q \cdot R_g \ll 1$, the Zimm equation was used to analyse the static light scattering data see equation (2.6). Usually, the coefficient $A_2 \cdot C$ was also negligible and the apparent molar mass determined for $q \rightarrow 0$ was equal to the true molar mass of the scatterers M_w .

$$\frac{KC}{R_{\theta}} = \left(\frac{1}{M_w} + 2A_2 C \right) \left(1 + \frac{q^2 R_g^2}{3} \right) \quad (2.6)$$

A last parameter widely used in this work is the aggregation number (N_{agg}) defined by equation (2.7) when aggregates were formed. N_{agg} is the number of hydrophobic blocks in a macromolecular aggregate, which equals the number of aggregated chains in the case of mono and diblocks.

$$N_{agg} = \frac{M_w}{M_{w,unimère}} \quad (2.7)$$

I.2.4. Dynamic light scattering (DLS)

a) Principle

For dynamic light scattering (DLS), the fluctuations of the scattered light intensity over time are studied. Due to brownian motion, the inhomogeneities, coming from the spatial density and concentration fluctuations are time-dependent and affect the scattered light intensity. The fluctuations of the intensity originate from the fluctuations of the electrical field. The electrical field is not directly measurable, but its autocorrelation function is described by equation (2.8).

$$g_1(t) = \langle E(t_0).E^*(t_0 + \Delta t) \rangle \quad (2.8)$$

In DLS, only intensity measurements are performed and the normalised intensity autocorrelation function is defined by equation (2.9).

$$g_2(t) = \frac{G_2(t)}{\langle I(t) \rangle^2} = \frac{\langle I(0).I(t) \rangle}{\langle I(t) \rangle^2} \quad (2.9)$$

In the case of a Gaussian distribution of intensity fluctuations, the electrical field fluctuations and intensity fluctuations are related by the Siegert equation see (2.10). The Siegert equation holds for a diffusive volume larger than the correlation length of the concentration fluctuation.

$$g_2(t) = 1 + a|g_1(t)|^2 \quad (2.10)$$

With “a” a constant between 0 and 1 which depends on the apparatus.

The origins of the variation of the electrical field are the particle relaxation mechanisms. It can be diffusion, rotation, translation or others. In this work, only the diffusion relaxation mechanism contributes to $g_2(t)$.

For monodisperse diffusive particles, the autocorrelation function of the electrical field can be described with equation (2.11).

$$g_1(t) = \exp\left(-\frac{t}{\tau}\right) = \exp(-D.q^2.t) \quad (2.11)$$

where τ is the relaxation time and D the diffusion coefficient of the particles.

With polydisperse systems equation (2.11) is replaced by a sum of exponentials corresponding to the contribution of each species, see equation (2.12).

CHAPTER 2: MATERIALS AND METHODS

$$g_1(t) = \int A(\tau) \cdot \exp\left(-\frac{t}{\tau}\right) d\tau \quad (2.12)$$

with $A(\tau)$ the intensity-weighted proportion of scatterers with relaxation time τ .

Therefore, by fitting equation (2.12) it is possible to deduce the z-average apparent diffusion coefficient D_{app} by applying equation (2.13), an indication of the dispersity is calculated using equation (2.14). Details on the data treatment are given in section I.2.4b).

$$D_{app} = \left\langle \frac{1}{\tau} \right\rangle \cdot \frac{1}{q^2} \quad (2.13)$$

$$Dispersity = \frac{1}{\left\langle \tau \right\rangle} \cdot \left\langle \frac{1}{\tau} \right\rangle \quad (2.14)$$

The diffusion coefficient D_i is extrapolated to $C \rightarrow 0$ by using equation (2.15).

$$D = D_0(1 + k_D C + \dots) \quad (2.15)$$

where k_D is the second dynamic virial coefficient.

The z-average hydrodynamic radius can be calculated by using the Stokes-Einstein equation assuming that the particles are spherical, see equation (2.16).

$$R_{h,z} = \frac{k_B T}{6\pi\eta D_0} \quad (2.16)$$

where k_B is the Boltzmann constant, T the absolute temperature and η the solvent viscosity.

b) Data treatment

The aim of the data treatment is to determine the distribution of relaxation times $A(\tau)$. A software called Gendist was used in order to solve equation (2.17) which is a combination of equation (2.10) and equation (2.12).

$$g_2(t) = 1 + \beta \left[\int A(\tau) \cdot \exp\left(-\frac{t}{\tau}\right) d\tau \right]^2 \quad (2.17)$$

Since no general analytical resolution is possible, two models were used for $A(\tau)$ to fit this equation: REPES and GAUSS-GEX.

The first model, REPES, assumes that $A(\tau)$ is a sum of discrete relaxation times. This method can treat most of the results but might generate $A(\tau)$ without physical meaning. A

regularization parameter is used to smooth the data, also called probability (p), and eliminates meaningless peaks. However, the regularization parameter must be used carefully since it may also merge meaningful distinct peaks.

The GAUSS-GEX model can be used with systems having one or two populations. It uses two equations, (2.18) and (2.19), of relaxation time distributions $A(\tau)$ to fit the data. In the case of a unimodal system, only the GAUSS equation was used.

$$A(\tau_{GAUSS}) = \frac{1}{\beta\tau\sqrt{\pi}} \cdot \exp\left(-\frac{\left[\ln\left(\frac{\tau}{\tau_0}\right)\right]^2}{\beta^2}\right) \quad (2.18)$$

where β determines the curve's width.

When two populations are expected, GEX equation is added to the GAUSS equation with a weight parameter.

$$A(\tau_{GEX}) = N \cdot \tau^{p-1} \cdot \tau_a^{-p} \cdot \exp\left(-\left(\frac{\tau}{\tau_a}\right)^s\right) \quad (2.19)$$

N is a normalisation constant, τ_a determines the relaxation time, p determines the width and s the asymmetry of the curve. GEX has an additional degree of freedom to describe broad monomodal distributions. Using GEX for $A(\tau)$ allows one to describe broad monomodal distributions for which REPES would generate multimodal responses.

c) Correction of SLS with DLS

In the case of multimodal systems, the amplitude of each mode in DLS can be used to obtain, from the average scattered light intensity, the molar mass of each scattering particles if the weight concentration is known. Typically the weight concentration of the slow mode is considered negligible.

For example, let us focus on a polymer in solution that contains a small weight fraction of large spurious particles,¹ these large particles which contribute significantly to the total scattered light even though they represent only a negligible weight fraction. We illustrate the method for the diblock DH40 at an ionization degree of 0.6, $[Na^+]=0.1$ mol/L and a polymer concentration of 2 g/L. SLS indicates a molar mass of 2×10^5 g/mol, but DLS analysis (Gauss-Gex here) shows a bimodal relaxation time distribution with up to ~80% of the scattered light

intensity coming from spurious aggregates that cause the slow relaxation mode, as depicted in Figure 2.4a. By considering the relative amplitude of the fast mode (~20 %) the apparent molar mass can be corrected and decreases down to 5×10^4 g/mol as shown in Figure 2.4b.

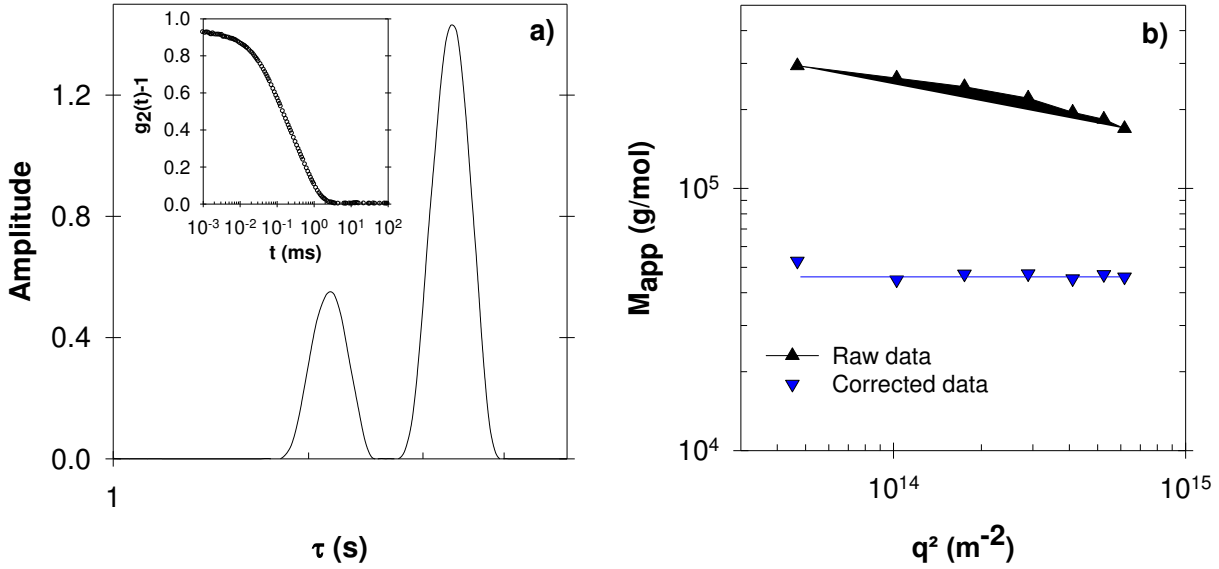


Figure 2.4. (a) Relaxation time distribution and correlation function (inset) (b) Evolution of M_{app} as a function of q^2 for DH40 at $\alpha=0.6$, $[Na^+]=0.1$ M, $C(DH40)=2$ g/L, with and without correction of the SLS data using the DLS results.

I.3. Rheology

I.3.1. Shear flow measurement

Rheology is the science and the study of the flow of matter. In the case of a laminar flow between an immobile and a mobile surface, the fluid is considered as a superposition of thin layers, parallel to each other, without any matter transfer between them. The movement of the mobile surface generates a shear force (F), which defines the shear stress ($\sigma=F/S$) on a surface S. The sample flow is characterized by its deformation (γ =displacement/thickness) and its derivative with respect to time the shear rate ($\dot{\gamma}$). The viscosity (η) is defined in equation (2.20)

$$\eta \text{ (Pa.s)} = \frac{\sigma \text{ (Pa)}}{\dot{\gamma} \text{ (s}^{-1}\text{)}} \quad (2.20)$$

All measurements were done under steady-state flow i.e. when the results become independent of time. Shear flow measurements were used when $C < C_p$, C_p being the

percolation concentration, and above C_p when possible i.e. when the viscosity was not too high.

I.3.2. Oscillatory shear measurement

In oscillatory shear measurement, a sinusoidal, time dependent, deformation of pulsation ω (rad.s^{-1}) is applied to the sample. This results in a stress ($\sigma(t)$) described by equation (2.21).

$$\sigma(t) = \sigma_0 \sin(\omega t + \delta) = \sigma_0 \sin(\omega t)\cos(\delta) + \sigma_0 \cos(\omega t)\sin(\delta) \quad (2.21)$$

With δ the characteristic phase shift ($\delta=0$ for an ideal solid and $\delta=\pi/2$ for a Newtonian liquid)

Both elastic (G') and viscous (G'') moduli are defined by dividing equation (2.21) by γ_0 , as shown in equation (2.22).

$$G(t) = G' \sin(\omega t) + G'' \cos(\omega t) \quad (2.22)$$

With $G' = \frac{\sigma_0}{\gamma_0} \cos(\delta)$ and $G'' = \frac{\sigma_0}{\gamma_0} \sin(\delta)$

In this work, oscillatory shear measurements were conducted in the linear regime i.e. when both G' and G'' are independent of the stress. Strain sweeps were performed prior to oscillatory shear measurement to determine the proper stress to apply to remain in the linear regime while obtaining a sufficient signal to noise ratio. The viscosities of viscoelastic fluids ($C > C_p$) were computed by oscillatory shear measurements by using equation (2.23) and compared to flow measurements when possible.

$$\eta = G_{el} * \tau \quad (2.23)$$

with G_{el} (Pa) the elastic modulus and τ (s) the relaxation time.

I.3.3. Rheometers used

All rheometers used for this work were stress-imposed apparatuses with cone-plate geometry. The geometry sizes range from 20 to 60 mm. The temperature was controlled by a Peltier system and a water bath. To prevent water evaporation during measurement paraffin oil was added. The main characteristics of the geometry used are given in Table 2-1.

Table 2-1. Main characteristics of the geometries used in rheology experiments.

Name of the apparatus	Diameter (mm)	Angle (°)	Truncation (µm)	Serial Number
ARG2	20	4	118	994327
	40	2	54	988015
	60	1	27	989003
MCR301	25	2	103	29256
	50	1	50	15815
DHR3	20	3	96	987285
	40	2	59	998173
	60	1	27	996962
AR2000	40	2	55	991073

I.4. Size exclusion chromatography

I.4.1. Polymers made of *t*BA and *n*BA

Size exclusion chromatography analysis was done with an equipment consisting of a guard column (5 µm, 50 mm × 7.5 mm) connected to a PLgel Mixed-D column (5 µm, 300 mm × 7.5 mm) and a PLgel “individual pore size” column (5 µm, 50 mm × 7.5 mm) operating at room temperature in THF with a flow rate of 1 mL.min⁻¹. After filtration through a 0.2 µm pore size membrane, injection was done at a polymer concentration of ~5 mg.mL⁻¹ in THF. In all cases except DH50 which had been synthesized and analyzed previously, absolute average molar masses were calculated using a light scattering (miniDAWN TREOS from Wyatt) and an Online refractive index (RID10A from Shimadzu) detectors with a specific refractive index increment of the polymer in THF of 0.057 mL/g.³ For the precursor of DH50, molecular weights were determined as PS-equivalents using PS-standards for calibration of the SEC.

I.4.2. Polymers made of DMAEMA and *n*BMA

Size exclusion chromatography was performed using a EcoSEC semi-micro CPG Tosoh system equipped with a 3 PSS GRAM (10 µm, 300 x 7,5mm) column with DMF with 0.01M

of LiBr as eluent (flow rate = 0.8 mL/min), at 60°C, and using refractometry for detection (Shodex RI 71 refractometer, Showa Denko). The number-average molecular weight (M_n) and dispersity (M_w/M_n) were determined using poly(methyl methacrylate) standards for calibration ranging from 580 to 3×10^6 g/mol. It should be noted that this conventional calibration of SEC yields apparent values of M_n , M_w , and dispersity (M_w/M_n). The molecular weights of the final polymers were calculated from the conversion assuming that termination and transfer reactions were negligible.

I.5. Gas Chromatography

Gas chromatography experiments were performed to follow the kinetics of polymerization on a Shimadzu GC-2014 apparatus equipped with an Equity-1 column (length: 30 m, internal diameter: 0.25 mm, thickness of the poly(dimethylsiloxane) stationary phase: 0.25 μ m, T_{max} : 320 °C, T_{min} : -60 °C), an AOC-20i injector using a 10 μ L syringe and an FID (Flame Ionization Detector). Nitrogen was used as mobile phase.

The injector temperature was 250 °C and the temperature program to measure the samples consisted of a plateau for 1 min at 60 °C followed by a temperature increment at 60 °C/min up to 150 °C and finally another temperature plateau at 150 °C for 2.5 min. This method was used to determine the evolution as a function of time of the *n*BA and *t*BA contents with respect to anisole used as internal standard. The data were treated using the GCSolution software.

I.6. NMR

^1H and ^{13}C NMR spectra were recorded on a Bruker DPX 200MHz and a Bruker Advance 400MHz. Chemical shifts (δ) used TMS (tetramethylsilane) as internal reference ($\delta=0$ ppm). Samples were dissolved in CDCl_3 , THF- D_8 or MeOD. Data were treated with the MestRec software.

II. Polymer based on acrylic acid (AA) and *n*-butyl acrylate (*n*BA)

II.1. Synthesis of linear copolymers

Several copolymers of *n*-butyl acrylate and acrylic acid were synthesized during this PhD. However, some of the copolymers used for this study were synthesised by others (the

monoblocks MH50, the diblock DH50, and the triblocks TH40 and TH60) as described in previous publications^{2,3}. The main characteristics of the polymers are given in Table 2-3.

a) Synthesis of the MHx precursors: $P(nBA_{1-x}\text{-stat-}tBA_x)_{100}\text{-Br}$

The global strategy for the synthesis of the MHx precursors is depicted in Figure 2.5.

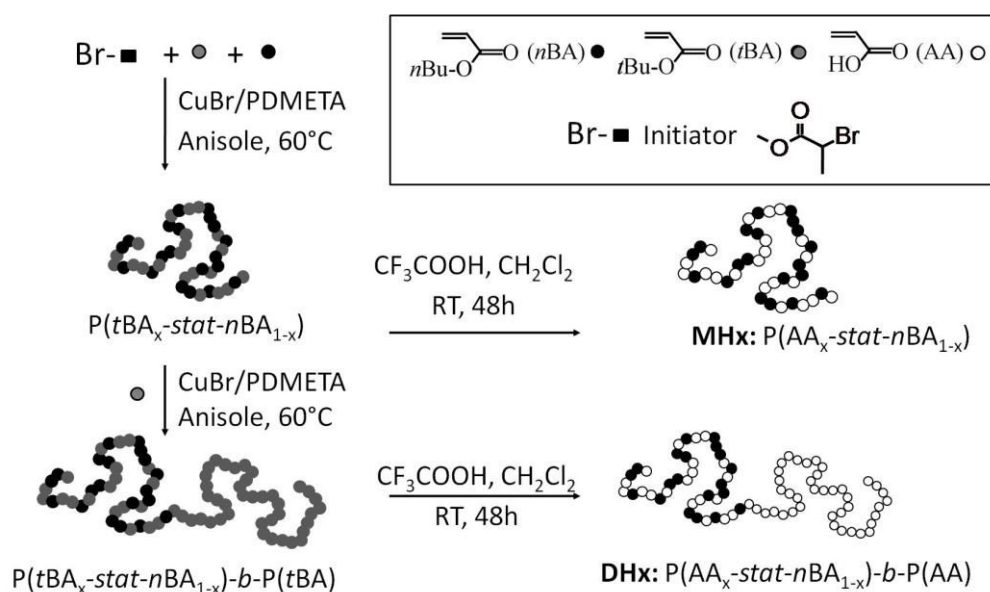


Figure 2.5. Global synthesis strategy of random associating blocks MHx and diblocks DHx, adapted from ref.⁴.

For the synthesis of $P(nBA_{0.6}\text{-stat-}tBA_{0.4})_{100}\text{-Br}$, *tert*-butyl acrylate (60 g, 4.69×10^{-1} mol), *n*-butyl acrylate (90 g, 7.03×10^{-1} mol), Cu(II)Br_2 (0.049 g, 2.23×10^{-4} mol), and methyl 2-bromopropionate (1.02 g, 6.10×10^{-3} mol) were introduced in a 500 mL round-bottom flask. The flask was closed with a screw cap equipped with a septum and degassed by argon bubbling for 1 hour. The composition after argon bubbling was verified and always equal to the initial composition. The flask was then slightly opened to introduce CuBr (0.64 g, 4.43×10^{-3} mol) under a back-flow of argon and the solution was then degassed again by argon bubbling. PMDETA (0.798 g, 4.60×10^{-3} mol), and anisole (17 g) were introduced in a 50 mL vial. The flask was closed with a screw cap equipped with a septum and degassed by argon bubbling for 10 min. The degassed PMDETA solution was then transferred in the flask under argon using a double-tipped needle. A few drops of the solution were taken as sample t_0 , and the flask was dipped in an oil bath at 60 °C. The molar ratios were as follows $[tBA+nBA]:[MBP]:[\text{CuBr}]:[\text{PMDETA}] = 192 : 1 : 0.73 : 0.75$.

As reported elsewhere, samples were withdrawn throughout the reaction to follow the kinetics^{5,6}. The reaction was stopped at 52 % conversion by cooling the flask to 0 °C and injecting air. The polymer was purified by column chromatography (SiO₂/CHCl₃) followed by two precipitations at room temperature in methanol/water (90/10 vol/vol), yielding a sticky yellowish powder. Size exclusion chromatography (SEC) in THF was performed on the final polymer and on samples taken during the reaction to determine the number (M_n) and weight (M_w) average molar masses and the dispersity. The copper was removed prior to SEC analysis using a small column (SiO₂/CHCl₃), but no precipitation was done in order to avoid fractionation of the polymer. ¹H NMR in CDCl₃ demonstrated that the *t*BA/*n*BA ratio in the final polymer was the same as in the initial monomer feed, see Table 2-3. After purification, the yield was 96% and 58.6 g of polymer were obtained.

The precursor of MH60 was synthesized according to the same procedure but using a 60/40 *t*BA/*n*BA monomer ratio, see Table 2-2. The polymer characteristics are summarized in Table 2-3.

b) Synthesis of the DHx precursor: P(*n*BA_{1-x}-stat-*t*BA_x)₁₀₀-*b*-P(*t*BA)₁₀₀

The synthesis of the P(*n*BA_{0.6}-stat-*t*BA_{0.4})₁₀₀-*b*-P(*t*BA)₁₀₀ diblock copolymer was done similarly to that of the P(*n*BA_{0.6}-stat-*t*BA_{0.4})₁₀₀-Br macroinitiator described above, but with the following conditions: *tert*-butyl acrylate (45 g, 3.51 x10⁻¹ mol), Cu(II)Br₂ (0.019 g, 8.60 x10⁻⁵ mol), P(*n*BA_{0.6}-stat-*t*BA_{0.4})₁₀₀ (21.5 g, 1.76 x10⁻³ mol), CuBr (0.26g, 1.79 x10⁻³ mol), PMDETA (0.33 g, 1.90 x10⁻³ mol), and anisole (5 g). Here, P(*n*BA_{0.6}-stat-*t*BA_{0.4})₁₀₀-Br was the MH40 precursor whose synthesis was described in the previous section, see Figure 2.5. The molar ratios were as follows [*t*BA]: [P(*n*BA_{0.6}-stat-*t*BA_{0.4})₁₀₀]:[CuBr]:[PMDETA] = 200: 1 : 1.02 : 1.08.

The reaction was stopped at 51% conversion and the polymer was purified as described in the previous section. ¹H NMR in CDCl₃ demonstrated that the *t*BA/*n*BA ratio in the final polymer was the same as in the initial monomer feed, see Table 2-3. After purification, the yield was at 90% and 39.6 g of polymer were obtained.

The precursor of DH60 was synthesized according to the same procedure but starting from the MH60 precursor as macroinitiator, see Table 2-2. The polymer characteristics are available in Table 2-3.

c) Acidolysis

The final polymers were obtained by respectively dissolving $P(nBA_{1-x}\text{-stat-}tBA_x)_{100}$ or $P(nBA_{1-x}\text{-stat-}tBA_x)_{100}\text{-}b\text{-}P(tBA)_{100}$ in dichloromethane at $C \sim 150$ g/L and stirring the solution at room temperature for more than 24 h with 5 equivalents of trifluoroacetic acid (CF_3COOH) relative to the amount of tBA units, as previously reported.^{5, 6} The polymer was finally recovered by precipitation of the crude reaction mixture twice in pentane with yields higher than 95% each time.

^{13}C NMR revealed the absence of significant quantities of residual CF_3COOH and complete acidolysis after drying as already published. 1H NMR in THF- D_8 demonstrated that the AA/ nBA ratio after acidolysis was the same as the tBA/nBA ratio of the corresponding precursors, see Table 2-3. The polymer characteristics are available in Table 2-3.

Table 2-2. Conditions of the synthesis of the associating blocks MH40, MH60, of the diblocks DH40, DH60 and of the triblock TH50.

Type	Name	[Monomers]:[Initiator]:[CuBr]:[Ligand]
Monoblock	MH40	192 : 1 : 0.73 : 0.75
	MH60	197 : 1 : 0.69 : 0.74
Diblock	DH40	200 : 1 : 1.02 : 1.08
	DH60	200 : 1 : 0.75 : 0.81
Triblock	TH50	400:1:2:2.10

Table 2-3. Characteristics of the copolymers synthesized. ^aTheoretical M_n calculated from the conversion. ^bTheoretical M_n calculated assuming 100% acidolysis. ^c Copolymers synthesized in former studies ^{2, 3}.

Name	Before acidolysis					After acidolysis		
	$M_{n, GC}$ (g/mol) ^a	$M_{n, SEC}$ (g/mol)	\bar{D}	% tBA, th	% tBA, NMR	M_n (g/mol) ^b	% AA, th	% AA, NMR
MH40	1.2×10^4	1.2×10^4	1.2	40	41	1.1×10^4	40	39

MH50 ^c	1.3 x10 ⁴	1.2 x10 ⁴	1.1	50	51	1.0 x10 ⁴	50	51
MH60	1.3 x10 ⁴	1.4 x10 ⁴	1.3	60	61	9.2 x10 ⁴	60	60
DH40	2.5 x10 ⁴	2.5 x10 ⁴	1.2	70	72	1.7 x10 ⁴	70	70
DH50 ^c	2.5 x10 ⁴	2.6 x10 ⁴	1.1	76	78	1.7 x10 ⁴	76	78
DH60	2.5 x10 ⁴	2.7 x10 ⁴	1.1	80	82	1.6 x10 ⁴	80	81
TH40 ^c	5.3 x10 ⁴	5.4 x10 ⁴	1.0	70	71	3.5 x10 ⁴	70	71
TH50	5.2 x10 ⁴	4.9 x10 ⁴	1.1	75	n/a	3.4 x10 ⁴	75	76
TH60 ^c	5.3 x10 ⁴	5.0 x10 ⁴	1.0	81	78	3.3 x10 ⁴	81	78

II.2. Synthesis of graft copolymers

a) Global strategy

The synthetic strategy of graft copolymers was partly adapted from references^{7, 8} and from our previous ATRP work⁶ and is illustrated in Figure 2.6.

First, a functional monomer, called BIEA was prepared by esterification of 2-hydroxyethyl acrylate with α -bromoisobutyryl bromide. After purification, BIEA was copolymerized with *tert*-butyl acrylate by free radical polymerization. These steps allowed the formation of a *PtBA* backbone bearing ATRP initiating sites, *P(tBA-stat-BIEA)*. *Tert*-butyl acrylate and *n*-butyl acrylate were subsequently copolymerized in a statistical manner from these initiating sites by ATRP according to a grafting from strategy.⁹ Finally, the graft copolymer formed, *P(tBA)-g-P(nBA-stat-tBA)*, was acidolysed with CF₃COOH to obtain the final polymer *P(AA)-g-P(nBA-stat-AA)*.

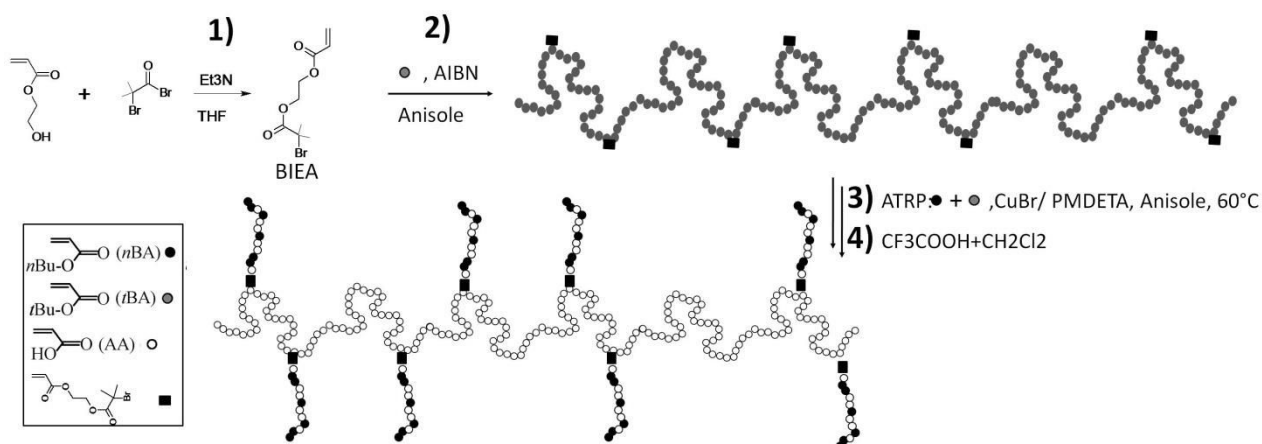


Figure 2.6. Global synthesis strategy of the graft copolymers.

b) Functional monomer

For the synthesis of the functional monomer, 2-(2-bromoisobutyryloxy)ethyl acrylate (BIEA), 2-hydroxyethyl acrylate (5.52 g, 4.75×10^{-2} mol), triethylamine (5.29 g, 5.23×10^{-2} mol), 4-methoxyphenol (5.9 mg, 4.75×10^{-4} mol), and dry THF (52 g) were mixed in a double-neck flask at 0 °C. A dropping funnel containing α -bromoisobutyryl bromide (19.8 g, 8.61×10^{-2} mol) and dry THF (20 g) was adjusted on the double-neck flask. A septum was placed on the other neck. The dropping funnel was gently opened to add dropwise, at 0 °C under stirring, the α -bromoisobutyryl bromide solution to the 2-hydroxyethyl acrylate solution. The mixture was let reacting for 22 hours at room temperature.

The solution was filtered on a Büchner to remove the insoluble triethylammonium bromide salt and THF was evaporated under reduced pressure ($T=40^{\circ}\text{C}$). An orange liquid was recovered.

To remove impurities, the liquid was diluted in CHCl_3 (40 mL) and extracted five times with a saturated solution of NaHCO_3 (87g/L) to hydrolyze and neutralize the excess of α -bromoisobutyryl bromide, then twice with salted water (25 mL at 200 g/L) and once with water (10 mL). Finally, the organic phase was dried with MgSO_4 and CHCl_3 was removed by rotary evaporation (40°C). Despite our efforts impurities remained in the product, as illustrated by the double peaks at $\delta=1.9$ ppm in ^1H NMR, see Figure 2.7. We do believe that it comes from side reactions between HEA and BIBB since hydrolysed BIBB should be totally removed after these purifications. The final product 11.2 g (yield of 95%) was analysed by gas chromatography confirming the existence of a minority side product corresponding to 12% (in area) of the Flame Ionization Detector signal.

Since the next step involves copolymerisation and precipitation, it is believed that this side product should not affect the reaction and will be removed with the polymer precipitation.

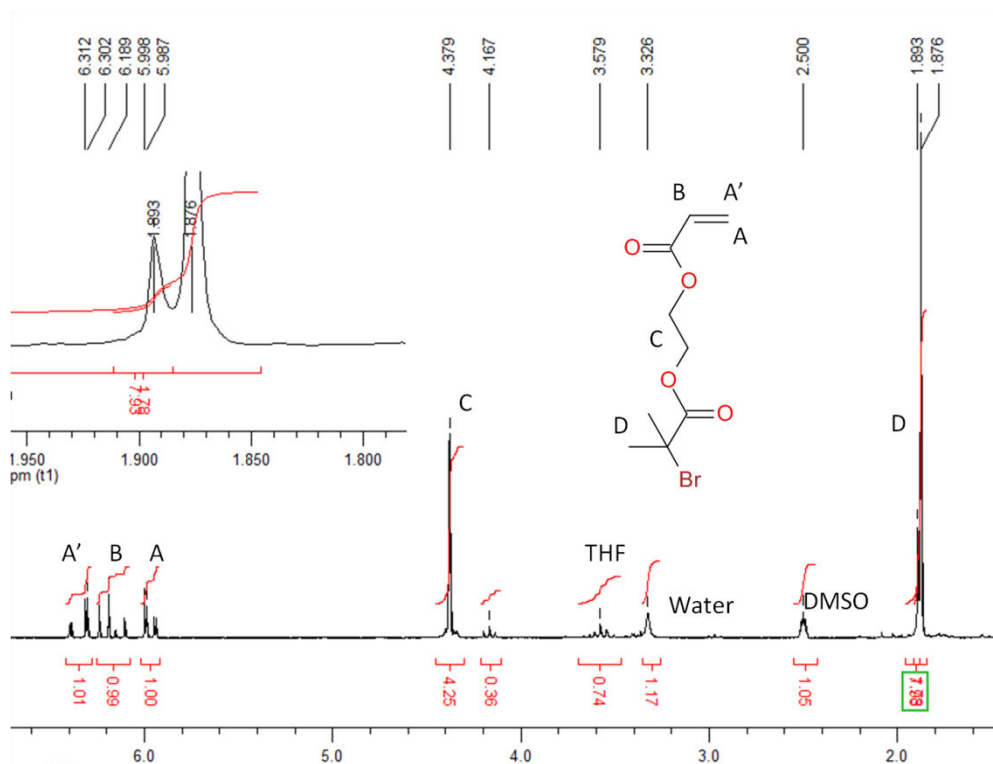


Figure 2.7. 200MHz ^1H NMR of the 2-(2-bromoisobutryl)ethyl acrylate after purification in DMSO. δ (ppm) = 1.9 (s, 2H BIEA+impurity, H-d) ; δ (ppm) = 4.4 (m, 4H BIEA+impurity, H-c) ; δ (ppm) = 6.0 (dd, 1H BIEA, H-a) ; δ (ppm) = 6.2 (dd, 1H BIEA, H-b) ; δ (ppm) = 6.4 (dd, 1H BIEA, H-a).

c) Backbone synthesis

Here, the synthesis of the backbone of G7H50 is detailed. The others backbones were prepared by adjusting the functional monomer to *t*BA ratio.

For the backbone synthesis, *tert*-butyl acrylate (39 g, 3.05×10^{-1} mol), BIEA (1.04 g, 3.9×10^{-3} mol), anisole (4.56 g, 4.2×10^{-2} mol), toluene (119 g) and azobisisobutyronitrile (9.2×10^{-2} g, 5.6×10^{-4} mol) were introduced in a 250 mL round-bottom flask. The flask was closed with a screw cap equipped with a septum, degassed by argon bubbling for 30 min and dipped in an oil bath at 60 °C. The mixture was let reacting for 24 hours. The reaction was stopped by cooling the flask to 0 °C. The polymer was precipitated twice in methanol/water (90/10 vol/vol), yielding a white powder. ^1H NMR in CDCl_3 was performed on the final polymer to confirm its composition, see Figure 2.8. Size exclusion chromatography (SEC) in THF yielded the number (M_n) and weight (M_w) average molar masses and the dispersity, see Figure 2.11a. For the three backbones, M_n was around 6.0×10^4 g/mol with $\text{Đ} \sim 2.7$.

CHAPTER 2: MATERIALS AND METHODS

The ^1H NMR gave a molar BIEA/*t*BA ratio of 1.48% assuming no impurity in agreement with the theoretical value of 1.44%, see Table 2-5.

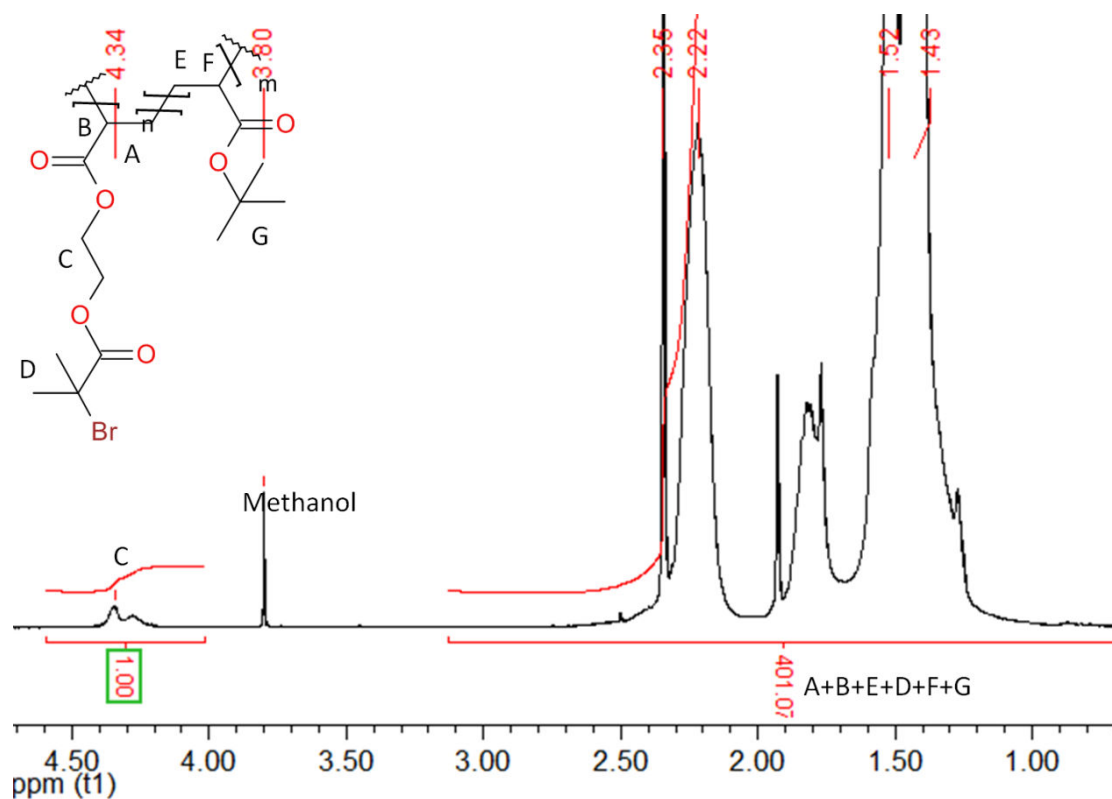


Figure 2.8. 200MHz ^1H NMR of the polymer backbone of G7H50 in CDCl_3 after purification. δ (ppm) = 1.4-2.5 (m, 21H, H-a-b-d-e-f-g) ; δ (ppm) = 3.7 (s, 4H BIEA, H-c).

d) Grafting from step

Here, the synthesis of the graft copolymer precursor of G7H50 is detailed. The others graft copolymers precursors were prepared by adjusting the polymer to monomers ratio.

For the graft copolymer $\text{P}(t\text{BA})_{500-g}\text{-}[\text{P}(n\text{BA}_{0.5}\text{-stat-}t\text{BA}_{0.5})_{100}]_7$, *tert*-butyl acrylate (41.2 g, 3.22×10^{-1} mol), *n*-butyl acrylate (41.3 g, 3.23×10^{-1} mol), Cu(II)Br_2 (0.038 g, 1.7×10^{-4} mol) and $\text{P}(t\text{BA}\text{-stat-BIEA})$ (32.8 g, 1.44% BIEA) were introduced in a 500 mL round-bottom flask. PMDETA (0.62 g, 3.58×10^{-3} mol) and anisole (9.2 g) were introduced in a 50 mL vial. The flask and the vial were closed with screw caps equipped with a septum, and degassed by argon bubbling for 2 hours (a long degassing time was selected because of the viscosity of the polymer solution) and 10 min respectively. CuBr (0.479 g, 3.34×10^{-3} mol) was introduced in the 500 mL round-bottom flask under a counter-flux of argon and the solution was degassed again after that. The molar ratios are as follows $[t\text{BA}+n\text{BA}]:[\text{active Br in P}(t\text{BA}\text{-stat-}$

BIEA)]:[CuBr]:[PMDETA] = 200:1:1:1.05. The PMDETA solution was finally transferred in the flask under argon using a double-tipped needle. A few drops of the solution were taken as sample t_0 , and the flask was dipped in an oil bath at 60 °C. Kinetics were followed by gas chromatography using anisole as internal standard, see Figure 2.10. $\ln([M]_0/[M])$ evolved linearly with time for G7H50 and G30H50, whereas it was linear versus $t^{2/3}$ for G2H50 due to the lower concentration in propagating species needed to reduce the bulk viscosity. Conversion of both t BA and n BA were equal throughout the reaction meaning that statistical grafts were formed as previously observed.^{6, 10}

The reaction was stopped at 50% conversion. The copper was removed by three liquid-liquid extractions with EDTA solution (1% (w/w) EDTA, 2:1 NaHCO₃/EDTA and 20% (w/w) NaCl) since purification by flash column chromatography on SiO₂ was not possible due to the viscosity of the polymer solution. Thereafter, the solution was washed three times with water. The polymer was precipitated twice in methanol/water (90/10 vol/vol), yielding a white powder. Size exclusion chromatography (SEC) in THF yielded the number (M_n) and weight (M_w) average molar masses and the dispersity, see Figure 2.11b and Table 2-5. The n BA/ t BA ratio was measured by ¹H NMR in CDCl₃ and compared to the expected values, see Table 2-6 and Figure 2.9.

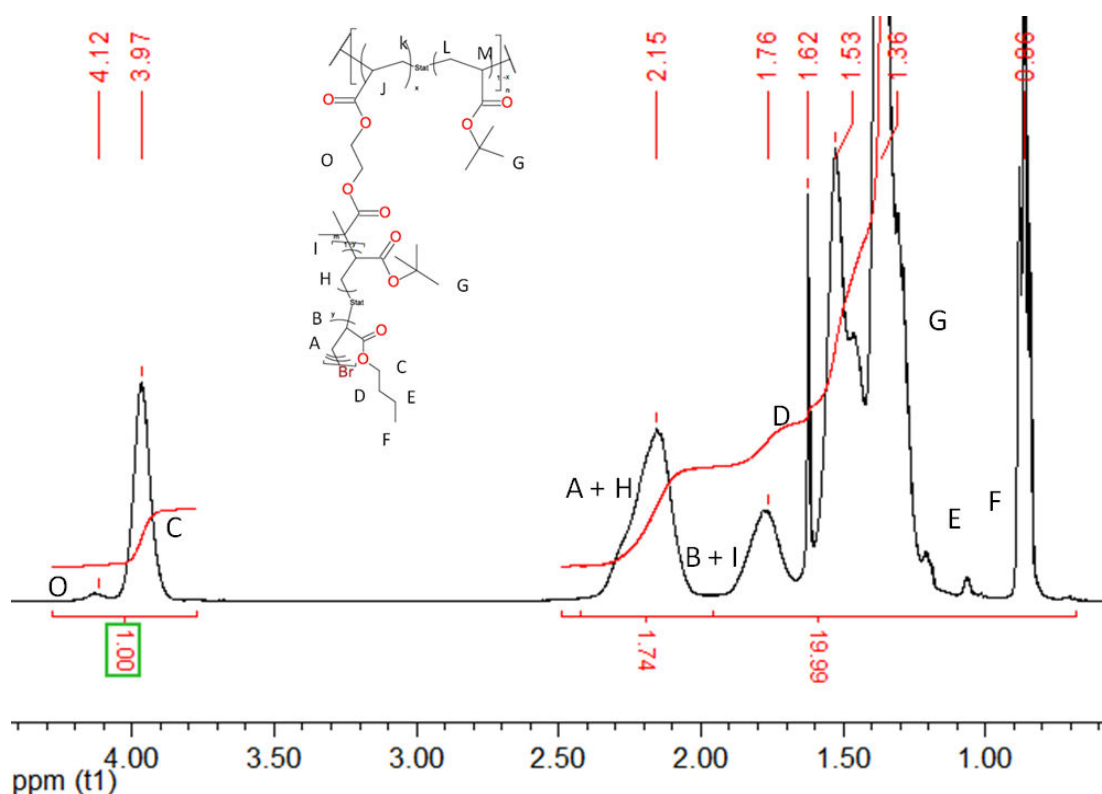


Figure 2.9. 200MHz ^1H NMR of the G7H50 graft copolymer precursor (unacidolyzed) in CDCl_3 after purification. δ (ppm) = 0.96 (t, 3H, nBA, H-f) ; δ (ppm) = 1.2-1.5 (m, 13H, nBA+tBA, H-d+e+g) ; δ (ppm) = 1.78 (s, 2H, nBA+tBA, H-b+i) ; δ (ppm) = 2.15 (s, 4H, nBA+tBA, H-a+h); δ (ppm) = 3.97 (s, 2H, nBA, H-c).

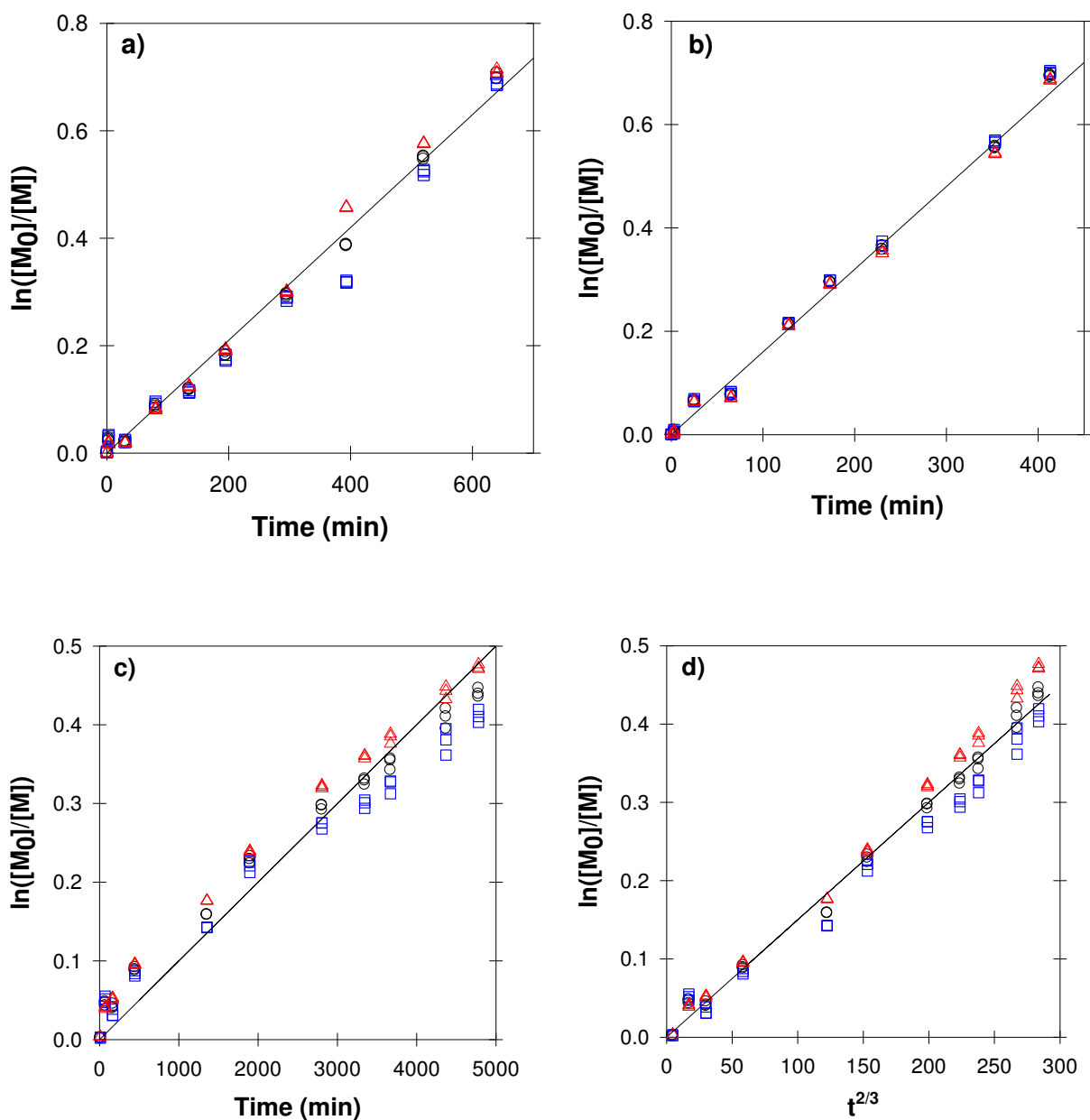


Figure 2.10. Kinetics of the polymerisation for the synthesis of the $P(n\text{BA}_{50\%}\text{-stat-tBA}_{50\%})_{100}$ grafts from the PtBA functional backbones (step 3 in Figure 2.6) with $[t\text{BA}+n\text{BA}]:[P(t\text{BA}\text{-stat-BIEA})]:[\text{CuBr}]:[\text{PMDETA}]$ ratios of 200:1:1:1.05 for G7H50 (a), 200:1:1:1.05 for G30H50 (b) and 245:1:1:1.05 for G2H50 (c+d). The monomer consumption of tBA (Δ), nBA (\square) and total (\circ) were measured by gas chromatography.

e) Acidolysis

The polymer was dissolved in dichloromethane (C~150 g/L) and stirred at room temperature for more than 24 h with 5 equivalents of trifluoroacetic acid (CF₃COOH) relative to the amount of *t*BA units, as previously reported. The polymer was finally precipitated twice in pentane. The *n*BA/AA ratios were measured by ¹H NMR and compared to the inputs, see Table 2-6. ¹³C NMR revealed the absence of significant quantities of residual CF₃COOH and complete acidolysis after drying as already reported elsewhere.⁶

Table 2-4. Synthesis conditions of the grafts for the graft copolymers.

Name	Backbone	Grafts			
	% BIEA (mol/mol)	[Monomers]:[Br functions]:[CuBr]:[Ligand]	t (hr)	DP _{GC}	Conversion %
G2H50	0.5%	245: 1 : 1 : 1.05	80	100	36
G7H50	1.4%	200: 1 : 1 : 1.05	10	92	50
G30H50	5.8%	200: 1 : 1 : 1.05	7	100	50

Table 2-5. Characteristics of the synthesized copolymers. Theoretical M_n calculated assuming 100% acidolysis of the *t*BA units into AA ones.^a

Name	Backbone		Graft copolymer		
	% BIEA (mol/mol) th.	% BIEA (mol/mol) ¹ H NMR	$M_{n,SEC}$ (g/mol)	\bar{D}	M_n (g/mol) ^a
G2H50	0.54	0.55	1.1×10^5	2.5	5.6×10^4
G7H50	1.44	1.48	1.7×10^5	2.5	8.6×10^4
G30H50	5.81	5.96	5.2×10^5	2.5	3.4×10^5

Table 2-6. tBA/nBA and AA/nBA ratios of the GxH50 copolymers synthesized.

Name	% tBA (mol/mol, th.)	% tBA (mol/mol, exp.)	% AA (mol/mol, th.)	% AA (mol/mol, exp.)
G2H50	85.0	85.2	85.0	83.4
G7H50	71.0	71.4	71.0	72.8
G30H50	58.0	57.6	58.0	56.1

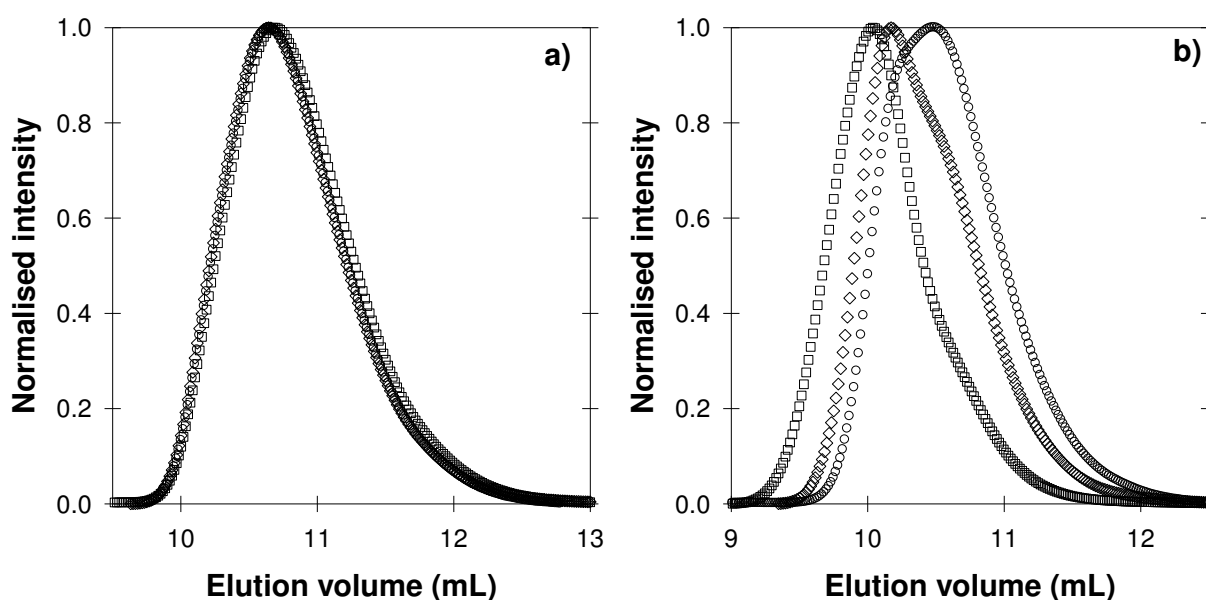


Figure 2.11. Size exclusion chromatograms for the backbones of G2H50 (\diamond), G7H50 (\circ) and G30H50 (\square) (a), and for the unacidolyzed graft copolymers G2H50 (\diamond), G7H50 (\circ) and G30H50 (\square) (b). The light scattering intensity detector was used.

II.3. Sample preparation

Aqueous samples of MHx, DHx, THx and GHx were prepared by dissolving the copolymers in demineralized water (Millipore) containing the required amount of NaOH to reach an ionization degree $\alpha_0 \sim 0.9$. Dissolution was done under vigorous stirring for at least 24 hours at room temperature. For the graft copolymer with a high grafting density the temperature was

increased to 60 °C and two or three days were needed to obtain transparent and homogeneous solutions at high polymer concentrations. All the systems formed homogeneous and transparent solutions unless specified otherwise.

To obtain the desired ionization degree (α), the required amount of D-glucono- δ -lactone (GDL) was added to the solutions at $\alpha_0 \sim 0.9$ prior to analysis. As explained in detail in the supporting information of reference,¹¹ the hydrolysis of GDL takes around $\sim 10^5$ s at 20 °C and produces gluconic acid which has a pKa of 3.4. The final ionization degree can be calculated with equation (2.24) if the polymers and the gluconic acid are considered as strong acids.

$$\alpha = \frac{[AA^-]}{[AA]_{total}} = \alpha_0 - \frac{[GDL]}{[AA]_{total}} \quad (2.24)$$

$$\text{with } [AA]_{total} = \frac{x_{AA}}{x_{AA}M_{AA} + x_{nBA}M_{nBA}} C_{polymer} = \frac{DP(AA)}{M_n} C_{polymer}$$

with α_0 the initial ionization degree, x_{AA} and x_{nBA} the molar fractions of each monomers, $C_{polymer}$ the polymer concentration and $DP(AA)$ the number of acrylic acid units per chain.

At low ionization degrees, the pKa of the AA units of the polymer becomes too close to that of gluconic acid so that the acid-base reaction is no longer complete. Furthermore, the pKa of the polymers varies with α . Therefore, a different calculation is needed to compute α accurately, especially when it is small. This is illustrated in Figure 2.12 where it is shown that the true ionization degree is higher than that assuming complete reaction with GDL at low α . The true α was calculated by solving equation (2.25).

$$\alpha_{true} = \alpha_0 - \frac{n(GDL)_0}{n(AAH)_0} \cdot \frac{A(y+1) + \sqrt{(A(y+1))^2 - 4(y(A-1))}}{2(yA-1)} \quad (2.25)$$

$$\text{with } A = \frac{K_{a,GDL}}{K_{a,polymer}(\alpha)} \text{ and } y = \frac{n(GDL)_0}{n(polymer)_0}$$

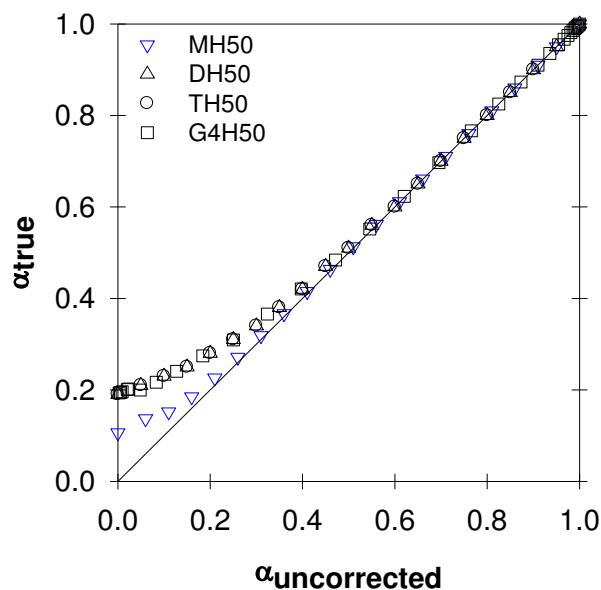


Figure 2.12. Determination of the true ionization degree upon addition of GDL calculated using eq. 1.25 as a function of $\alpha_{uncorrected}$ using eq. 1.24. $T=20^{\circ}\text{C}$ $[\text{Na}^+]=0.5\text{ mol/L}$. See SI of ref¹².

This sample preparation method allows the formation of homogenous samples even for the lowest ionization degrees where the systems exhibit very long relaxation times and where the triblock copolymers lead to non flowing hydrogels.¹

The drawback of this technique is that it introduces a certain amount of sodium and gluconate ions, affecting the ionic strength. In light scattering experiments, the sodium concentration was kept constant (0.1 or 0.5 mol/L) by addition of NaCl using equation (2.26). Addition of NaCl was done after complete dissolution of the polymer.

$$[\text{Na}^+]_{total} = \frac{x_{AA}}{x_{AA}M_{AA} + x_{nBA}M_{nBA}} C_{polymer} + [\text{NaCl}]_{add} \quad (2.26)$$

For light scattering analysis, the samples were filtered through 0.2 μm pore size Acrodisc filters. For rheology measurements, the samples were degassed under vacuum, when needed, to remove the bubbles.

II.4. Potentiometric titration

The procedure used to titrate the polymer was described in ref.¹³.

II.4.1. Potentiometric titration

Titration experiments were performed on an automatic titrator TIM 856 equipped with TitraMaster 85 software. The electrode probe was a Radiometer Analytical pHC2401-8, the pH ranging from 2 to 11. Measurements were done at room temperature at an addition rate of titrant of 0.1 mL/min. The titrant used was either NaOH or HCl at 1 mol/L.

II.4.2. Determination of the AA contents in the polymers

In order to calculate the amount of AA (n_{AAH}) within a polymer chain, potentiometric titrations were systematically performed.

First, the polymer was dissolved in demineralized water (Millipore) containing the required amount of NaOH to reach $\alpha=1$. Then, a solution of sodium hydroxide was added to reach ~10 % of NaOH in excess. The total amount of sodium hydroxide was not added before the dissolution of the polymer to avoid hydrolysis of *n*-butyl acrylate functions. The salt concentration was adjusted by adding the required amount of a 4 M NaCl solution. The polymer weight concentration was adjusted to have a theoretical AA concentration of 0.043 mol/L. Thereafter, the solution was back-titrated using HCl at 1 mol/L to decrease the ionization degree while measuring the pH.

Let us consider the example in Figure 2.13 which corresponds to the titration of a P(AA) in the presence of 0.5 mol/L of NaCl. Two pH jumps appeared, the first around pH=9 and the second between pH 4-2. Three reactions are involved in the titration. First, the strong acid HCl and the strong base NaOH react quantitatively until the first pH jump at $pH_{V_{eq1}} \sim 9$ for a HCl volume V_{eq1} . Then, HCl reacts with the acrylate ions AA^- to form acrylic acid AAH until the second pH jump. The third reaction is the dissociation of HCl in water.

In a previous publication¹³, details of the data treatment of the titration curves were given. Here, only equation (2.27) giving n_{AAH} , the amount of protonated AAH units formed (= the amount of AA^- units titrated), as a function of V_{HCl} is presented. It was used to plot the inset in Figure 2.13.

$$n_{AAH} = (V_{HCl,add} - V_{eq1}) \cdot [HCl]_{stock} - \left[(V_{initial} + V_{eq1}) \cdot 10^{-14+pH_{V_{eq1}}} - (V_{initial} + V_{HCl,add}) \cdot 10^{-14+pH} \right] - \left[(V_{initial} + V_{HCl,add}) \cdot 10^{-pH} - (V_{initial} + V_{eq1}) \cdot 10^{-pH_{V_{eq1}}} \right] \quad (2.27)$$

CHAPTER 2: MATERIALS AND METHODS

Three stages are observed in the evolution of n_{AAH} . First, $n_{AAH} \sim 0$ corresponds to the domain where the excess NaOH is titrated. In this region, equation (2.27) is not perfectly reliable which explains why $n_{AAH} < 0$ rather than $n_{AAH} = 0$. The second stage is a linear increase of n_{AAH} until a maximum. This represents the reaction between HCl and AA^- and the production of AAH. In the last stage, the total amount of AAH in solution hardly varies because only the dissociation of HCl occurs and all AA units are already protonated.

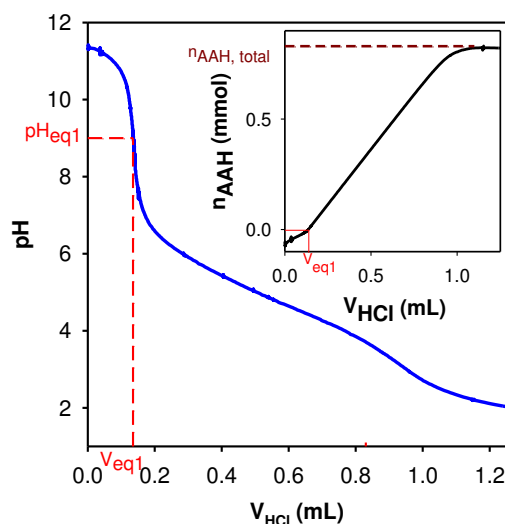


Figure 2.13. pH evolution as a function of the HCl (1M) volume added during the titration of a PAA solution at $[AA]=0.043$ mol/L, $[Na^+]=0.5$ mol/L with an addition rate of HCl of 0.1 mL/min. The inset represents the evolution of the amount of protonated AAH units.

II.4.3. Calculation of the ionization degree (α) and pKa

As previously reported¹³, the ionization degree and the pKa can be determined for each pH by treating the titration curve with equations (2.28) and (2.29). From the example illustrated in the previous section the Figure 2.14 was obtained.

$$\alpha = \frac{[AA^-]}{[AA]_{tot}} = 1 - \frac{n_{AAH}}{n_{AA-tot}} \quad (2.28) \quad pK_a = pH - \log\left(\frac{\alpha}{1-\alpha}\right) \quad (2.29)$$

Here we wish to highlight that in the case of polyelectrolytes the acidity constant K_a depends on the ionization degree and therefore on the pH. The more ionized the polymer already is, the more difficult it becomes to create more charges on its backbone, because of electrostatic repulsions of the neighbouring AA^- units. As a consequence the pKa increases with α .¹⁴

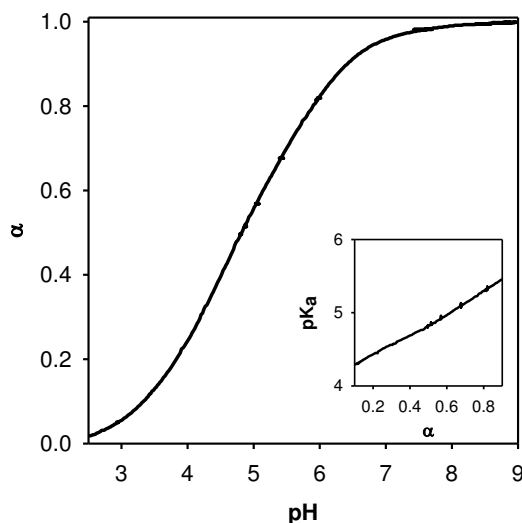


Figure 2.14. Evolution of the ionization degree as a function of the pH during the titration of a PAA solution at $[AA]=0.043$ mol/L, $[Na^+]=0.5$ mol/L with addition rate of 0.1 mL/min. The inset represents the evolution of the pK_a as a function of α .

II.5. Refractometry

All measurements of the refractive index increments (dn/dc) conducted during this work are reported in Figure 2.15. The specific refractive index increment was found to depend linearly on the overall fraction of charged AA units: $dn/dc = 0.126 + 0.10 \cdot f_{AA^-}$ at 0.1 M NaCl and $dn/dc = 0.121 + 0.051 \cdot f_{AA^-}$ at 0.5 M NaCl (see Figure 2.15) with $f_{AA^-} = [AA^-]/([AA^-] + [AAH] + [nBA])$. In first approximation, the increase in dn/dc with increasing charge density can be explained by the contribution of the sodium counter-ions to the refractive index. The dependence of dn/dc on α was stronger than for pure PAA reported in the literature by Kitano et al. see the dashed lines in Figure 2.15.

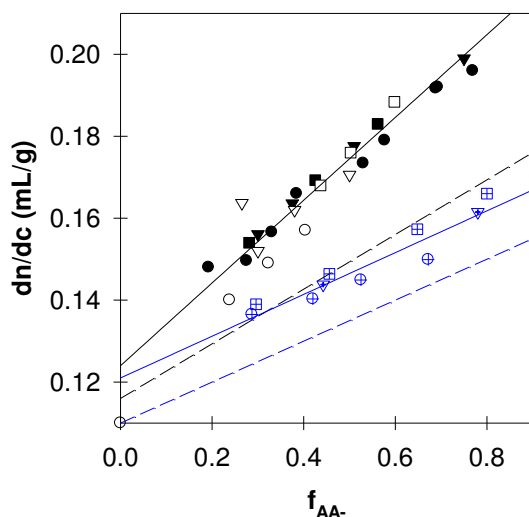


Figure 2.15. Evolution of the specific refractive index increment over the fraction of charged AA units for MH40 (\circ), MH50 (∇), MH60 (\square), DH40 (\bullet), DH50 (\blacktriangledown) and DH60 (\blacksquare) at $[Na^+] = 0.1$ mol/L and DH40 (\oplus), DH50 (∇), DH60 (\boxplus) at $[Na^+] = 0.5$ mol/L. The solid lines correspond to $dn/dc = 0.126 + 0.101 \cdot f_{AA}$ (in dark) and $dn/dc = 0.121 + 0.051 \cdot f_{AA}$ (in blue). The dashed lines correspond to the evolution reported for PAA in the literature at the same NaCl concentrations.¹⁵

III. Polymer based on DMAEMA and *n*BMA

Until now, the focus was on copolymers using acrylic acid and *n*-butyl acrylate as monomers. In this section, details will be given on polymers based on dimethylaminoethyl methacrylate (DMAEMA) and *n*-butyl methacrylate (*n*BMA).

III.1. Synthesis

The BAB triblock copolymer TH70c consisting of a central PDMAEMA₂₀₀ A block and two statistical P(*n*BMA_{0.3}-*stat*-DMAEMA_{0.7})₁₀₀ B blocks was synthesized by RAFT¹⁶ according to the detailed procedure described below adapted from results obtained by a master student of our group, Julien Santarelli (M2, 2014-2015) who synthesized TH50c: P(*n*BMA_{0.5}-*stat*-DMAEMA_{0.5})₁₀₀-*b*-P(DMAEMA)₂₀₀-*b*-P(*n*BMA_{0.5}-*stat*-DMAEMA_{0.5})₁₀₀. TH50c adapting the ratio of comonomers for the synthesis of the lateral blocks.

a) First block: P(*n*BMA_{0.3}-*stat*-DMAEMA_{0.7})₁₀₀

For the first block P(*n*BMA_{0.3}-*stat*-DMAEMA_{0.7})₁₀₀, *n*-butyl methacrylate (3.31 g, 2.33×10^{-2} mol), dimethylaminoethyl methacrylate (8.52 g, 5.42×10^{-2} mol), azobisisobutyronitrile (AIBN, 2.16×10^{-2} g, 1.31×10^{-4} mol), cumyl dithiobenzoate (CDTB, 0.10 g, 3.77×10^{-4} mol) and dioxane (14.5 g) were introduced in a 500 mL round-bottom flask. The flask was closed with a screw cap equipped with a septum, and degassed by argon bubbling for 20 min. The molar ratios were as follows [*n*BMA+DMAEMA]:[CDTB]:[AIBN]=205:1:0.35.

A few drops of the solution were taken as sample t_0 , and the flask was dipped in an oil bath at 70 °C. To follow the kinetics, samples were withdrawn throughout the reaction. The conversion was determined by ^1H NMR.¹⁷ The reaction was stopped at 49 % conversion by cooling the flask to 0 °C and injecting air. The polymer was purified by two precipitations in pentane, yielding a dark pink powder (3.93g, yield of the precipitation = 65%). Size exclusion chromatography (SEC) in DMF calibrated with poly(methyl methacrylate) standards was performed in Lyon by Olivier Boyron (UMR5265) on the final polymer to determine the number (M_n) and weight (M_w) average molar masses as well as the dispersity, see Figure 2.19. ^1H NMR demonstrated that the DMAEMA/*n*BMA ratio was the same as in the initial monomer feed and the copolymerization was statistical, see Figure 2.16. The polymer characteristics are summarized in Table 2-7.

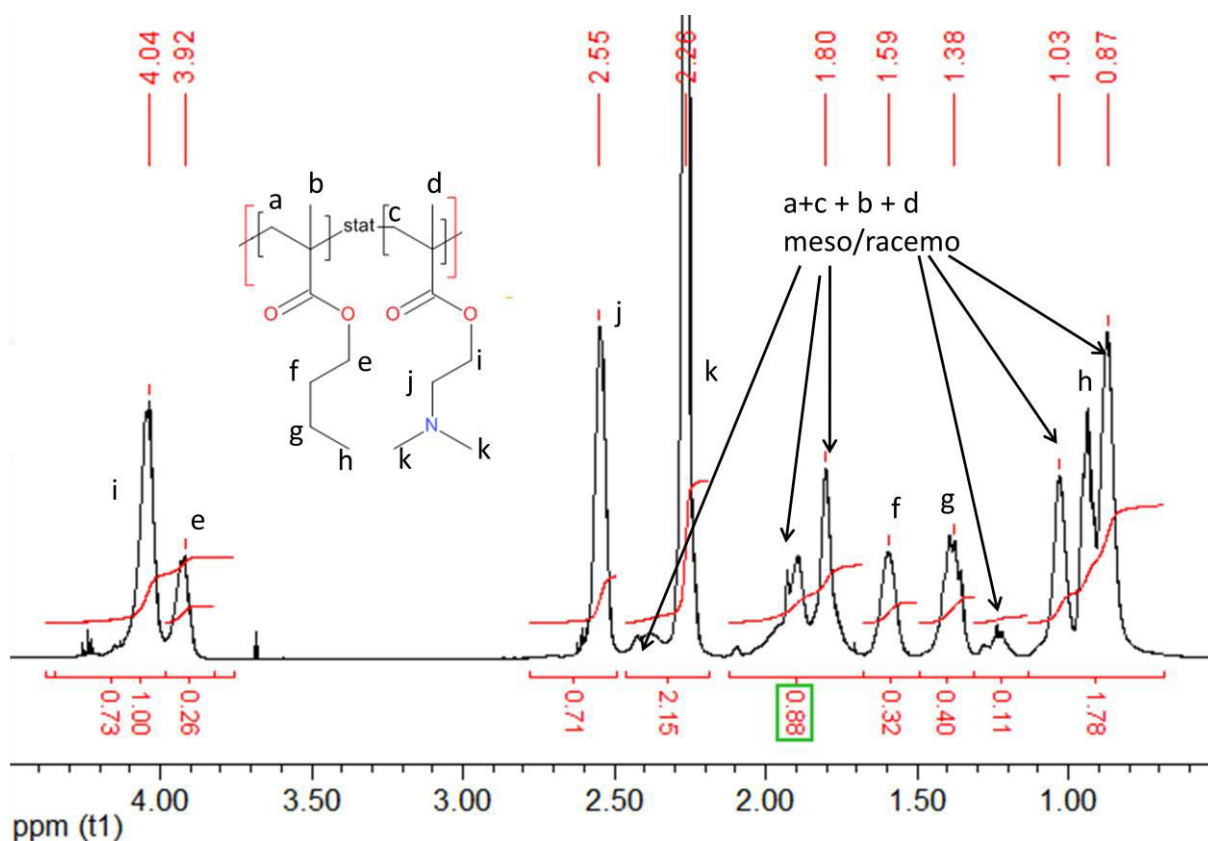


Figure 2.16. ^1H NMR of MH70c after purification in CDCl_3 . δ (ppm) = 4.04 (t, 2H, H-i) ; δ (ppm) = 3.92 (t, 2H, H-e) ; δ (ppm) = 2.55 (m, 2H, H-j) ; δ (ppm) = 2.26 (s, 6H, H-k) ; δ (ppm) = 1.59 (m, 2H, H-f) ; δ (ppm) = 1.38 (m, 2H, H-g) ; δ (ppm) = 0.93 (t, 3H, H-h) ; δ (ppm) = 2.40+1.93+1.80+1.30+1.03+0.87 (m, 6H, H-a+c+b+d).

b) Second block: $\text{P}(\text{nBMA}_{0.3}\text{-stat-DMAEMA}_{0.7})_{100}\text{-b-P}(\text{DMAEMA})_{200}$

For the diblock copolymer $\text{P}(\text{nBMA}_{0.3}\text{-stat-DMAEMA}_{0.7})_{100}\text{-b-P}(\text{DMAEMA})_{200}$ a similar procedure was used with the following amounts of reagents: dimethylaminoethyl methacrylate (15.3 g, 9.73×10^{-2} mol), azobisisobutyronitrile (1.4×10^{-2} g, 8.77×10^{-5} mol), $\text{P}(\text{nBMA}_{0.3}\text{-stat-DMAEMA}_{0.7})_{100}$ (3.72 g, 2.44×10^{-4} mol) and dioxane (9.31 g). The molar ratios were as follows $[\text{DMAEMA}] : [\text{P}(\text{nBMA}_{0.3}\text{-stat-DMAEMA}_{0.7})_{100}] : [\text{AIBN}] = 399 : 1 : 0.36$. The reaction was stopped at 49% conversion and the polymer was recovered by two precipitations in pentane which gave 8.1 g of a pink powder (yield of the precipitation = 71%). The same analyses as for the first block were achieved, see Figure 2.19, Figure 2.17 and Table 2-7.

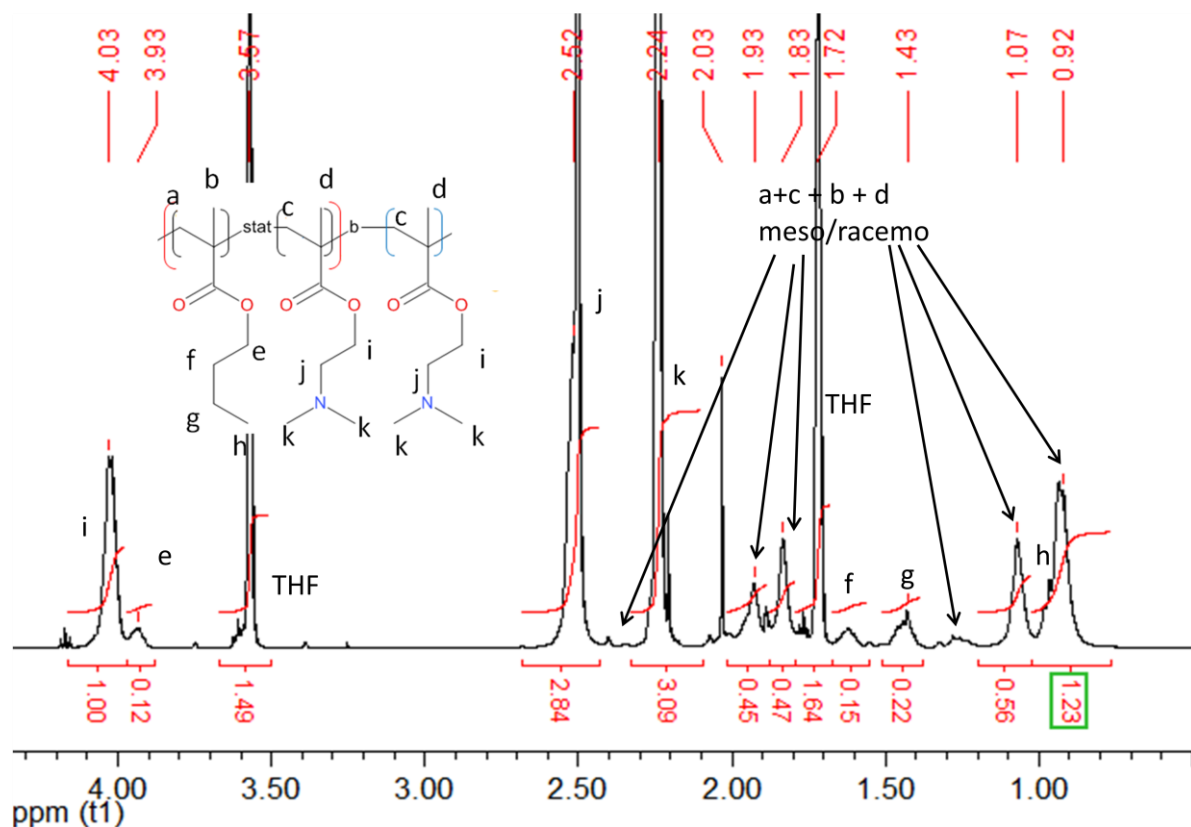


Figure 2.17. ^1H NMR of DH70c after purification in THF- D_8 . δ (ppm) = 4.03 (t, 2H, H-i); δ (ppm) = 3.93 (t, 2H, H-e); δ (ppm) = 2.52 (m, 2H, H-j); δ (ppm) = 2.24 (s, 6H, H-k); δ (ppm) = 1.62 (m, 2H, H-f); δ (ppm) = 1.43 (m, 2H, H-g); δ (ppm) = 0.93 (t, 3H, H-h); δ (ppm) = 2.40+1.93+1.80+1.30+1.03+0.87 (m, 6H, H-a+c+b+d).

c) Third block: $\text{P}(n\text{BMA}_{0.3}\text{-stat-DMAEMA}_{0.7})_{100}\text{-b-P(DMAEMA)}_{200}\text{-b-P}(n\text{BMA}_{0.3}\text{-stat-DMAEMA}_{0.7})_{100}$

For the triblock copolymer $\text{P}(n\text{BMA}_{0.3}\text{-stat-DMAEMA}_{0.7})_{100}\text{-b-P(DMAEMA)}_{200}\text{-b-P}(n\text{BMA}_{0.3}\text{-stat-DMAEMA}_{0.7})_{100}$, a similar procedure was used with the following amounts of reagents: *n*-butyl methacrylate (1.48 g, 1.04×10^{-2} mol), dimethylaminoethyl methacrylate (3.91 g, 2.49×10^{-2} mol), azobisisobutyronitrile (9.20×10^{-3} g, 5.60×10^{-5} mol), $\text{P}(n\text{BMA}_{0.3}\text{-stat-DMAEMA}_{0.7})_{100}\text{-b-P(DMAEMA)}_{200}$ (7.96 g, 1.70×10^{-4} mol) and dioxane (6.62 g). The molar ratios were as follows $[\text{nBMA}+\text{DMAEMA}]:[\text{P}(n\text{BMA}_{0.3}\text{-stat-DMAEMA}_{0.7})_{100}\text{-b-P(DMAEMA)}_{200}]:[\text{AIBN}]:207:1:0.33$.

CHAPTER 2: MATERIALS AND METHODS

The reaction was stopped at 50% conversion resulting in 9.3 g of a pink powder (yield of the precipitation = 88%) after two precipitations in pentane. The same analyses as for the first and second blocks were achieved see Figure 2.19, Figure 2.18 and Table 2-7.

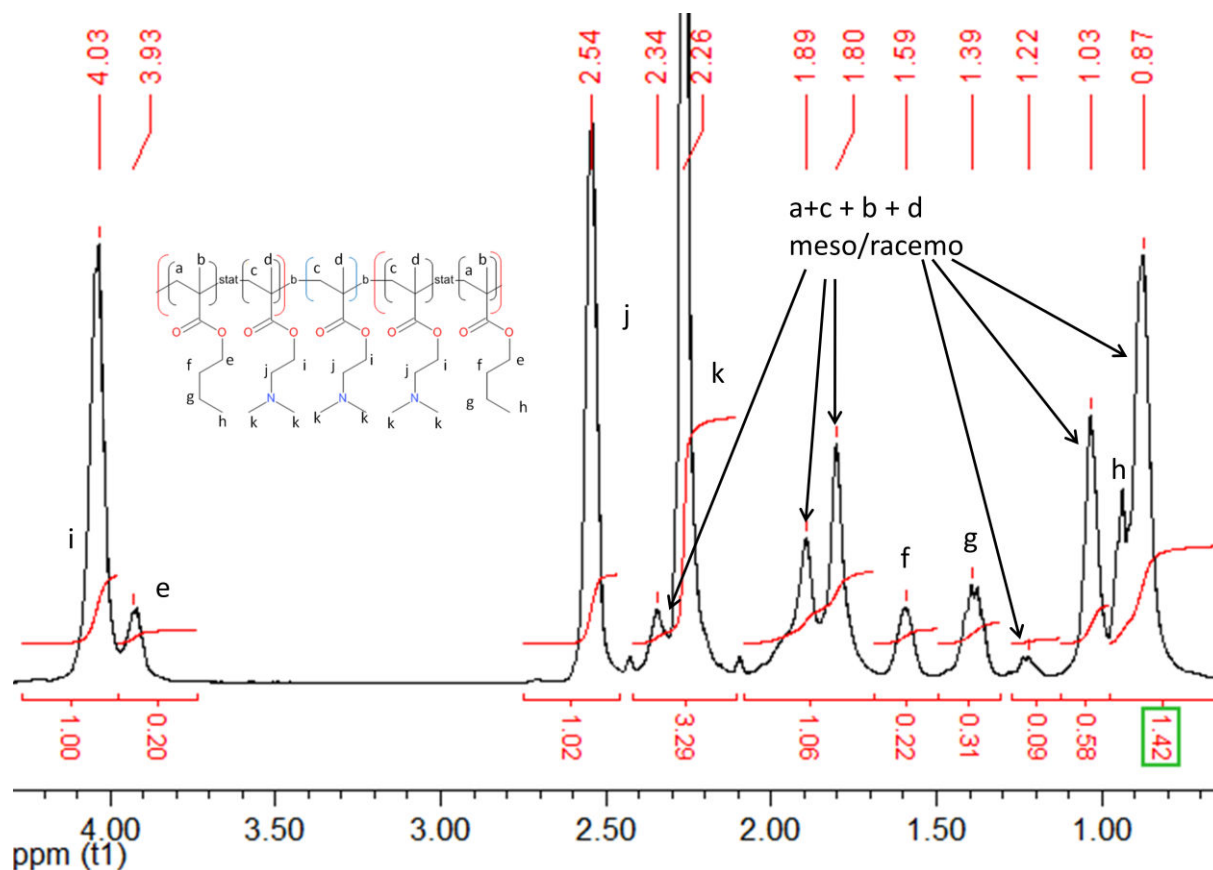


Figure 2.18. ^1H NMR of TH70c after purification in CDCl_3 . δ (ppm) = 4.03 (t, 2H, H-i) ; δ (ppm) = 3.93 (t, 2H, H-e) ; δ (ppm) = 2.54 (m, 2H, H-j) ; δ (ppm) = 2.26 (s, 6H, H-k) ; δ (ppm) = 1.59 (m, 2H, H-f) ; δ (ppm) = 1.39 (m, 2H, H-g) ; δ (ppm) = 0.90 (t, 3H, H-h) ; δ (ppm) = 2.40+1.93+1.80+1.30+1.03+0.87 (m, 6H, H-a+c+b+d).

Table 2-7. Characteristics of the synthesized copolymers. ^a Copolymers made by J. Santarelli (M2, 2014-2015).

Name	% DMAEMA th.	% DMAEMA NMR	$M_{n, th}$ (g/mol)	$M_{n, SEC}$ (g/mol)	\bar{D}
MH50c ^a	50	50	1.5×10^4	1.7×10^4	1.2
MH70c	70	70	1.5×10^4	9.5×10^3	1.2
DH50c	83	84	4.7×10^4	3.4×10^4	1.2
DH70c	89	90	4.7×10^4	2.3×10^4	1.2
TH50c ^a	76	76	6.1×10^4	4.3×10^4	1.4
TH70c	85	85	6.2×10^4	3.7×10^4	1.3

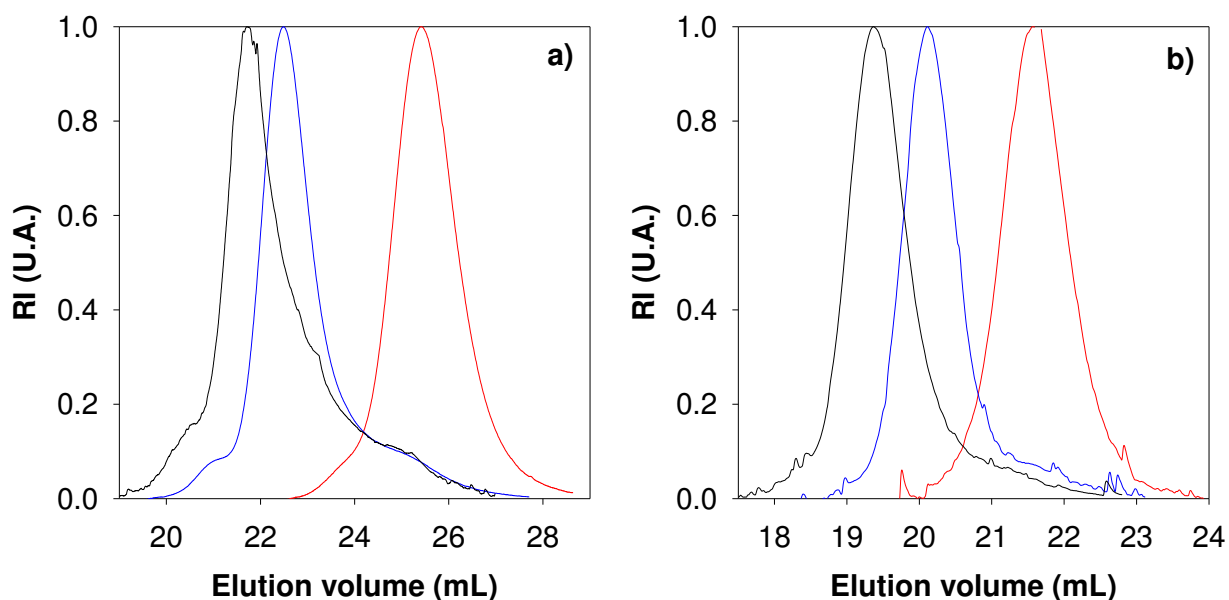


Figure 2.19. Size exclusion chromatograms of the first block MHxc (red), second block (blue) DHxc and triblock THxc (black) of TH50c (a) TH70c (b) in DMF with 0.01 M LiBr at 60°C

III.2. Sample preparation

Aqueous solutions of cationic polymers were prepared by dissolving the copolymer in demineralized water (Millipore) containing the required amount of HCl to reach an ionization degree of $\alpha_0 \approx 0.9$. Being a strong acid, HCl was used in stoichiometric quantities to obtain the desired amount of DMAEMA⁺ units ($[\text{DMAEMA}^+] = [\text{HCl}]$). Dissolution was done under

CHAPTER 2: MATERIALS AND METHODS

strong stirring for at least 24 hours at room temperature. Transparent, slightly pink and homogeneous solutions were obtained.

To obtain the desired ionization degree (α), the required amount of NaOH was subsequently added. Dilute NaOH solution had to be used and the addition had to be done under vigorous stirring in order to limit the formation of heterogeneities. The final ionization degree can be calculated utilizing equation (2.30).

$$\alpha = \frac{[\text{DMAEMA}^+]}{[\text{DMAEMA}]_{\text{total}}} = \alpha_0 - \frac{[\text{NaOH}]}{[\text{DMAEMA}]_{\text{total}}}$$
$$\text{with } [\text{DMAEMA}]_{\text{total}} = \frac{x_{\text{DMAEMA}}}{x_{\text{DMAEMA}}M_{\text{DMAEMA}} + x_{n\text{BmA}}M_{n\text{BmA}}} C_{\text{polymer}} \quad (2.30)$$
$$= \frac{DP(\text{DMAEMA})}{M_n} C_{\text{polymer}}$$

with $[\text{DMAEMA}^+]$ and $[\text{DMAEMA}]_{\text{total}}$ the concentrations in mol/L of charged DMAEMA and total amount of DMAEMA, respectively.

III.3. Titration

The titration procedure was adapted from the one already published¹³ and explained in section II.4.

III.3.1. Determination of the DMAEMA content

In order to calculate the amount of DMAEMA (n_{DMAEMA}) in a polymer chain, potentiometric titrations were performed.

First, the polymer was dissolved in demineralized water (Millipore) containing the required amount of HCl so that ~10 % of the HCl was in excess. The salt concentration was adjusted by adding the required amount of a 4 M NaCl solution. The polymer concentration was calculated to have a theoretical concentration of DMAEMA units of 0.043 mol/L. Thereafter, the solution was back-titrated using NaOH at 1 mol/L to decrease the ionization degree.

Let us consider the example in Figure 2.20 which corresponds to the titration of TH70c in the presence of 0.5 mol/L of NaCl. Two pH jumps appeared, the first around pH=3 and the second at pH 9. Three reactions are involved in the titration. First, the strong base NaOH and the strong acid HCl react quantitatively until the first pH jump characterized by pH_{Veq1} and

V_{eq1} . Then, NaOH reacts with the DMAEMA⁺ units to form DMAEMA until the second pH jump. The third reaction corresponds to the dissociation of NaOH in water. The total amount of DMAEMA was calculated from the volume of added NaOH between the two pH jumps.

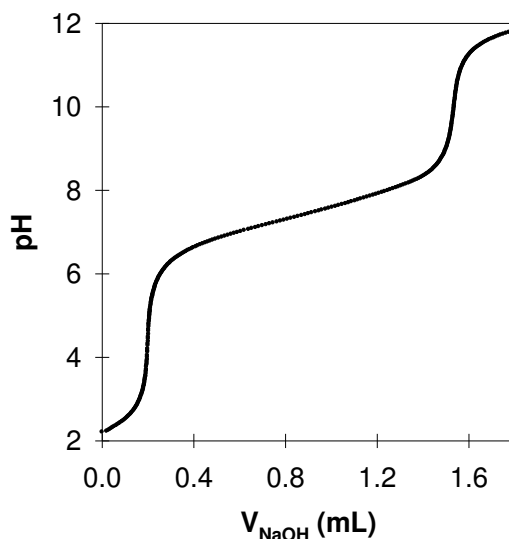


Figure 2.20. pH evolution as a function of the volume of NaOH (1M) added during the titration of a TH70c solution at $[DMAEMA]=0.043$ mol/L, $[NaCl]=0.5$ mol/L and an addition rate of 0.1 mL/min.

III.3.2. Calculation of the ionization degree (α) and pKa

The ionization degree and the pKa can be determined for each pH using equations (2.31) and (2.32). In this way Figure 1.20 is obtained for the example shown in the previous section

$$\alpha = \frac{[DMAEMA^+]}{[DMAEMA]_{tot}} = 1 - \frac{n_{DMAEMA}}{n_{DMAEMA-tot}} \quad (2.31)$$

$$pK_a = pH - \log\left(\frac{\alpha}{1-\alpha}\right) \quad (2.32)$$

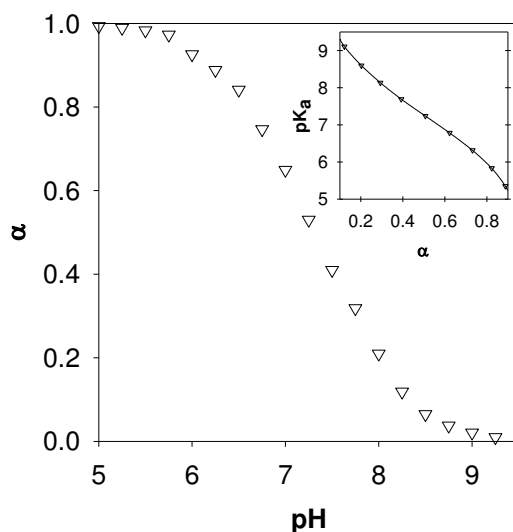


Figure 2.21. Evolution of the ionization degree as a function of the pH for TH70c at $[\text{DMAEMA}] = 0.043 \text{ mol/L}$, $[\text{Na}^+] = 0.5 \text{ mol/L}$. The inset represents the evolution of the pKa as a function of α .

IV. References

1. Chassenieux, C.; Nicolai, T.; Durand, D. *Macromolecules* **1997**, 30, (17), 4952-4958.
2. Lejeune, E. Synthèse, caractérisation et mise en oeuvre de copolymères diblocs amphophiles : vers des assemblages à dynamique stimuable. Université du Maine, Le Mans, 2010.
3. Charbonneau, C.; Chassenieux, C.; Colombani, O.; Nicolai, T. *Macromolecules* **2012**, 45, (2), 1025-1030.
4. Lauber, L.; Chassenieux, C.; Nicolai, T.; Colombani, O. *Macromolecules* **2015**, 48, (20), 7613-7619.
5. Colombani, O.; Langelier, O. I.; Martwong, E.; Castignolles, P. *J. Chem. Educ.* **2011**, 88, (1), 116-121.
6. Lejeune, E.; Drechsler, M.; Jestin, J.; Muller, A. H. E.; Chassenieux, C.; Colombani, O. *Macromolecules* **2010**, 43, (6), 2667-2671.
7. Zehm, D.; Laschewsky, A.; Heunemann, P.; Gradzielski, M.; Prevost, S.; Liang, H.; Rabe, J. P.; Lutz, J.-F. *Polym. Chem.* **2011**, 2, (1), 137-147.
8. Krivorotova, T.; Jonikaite-Svegziene, J.; Radzevicius, P.; Makuska, R. *React. Funct. Polym.* **2014**, 76, 32-40.
9. Lee, H. I.; Pietrasik, J.; Sheiko, S. S.; Matyjaszewski, K. *Prog. Polym. Sci.* **2010**, 35, (1-2), 24-44.
10. Shedge, A.; Colombani, O.; Nicolai, T.; Chassenieux, C. *Macromolecules* **2013**, 47, (7), 2439-2444.
11. Klymenko, A.; Nicol, E.; Nicolai, T.; Colombani, O. *Macromolecules* **2015**, 48, (22), 8169-8176.
12. Klymenko, A.; Nicolai, T.; Benyahia, L.; Chassenieux, C.; Colombani, O.; Nicol, E. *Macromolecules* **2014**, 47, (23), 8386-8393.
13. Colombani, O.; Lejeune, E.; Charbonneau, C.; Chassenieux, C.; Nicolai, T. *J. Phys. Chem. B* **2012**, 116, (25), 7560-7565.

14. Dautzenberg, H.; Jaeger, W.; Kötz, J.; Philippe, B.; Seidel, C.; Stscherbina, D., *Polyelectrolytes : Formation, Characterization and Application*. Hanser: 1994; p 248.
15. Kitano, T.; Taguchi, A.; Noda, I.; Nagasawa, M. *Macromolecules* **1980**, 13, (1), 57-63.
16. Moad, G.; Rizzardo, E.; Thang, S. H. *Aust. J. Chem.* **2005**, 58, (6), 379-410.
17. Dutertre, F.; Boyron, O.; Charleux, B.; Chassenieux, C.; Colombani, O. *Macromol. Rapid Commun.* **2012**, 33, (9), 753-759.

CHAPTER 3: PRINCIPAL RESULTS

In this chapter, the main results are presented in four sections. First, the self-assembly in aqueous medium of the random associative blocks $P(nBA_{1-x}\text{-stat-AA}_x)_{100}$ was studied by light scattering and related to that of the diblocks $P(AA)_{100}\text{-b-}P(nBA_{1-x}\text{-stat-AA}_x)_{100}$. Secondly, the comicellisation of mixtures of diblocks was analysed to understand the rheological properties of mixtures of triblocks $P(nBA_{1-x}\text{-stat-AA}_x)_{100}\text{-b-}P(AA)_{200}\text{-b-}P(nBA_{1-x}\text{-stat-AA}_x)_{100}$. Thereafter, graft copolymers, $P(AA)_{500}\text{-g-}[P(nBA_{1-x}\text{-stat-AA}_x)_{100}]_y$, were studied as alternatives of triblocks. Finally, to extend our concept to a different pH range and bring new thermo-sensitive properties, cationic triblock copolymers, $P(nBMA_{1-x}\text{-stat-DMAEMA}_x)_{100}\text{-b-}P(DMAEMA)_{200}\text{-b-}P(nBMA_{1-x}\text{-stat-DMAEMA}_x)_{100}$, were investigated. The structures of the copolymers studied in this work are shown in Figure 3.1.

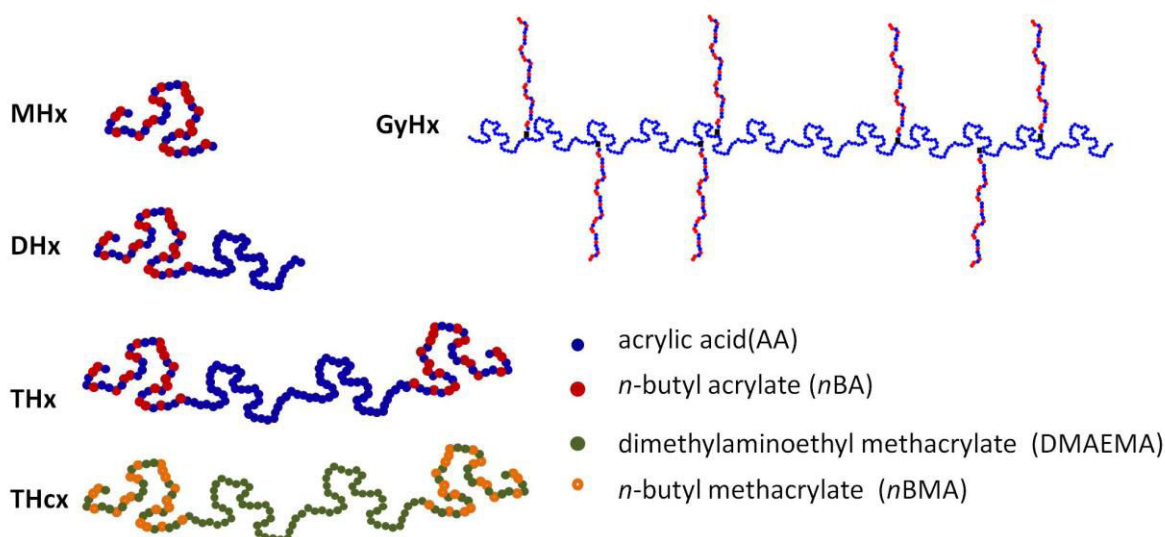


Figure 3.1. Schematic representation of the copolymers used.

This chapter is based on four articles presented in the next four chapters. Two appendices are added and are referred to when needed.

I. Highlighting the Role of the Random Associating Block in the Self-Assembly of Amphiphilic Block–Random Copolymers

It was shown in the literature that the amount of hydrophobic monomers in the random associating block can tune both the LCST¹ and the dynamic exchange². However, the effect

CHAPTER 3: PRINCIPAL RESULTS

on the structure was not investigated and the relationship between the self-association of the random associating block and that of the di/triblocks is only mentioned once.¹ Therefore, the self-association in aqueous medium of three statistical copolymers consisting of acrylic acid and *n*-butyl acrylate, $P(nBA_{1-x}\text{-stat-AA}_x)_{100}$ (MHx), with different *x* ratios was studied by light scattering and compared to that of their diblocks homologues (DHx) having a PAA hydrophilic block.^{3,4}

First, the self-association of the three MHx was studied by light scattering. The amount of AA units varied from 40 to 60 % (mol/mol) while the polymerisation degrees were kept constant at ~ 100 and the dispersities remained low ($\mathcal{D} \sim 1.1$) for the three statistical copolymers (MHx). In Figure 3.2a, at high ionization degree (α), the three MHx were dissolved as unimers since their molar masses were around 1.2×10^4 g/mol similar to the one of their unimers. When the ionization degree decreased, the molar mass and the hydrodynamic radius increased, implying that MHx aggregated. At low ionization degree, the molar mass sharply increased indicating that the electrostatic repulsions were no longer strong enough to stop the aggregation and the polymer eventually precipitated. The onset of precipitation depended on the amount of AA units, *x*. When *x* increased, the divergence occurred at lower α . The self-association of the three MHx can be compared as a function of the fraction of charged units (f_{MHx}), i.e. the amount of charges, inside the random block, as illustrated in Figure 3.2b. The evolutions of the molar masses are much closer as function of f_{MHx} highlighting the importance of this parameter to tune the extent of self-assembly.

Here the balance between the electrostatic repulsions and the hydrophobic attraction allows tuning the aggregate size by adjusting the amount of charges within the statistical copolymer either by adjusting the pH or the AA content. The chemical structure of a polymer can be designed to reach the desired aggregation state at a specific pH. MHx can be used as hydrophobic blocks for amphiphilic diblocks consisting of this block connected to a pure PAA block, $P(AA)_{100}\text{-}b\text{-}P(nBA_{1-x}\text{-stat-AA}_x)_{100}$ (DHx).

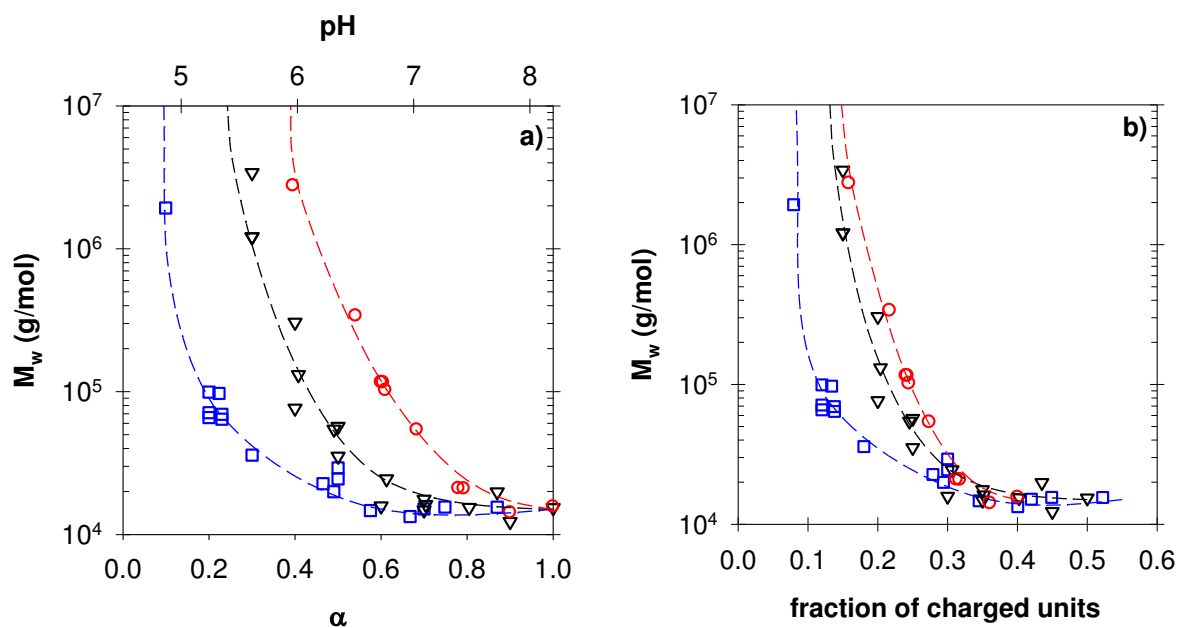


Figure 3.2. Evolution of the molar mass of MHx (MH40: \circ , MH50: ∇ , MH60: \square) as a function of a) the ionization degree, b) the fraction of charged units of MHx blocks. The dashed lines are guides to the eye.

Figure 3.3a reveals that, at high ionization degree, the molar mass of the diblocks was equal to the value expected for unimers around 1.8×10^4 g/mol. A decrease in the ionization degree led to an increase of the molar mass indicating self-assembly. By increasing the AA content x within the hydrophobic block, self-assembly started at lower α . Overall, the behavior of the DHx was qualitatively very similar to that of the neat MHx blocks. However, unlike MHx, diblocks did not precipitate because of their PAA hydrophilic block. They rather formed star-like micelles of finite size at low ionization degree.

As explained by Colombani et al., for a global ionization degree (α) the ionization degree of the hydrophobic blocks of the diblocks (α_{MHx}) is smaller.⁵ Therefore, to compare the self-association of MHx and DHx, α_{MHx} is more relevant. Figure 3.3a reveals that the self-assembly of DHx was directly related to that of MHx. The self-assembly of the diblock and of the neat MHx block roughly started at the same α_{MHx} . The major difference was the precipitation of MHx at low α_{MHx} while DHx formed star-like micelles of finite size. In addition, the PAA corona slightly hindered the aggregation since N_{agg} was always slightly lower for DHx than for MHx at the same α_{MHx} . For example, MH50 aggregated when α_{MHx} decreased until it diverged around $\alpha_{\text{MHx}} \sim 0.3$, whereas DH50 aggregated when α_{MHx} decreased until the aggregate size stagnated around $\alpha_{\text{MHx}} \sim 0.25$.

CHAPTER 3: PRINCIPAL RESULTS

It was previously shown that the amount of charges within the hydrophobic blocks of the triblocks THx also strongly determines their rheological properties.² Indeed, the evolution of the relaxation time as a function of the fraction of charged units ($= x \cdot \alpha_{MHx}$) roughly superimposed for the three THx, x varying from 40 to 60%. As depicted in Figure 3.3b, the increase of the relaxation time of TH50 transient networks roughly starts when the N_{agg} of DH50 starts to increase. Here, for the sake of clarity, only systems with $x=50\%$ are shown. Since the relaxation time of the triblock is related to the dynamic exchange of the micelle, these results imply that the amount of charges within the self-assembling block of this family of diblocks and triblocks controls both their exchange dynamics and their extent of self-assembly. A direct consequence is that a good understanding of the self-assembly of the neat associative blocks (monoblocks MHx) may allow predicting both the aggregation behavior and the exchange dynamics of the diblock/triblock copolymers.

To conclude, random copolymers appear to be a simple way to produce aggregates of different sizes as function of the pH with only two monomers. In addition, random block copolymers allow tuning the associative properties of diblocks using random block copolymers as hydrophobic blocks since the behavior of the system can be understood by knowing the fraction of charged units in the hydrophobic blocks for a specific pH. However, with triblock copolymers forming transient networks, to reach the desired rheological properties for a specific pH, new polymer syntheses are needed to change the monomer ratio i.e. the x value. To avoid this synthesis step, investigation of the behavior of mixtures of triblock copolymers was done in order to see whether it was possible to tune their rheological properties for a specific pH by formulation. This will be described in the next section.

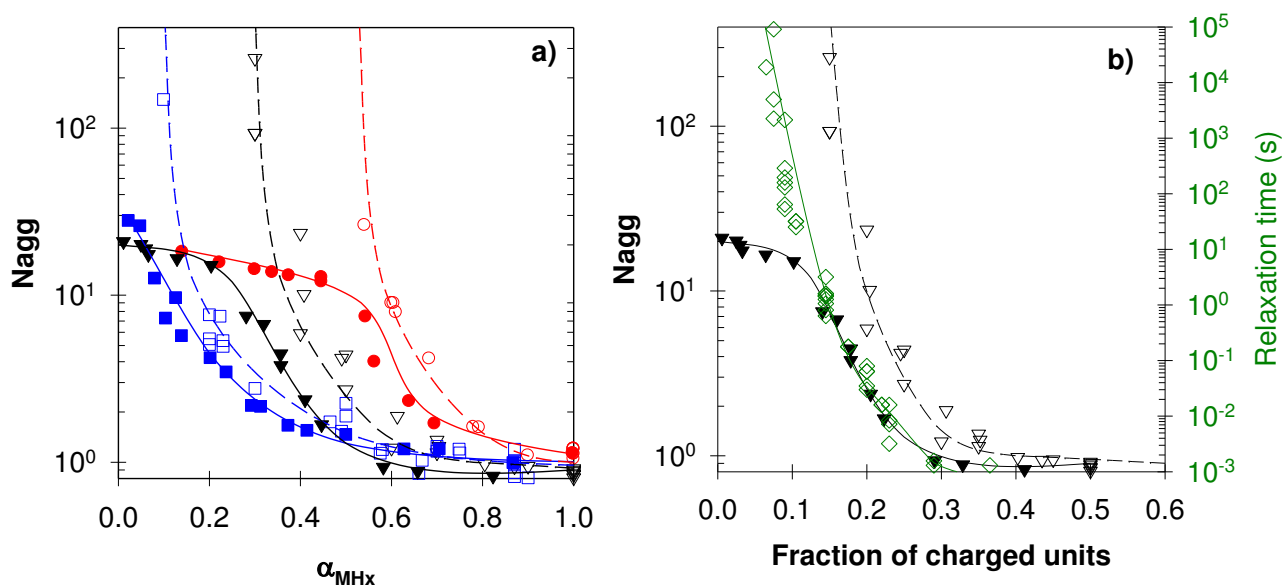


Figure 3.3. (a) Evolution of the aggregation number of MHx (MH40: \circ , MH50: ∇ , MH60: \square) and DHx (DH40: \bullet , DH50: \blacktriangledown , DH60: \blacksquare) as a function of the ionization degree of MHx blocks. The lines are guides to the eye, diblocks (solid lines) random associating blocks (dashed lines). (b) Evolution of the aggregation number of MH50 (∇) and DH50 (\blacktriangledown) and evolution of the relaxation time of TH50 (\diamond) as a function of the fraction of charged units within the MHx blocks.⁶

II. pH-Controlled Rheological Properties of Mixed Amphiphilic Triblock Copolymers

The literature contains very few examples of mixtures of triblock copolymers to tune the rheological properties of hydrogels and none of them are with copolyelectrolytes. However, such mixtures could be interesting in order to easily change the rheological properties without new polymer synthesis. Furthermore, mixtures of frozen copolymers with (very) dynamic ones could lead to an overall dynamic system since the dynamic system may enhance the exchange rate of the frozen one as was already observed for mixtures with surfactants which were shown to increase the exchange rate of diblock copolymers by Stam *et al.*⁷⁻⁹

In order to facilitate understanding of the rheological properties of mixtures of triblock copolymers THx, the conditions of co-micellisation were studied by light scattering for mixtures of diblock copolymers DHx.

II.1. Self-Assembly of mixtures of diblock copolymers

By titrating three triblock copolymers THx with x varying from 40% to 60%, Shedge et al. demonstrated that for such copolymers the dependence of the ionization degree on the pH was similar.² The same results were found for DHx entailing that two polymer solutions prepared at the same α had the same pH and that mixing them did not alter significantly their α (or pH⁵).

DH40 and DH60 were mixed at different weight fractions of DH40 (F_{40}) and a constant global polymer concentration (2 g/L) for several values of the ionization degree α of both polymers, see Figure 3.4. The average aggregation numbers (N_T) were calculated from molar mass measured by light scattering for each composition. At high ionization degree, $\alpha=0.77$, when DH60 remained as unimers and DH40 had an aggregation number (N_T) around 12, no co-micellisation occurred since the measured N_T (see points) was equal to the one calculated for unhybridized polymers (see solid line). At lower ionization degree, $\alpha=0.2$ and $\alpha=0.4$, when both DH40 and DH60 were aggregated, co-micellisation occurred. Similar observations were made at several ionic strengths and for mixtures of DH40 and DH50.

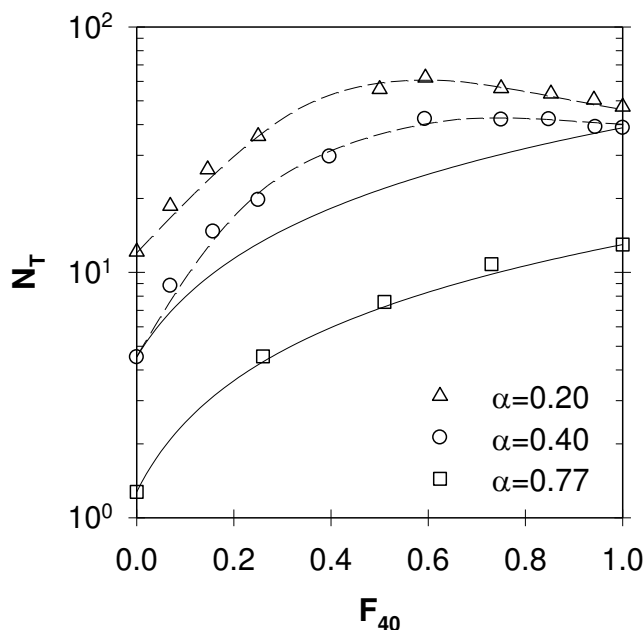


Figure 3.4. Evolution of the total aggregation number (N_T) as a function of the weight fraction of DH40 (F_{40}) in solutions of DH40 and DH60 at $[Na^+] = 0.5 \text{ mol/L}$. Different ionization degrees were investigated as indicated in the figures. The values for mixtures in the absence of co-micellisation are shown for a number of systems by the solid lines.

Studies on the diblocks therefore indicated that co-micellisation occurs only when both copolymers aggregated as illustrated in Figure 3.5. This behaviour was expected from the literature since comicellisation usually occurs when the cmc (or the cmt) of both polymers in the mixture is reached and as long as the difference of the spontaneous curvature of the interface is not too large. This was shown theoretically¹⁰⁻¹² and experimentally^{11, 13, 14}. Interestingly, Wright *et al.* demonstrated that the co-micellisation can be forced with mixtures of diblocks with P(DMAEMA) as hydrophilic block and P(DMAEMA-*stat*-DEAEMA) as hydrophobic blocks with different amounts of DEAEMA units within the hydrophobic block.¹⁵ The major differences with the systems studied here is the aggregation number, which is around 5 for the present system and around 80 for the system studied by Wright *et al.* In addition, Wright *et al.* prepared all mixtures at $\alpha \sim 0$ removing the polyelectrolyte effect.

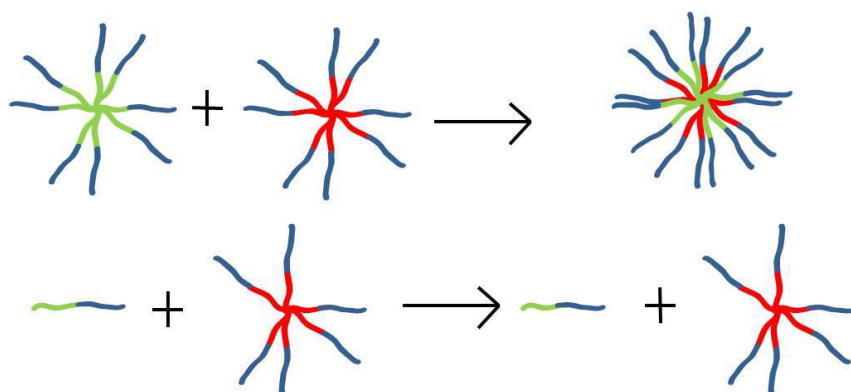


Figure 3.5. Schematic illustration of the self-association of mixtures of diblocks DHx. In green is the hydrophobic block with the highest amount of AA units in the hydrophobic block, in red with the lowest amount.

II.2. Rheological Properties of Mixed Amphiphilic Triblock Copolymers

Two types of mixtures of triblock copolymers were studied: TH40/TH60 and TH40/TH50. Based on the results on the diblocks, mixtures were analysed in conditions where co-micellisation occurred or not by adjustment of the overall ionization degree.

First, mixtures of triblock copolymers TH40/TH60 were made at $\alpha=0.64$ with a constant global polymer concentration (30 g/L), which corresponds to conditions where DH60 forms unimers and DH40 is aggregated^{2, 3, 16}. As explained for diblocks, no co-micellisation occurs

CHAPTER 3: PRINCIPAL RESULTS

at these conditions. The viscosity and relaxation time of the system were the same for mixtures of TH40 and TH60 at different weight fractions of TH40 (F_{40}) and for solutions of pure TH40 at the same concentration as in the mixtures, see Figure 3.6. In other words, without hybridisation TH60 had no effect on the behaviour of TH40 as expected, and only a simple dilution effect of TH40 is observed.

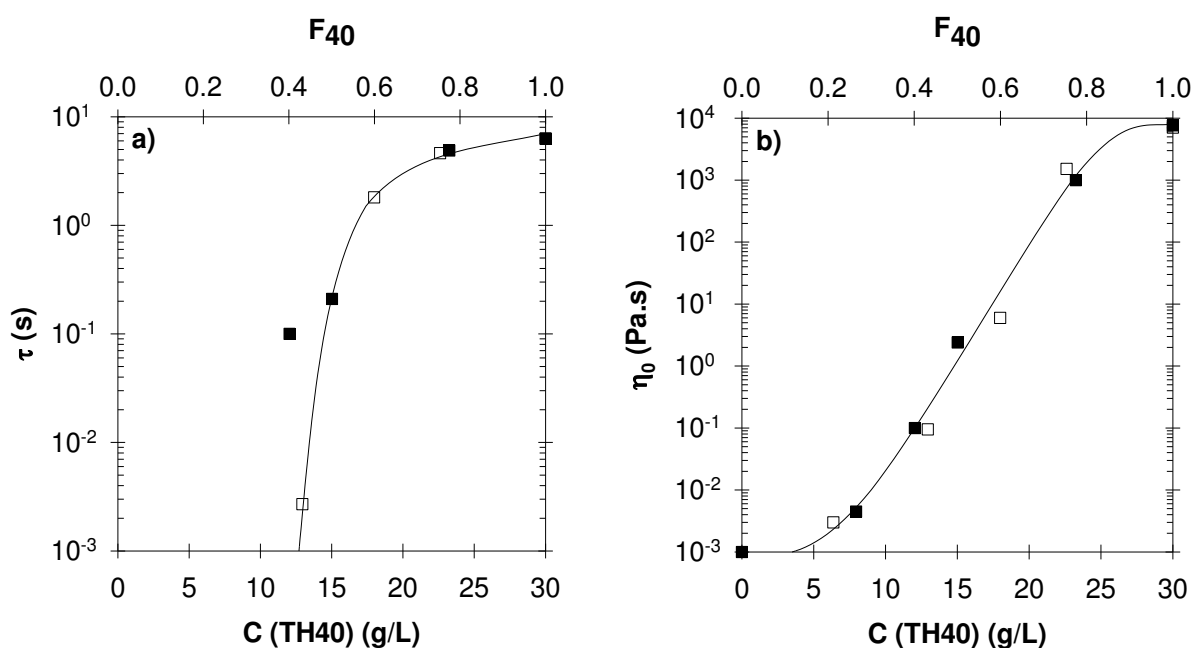


Figure 3.6. Dependence of the relaxation time (a) and the viscosity (b) as a function of the TH40 concentration (bottom axis) or F_{40} (top axis) for mixtures of TH60 and TH40 at $\alpha=0.65$, $C=30$ g/L and $T=20$ °C without added salt. The results for the mixtures (open symbols) are compared with those for pure TH40 solutions (closed symbols). The solid lines are guides to the eye.

In mixtures of TH40/TH60 triblocks where both THx associated, $\alpha=0.2$, the behaviour was strongly different. At these conditions, co-micellisation occurred and gave the rheological response depicted in Figure 3.7. At $\alpha=0.2$, pure TH40 formed frozen networks, whereas pure TH60 formed a dynamic network with a relaxation time of 1.3×10^{-2} s. The evolution of the elastic modulus of the mixture as a function of the angular frequency, in Figure 3.7, indicates that the rheological properties strongly depended on F_{40} , with a relaxation time ranging from 1.3×10^{-2} s to infinity. For $F_{40} \leq 0.33$, the mixture formed a viscoelastic network with a relaxation time increasing with increasing F_{40} while becoming more and more polydisperse. For $F_{40} \geq 0.43$, frozen networks were formed showing a plateau modulus at low frequencies the value of which increased sharply with increasing F_{40} .

Since co-micellisation occurred, it was concluded that a mixed network was formed with two types of junctions the relaxation of which was responsible for the overall rheological response. Unlike what was observed for alkyl-PEO-alkyl networks,^{8, 9} the relaxation time of each bridge was different in the hybrid network or in networks formed by only one component of the mixture. For TH60, the more dynamic copolymer, the relaxation time was slowed down by the incorporation of TH40 as is clearly seen for $F_{40}=0.33$ in Figure 3.7. For TH40, the result was not clear since the relaxation time was immeasurably long. At $F_{40}=0.33$, corresponding to a TH40 concentration of 10 g/L, the hybrid network still exhibited the behaviour of a transient network able to relax. Considering that the percolation concentration of TH40 alone at $\alpha=0.2$ is 5 g/L and that the obtained network is frozen, it can be concluded that either the exchange rate or the percolation concentration of TH40 increased in the presence of TH60. It is not possible to discriminate either scenario for TH40/TH60 mixtures, which is why experiments on mixtures of TH40/TH50 were conducted.

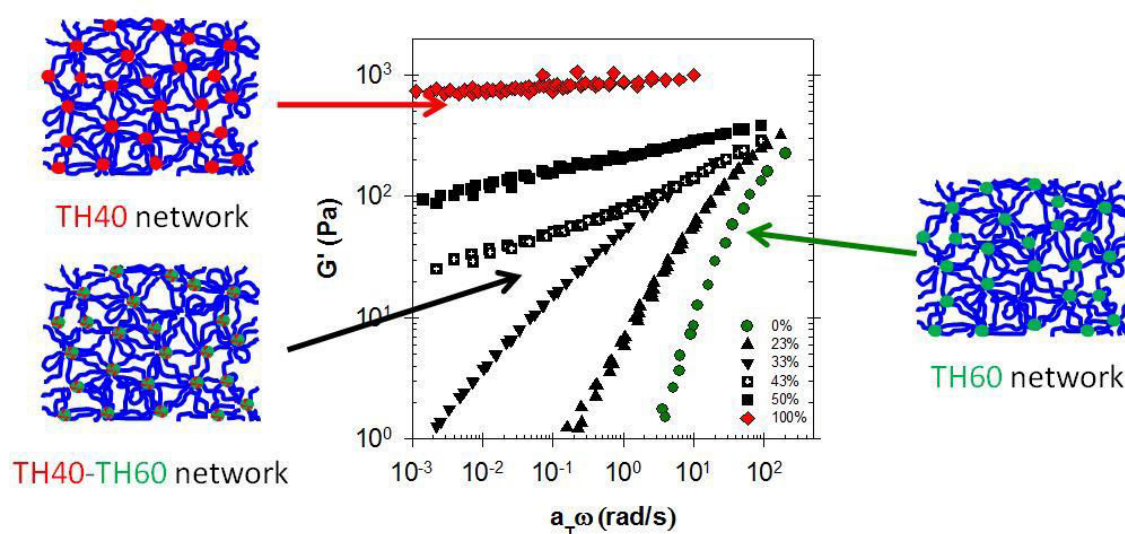


Figure 3.7. Master curves obtained by frequency-temperature superposition of the storage shear modulus at $T_{ref}=20$ °C for mixtures of TH40 and different fractions of TH40 indicated in the figure at $C=30$ g/L and $\alpha=0.2$ without added salt. For clarity, not all data points are shown.

With mixtures of TH40/TH60, no condition exists where TH40 and TH60 are dynamic and self-assemble for the same α . However, such conditions occur with TH40/TH50 at $\alpha=0.60$, their relaxation times being 1×10^3 s and 2×10^{-2} s respectively. With mixtures of TH40 and TH50, tuning the relaxation time over the whole range of F_{40} was possible as illustrated in Figure 3.8. The sharp increase of the relaxation time (and viscosity, data shown in chapter 5 at

CHAPTER 3: PRINCIPAL RESULTS

F_{40} between 0.3 and 0.4 roughly occurred for the percolation concentration of pure TH40. Interestingly, the dispersity of the master curves varied as a function of F_{40} . It reached a maximum for $F_{40} \sim 0.5$ as shown in Figure 3.8. Again, the rheological properties can be explained by the formation of a mixed network with two types of junctions. Since the relaxation time of each type of junction is already polydisperse and the exchange rates of both triblock copolymers were mutually influenced by the presence of the other triblock copolymers, an extremely broad relaxation distribution was observed rather than two distinct relaxation events.

Here TH50 does accelerate unambiguously the exchange rate of TH40 since the percolation concentration of the latter is similar in mixtures and alone, see chapter 5. It is believed that this phenomenon arises from the polyelectrolyte nature of the systems: blending of both types of hydrophobic blocks in the same micellar core might affect the charge density in the blocks due to a change of the dielectric constant.⁵

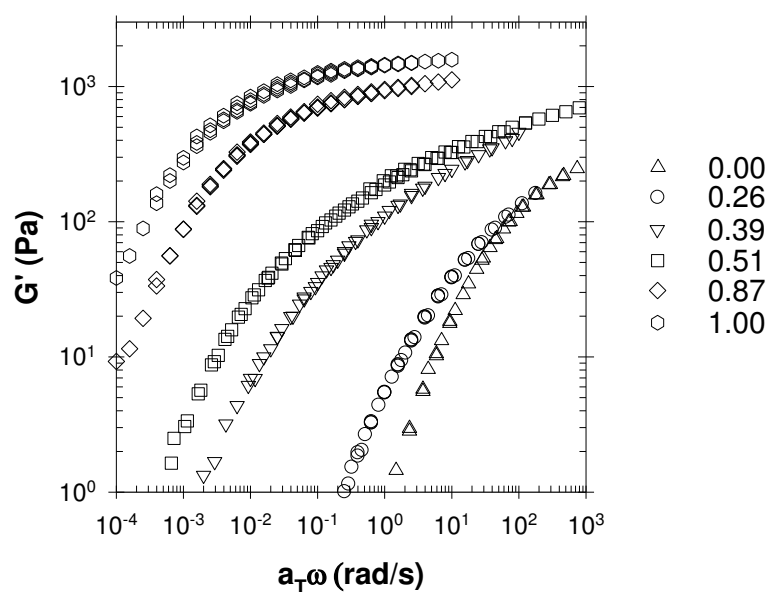


Figure 3.8. Master curves obtained by frequency-temperature superposition of the shear moduli at $T_{ref}=20$ °C for mixtures of TH40/TH50 and different fractions of TH40 indicated in the figure at $C=30$ g/L and $\alpha=0.60$ without added salt. For clarity, not all data points are shown.

To summarize, co-micellisation occurs only when both copolymers aggregate in agreement with the literature. Rheological properties are affected only at conditions at which co-micellisation occurred, i.e. when hybrid networks of THx were formed. The viscoelastic relaxation time and/or viscosity could be tuned as a function of the mixing ratio of triblock copolymers THx. The exchange rate of each THx was mutually affected by the presence of

the other copolymer. For neutral polymers, Annable *et al.* demonstrated that mixtures of triblock copolymers led to co-networks with several relaxation times equal to those of the neat components.¹⁷ The difference between the systems studied by Annable *et al.* and those studied here may be due to the polyelectrolyte nature of the latter.

That the rheological properties of mixtures of triblock copolymers can be controlled by the mixing ratio is interesting from a practical point of view.

III. pH-Responsive Transient Networks Formed By Amphiphilic Graft Copolymers

As explained in chapter 2 and in the previous section, THx triblock copolymers self-assemble in aqueous medium and form hydrogels with adjustable rheological properties. The production of this kind of triblock copolymers at an industrial scale can be challenging and expensive at high molecular weight. An alternative to triblock copolymers are graft copolymers which are easier to produce. Graft copolymers are also interesting since the grafting density can be varied to control further the rheological properties. Also, understanding the effect of the architecture on the rheological properties of polymers consisting of random associating blocks would be interesting since, to the best of our knowledge, the formation of hydrogels by copolymers with pH-sensitive grafts has not been reported in the literature.

Three graft copolymers, $P(AA)_{500-g-[P(nBA_{0.50-stat-AA_{0.50}})_{100}]_y$, were synthesized with y standing for the grafting density ($y = 2, 7$ and 30 grafts per chain in number average), the subscript 500 and 100 corresponding to the number average degrees of polymerization of the backbone and the grafts respectively and the subscripts 0.50 corresponding to the molar ratios of nBA and AA units. All the details of the synthesis are given in chapter 6. The backbones were synthesized by free radical polymerization and have large dispersities ($\mathcal{D} \sim 2.8$), implying that the number of grafts per chain is also polydisperse. On the contrary, the grafts were prepared by controlled radical polymerization (ATRP) and should therefore be rather monodisperse in terms of molecular weight and composition according to previous studies in similar conditions ($\mathcal{D} \sim 1.2$).^{2,3,4}

CHAPTER 3: PRINCIPAL RESULTS

In Figure 3.9, the relaxation time of the viscoelastic fluids formed by three graft copolymers above their α -dependent percolation concentration are reported as a function of the ionization degree. At high ionization degree the relaxation time was small ($\sim 10^{-3}$ s) and it increased as the ionization degree decreased. Since the relaxation time of G7H50 became independent of the polymer concentration, see chapter 6, the relaxation time was correlated to the exchange time of the hydrophobic grafts. In addition, the elastic moduli were lower than predicted by the rubber elasticity theory if all hydrophobic blocks contribute elastically to the transient network indicating the presence of defects.^{18, 19} These defects most probably come from intramolecular aggregation.

Qualitatively the results are similar for the three graft copolymers; the relaxation time increased with decreasing ionization degree. However, the grafting density changed the results from a quantitative point of view. Indeed, for higher grafting densities the relaxation time was lower for a given α . For instance, at $\alpha=0.5$ the relaxation times were 10^7 , 60 and 10^{-2} s for G2H50, G7H50 and G30H50 respectively, see Figure 3.9. For G7H50 and G30H50 the relaxation times became independent of the concentration and are therefore related to the exchange time of the grafts. This indicated that, at least for these two polymers, the exchange time is longer at the same α value for a lower grafting density. The results for G2H50 were more qualitative but follow the same trend.

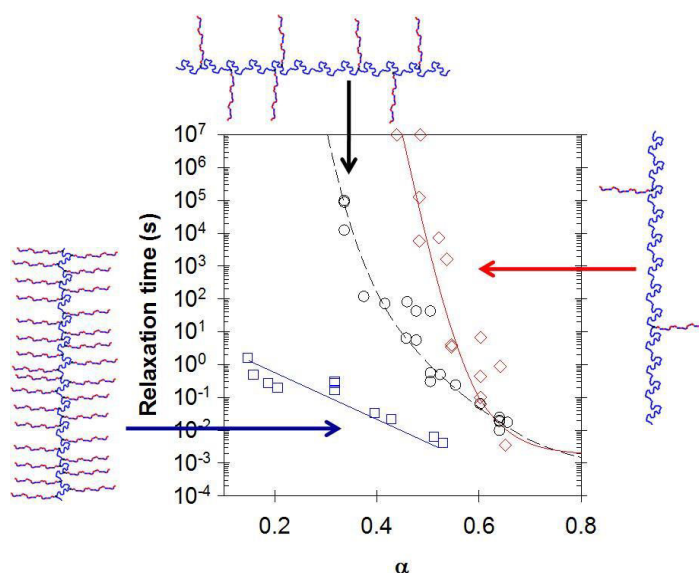


Figure 3.9. Evolution of the relaxation time as a function of the ionization degree for G2H50 (\diamond), G7H50 (\circ) and G30H50 (\square). The solid lines are guides to the eye. The dashed line is guide to the eye for TH50 data.

As previously reported⁵ and explained in the bibliographic part, the ionization degree of the hydrophobic blocks is different from the overall ionization degree of the polymer ($\alpha_{\text{MHx}} < \alpha$). The relationship between α_{MHx} and α was determined from titration experiments, revealing a strong influence of the grafting density on this relationship, as illustrated in Figure 3.10. Since for the same overall ionization degree, the ionization of the grafts changed, it is interesting to compare the evolution of the relaxation time as a function of the fraction of charged units within the MH50 grafts ($f = \alpha_{\text{MHx}} \cdot x$, $x=0.50$ for all systems here), see Figure 3.11.

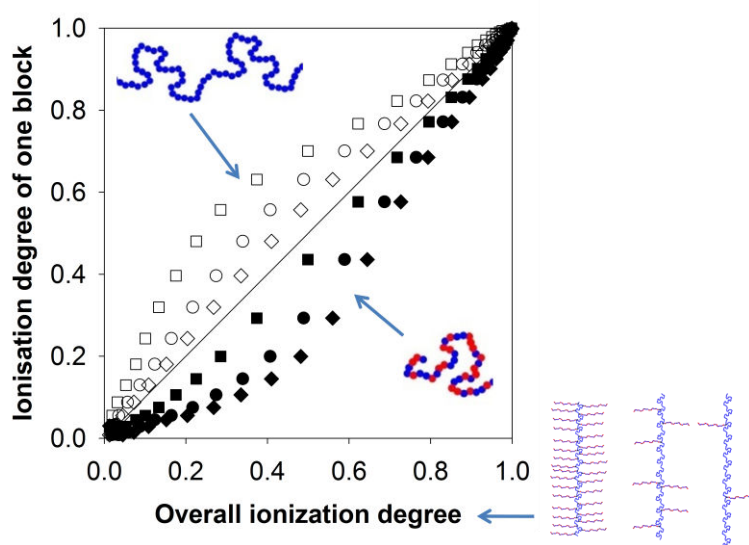


Figure 3.10. Degree of ionization of the backbone (open symbols) and of the grafts (closed symbols) as a function of the overall degree of ionization of the graft copolymers G2H50 (\diamond), G7H50 (\circ) and G30H50 (\square).

G7H50 and G2H50 have similar relaxation time dependencies on the fraction of charges within the grafts. The evolution of the relaxation time is moreover equivalent to the one already observed for TH50 as shown in Figure 3.11.² Interestingly, G7H50 exhibits the same evolution of the relaxation time as TH50 even though the dispersity of its backbone was much higher than the dispersity of the hydrophilic block of TH50. This confirms that the relaxation times of both systems were mainly controlled by the charge density of the hydrophobic block, whereas the dispersity of the hydrophilic block (or backbone) had a negligible effect.

Interestingly, at high grafting density, the fraction of charges does not entirely explain the rheological behavior. Indeed, the behavior of G30H50 did not superimpose with that of the other graft copolymers especially at low fraction of charges within the grafts. The high grafting density clearly lowers the relaxation time for a specific fraction of charge. It should

CHAPTER 3: PRINCIPAL RESULTS

be reminded here that the relaxation time of G30H50 did not depend on the concentration within the investigated range.

The origin of the strong difference between the behaviour of G30H50 and that of the two other graft copolymers is not clear. However, it is speculated that intramolecular interactions between the grafts can be favoured compared to intermolecular interactions. At such high grafting density, G30H50 might have a rod-like shape instead of a coil-like shape leading to a different self-assembly at the nanoscale and to a different relaxation mechanism. Light scattering experiments were undertaken to determine the morphology of the aggregates as shown in appendix, however, due to the high polydispersity of the backbones no conclusion could be drawn.

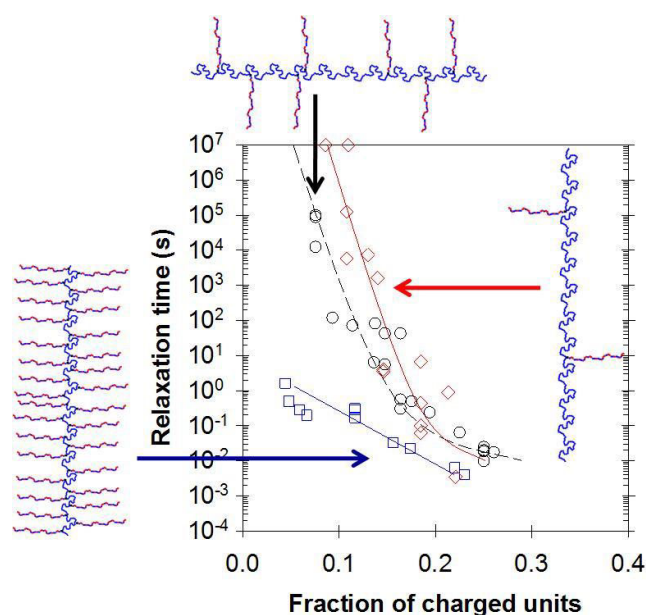


Figure 3.11. Evolution of the relaxation time as function of the fraction of charged units in the hydrophobic blocks for G2h50 (\diamond), G7H50 (\circ) and G30H50 (\square). The solid lines are guides to the eye. The dashed line is guide to the eye for TH50 data.

In conclusion, graft copolymers, $P(AA)_{500-g}-[P(nBA_{1-x}stat-AA_x)_{100}]_y$, with $y=2$ and 7 were able to form viscoelastic fluids with pH-sensitive exchange dynamics mostly controlled by the fraction of charged units of the grafts ($f=x \cdot \alpha_{MHx}$) without significant effect of the high dispersity of the backbones. These graft copolymers are the first with pH-sensitive grafts used to form hydrogels. In addition, for moderate grafting density, their behavior was similar to the one of the triblock TH50 implying that the relaxation time was hardly affected by the polymer architecture. Only at high grafting density, $y=30$, were architectural effects involved. They lowered the relaxation times probably because of stronger intramolecular interactions. An

optimum of the grafting density should be found for large-scale applications but a small grafting density seems desirable.

IV. pH and thermo-responsive self-assembly of cationic triblock copolymers with controlled dynamics

So far, the focus was on systems based on acrylic acid and *n*-butyl acrylate. Literature results suggest that the strategy consisting of incorporating hydrophilic monomers in the hydrophobic block may be a universal way to control the exchange dynamics of amphiphilic copolymers. However, until now it was demonstrated quantitatively only for THx that the exchange dynamics were indeed affected and controlled by the addition of hydrophilic monomers. In order to assess whether dynamic exchange can be induced and tuned by incorporation also of other hydrophilic units, to extend the accessible pH range and to add thermo-sensitiveness to the hydrogels, triblock copolymers with dimethylaminoethyl methacrylate (DMAEMA) hydrophilic units were investigated.

Recent work in our group demonstrated that diblock copolymers made of DMAEMA and *n*-butyl methacrylate (*n*BMA) were able to form star-like micelles with pH-tunable aggregation numbers.²⁰ Therefore, triblock copolymers made of DMAEMA and *n*BMA were synthesized by RAFT and evaluated: P(*n*BMA_{1-x}-*stat*-DMAEMA_x)₁₀₀-*b*-P(DMAEMA)₂₀₀-*b*-P(*n*BMA_{1-x}-*stat*-DMAEMA_x)₁₀₀ (THxc) with x at 50 and 70 %. The polymer dispersities remained below 1.4.

The diblock copolymers made of DMAEMA and *n*BMA were previously synthesized by our group using ATRP.²⁰ However, due to only partial reinitiation for the synthesis of the second block, RAFT polymerization was preferred here. It is important to remark that the polymer block length was similar for THx and THxc.

Results at 20°C will first be described followed by the effect of the temperature. It is important to note already however that the effect of temperature was partly irreversible preventing the construction of master curves by frequency-temperature superposition. A master curve at T=20°C could be obtained by shifting the results obtained at different ionization degrees for TH50c and TH70c, see Figure 3.12. In this manner relaxation times up to 10⁴ s could be determined.

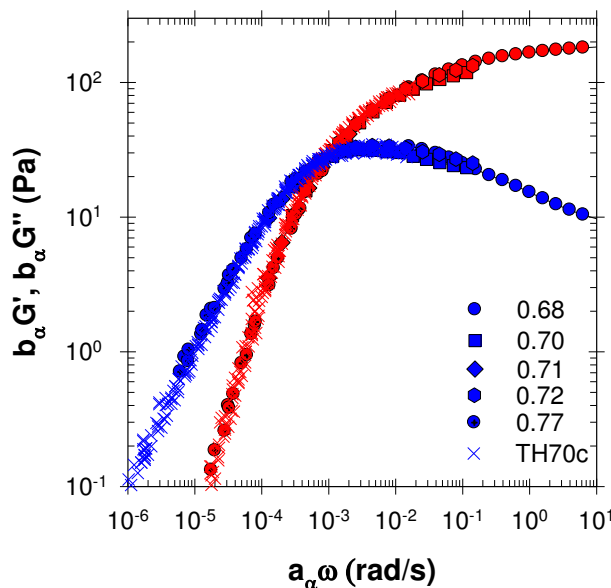


Figure 3.12. Master curves obtained by frequency- α superposition for TH50c at $C = 50$ g/L and for TH70c at $C=80$ g/L, with $\alpha_{ref}=0.68$ for TH50c and $\alpha_{ref}=0.29$ for TH70c.

At $T=20^{\circ}\text{C}$, the copolymers formed viscoelastic fluids above their α -dependent percolation concentrations. In Figure 3.13a, the evolution of the relaxation time of both TH50c and TH70c as a function of the ionization degree is reported. There is a strong dependence of the relaxation time on the ionization degree. When the ionization degree decreased, the relaxation time increased, sharply for TH50c. The relaxation times were higher than 10^4 s for TH50c below $\alpha = 0.6$ and were no longer measurable. In Figure 3.13b, the evolution of the elastic modulus as a function of the ionization degree is reported. The elastic modulus increased with the decrease of α until a maximum. For TH50c, at high polymer concentration (80 g/L) and low ionization degree, the elastic modulus reached the theoretical value for purely entropic elasticity ($G_e=v.R.T$ with $v=C/M_n$ for ideal rubber elastic networks)¹⁸ and the relaxation time became independent of the polymer concentration; in other words, TH50c formed an ideal network at low α and high concentration. The terminal relaxation times measured for ideal networks of TH50c at low ionization degrees ($\alpha<0.70$) and $C>35$ g/L are related to the exchange rate of the hydrophobic blocks of TH50c.

Qualitatively, the behavior of the cationic triblock copolymers (THxc) was similar to that of the anionic triblock copolymers (THx). Therefore, the exchange dynamics can be controlled by the pH with cationic copolymers similarly to anionic copolymers, which supports the suggestion that the method may be generally applicable. This statement is further verified

qualitatively with TH70c, even if only one concentration was investigated since the percolation concentration was high. For TH70c, when $\alpha < 0.2$, the elastic modulus was independent of the ionization degree and was the one expected for ideal networks. The relaxation time at low ionization degree was related to the extraction of hydrophobic blocks, whereas at higher α the extraction time was underestimated due to the presence of defects such as superbridges.¹⁹

It is interesting to note that the increase of the relaxation time with decreasing ionization degree is much sharper for TH50c than for TH50. As shown in the chapter 7, for TH50c, the evolution of the fraction of charged units within the hydrophobic blocks as a function of the ionization degree was also sharper for TH50c. Also for TH50c the fraction of charged units within the hydrophobic blocks is an important factor that controls the properties and explains to a large extent why variation of the amount of DMAEMA led to a variation of the exchange dynamics for a given α .

At room temperature, the behavior of the cationic copolymers was similar to that of the anionic ones. However, the response under heating was strongly different.

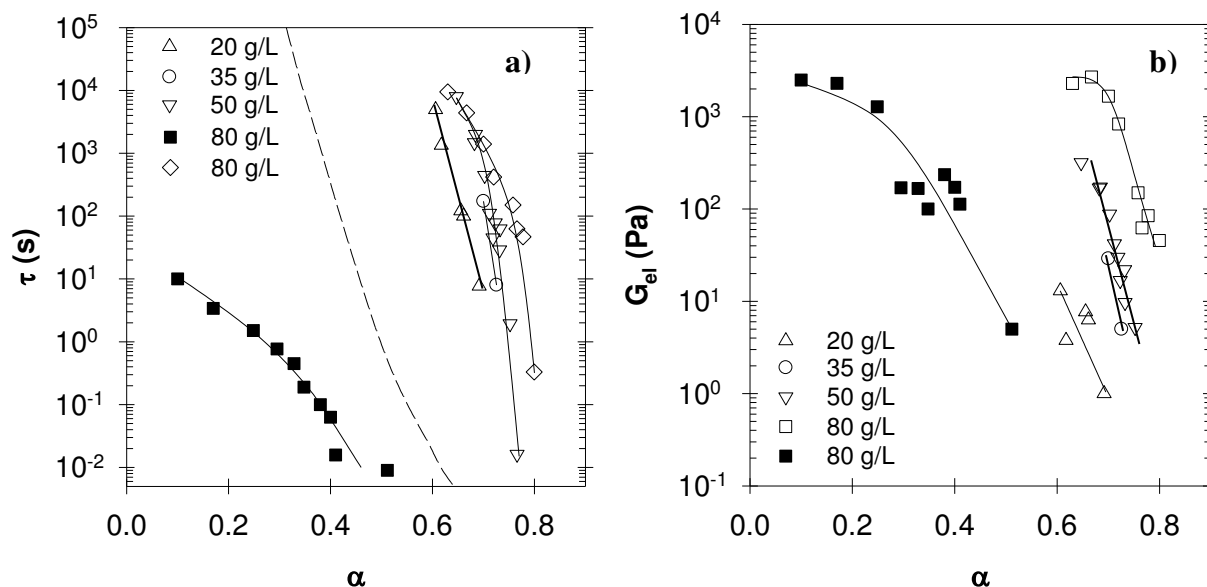


Figure 3.13. Evolution of the relaxation time (a) and of the elastic modulus (b) as a function of the ionization degree for TH50c (open symbols) and TH70c (closed symbols) at different polymer concentrations, $T=20^\circ\text{C}$ and $[Cl^-]=0.5M$.

The effect of temperature for the cationic triblock copolymers was observed to be complex and even irreversible to some extent. Here, we focused on the temperature range below 50°C where no irreversible phenomena were observed. Irreversible transformations can occur at

CHAPTER 3: PRINCIPAL RESULTS

higher temperatures as shown in chapter 7, leading to out-of-equilibrium systems which are not described here.

For TH50c, the relaxation time decreased upon increasing the temperature except at low ionization degrees. Indeed, for ionization degrees below 0.70 the relaxation time increased when the temperature increased. For TH70c the relaxation time increased upon heating for all ionization degrees. Figure 3.14 represents the evolution of the relaxation time at 50°C normalised by its original value at 20°C as a function of the fraction of charged units within the hydrophobic blocks (f). The relaxation time increased upon heating at low fraction of charged units and decreased at high fraction of charged units.

These results are in contrast with those observed for the anionic triblock copolymers TH50 where the relaxation time decreased upon heating with an Arrhenius dependence characterized by $E_a \sim 120$ kJ/mol independent of α and the concentration. This unusual effect could be explained by the pH-dependent LCST of the DMAEMA units, which is well-known to induce temperature-responsiveness sensitive to the pH. Indeed, Plamper *et al.* showed that the LCST of DMAEMA increases from 45 °C at pH=10 to 80°C at pH=7.²¹

In conclusion, cationic copolymers formed viscoelastic fluids with exchange dynamics controlled by α , similarly to THx. The strategy consisting of incorporating hydrophilic units inside the hydrophobic blocks could be extended to other monomer units than n BA/AA ones to induce and control the exchange dynamics of self-assembled amphiphilic copolymers. The use of DMAEMA as hydrophilic monomers allowed controlling the exchange dynamics with temperature and gave access to interesting new rheological properties, although the effect of temperature is very complex and partly irreversible.

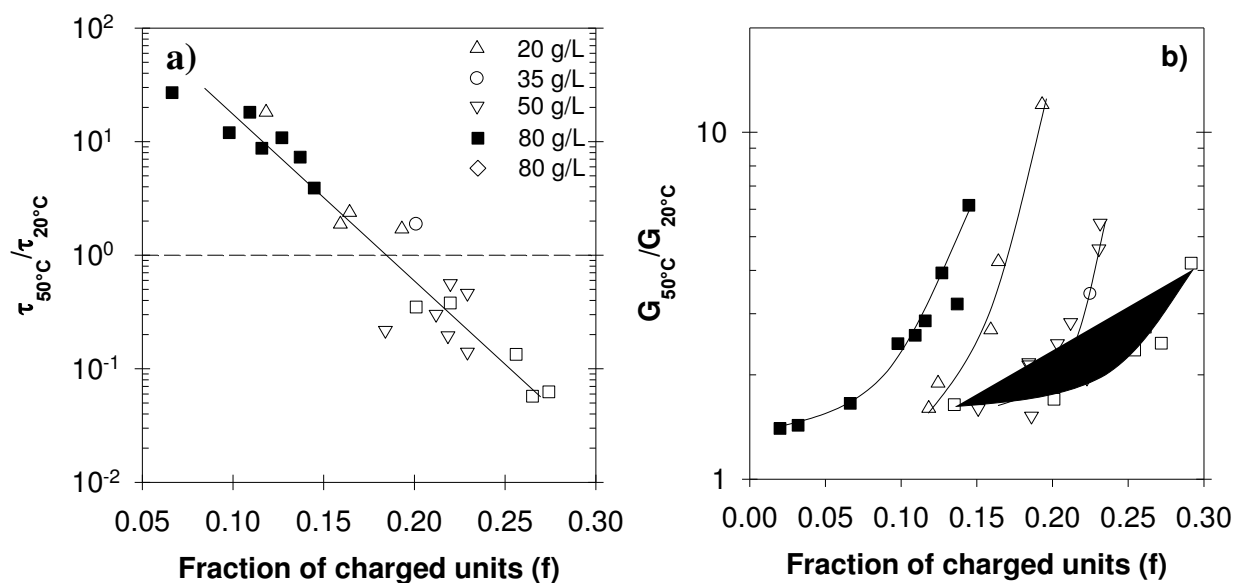


Figure 3.14. Evolution of the relaxation time (a) and of the elastic modulus (b) at 50°C normalized by its value at 20°C as a function of the fraction of charged units in the hydrophobic blocks at different concentration for TH50c (open symbols) and at 80 g/L for TH70c (closed symbols), $[\text{Cl}^-]=0.5\text{M}$.

V. Block-random copolymers: a universal way to control exchange dynamics

Anionic triblock, anionic graft and cationic triblock copolymers were shown to form viscoelastic fluids and had pH-controlled rheological properties. The properties of the systems were controlled by the pH and the amount of hydrophilic units inside the hydrophobic blocks/grfts i.e. by the fraction of charged units. A potentially universal behavior appeared from the different studies. Indeed, as depicted in Figure 3.15 with the superposition of the master curves at 20°C , the same relaxation process occurred with the three different types of polymers. This general relaxation process was controlled to a large extent by the fraction of charged units in the hydrophobic blocks. As a consequence, the relaxation time could be tuned by the pH. It is important to remark that the ionization degree of the hydrophobic blocks evolved differently with the pH for each polymer, changing the pH-range at which a given relaxation time is obtained.

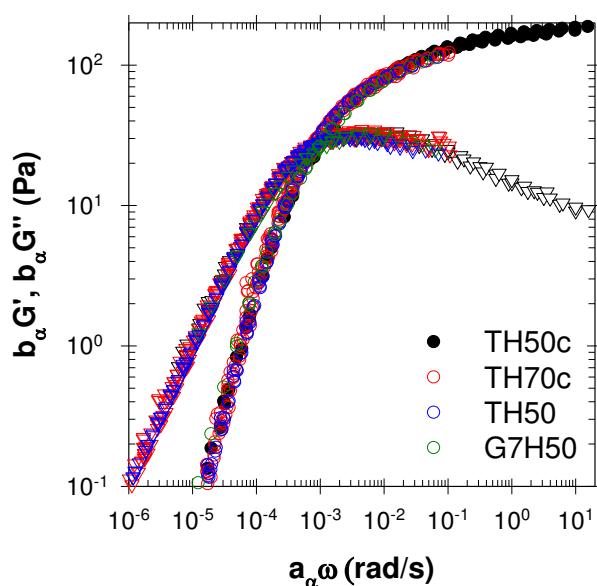


Figure 3.15. Superposition of master curves of the angular frequency dependence of the storage and loss moduli for different systems at $T_{ref}=20^{\circ}\text{C}$ without salt for TH50 and G7H50 and $[\text{Na}^+]=0.5\text{M}$ for TH50c and TH70c.

The relaxation time and therefore the exchange dynamics were controlled over more than 10 decades in different pH-ranges as illustrated in Figure 3.16. Figure 3.16 also implies that different rheological properties can be reached at the same pH depending on the selected chemical structure of the polymer. Alternatively, it is possible to reach the desired rheological properties in a large range of pH by using mixtures of polymers rather than synthesizing a new polymer for each application.

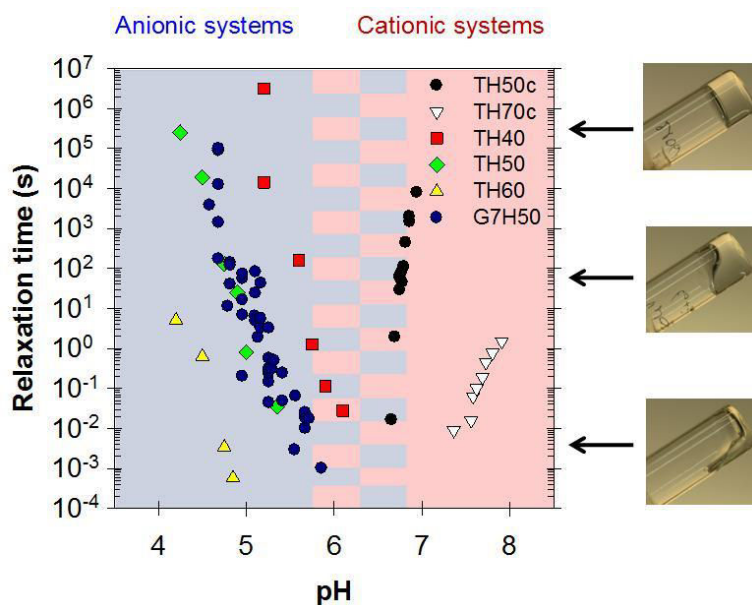


Figure 3.16. Evolution of the relaxation time as a function of the pH at different concentrations for different systems, $T_{ref}=20^{\circ}C$.

Moreover, the study of the neat random associating block by titration and light scattering revealed that the behavior of this polymer guides that of the diblock, triblock and graft copolymers both in terms of aggregation and exchange dynamics. This observation can be utilized to rationally design new copolymers with tunable aggregation and dynamics. Indeed, full understanding of the behavior of the neat hydrophobic blocks by light scattering and potentiometric titration can drive the synthesis efforts as illustrated in Figure 3.17. First only neat hydrophobic blocks with various compositions are synthesized. Then, titration experiments may be used to predict the charge repartition within the hydrophobic segments (blocks or grafts) as a function of the overall ionization degree/pH of triblock or graft copolymers containing these hydrophobic segments as previously reported.⁵ Thereafter, the evolution of the aggregation numbers of the random copolymer(s) as a function of the ionization degree can be studied by light scattering.

Results of both potentiometric titration and light scattering studies of the neat hydrophobic block could predict roughly the rheological properties of triblock and graft copolymers as a function of the pH without needing to synthesize them. Hence, the preliminary study of different hydrophobic segments alone may save a lot of synthetic efforts to rationally design triblock and graft copolymers containing the proper amount of hydrophilic and hydrophobic units to fulfill a target application.

CHAPTER 3: PRINCIPAL RESULTS

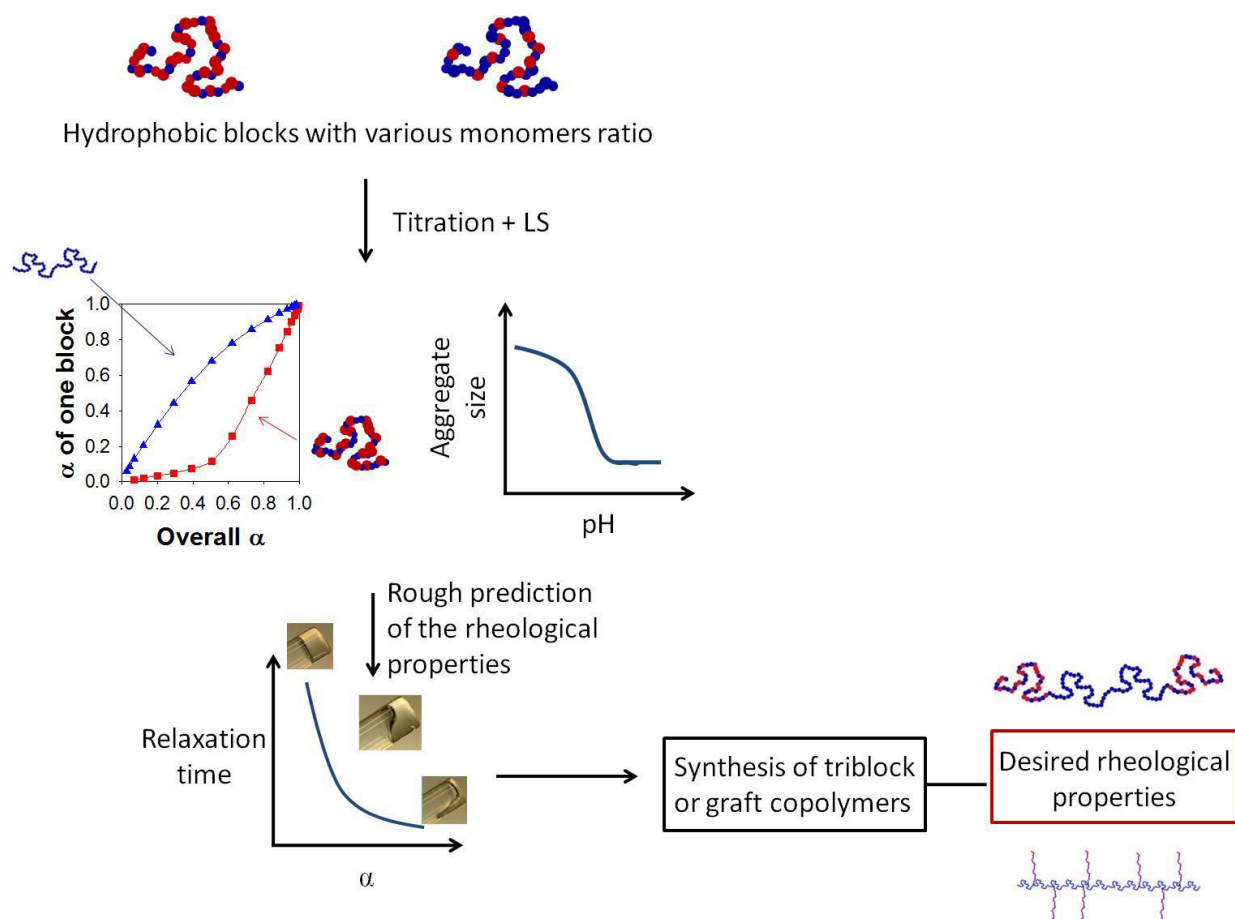


Figure 3.17. Conceptual illustration of the system.

VI. References

1. Gotzamanis, G.; Tsitsilianis, C. *Macromol. Rapid Commun.* 2006, 27, (20), 1757-1763.
2. Shedge, A.; Colombani, O.; Nicolai, T.; Chassenieux, C. *Macromolecules* 2013, 47, (7), 2439-2444.
3. Charbonneau, C.; Lima, M. M. D.; Chassenieux, C.; Colombani, O.; Nicolai, T. *Phys. Chem. Chem. Phys.* 2013, 15, (11), 3955-3964.
4. Lejeune, E.; Chassenieux, C.; Colombani, O., pH Induced Desaggregation Of Highly Hydrophilic Amphiphilic Diblock Copolymers. In *Trends in Colloid and Interface Science Xxiv*, Starov, V.; Prochazka, K., Eds. 2011; Vol. 138, pp 7-16.
5. Colombani, O.; Lejeune, E.; Charbonneau, C.; Chassenieux, C.; Nicolai, T. *J. Phys. Chem. B* 2012, 116, (25), 7560-7565.
6. Charbonneau, C.; Chassenieux, C.; Colombani, O.; Nicolai, T. *Macromolecules* 2011, 44, (11), 4487-4495.
7. Creutz, S.; van Stam, J.; De Schryver, F. C.; Jerome, R. *Macromolecules* 1998, 31, (3), 681-689.
8. Van Stam, J.; Creutz, S.; De Schryver, F. C.; Jérôme, R. *Macromolecules* 2000, 33, (17), 6388-6395.
9. Okay, O., Self-Healing Hydrogels Formed via Hydrophobic Interactions. In *Supramolecular Polymer Networks and Gels*, Seiffert, S., Ed. Springer International Publishing: Cham, 2015; pp 101-142.
10. Shim, D. F. K.; Marques, C.; Cates, M. E. *Macromolecules* 1991, 24, (19), 5309-5314.
11. Sens, P.; Marques, C. M.; Joanny, J. F. *Macromolecules* 1996, 29, (14), 4880-4890.
12. Borovinskii, A. L.; Khokhlov, A. R. *Macromolecules* 1998, 31, (22), 7636-7640.
13. Alexandridis, P.; Holzwarth, J. F.; Hatton, T. A. *Macromolecules* 1994, 27, (9), 2414-2425.
14. Renou, F. d. r.; Benyahia, L.; Nicolai, T.; Glatter, O. *Macromolecules* 2008, 41, (17), 6523-6530.
15. Wright, D. B.; Patterson, J. P.; Pitto-Barry, A.; Cotanda, P.; Chassenieux, C.; Colombani, O.; O'Reilly, R. K. *Polym. Chem.* 2015, (6), 2761-2768.
16. Lauber, L.; Chassenieux, C.; Nicolai, T.; Colombani, O. *Macromolecules* 2015, 48, (20), 7613-7619.
17. Annable, T.; Buscall, R.; Ettelaie, R.; Whittlestone, D. J. *Rheol.* 1993, 37, (4), 695-726.
18. Green, M. S.; Tobolsky, A. V. *J. Chem. Phys.* 1946, 14, (2), 80-92.
19. Annable, T.; Buscall, R.; Ettelaie, R.; Whittlestone, D. J. *Rheol.* 1993, 37, (4), 695-726.
20. Dutertre, F.; Boyron, O.; Charleux, B.; Chassenieux, C.; Colombani, O. *Macromol. Rapid Commun.* 2012, 33, (9), 753-759.
21. Plamper, F. A.; Ruppel, M.; Schmalz, A.; Borisov, O.; Ballauff, M.; Muller, A. H. E. *Macromolecules* 2007, 40, (23), 8361-8366.

CONCLUSIONS AND PERSPECTIVES

Conclusions and perspectives

The bibliographic study revealed that diblock (DHx) and triblock (THx) copolymers based on a poly(acrylic acid) (PAA) hydrophilic block and one or two poly(*n*-butyl acrylate-*co*-acrylic acid) (MHx) hydrophobic end block(s) exhibited pH-tunable aggregation numbers and exchange dynamics. The AA content (*x*) strongly affected the dynamic exchange of THx due to the modification of the fraction of charged units within the hydrophobic blocks MHx.

The aim of this PhD work was to rationalize the parameters allowing a control of the exchange dynamics and of the resulting rheological properties of amphiphilic copolymers in aqueous medium in order to design smart materials such as hydrogels potentially relevant for industrial applications.

In the present work, the self-assembly of MHx with different *x* contents was investigated in aqueous medium by light scattering. These polymers were found to form aggregates with a size and aggregation number drastically depending on their amount of charges. A strong relationship between the self-assembly of the neat hydrophobic block (MHx) and that of the diblocks (DHx) was observed since the size of the DHx diblocks was mainly controlled by the amount of charges within their hydrophobic blocks. The amount of charges within the hydrophobic block(s) therefore controlled both the structure and the exchange dynamics of such copolymers.

To easily tune the rheological properties of hydrogels by formulation rather than by synthesis, mixtures of triblocks were studied. Mixtures of two dynamic triblock copolymers were already described in the literature for neutral copolymers and always led to visco-elastic fluids with two relaxation times corresponding to the exchange time of each triblock. It appeared that for our copolymers co-micellisation occurred only when both copolymers aggregated as was reported for other systems in the literature. When co-micellisation occurred, the relaxation time and the viscosity were affected by the mixing ratio of triblock copolymers THx. Furthermore, the exchange rate of each THx was mutually affected by the presence of the other copolymer, broadening the relaxation time distribution. The difference between neutral copolymer mixtures and our systems may come from the polyelectrolyte nature of the THx. This may indeed have resulted in a different expression of the charges within a hybrid core compared to a hydrophobic core composed of only one type of associating blocks.

CONCLUSIONS AND PERSPECTIVES

Graft copolymers, $P(AA)_{500-g-[P(nBA_{1-x}stat-AA_x)_{100}]_y}$, with $y=2, 7$ and 30 were synthesized and characterized to better understand the effect of topology on the rheological properties and because graft copolymers are more relevant for large-scale applications than triblock copolymers. The graft copolymers formed viscoelastic fluids with pH-sensitive exchange dynamics. When $y=2$ or 7 the properties were mostly controlled by the fraction of charged units of the grafts ($f=x \cdot \alpha_{MHx}$) without significant effect of the high dispersity of the hydrophilic backbones. In addition, their behavior was similar to the one of the triblock TH50 implying that the relaxation time is hardly impacted by the polymer architecture. Only at high grafting density, $y=30$, were architectural effects involved, lowering the relaxation times probably because of stronger intramolecular interactions.

In order to assess whether dynamic exchange can be induced and tuned by incorporation of any other hydrophilic units, to extend the pH range of use of such copolymers and to add thermo-sensitivity to the hydrogels, triblock copolymers composed of dimethylaminoethyl methacrylate (DMAEMA) and *n*-butyl methacrylate (*n*BMA) were synthesized and investigated. The incorporation of hydrophilic units inside the hydrophobic blocks appeared as a universal strategy to induce and control exchange dynamics of self-assembled amphiphilic copolymers. In addition, the use of DMAEMA as hydrophilic monomers allowed to control the exchange dynamics with temperature to some extent and gave access to interesting new rheological properties. It must however be noted that the effect of temperature was not fully reversible.

From a more general point of view, both the structure and the rheological properties of all these copolymers were mostly controlled by the fraction of charged units in the hydrophobic blocks. It appeared that a deep understanding of the self-assembly of the neat random associating block in aqueous medium gives tools to roughly predict the self-association of diblock copolymers and to estimate the rheological properties of the triblock/graft copolymers.

Despite these interesting results, many questions remain partially or totally unsolved. As shown in appendix, preliminary results indicate that gradient triblock copolymers may form viscoelastic materials with relaxation times tuned by the pH. However, gradient triblock copolymers of similar sizes as TH x are needed to draw conclusions on the effect of the monomer repartition on the exchange dynamics. Moreover, unlike our systems, graft copolymers with longer backbones might have pronounced non-linear rheological properties such as shear-thickening or even shear induced gelation.

CONCLUSIONS AND PERSPECTIVES

During this PhD, a master student of our group used a triblock copolymer TH50 to stabilize water/(do)decane emulsions. These preliminary results were interesting, emulsions were stable with small amounts of polymer, and this work could be extended.

CHAPTER 4: ARTICLE 1

CHAPTER 4 : ARTICLE 1

**Highlighting the Role of the Random Associating Block in the
Self-Assembly of Amphiphilic Block-Random Copolymers**

*Lionel Lauber, Christophe Chassenieux, Taco Nicolai and Olivier Colombani**

LUNAM Université, Université du Maine, IMMM-UMR CNRS 6283, Equipe Polymères,
Colloïdes et Interfaces, av. O. Messiaen, 72085 Le Mans cedex 9, France

AUTHOR EMAIL ADDRESS: olivier.colombani@univ-lemans.fr

CHAPTER 4: ARTICLE 1

ABSTRACT: pH-sensitive random $P(nBA_{1-x}\text{-stat-AA}_x)_{100}$ (MHx) and block-random $P(nBA_{1-x}\text{-stat-AA}_x)_{100}\text{-}b\text{-PAA}_{100}$ (DHx) amphiphilic copolymers have been synthesized, x standing for the molar ratios of pH-sensitive hydrophilic acrylic acid (AA) units statistically distributed with hydrophobic *n*-butyl acrylate (*n*BA) ones within the random block. Static and dynamic light scattering revealed that self-assembly of the random associating block (MHx) and block-random (DHx) copolymers is strongly affected by the pH and ionic strength of the solution, but also by the amount of AA units within the MHx blocks. Below a characteristic pH, MHx self-assembles into finite size spherical particles that grow in size with decreasing pH until they eventually become insoluble. DHx self-assembles into similar spherical particles, but the hydrophilic PAA₁₀₀ corona surrounding the MHx core prevents insolubility at low pH. Self-assembly of DHx at higher pH is fully correlated to that of the neat MHx blocks, indicating that it is possible to control precisely the extent of self-assembly of diblock copolymers by tuning the hydrophobic character of their associating block. Here, this was done by controlling the fraction of charged units within the random associating block.

KEYWORDS: Micelle, acrylic acid, *n*-butyl acrylate, stimuli responsive, gradient.

I. Introduction

Self-assembly of amphiphilic copolymers in aqueous solution has been studied intensively over the last few decades.^{1, 2} Their amphiphilic nature is due to the combination of hydrophobic and hydrophilic monomers within the same macromolecule. The hydrophobicity of the corresponding units can be permanent or tunable in a reversible way through external parameters such as pH and temperature.³ The distribution of hydrophilic and hydrophobic units within the polymer chain can vary between the two limiting cases of random and diblock copolymers; which plays a key role on the properties of the copolymer both in bulk and in solution.

Amphiphilic random copolymers are macromolecules in which hydrophobic and hydrophilic units are statistically distributed.⁴⁻⁶ This causes them to display average properties with respect to the two corresponding homopolymers in terms of glass transition temperature and mechanical properties in bulk⁷ or of LCST⁸ or UCST⁹ in solution. Studies of the self-assembly of such copolymers in aqueous solution have mainly been done in the past with hydrophobic polyelectrolytes, such as sulfonated polystyrene (PSS) or hydrophobically modified polyelectrolytes. Experimental work¹⁰⁻¹² in this field has been complemented with theoretical predictions.¹³⁻¹⁶ It has been shown that in dilute solution and at low ionic strength, the chains self-assemble and adopt a “pearl-necklace” morphology. Intermolecular aggregation has also been observed experimentally.^{6, 17-20} Copolymers that consist of short sequences of hydrophobic units separated by short sequences of charged hydrophilic units have also been studied as models for proteins.²¹⁻²⁴ It was shown that with an appropriate arrangement of the hydrophobic and charged sequences the polymer chains collapse into single-chain globules similar to the coil-to-globule transition of proteins.

Diblock copolymers consist of a pure hydrophilic block connected to a pure hydrophobic block.²⁵⁻²⁹ Once dispersed in solution, they may self-assemble into very well defined aggregates of various shapes. It must be noted though that most of these block copolymers lead to frozen aggregates, i.e. out of equilibrium nano-objects, whose characteristics depend both on thermodynamics and kinetics.³⁰ The reason is that a high glass transition temperature and/or a too strong hydrophobic character of the hydrophobic block inhibits its escape from the core of the aggregates.

Dynamic exchange can be induced by incorporating in a controlled way hydrophilic units within the hydrophobic associating block leading to amphiphilic block-random copolymers, i.e. block copolymers which contain at least one random block rather than only pure blocks.

CHAPTER 4: ARTICLE 1

This new type of amphiphilic copolymers combines the advantages of both extremes as recently reviewed in the literature.³¹ Their diblock architecture leads to the formation of well-defined aggregates, whereas the randomness of the associating block allows fine-tuning of the self-assembling properties.³²⁻³⁶ The block-random architecture has been used by Bendejacq³⁷, Wright³⁸, Gotzamanis³⁹ and ourselves^{40, 41} to control the structure and/or dynamics of self-assembly of amphiphilic block copolymers. In our research group we have studied diblock and triblock copolymers consisting of a pure hydrophilic poly(acrylic acid) (PAA) block connected respectively to one or two associating random blocks of *n*-butyl acrylate (*n*BA) and acrylic acid (AA): $P(nBA_{(1-x)}-stat-AA_x)_{100}-b-PAA_{100}$ (DHx) and $P(nBA_{(1-x)}-stat-AA_x)_{100}-b-PAA_{200}-P(nBA_{(1-x)}-stat-AA_x)_{100}$ (THx).^{40, 41} Pure $PnBA-b-PAA$ diblocks formed frozen aggregates^{42, 43} unable to exchange unimers due to the strong hydrophobic character of the pure *Pn*BA block, but DHx and THx formed aggregates with exchange rates that could be controlled by the pH.^{40, 41} Although preliminary results⁴⁴ highlighted the importance of *x*, the amount of charged units within the hydrophobic block of THx copolymers, there has been to the best of our knowledge only one investigation of the relationship between the self-assembly of a block-random copolymer (A-*co*-B)-*b*-B and that of its random associating block (A-*co*-B) by itself.³⁹ Here, we report on the self-assembly of three MHx with nearly identical degrees of polymerization and dispersity, but different AA contents and compare it to the self-assembly of corresponding diblock copolymers DHx consisting of the same MHx blocks connected to a PAA₁₀₀ block.

II. Materials and methods.

1. Synthesis of the copolymers. All copolymers have been synthesised following already published procedures,⁴⁰ see Figure 1. First, $P(nBA_{(1-x)}-stat-tBA_x)_{100}$ blocks with various molar ratios, *x*, of *tert*-butyl acrylate (*t*BA) were synthesized by Atom Transfer Radical Polymerization (ATRP). A fraction of these polymers were used as ATRP macroinitiators to yield $P(nBA_{(1-x)}-stat-tBA_x)_{100}-b-PtBA_{100}$ diblock copolymers in a second step. Finally, the *t*BA units of both the random $P(nBA_{(1-x)}-stat-tBA_x)_{100}$ and the block-random $P(nBA_{(1-x)}-stat-tBA_x)_{100}-b-PtBA_{100}$ copolymers were selectively and quantitatively acidolysed with trifluoroacetic acid (CF₃COOH) into AA units to yield MHx and DHx, respectively, where *x* was equal to 40, 50 or 60 %. Dispersity remained low for all copolymers ($\mathcal{D} \sim 1.1$), see section 1 of supporting information for more details.

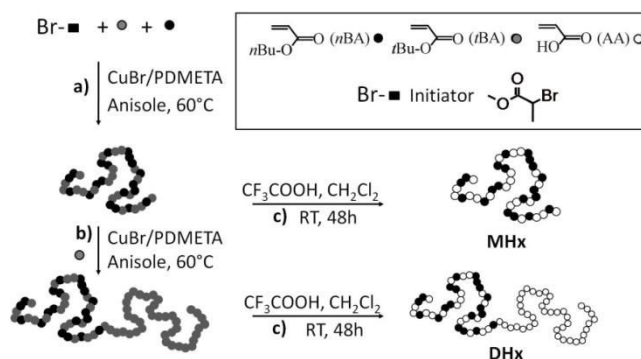


Figure 1. Steps of the synthesis of $P(nBA_{(1-x)}\text{-stat-AA}_x)_{100}$ (MHx) and of $P(nBA_{(1-x)}\text{-stat-AA}_x)_{100}\text{-b-P(AA)}_{100}$ (DHx) by Atom Transfer Radical Polymerization (ATRP): a) synthesis of the macroinitiator $P(nBA_{(1-x)}\text{-stat-tBA}_x)_{100}$ b) synthesis of the $P(nBA_{(1-x)}\text{-stat-tBA}_x)_{100}\text{-b-P(tBA)}_{100}$ diblock copolymers and c) acidolysis into MHx and DHx.

2. *Potentiometric Titration.* Potentiometric titration was done according to the procedure published in ref.⁴⁵ at room temperature with an automatic titrator (TIM 856, Radiometer Analytical) controlled by the TitrMaster 85 software. For each titration, 30 mL of polymer solution at an overall AA concentration $[AA] = 0.043$ mol/L and containing $[NaCl] = 0.1$ mol/L were first prepared by dissolving the polymer in the presence of 1.1 equivalent of sodium hydroxide (the NaCl concentration was adjusted with 4 M NaCl after the polymer was dissolved) and were then back titrated with HCl (1 M) at a rate of addition of 0.1 mL/min. From the titration data, the total amount of titrable AA units and the evolution of the pH of the solution as a function of its ionization degree $\alpha = [AA^-]/([AAH] + [AA^-])$ were determined, where $[AA^-]$ and $[AAH]$ are the concentrations of charged and protonated AA units, respectively. All acrylic acid units within a DHx copolymer could be ionized no matter whether they belonged to the pure PAA_{100} block or the statistical $P(nBA_{1-x}\text{-stat-AA}_x)_{100}$ block. However, the AA units within the PAA_{100} block are more acidic than those of the $P(nBA_{1-x}\text{-stat-AA}_x)_{100}$ block. It was shown that for a given overall ionization degree of the diblock (α_{DHx}) the specific ionization degree of the AA units within each block, α_{MHx} and α_{PAA} could be determined quantitatively.⁴⁵ Therefore, the fraction of charged units within the random associating block can be calculated as: $f_{MHx} = [AA^-]_{MHx}/([AA^-] + [AAH] + [nBA]_{MHx}) = x \cdot \alpha_{MHx}$.

3. *Sample Preparation.* For light scattering, stock solutions were prepared by dissolving the polymers with demineralized water (Millipore) in the presence of the required amount of NaOH to reach an ionization degree $\alpha \sim 0.9\text{-}1$ while stirring overnight. For the final solutions,

CHAPTER 4: ARTICLE 1

α was decreased by adding the desired amount of either a hydrochloric acid solution (HCl) or a freshly prepared solution of D-glucono- δ -lactone (GDL). D-glucono- δ -lactone is slowly hydrolyzed into gluconic acid, a weak acid with a pK_a of 3.4^{44, 46} which causes a decrease of α . The solutions were prepared at least 24 hours prior to measurements to insure full hydrolysis of GDL into gluconic acid. The fact that the acid-base reaction between GDL and DHx is no longer complete below $\alpha = 0.4$ was taken into account when lower values of α were targeted, see Supporting Information of ref⁴⁷ for details. For MHx the correction is necessary only below $\alpha = 0.2$ because MHx has a higher pK_a . The solutions were filtered through 0.2 μm pore size GHP Acrodisc filters. Solutions at lower concentrations were obtained by simple dilution of the stock solutions with filtered NaCl solutions at the proper NaCl concentration. The $[\text{Na}^+]$ was kept constant as explained previously.⁴¹

4. Light scattering. Light scattering measurements were performed at 20 °C with a standard ALV-CGS-8F system equipped with an ALV-5003 multi tau correlator system (ALV GmbH, Germany). A vertically polarised Helium-Neon laser with wavelength $\lambda=632.8$ nm was used as light source. Measurements were done at angles varying from 12 to 150° corresponding to scattering wave vectors ($q=4\pi n \sin(\theta/2)/\lambda$, with θ the angle of observation and n the refractive index of the solvent) ranging from 2.5×10^6 to 2.7×10^7 m^{-1} .

Dynamic light scattering. The measured normalized autocorrelation function of the scattered light intensity ($g_2(t)$) is related to the electric field autocorrelation function ($g_1(t)$) through the Siegert equation: $g_2(t)=1+\beta g_1^2(t)$, where β is the spatial coherence factor.⁴⁸ The electric field autocorrelation function $g_1(t)$ was analyzed in terms of a relaxation time (τ) distribution ($A(\tau)$) using the REPES routine.

$$g_1(t) = \int A(\tau) \exp(-t/\tau) d\tau \quad (1)$$

The calculated average relaxation rate was q^2 -dependent indicating cooperative diffusion of the solute and the diffusion coefficient was calculated as $D_c = \langle \tau^{-1} \rangle / q^2$. The z-average hydrodynamic radius of the solute was calculated from D_c in dilute solution using the Stokes-Einstein equation:

$$R_h = \frac{kT}{6\pi\eta D_c} \quad (2)$$

with k Boltzmann's constant and η the viscosity of the solvent.

For DHx solutions a second slow relaxation mode was sometimes observed that was caused by the scattering of a small weight fraction of large particles (spurious scatterers).⁴¹

Static light scattering. The Rayleigh ratio, R_θ , was calculated as:

$$R_\theta = \frac{I_{\text{solution}}(\theta) - I_{\text{solvent}}(\theta)}{I_{\text{toluene}}(\theta)} \left(\frac{n_{\text{solvent}}}{n_{\text{toluene}}} \right)^2 R_{\text{toluene}} \quad (3)$$

where I_{solution} , I_{solvent} , and I_{toluene} are the average intensities scattered, respectively, by the solution, the solvent, and the reference (toluene). The refractive index of the solvent (water) and the reference are $n_{\text{solvent}}=1.333$ and $n_{\text{toluene}}=1.496$ and the Rayleigh ratio of the reference is $R_{\text{toluene}}=1.35 \times 10^{-5} \text{ cm}^{-1}$. When a slow mode was observed in DLS, R_θ was corrected for the contribution of the spurious scatterers by multiplying it with the relative amplitude of the fast mode.⁴⁹

The apparent molar mass (M_{app}) of the solute was calculated from the Rayleigh ratio of the solution as:

$$R_\theta = K \cdot C \cdot M_{\text{app}} \cdot S(q) \quad (4)$$

where $S(q)$ is the structure factor and K a constant:

$$K = \frac{4\pi^2 n_{\text{solvent}}^2}{\lambda^4 N_a} \left(\frac{\partial n}{\partial C} \right)^2 \quad (5)$$

Here N_a is Avogadro's number and $\partial n / \partial C$ is the specific refractive index increment of the solute. For all systems studied here $S(q)$ was close to unity over the whole q -range investigated. M_{app} is equal to the weight average molar mass (M_w) in dilute solution when interactions can be neglected.

Specific refractive index increment measurement. dn/dc has been measured with a differential refractometer, Optilab rEX Wyatt-822, equipped with a laser light source ($\lambda=633 \text{ nm}$). The refractive index was determined for each polymer at five concentrations between 1 and 5 g/L in the presence of 0.1 or 0.5 mol/L NaCl.

The specific refractive index increment was found to depend linearly on the overall fraction of charged AA units: $dn/dc=0.126+0.10 \cdot f_{\text{AA}^-}$ at 0.1 M NaCl and $dn/dc=0.121+0.051 \cdot f_{\text{AA}^-}$ at 0.5 M NaCl, see Figure 2, with $f_{\text{AA}^-} = [\text{AA}^-]/([\text{AA}^-] + [\text{AAH}] + [n\text{BA}])$. In first approximation, the increase of dn/dc with increasing charge density can be explained by the contribution of the sodium counterions to the refractive index. The dependence of dn/dc on α was stronger than for pure PAA reported in the literature by Kitano et al.⁵⁰, see dashed lines in Figure 2.

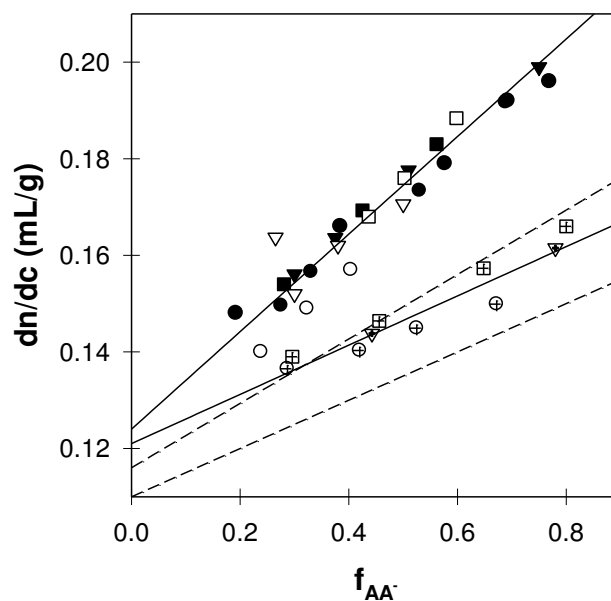


Figure 2. Evolution of the specific refractive index increment over the fraction of charged AA units for MH40 (○), MH50 (▽), MH60 (□), DH40 (●), DH50 (▼) and DH60 (■) at $[\text{Na}^+] = 0.1$ mol/L and DH40 (⊕), DH50 (▽), and DH60 (⊞) at $[\text{Na}^+] = 0.5$ mol/L. The solid line corresponds to $\text{dn}/\text{dc} = 0.126 + 0.101 \cdot f_{\text{AA}}$ and $\text{dn}/\text{dc} = 0.121 + 0.051 \cdot f_{\text{AA}}$. The dashed line corresponds to the evolution reported for PAA in the literature at the same NaCl concentrations.⁵⁰

III. Results and discussion.

1. Statistical $\text{P}(n\text{BA}_{(1-x)\text{-stat-AA}_x})_{100}$ blocks (MH x)

1.1. MH50

In first instance, self-assembly in aqueous solution of $\text{P}(n\text{BA}_{50\%\text{-stat-AA}_{50\%})_{100}$ (MH50) has been studied as a function of both α and polymer concentration. NaCl was added to all solutions to maintain a constant Na^+ concentration of 0.1 M. This value was chosen as a compromise between suppressing the polyelectrolyte effect classically observed in light scattering for salt-free polyelectrolyte solutions⁵¹ and limiting macroscopic phase separation which occurs at low α and high ionic strength (see below and Supporting Information in section 2, Figure S1-4).

For $\alpha \geq 0.7$, the weight average molar mass of the scatterers ($M_w = 1.2 \times 10^4$ g/mol), corresponding to their apparent molecular weight M_{app} at low concentrations where interactions can be neglected, corresponded to that of the unimers ($M_w(\text{MH50}) = 1.1 \times 10^4$ g/mol), indicating that MH50 was not aggregated at these ionization degrees, see Figure 3.

For $\alpha = 0.9$, M_{app} decreased while the concentration increased due to repulsive interactions between unimers. For $0.7 \geq \alpha \geq 0.3$, M_{app} was independent of the polymer concentration up to 30 g/L. This behavior is in contrast with that of DH50 for which strong repulsive interactions were observed above 5 g/L.⁴¹ The difference between MH50 and DH50 can be understood by the fact that the aggregates formed by MH50 lack the PAA corona of DH50 which generates much stronger steric and electrostatic repulsive interactions between aggregates.

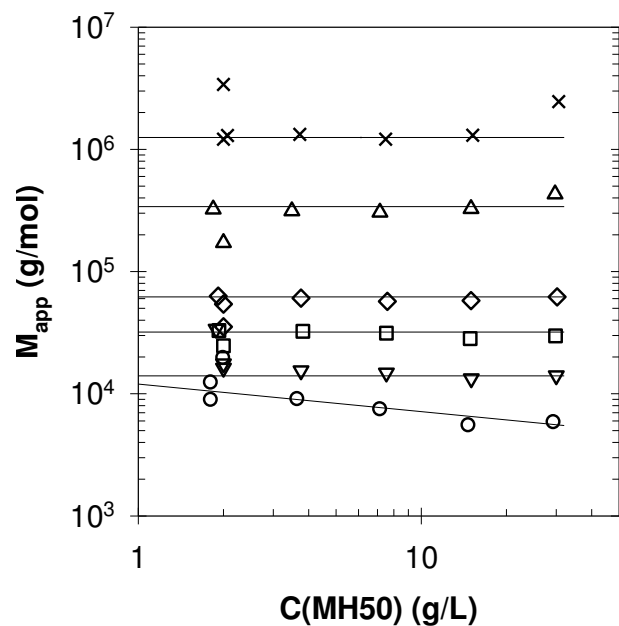


Figure 3. Concentration dependence of the apparent molar mass M_{app} for MH50 at $\alpha=0.9$ (○), 0.7 (▽), 0.6 (□), 0.5 (◇), 0.4 (△) and 0.3 (×) in the presence of 0.1 M Na^+ . The solid lines are guides to the eye.

Figure 4 shows that M_w increased when α decreased below 0.7, revealing a progressive association of the unimers. The size of the aggregates increased sharply with decreasing α and diverged at $\alpha = 0.3$. At lower charge densities, electrostatic interaction was no longer sufficient to limit the growth of the aggregates and the polymer precipitated.

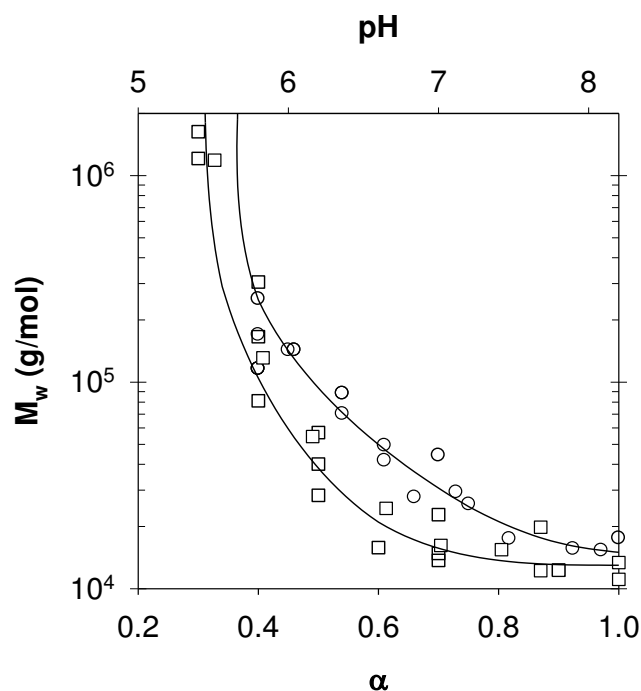


Figure 4. Dependence of the molar mass on the degree of ionization for MH50 at 0.1 (\square) and 0.5 (\circ) mol/L Na^+ . The solid lines are guides to the eye.

Figure 5 shows that the dependence of the hydrodynamic radius (R_h) on M_w is compatible with spherical objects ($R_h \sim M_w^{1/3}$) with a density of 0.5-1 g/mL. The density of the particles was smaller than that of PnBA ($\rho_{\text{PnBA}} = 1.04 \text{ g/mL}^{42}$) or of PAA ($\rho_{\text{PAA}} > 1.2 \text{ g/mL}^{52}$), indicating that they contained water.

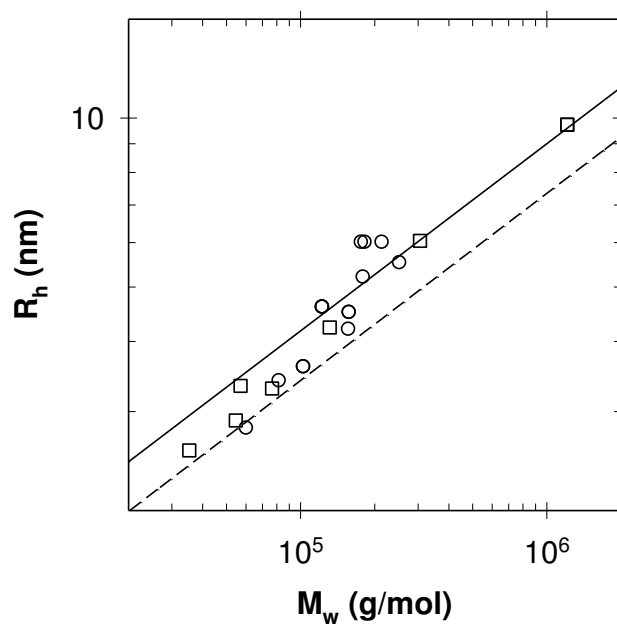


Figure 5. Dependence of the hydrodynamic radius R_h as a function of M_w for MH50 at 0.1 (\square) and 0.5 (\circ) mol/L Na^+ . The solid and dashed lines represent $R_h \propto M_w^{1/3}$ with densities 0.5 g/mL and 1 g/mL, respectively.

Formation of finite size aggregates has already been observed for colloidal and associating polyelectrolytes systems^{16, 21, 53-58} and can be rationalized as follows. The n BA units within MH50 chains are not soluble in water and trigger the aggregation. However, the latter leads to increasing electrostatic interactions between the charged AA units, which is reduced by condensation of Na^+ counter ions causing a loss of translational entropy. The equilibrium size of the aggregates is determined by the balance between the hydrophobic interactions of n BA units and the charge accumulation and will therefore increase with decreasing charge density of MH50. The equilibrium size did not depend on the polymer concentration, at least between 2 and 30 g/L implying that the contribution of translational entropy of the polymers was not significant in this concentration range.

The self-assembly of MH50 was also studied at $[\text{Na}^+] = 0.5$ M, see Figure 4. Qualitatively, the behavior of MH50 at this ionic strength was similar to what was observed at $[\text{Na}^+] = 0.1$ M. However, the size of the aggregates for a given α was larger and macroscopic precipitation started at a slightly higher α . A more detailed description of the effect of $[\text{Na}^+]$ on the aggregation of MH50 is given in the section 2 of the Supporting Information (Figure S1). For a given value of α the aggregate size increased with increasing ionic strength and precipitation was observed above a critical salt concentration. Qualitatively, these effects of increasing salt concentration can be understood by screening of electrostatic interaction and reduction of the loss of translational entropy of the counterions.

1.2. Effect of the fraction of charged units: MH40, MH50 and MH60

The self-assembly of MH50 was compared to that of MH40 and MH60 at $[\text{Na}^+] = 0.1$ M, see Figure 6a. Note that the three MHx differ only by their molar content x of AA units within the polymer while degrees of polymerization, distributions of the units within the chains and dispersities are nearly identical. The three MHx showed the same trends. At high ionization degree, the chains were present as unimers. With decreasing α , self-assembly occurred leading to an increase of M_w with no dependence of M_{app} on the polymer concentration up to at least 30 g/L (see Figure S5-6 in the section 3 of Supporting Information). Finally, a sharp

increase of M_w occurred close to a characteristic ionization degree below which the polymer precipitated.

Quantitatively, the self-assembly of MHx was strongly dependent on its AA content as the evolution of M_w vs. α shifted to higher α (i.e. higher pH) when x decreased, see Figure 6a. In other words, for the same ionization degree the aggregation number increased when the AA content decreased. Moreover, precipitation of the polymer occurred at higher α when x was lowered. The effect of x can be understood by plotting the evolution of M_w as a function of the fraction of charged units within the MHx ($f_{MHx} = x.\alpha$), see Figure 6b. In this representation, the curves are much closer which shows that the fraction of charged units is a key parameter controlling the self-assembly of these polymers. Of course, the contribution of the hydrophobic nBA units is different from that of the hydrophilic uncharged AA units, which probably explains why the curves of MH40, MH50 and MH60 do not fully superimpose in this representation.

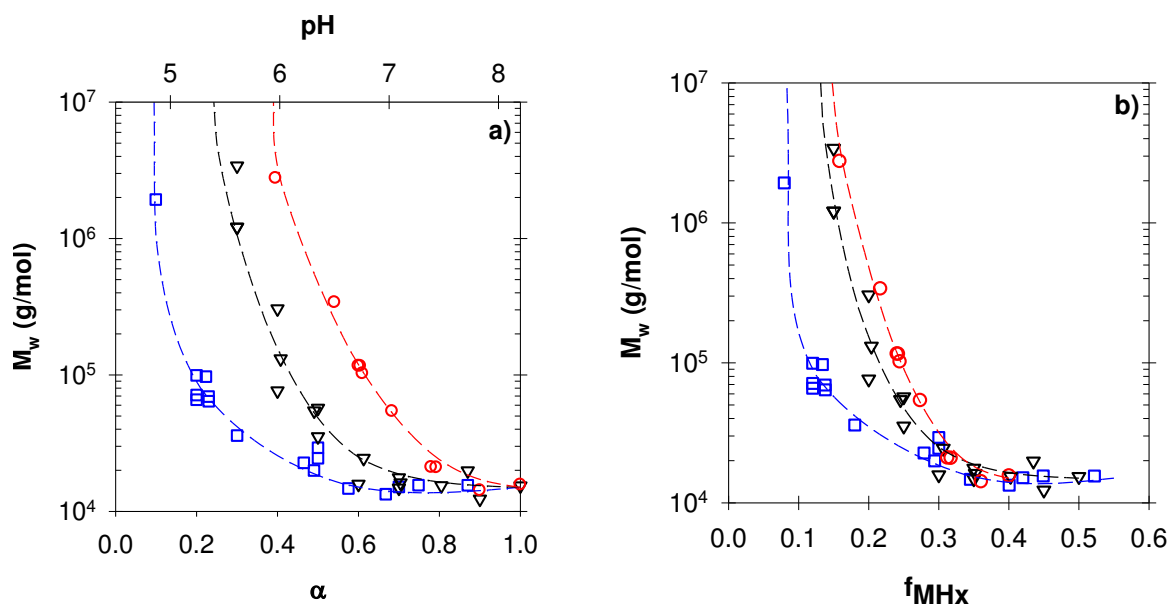


Figure 6. Dependence of M_w on the degree of ionization (a) on the fraction of charged units (b) for MH40 (○) MH50 (▽) and MH60 (□) at 0.1 M Na^+ . The dashed lines are guides to the eye.

2. $P(n\text{BA}_{(1-x)\text{-stat-AA}_x})_{100}\text{-}b\text{-PAA}_{100}$ diblock copolymers (DHx)

The self-assembly of the DHx diblock copolymers has been studied as a function of both α and polymer concentration at $[\text{Na}^+] = 0.1$ M in order to compare the behavior of these polymers with that of their random associating block (MHx). The concentration dependence

of M_{app} is shown in section 3 of Supporting Information, Figure S7-S8. In Figure 7, M_w and R_h of the three DHx samples are plotted as a function of α_{DHx} . Let us focus first on DH50. This diblock copolymer remained in the form of unimers for $\alpha_{DH50} \geq 0.6$. Below $\alpha_{DH50} = 0.6$, DH50 self-assembled into aggregates with a size that increased with decreasing α_{DH50} . The behavior of the other DHx is qualitatively equivalent. Similar to MHx, the increase of the aggregate size started at higher α_{DHx} when x decreased. However, whereas MHx precipitated below a characteristic value of α_{MHx} , for DHx the growth of the aggregate size with decreasing α_{DHx} stagnated.

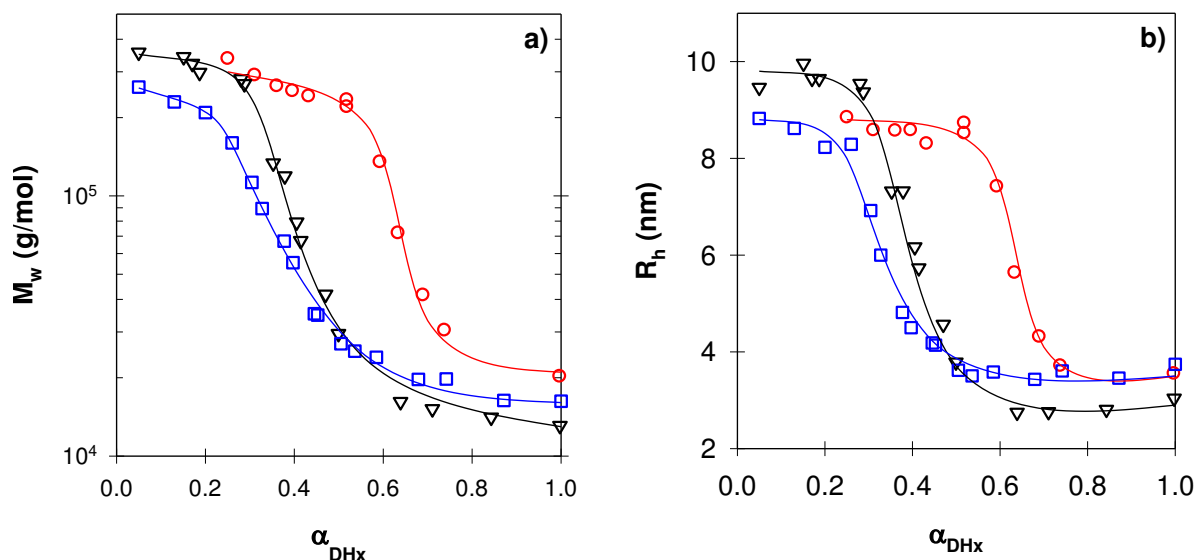


Figure 7. Dependence of M_w (a) and R_h (b) on the ionization degree for DH40 (\circ), DH50 (∇) and DH60 (\square) at $[Na^+] = 0.1$ M. The solid lines are guides to the eye.

3. Comparison of MHx and DHx

We have shown above that the self assembly of MHx was to a large extent controlled by their charge density. We suspected that the relevant parameter for the self assembly of DHx was the charge density of the random associating MHx block. Therefore we have compared the aggregation number ($N_{agg} = M_w/M_{uni}$) of DHx as a function of the ionization degree of their MHx block (α_{MHx}) with that of neat MHx blocks. Potentiometric titration was used to deduce α_{MHx} as a function of the ionization degree of DHx (α_{DHx}), see Supporting Information for details (section 4, Figure S9). The aggregation numbers of DHx and MHx are plotted in Figure 8 as a function of α_{MHx} . The key result displayed in Figure 8 is that the self-assembly

of the block random copolymers (DHx) and that of the neat random associating blocks (MHx) roughly occur for the same ionization degree of the MHx block (α_{MHx}). This implies that the self-assembly of the DHx random block copolymers can be understood and controlled through the behavior of their MHx random block. A similar close correlation was reported by Gotzamanis et al. who compared the temperature dependent self-assembly of individual thermo-sensitive random blocks with that of the corresponding block-random copolymers.³⁹ In spite of the strong correlation between the self-assembly of the MHx and that of the DHx, there are some quantitative differences. The increase of N_{agg} with decreasing α_{MHx} started systematically at lower values of α_{MHx} for DHx than for MHx. The implication is that the self-assembly of the hydrophobic block in DHx is slightly hindered by the presence of the PAA corona. In addition, as we noted above, the presence of the corona inhibited large scale aggregation and precipitation at low α_{MHx} as was earlier shown by Ward et al.⁵⁹ who compared random and triblock pH and thermosensitive amphiphilic copolymers.

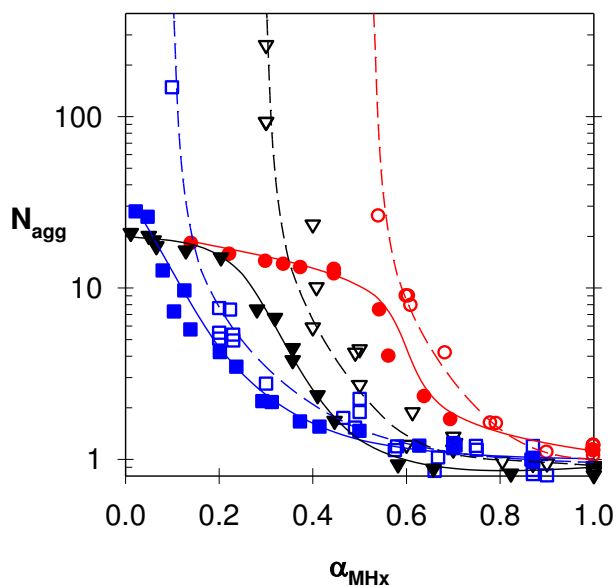


Figure 8. Evolution of the aggregation number of MHx (MH40:○, MH50:▽, MH60:□) and DHx (DH40:● DH50:▼ DH60:■) as a function of the ionization degree of MHx blocks. The lines are guides to the eye, diblocks (solid lines) random associating blocks (dashed lines).

IV. Conclusions

PAA with hydrophobic *n*BA units randomly distributed within the chain self-assembled below a certain degree of ionization into stable spherical aggregates. Their aggregation

number increased with decreasing α (resp. pH) and diverged at a characteristic value below which the polymers were no longer soluble. The association behavior shifted to higher α when more *n*BA were incorporated in the random associating block and can for a large part be understood in terms of the total fraction of charged units (= charge density). The charge density can be varied by varying the pH or the fraction of *n*BA units within the random copolymer. The effect of the pH on the self-assembly can therefore be controlled by varying the fraction of *n*BA units.

If the same random block MHx was attached to a PAA chain, it was observed that the self-assembly of the resulting block-random copolymer DHx was strongly correlated to that of the single MHx blocks. It demonstrates that it is possible to control and predict the pH dependent self-assembly of block-random copolymers by studying the behavior of their neat associating block. Small differences were however observed between the behavior of the MHx block and that of the DHx. In the block random copolymers, self-assembly indeed occurred at slightly lower charge densities of the MHx block than when this block was not connected to a PAA hydrophilic block. In addition, for the DHx, the increase of the aggregation number stagnated at lower α due to the presence of the polyelectrolyte corona.

We believe that the present results obtained on block random copolymers are relevant also for gradient amphiphilic copolymers, because block random copolymers may be considered as gradient copolymers with an extreme strength of the gradient of composition.⁶⁰ Reports in the literature have shown that the control of the gradient strength was an elegant way of driving the self-assembly of such amphiphilic copolymers.⁶¹⁻⁶³

ASSOCIATED CONTENT

Details on synthesis, titration, phase separation and polymer concentration effect are available in Supporting Information. This material is available free of charge via the Internet at <http://pubs.acs.org>.

CHAPTER 4: ARTICLE 1

REFERENCES

1. Madsen, J.; Armes, S. P. *Soft Matter* **2012**, 8, (3), 592-605.
2. Tsitsilianis, C. *Soft Matter* **2010**, 6, (11), 2372-2388.
3. Bajpai, A. K.; Bajpai, J.; Saini, R.; Gupta, R. *Polym. Rev.* **2011**, 51, (1), 53-97.
4. Guo, P.; Guan, W.; Liang, L.; Yao, P. *J. Colloid Interface Sci.* **2008**, 323, (2), 229-234.
5. Karayianni, M.; Mountrichas, G.; Pispas, S. *J. Phys. Chem. B* **2010**, 114, (33), 10748-10755.
6. Li, L.; Raghupathi, K.; Song, C.; Prasad, P.; Thayumanavan, S. *Chem. Commun.* **2014**, 50, (88), 13417-13432.
7. Penzel, E.; Rieger, J.; Schneider, H. A. *Polymer* **1997**, 38 (2), 325-337.
8. Lutz, J.-F.; Akdemir, ö.; Hoth, A. *J. Am. Chem. Soc.* **2006**, 128, (40), 13046-13047.
9. Seuring, J.; Agarwal, S. *Macromolecules* **2012**, 45, 3910-3918.
10. Baigl, D.; Ober, R.; Qu, D.; Fery, A.; Williams, C. E. *Europhys. Lett.* **2003**, 62, (4), 588.
11. Baigl, D.; Sferrazza, M.; Williams, C. E. *Europhys. Lett.* **2003**, 62, (1), 110.
12. Laschewsky, A., Molecular concepts, self-organisation and properties of polysoaps. In *Polysoaps/Stabilizers/Nitrogen-15 NMR*, Springer Berlin Heidelberg: 1995; Vol. 124, pp 1-86.
13. Dobrynin, A. V.; Rubinstein, M. *Macromolecules* **1999**, 32, (3), 915-922.
14. Dobrynin, A. V.; Rubinstein, M. *Macromolecules* **2000**, 33, (21), 8097-8105.
15. Dobrynin, A. V.; Rubinstein, M. *Macromolecules* **2001**, 34, (6), 1964-1972.
16. Vasilevskaya, V. V.; Klochkov, A. A.; Lazutin, A. A.; Khalatur, P. G.; Khokhlov, A. R. *Macromolecules* **2004**, 37, (14), 5444-5460.
17. Dutta, P.; Dey, J.; Ghosh, G.; Nayak, R. R. *Polymer* **2009**, 50, (6), 1516-1525.
18. Petit-Agnely, F.; Iliopoulos, I.; Zana, R. *Langmuir* **2000**, 16, (25), 9921-9927.
19. Sato, Y.; Hashidzume, A.; Morishima, Y. *Macromolecules* **2001**, 34, (17), 6121-6130.
20. Wu, X.; Qiao, Y.; Yang, H.; Wang, J. *J. Colloid Interface Sci.* **2010**, 349, (2), 560-564.
21. Murnen, H. K.; Khokhlov, A. R.; Khalatur, P. G.; Segalman, R. A.; Zuckermann, R. N. *Macromolecules* **2012**, 45, (12), 5229-5236.
22. Ashbaugh, H. S. *J. Phys. Chem. B* **2009**, 113, (43), 14043-14046.
23. Khokhlov, A. R.; Khalatur, P. G. *Curr. Opin. Colloid Interface Sci.* **2005**, 10, (1-2), 22-29.

24. Lozinsky, V. I., In *Conformation-Dependent Design of Sequences in Copolymers II*, Khokhlov, A. R., Ed. Springer-Verlag Berlin: Berlin, 2006; Vol. 196, pp 87-127.
25. Riess, G. *Prog. Polym. Sci.* **2003**, 28, (7), 1107-1170.
26. Borisov, O. V.; Zhulina, E. B.; Leermakers, F. M.; Müller, A. E., In *Self Organized Nanostructures of Amphiphilic Block Copolymers I*, Springer Berlin Heidelberg: 2011; Vol. 241, pp 57-129.
27. Nakashima, K.; Bahadur, P. *Adv. Colloid Interface Sci.* **2006**, 123-126, (0), 75-96.
28. Rodriguez-Hernandez, J.; Checot, F.; Gnanou, Y.; Lecommandoux, S. *Prog. Polym. Sci.* **2005**, 30, (7), 691-724.
29. Mai, Y.; Eisenberg, A. *Chem. Soc. Rev.* 41, (18), 5969-5985.
30. Nicolai, T.; Colombani, O.; Chassenieux, C. *Soft Matter* **2010**, 6, (14), 3111-3118.
31. Tsitsilianis, C.; Gotzamanis, G.; Iatridi, Z. *Eur. Polym. J.* **2011**, 47, (4), 497-510.
32. Soledad Lencina, M. M.; Iatridi, Z.; Villar, M. A.; Tsitsilianis, C. *Eur. Polym. J.* **2014**, 61, 33-44.
33. Iatridi, Z.; Mattheolabakis, G.; Avgoustakis, K.; Tsitsilianis, C. *Soft Matter* **2011**, 7, (23), 11160-11168.
34. Liu, H.; Guo, Z.; He, S.; Yin, H.; Fei, C.; Feng, Y. *Polym. Chem.* **2014**, 5, (16), 4756-4763.
35. Wang, W.; Liu, H.; Mu, M.; Yin, H.; Feng, Y. *Polym. Chem.* **2015**, 6, (15), 2900-2908.
36. Jin, N.; Zhang, H.; Jin, S.; Dadmun, M. D.; Zhao, B. *Macromolecules* **2012**, 45, (11), 4790-4800.
37. Bendejacq, D. D.; Ponsinet, V.; Joanicot, M. *Langmuir* **2005**, 21, (5), 1712-1718.
38. Wright, D. B.; Patterson, J. P.; Pitto-Barry, A.; Cotanda, P.; Chassenieux, C.; Colombani, O.; O'Reilly, R. K. *Polym. Chem.* **2015**, (6), 2761-2768.
39. Gotzamanis, G.; Tsitsilianis, C. *Polymer* **2007**, 48, (21), 6226-6233.
40. Charbonneau, C.; Chassenieux, C.; Colombani, O.; Nicolai, T. *Macromolecules* **2011**, 44, (11), 4487-4495.
41. Charbonneau, C.; Lima, M. M. D.; Chassenieux, C.; Colombani, O.; Nicolai, T. *Phys. Chem. Chem. Phys.* **2013**, 15, (11), 3955-3964.
42. Colombani, O.; Ruppel, M.; Burkhardt, M.; Drechsler, M.; Schumacher, M.; Gradzielski, M.; Schweins, R.; Müller, A. H. E. *Macromolecules* **2007**, 40, (12), 4351-4362.
43. Jacquin, M.; Muller, P.; Cottet, H.; Theodoly, O. *Langmuir* **2010**, 26, (24), 18681-18693.

CHAPTER 4: ARTICLE 1

44. Shedje, A.; Colombani, O.; Nicolai, T.; Chassenieux, C. *Macromolecules* **2013**, 47, (7), 2439-2444.
45. Colombani, O.; Lejeune, E.; Charbonneau, C.; Chassenieux, C.; Nicolai, T. *J. Phys. Chem. B* **2012**, 116, (25), 7560-7565.
46. Pocker, Y.; Green, E. *J. Am. Chem. Soc.* **1973**, 95, (1), 113-119.
47. Klymenko, A.; Nicol, E.; Nicolai, T.; Colombani, O. *Macromolecules*, revision submitted to journal.
48. Pecora, R., In *Dynamic Light Scattering: With Applications to Chemistry, Biology, and Physics*, Berne, B., Ed. John Wiley Sons, Inc.: Oxford, 1976; pp 245-275.
49. Chassenieux, C.; Nicolai, T.; Durand, D. *Macromolecules* **1997**, 30, (17), 4952-4958.
50. Kitano, T.; Taguchi, A.; Noda, I.; Nagasawa, M. *Macromolecules* **1980**, 13, (1), 57-63.
51. Borukhov, I.; Andelman, D.; Borrega, R.; Cloitre, M.; Leibler, L.; Orland, H. *J. Phys. Chem. B* **2000**, 104, (47), 11027-11034.
52. Bendejacq, D. D.; Ponsinet, V. *J. Phys. Chem. B* **2008**, 112, (27), 7996-8009.
53. Khokhlov, A. R.; Khalatur, P. G. *Curr. Opin. Colloid Interface Sci.* **2005**, 10, (1&2), 22-29.
54. Potemkin, II; Vasilevskaya, V. V.; Khokhlov, A. R. *J. Chem. Phys.* **1999**, 111, (6), 2809-2817.
55. Lu, P. J.; Conrad, J. C.; Wyss, H. M.; Schofield, A. B.; Weitz, D. A. *Phys. Rev. Lett.* **2006**, 96, (2), 028306.
56. Sciortino, F.; Tartaglia, P. *Adv. Phys.* **2005**, 54, (6-7), 471-524.
57. Sciortino, F.; Tartaglia, P.; Zaccarelli, E. *J. Phys. Chem. B* **2005**, 109, (46), 21942-21953.
58. Limberger, R. E.; Potemkin, I. I.; Khokhlov, A. R. *J. Chem. Phys.* **2003**, 119, (22), 12023-12028.
59. Ward, M. A.; Georgiou, T. K. *J. Polym. Sci., Part A: Polym. Chem.* **2013**, 51, 2850-2859.
60. Mok, M. M.; Pujari, S.; Burghardt, W. R.; Dettmer, C. M.; Nguyen, S. T.; Ellison, C. J.; Torkelson, J. M. *Macromolecules* **2008**, 41, 5818-5829.
61. Gallow, K. C.; Jhon, Y. K.; Genzer, J.; Loo, Y.-L. *Polymer* **2012**, 53, (5), 1131-1137.
62. Okabe, S.; Seno, K.-i.; Kanaoka, S.; Aoshima, S.; Shibayama, M. *Macromolecules* **2006**, 39, 1592-1597.
63. Zhao, Y.; Luo, Y.-W.; Li, B.-G.; Zhu, S. *Langmuir* **2011**, 27, 11306-11315.

Supporting information of article 1

Highlighting the Role of the Random Associating Block in the Self-Assembly of Amphiphilic Block-Random Copolymers

*Lionel Lauber, Christophe Chassenieux, Taco Nicolai and Olivier Colombani**

1) Synthesis

The synthesis of MH50 and DH50 by ATRP was already described¹⁻². The synthesis of the other $P(nBA_{(1-x)-stat-AA_x})_{100}$ (MHx) and $P(nBA_{(1-x)-stat-AA_x})_{100}-b-PAA_{100}$ (DHx), where x stands for the percentage of acrylic acid units in the hydrophobic block, was adapted from that of MH50 and DH50.

Briefly, methyl 2-bromopropionate (MBP), a monofunctional initiator, was used to prepare a monofunctional macroinitiator poly(*n*-butyl acrylate_(1-x)-*stat*-*tert*-butyl acrylate_x)₁₀₀-Br, $P(nBA_{(1-x)-stat-tBA_x})_{100}$ -Br. N,N,N',N',N''-pentamethyldiethyltriamine (PMDETA)/CuBr was used as catalyst in the following proportions: [nBA]:[tBA]:[MBP]:[CuBr]:[CuBr₂]:[PMDETA] = 100*(1-x):100*x:1:0.7:0.035:0.74. Anisole (monomers/anisole = 90/10 g/g) was used both as solvent and as internal standard to determine the monomer conversion by gas chromatography during the polymerization.³⁻⁴ The polymerization was allowed to proceed at 60°C until a conversion of 50%. The reaction was then stopped and the polymer was purified by column chromatography (silica/CHCl₃) followed by precipitation into methanol/water (90/10 vol/vol). Size exclusion chromatography (SEC) and ¹H NMR were used to characterise the polymer confirming its chemical structure as shown in Table S1.

To produce a $P(nBA_{(1-x)-stat-tBA_x})_{100}-b-PAA_{100}$ -Br diblock copolymer, the aforementioned macroinitiator $P(nBA_{(1-x)-stat-tBA_x})_{100}$ -Br was used to initiate the polymerisation of *tert*-butyl acrylate using the following proportions of reagents: [tBA]:[macroinitiator]:[CuBr]:[CuBr₂]:[PMDETA] = 200:1:0.7:0.035:0.74 and a monomer/anisole ratio of 90/10 g/g. After polymerization at 60°C, the reaction was again stopped at 50% conversion and purification was achieved as for the first block. The final step used trifluoroacetic acid to selectively and quantitatively transform the *tert*-butyl acrylate units into acrylic acid units by acidolysis.⁵ The MHx and DHx were obtained by respectively

CHAPTER 4: ARTICLE 1

acidolysing the corresponding $P(nBA_{(1-x)}-stat-tBA_x)_{100}-Br$ macroinitiator or the $P(nBA_{(1-x)}-stat-tBA_x)_{100}-b-PAA_{100}-Br$ diblock. After acidolysis, purification was done by precipitation into pentane. The final polymers were characterized by 1H , ^{13}C NMR and by titration, confirming quantitative and selective acidolysis.

1H , ^{13}C NMR spectra were recorded at 20 °C on a Brüker AC400 (400 MHz) spectrometer using $CDCl_3$, MeOD or THF- D_8 .

Size exclusion chromatography analysis was done with an equipment consisting of a guard column (5 μm , 50 mm \times 7.5 mm) connected to a PLgel Mixed-D column (5 μm , 300 mm \times 7.5 mm) and a PLgel "individual pore size" column (5 μm , 50 mm \times 7.5 mm) operating at room temperature in THF with a flow rate of 1 mL.min $^{-1}$. After filtration through a 0.2 μm pore size membrane, injection was done at a polymer concentration of ~ 5 mg.mL $^{-1}$ in THF. In all cases except DH50 which had been synthesized and analyzed previously, absolute average molar masses were calculated using a light scattering (miniDAWN TREOS from Wyatt) and an Online refractive index (RID10A from Shimadzu) detectors with a specific refractive index increment of the polymer in THF of 0.057 mL/g.³ For the precursor of DH50, molecular weights were determined as PS-equivalents using PS-standards for calibration of the SEC.

Table S1. Characteristics of the copolymers synthesized. ^a Theoretical M_n calculated from the conversion. ^b Theoretical M_n calculated assuming 100% acidolysis.

Name	Before acidolysis			After acidolysis
	$M_{n,theo}$ (g/mol) ^a	$M_{n,SEC}$ (g/mol)	\bar{D}	$M_{n,theo}$ (g/mol) ^b
MH40	1.22×10^4	1.25×10^4	1.17	1.00×10^4
MH50 ^c	1.28×10^4	1.25×10^4	1.10	1.00×10^4
MH60	1.26×10^4	1.36×10^4	1.34	1.03×10^4
DH40	2.55×10^4	2.52×10^4	1.17	1.74×10^4
DH50	2.54×10^4	2.56×10^4	1.10 ^c	1.72×10^4
DH60	2.50×10^4	2.72×10^4	1.13	1.59×10^4

2) Phase separation

Figure S1, Figure S2 and Figure S3 represent the dependences of M_w on the concentration of Na^+ at several ionization degrees at $C=2$ g/L, for MH50, MH40 and MH60, respectively. It appears that adding salt has two effects on MHx. It causes an increase of the aggregation

number at a given ionization degree and decreases the solubility of the polymer. For MH50, the aggregation number increases with increasing $[\text{Na}^+]$ at $\alpha=0.5$ and 0.7 until precipitation. However, at $\alpha=1$ unimers are present at all $[\text{Na}^+]$ until the system phase separates for $[\text{Na}^+]>1.5$ M.

There is a threshold value of $[\text{Na}^+]$ for each ionisation degree at which the polymer precipitated, characterized by clouding of the solutions. This critical value is represented as dashed lines and it decreases with the decrease of α . Phase separation leads to the formation of a viscous bottom phase containing most of the polymer. Light scattering measurements showed that the top phase contained a small amount of polymer at least just above the critical value (data not shown).

The salt induced phase separation occurred at different ionization degrees depending on x . The phase diagram of MH x as a function of $[\text{Na}^+]$ and the ionization degree is shown in Figure S4a. As might be expected a decrease in the fraction of AA units x favours phase separation.

The phase diagram of the MH x as a function of $[\text{Na}^+]$ and the fraction of charged units is shown in Figure S4b. Good correlation is found between $[\text{Na}^+]$ and the fraction of charged units for the three copolymers, demonstrating that the solubility of MH x is principally controlled by the charge density. The maximum fraction of charged units ($f_{\text{MH}x}$) when $\alpha=1$ is indicated by dashed lines on Figure S4b.

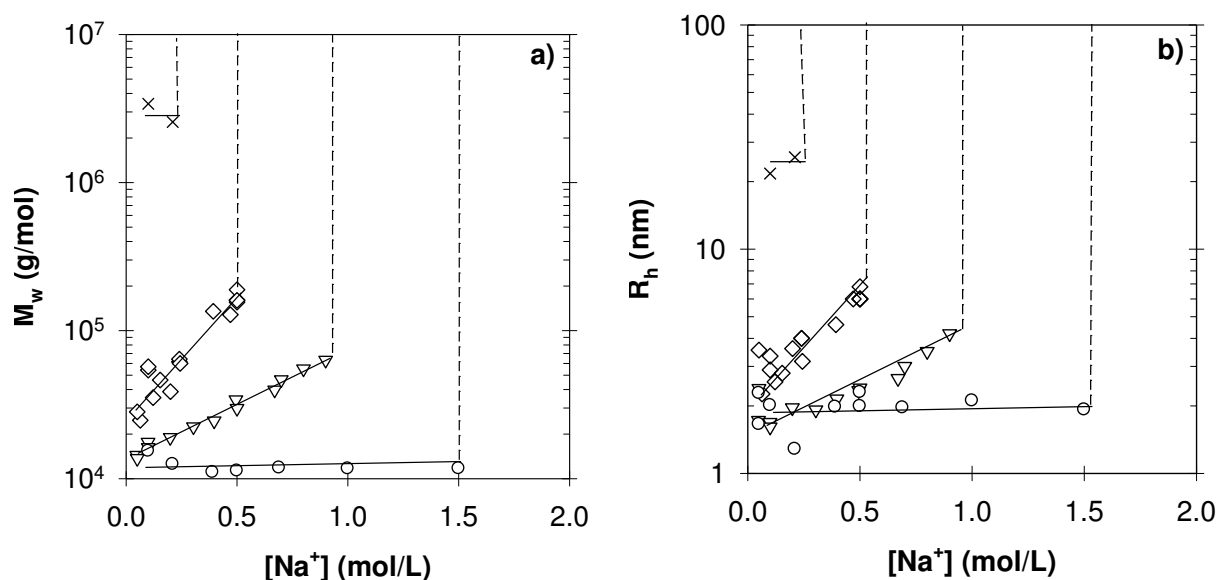


Figure S1. Molar mass M_w (a) and hydrodynamic radius R_h (b) as a function of the concentration of Na^+ for MH50 at 2 g/L and $\alpha=1$ (\circ), 0.7 (∇), 0.5 (\diamond) and 0.3 (\times). The solid lines are guides to the eye. The vertical dashed lines indicate the onset of phase separation.

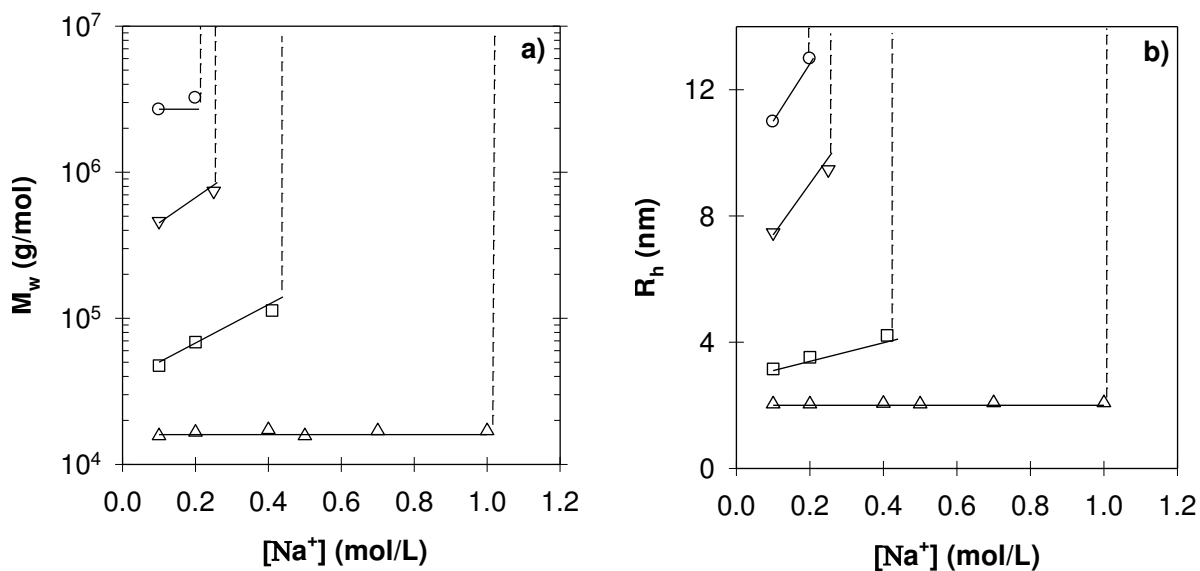


Figure S2. M_w (a) and hydrodynamic radius R_h (b) as a function of the concentration of Na^+ for MH40 at 2 g/L and $\alpha=1$ (Δ), 0.7 (\square), 0.5 (∇), 0.35 (\circ). The solid lines are guides to the eye. The vertical dashed lines indicate the onset of phase separation.

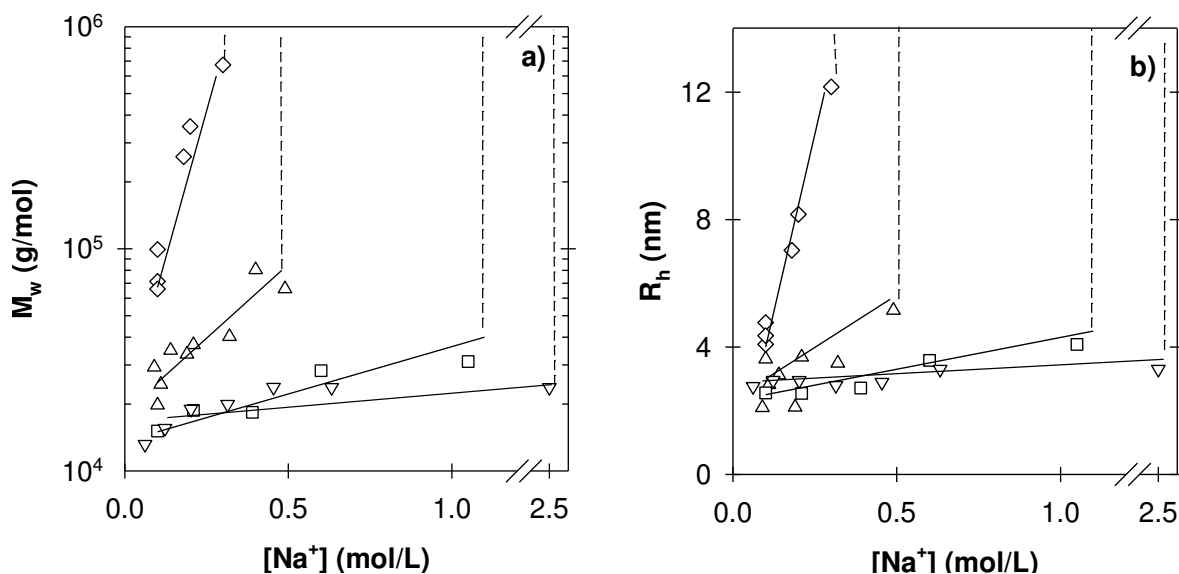


Figure S3. Molar mass M_w (a) and hydrodynamic radius R_h (b) as a function of the concentration of Na^+ for MH60 at 2 g/L and $\alpha=1$ (∇), 0.7 (\square), 0.5 (Δ), 0.2 (\diamond). The solid lines are guides to the eye. The vertical dashed lines indicate the onset of phase separation.

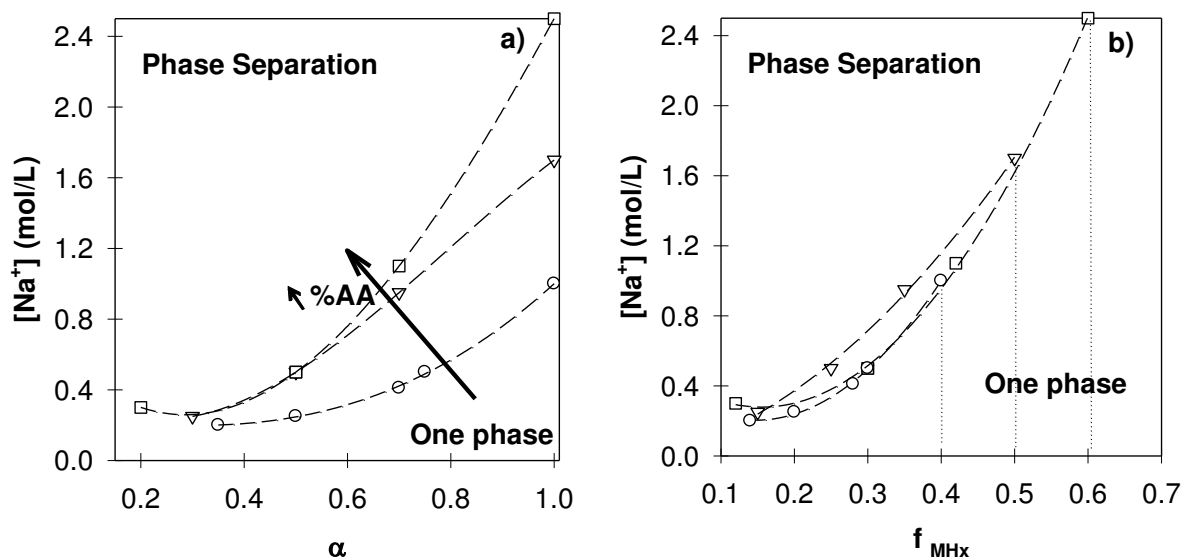


Figure S4. Phase diagram of MH40 (○) MH50 (▽) and MH60 (□) at different salt concentrations and ionization degrees (a) or fraction of charged units (b). The dashed lines are guides to the eye. The arrow in a) represents the increase of x , the AA content. The vertical dotted lines in b) correspond to the fraction of charged units within the MH x blocks for $\alpha = 1$.

3) Influence of the concentration

As explained in the “Material and Methods” section of the paper, the effects of the concentration were systematically checked in order to choose a suitable concentration to measure M_w . For all the copolymers, 2 g/L of copolymer is an appropriate polymer concentration where interactions between the scatterers can be neglected.

i. MH40

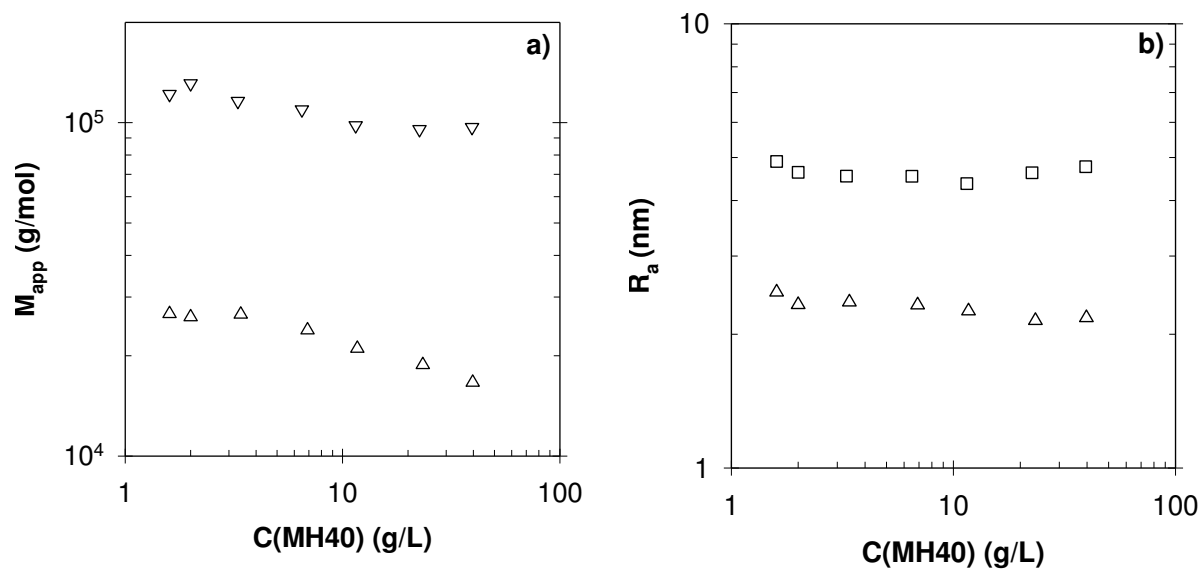


Figure S5. Apparent molar mass M_{app} (a) and apparent hydrodynamic radius R_a (b) as a function of the concentration of MH40 at $[\text{Na}^+]=0.1\text{M}$ and at $\alpha=0.6$ (\square) and 0.78 . The solid lines are guides to the eye.

ii. MH60

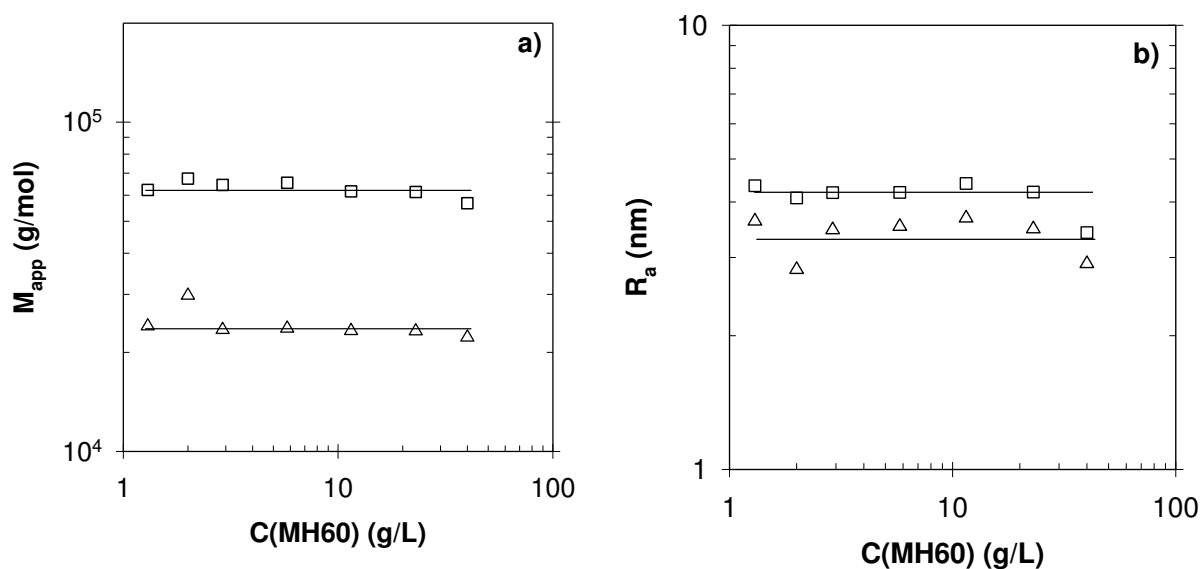


Figure S6. Apparent molar mass M_{app} (a) and apparent hydrodynamic radius R_a (b) as a function of the concentration of MH60 at $[\text{Na}^+]=0.1\text{M}$ and at $\alpha=0.23$ (\square) and 0.49 (Δ). The solid lines are guides to the eye.

iii. DH40

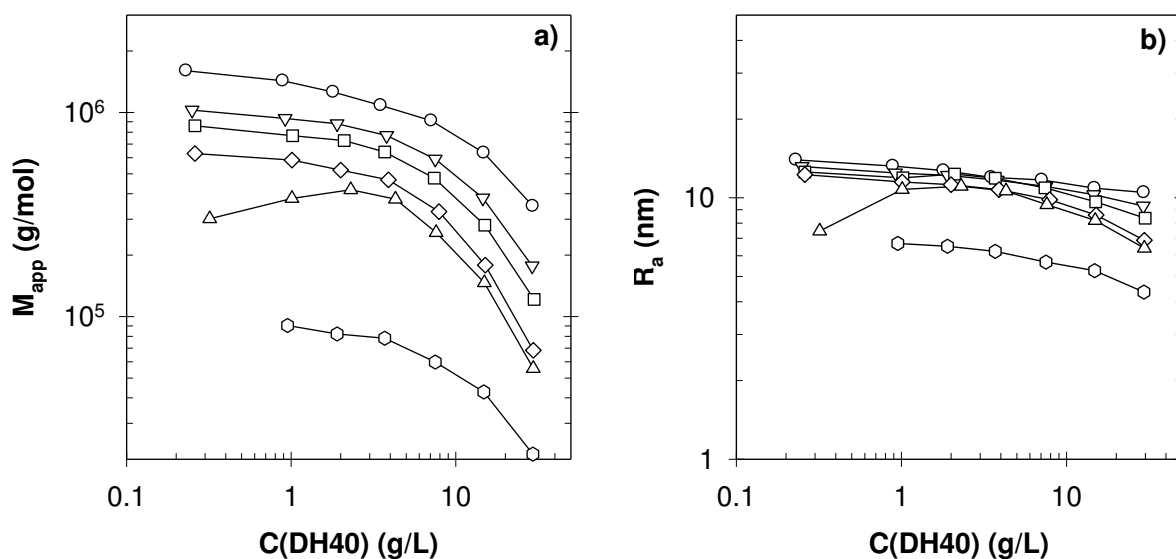


Figure S7. Apparent molar mass M_{app} (a) and apparent hydrodynamic radius R_a (b) as a function of the concentration of DH40 at $[\text{Na}^+] = 0.5\text{M}$ and at $\alpha = 0.24$ (○), 0.34 (▽), 0.42 (□), 0.53 (◇), 0.63 (△) and 0.79 (◊). The solid lines are guides to the eye.

iv. DH60

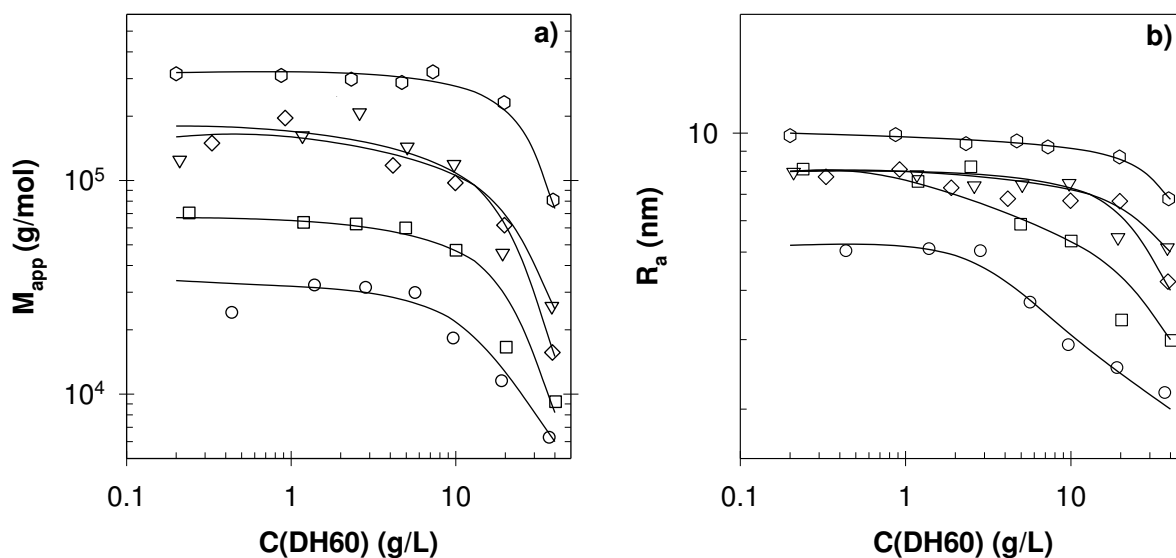


Figure S8. Apparent molar mass M_{app} (a) and apparent hydrodynamic radius R_a (b) as a function of the concentration of DH60 at $[\text{Na}^+] = 0.5\text{M}$ and at $\alpha = 0.09$ (○), 0.23 (◇), 0.27 (▽), 0.43 (□) and 0.77 (◊). The solid lines are guides to the eye.

4) Titration

For all $P(nBA_{(1-x)}\text{-stat-AA}_x)_{100}$ (MH x) and $P(nBA_{(1-x)}\text{-stat-AA}_x)_{100}\text{-}b\text{-PAA}_{100}$ (DH x) copolymers, all AA units eventually become ionized at $\text{pH} > 9$. However, due to differences of pK_a between the AA units in the hydrophilic corona PAA_{100} and in the associating block $P(nBA_{(1-x)}\text{-stat-AA}_x)_{100}$, preferential ionization of the AA units within the corona occurred as depicted on Figure S9. In other words, for a given overall ionization degree of the diblock, corresponding to the average ionization degree of all AA units within the polymer, the ionization degree is lower for the AA units in the $P(nBA_{(1-x)}\text{-stat-AA}_x)_{100}$ block than for those in the PAA_{100} block as depicted in Figure S9. Note that the experimental data represented on Figure S9 have been obtained according to an already published procedure⁷ and are in good agreement with extrapolations calculated in a previous article.³

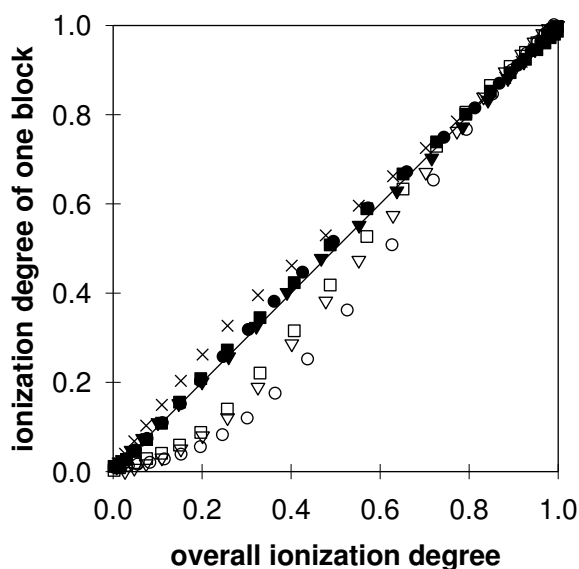


Figure S9. Degree of ionization of the AA units in the hydrophilic block PAA (\times) and in the hydrophobic blocks (MH40: \circ , MH50: ∇ , MH60: \square) as a function of the overall ionization degree of the AA units in the diblocks (DH40: \bullet , DH50: \blacktriangledown , DH60: \blacksquare). $[\text{Na}^+] = 0.1 \text{ mol/L}$ and $[\text{AA}] = 0.043 \text{ mol/L}$. The solid lines are guides to the eye.

REFERENCES

1. E. Lejeune; M. Drechsler; J. Jestin; A. H. E. Muller; C. Chassenieux; O. Colombani. *Macromolecules* **2010**, 43, (6), 2667-2671.
2. C. Charbonneau; C. Chassenieux; O. Colombani; T. Nicolai. *Macromolecules* **2011**, 44, (11), 4487-4495.

3. A. Shedge; O. Colombani; T. Nicolai; C. Chassenieux. *Macromolecules* **2013**, 47, (7), 2439-2444.
4. O. Colombani; O. I. Langelier; E. Martwong; P. Castignolles. *J. Chem. Educ.* **2011**, 88, (1), 116-121.
5. O. Colombani; M. Ruppel; M. Burkhardt; M. Drechsler; M. Schumacher; M. Gradzielski; R. Schweins; A. H. E. Müller. *Macromolecules* **2007**, 40, (12), 4351-4362.
6. J. L. Finney; D. T. Bowron. *Curr. Opinion Coll. Interface Sci.* **2004**, 9, (1-2), 59-63.
7. O. Colombani; E. Lejeune; C. Charbonneau; C. Chassenieux; T. Nicolai. *J. Phys. Chem. B* **2012**, 116, (25), 7560-7565.

CHAPTER 5: ARTICLE 2

CHAPTER 5 : ARTICLE 2

**pH-Controlled Rheological Properties of Mixed Amphiphilic
Triblock Copolymers**

Lionel Lauber, Olivier Colombani, Taco Nicolai and Christophe Chassenieux*

LUNAM Université, Université du Maine, IMMM-UMR CNRS 6283, Département
Polymères, Colloïdes et Interfaces, av. O. Messiaen, 72085 Le Mans cedex 9, France

AUTHOR EMAIL ADDRESS: olivier.colombani@univ-lemans.fr

CHAPTER 5: ARTICLE 2

ABSTRACT: Aqueous mixtures of pH-sensitive block random BAB triblock copolymers with different hydrophobic B blocks connected to the same hydrophilic A block were studied in order to investigate co-micellization and the impact on the dynamic mechanical properties. The B blocks were statistical copolymers of acrylic acid (AA) and *n*-butyl acrylate (*n*BA) copolymers, triblocks self-assembled into transient networks for which the mechanical relaxation time depended both on the AA content within the B blocks and on the pH, which affected the ionization of the AA units. Static and dynamic light scattering measurements were done on mixtures of equivalent AB diblock copolymers that showed that co-micellization occurred only at conditions at which both copolymers in the mixture self-assemble. It is shown that co-micellization influenced the viscoelastic properties of hydrogels formed by mixtures of triblock copolymers. Using binary mixtures of BAB triblock copolymers exhibiting pH-controlled dynamics allows control and fine tuning of the viscoelastic properties at constant pH by formulation without the need for to synthesize a large number of different polymers.

KEYWORDS: mixed micelle, pH-sensitive, hydrogel, acrylic acid, *n*-butyl acrylate.

I. Introduction

Amphiphilic diblock (AB) or triblock (BAB) copolymers consisting of hydrophobic B blocks and hydrophilic A blocks self-assemble in aqueous solution in order to reduce contact between the B blocks and water.¹ Triblock copolymers may form a network through bridging of hydrophobic micellar cores by the A blocks² with rheological properties that depend on the exchange time of the B blocks between the cores³, the polymer concentration and the block lengths. In particular, controlling the exchange time of the B blocks may lead to soft hydrogels or visco-elastic fluids with tunable viscosities relevant for applications such as in Enhanced Oil Recovery (EOR)^{4,5} or cosmetics^{5,6}. However, few attempts have been made at controlling the exchange time which increases exponentially with the length of the B blocks and with their hydrophobic character.^{7,8} Most amphiphilic triblock copolymers studied in the literature actually form networks with extremely long and poorly tuneable exchange times.⁷ It has been shown recently⁹⁻¹³ that incorporating hydrophilic units within the B blocks through controlled synthesis enables dynamic exchange even for relatively long B-blocks. In the past we have studied in some detail the amphiphilic triblock copolymers $P(nBA_{(1-x)}-stat-AA_x)_{100}-b-PAA_{200}-b-P(nBA_{(1-x)}-stat-AA_x)_{100}$ (THx) that consist of a poly(acrylic acid) (PAA) central A block and two lateral B blocks containing randomly distributed hydrophobic *n*-butyl acrylate (*n*BA) and hydrophilic acrylic acid (AA) units. Their exchange time could be varied over more than 10 orders of magnitude by modifying¹⁴ the content of AA units within the B blocks (*x*) and/or by changing the pH⁹ which affects the ionization degree $\alpha = [AA^-]/([AA^-] + [AAH])$ of the AA units¹⁵. Both parameters determine the fraction of ionized sodium acrylate units (AA^-) within the B blocks, which was shown to be a key parameter to tune the exchange time.¹⁴

Although this approach is useful to modify the relaxation time by changing the pH, modifying the relaxation time of aqueous solutions of THx at a given pH requires synthesis of polymers with different *x*.¹⁴ Here, we have explored the possibility to use mixtures of THx copolymers with different *x* to control the dynamic mechanical properties of the mixtures. Many studies of mixtures of AB amphiphilic diblock copolymers have been reported¹⁶⁻³⁵, but we are aware of only two relevant studies of mixtures of triblock copolymers, both using neutral copolymers^{3,36}. Annable et al.³ observed that the stress relaxation of the transient networks formed by mixtures of BAB triblock copolymers consisting of a poly(ethylene oxide) (PEO) A-block end capped with alkyl chains of different sizes were characterized by two distinct relaxation times corresponding to those of each individual BAB triblock. A similar observation was

reported by Rufier et al.³⁶ for mixtures of PEO end capped either with alkyls or fluorinated alkyls though in that case the incompatibility between fluorinated and alkyl end-chains may lead to their segregation.

Here we will show that by mixing THx with different compositions it is possible to modify and control the rheological properties of the solutions at a given pH. In order to investigate if and when comicellization occurs, we discuss mixtures of diblock copolymer homologues of THx: P(*n*BA_{(1-x)-stat-AA_x})₁₀₀-*b*-P(AA)₁₀₀ (DHx).

II. Materials and methods.

1. *Synthesis of the copolymers.* The synthesis of the P(*n*BA_{1-x-stat-AA_x})₁₀₀-*b*-P(AA)₁₀₀ diblock^{37,38} and of the P(*n*BA_{1-x-stat-AA_x})₁₀₀-*b*-P(AA)₂₀₀-*b*-P(*n*BA_{1-x-stat-AA_x})₁₀₀ triblock¹⁴ copolymers has been described elsewhere.³⁸ In each case, the number average degree of polymerization of each block was kept constant as indicated in subscripts while the AA content (x) was either 40, 50 or 60 %. The number average molecular weight and dispersity were, respectively, $M_n = 1.7 \times 10^4$ g/mol and $\mathcal{D} \sim 1.2$ for the diblocks and $M_n = 3.4 \times 10^4$ g/mol and $\mathcal{D} \sim 1.1$ for the triblocks. Diblocks are equivalent in mass and composition to triblocks cut in the middle.

2. *Light scattering.* Light scattering measurements were performed on an ALV-CGS-8F system equipped with an ALV-5003 multi tau correlator system (ALV GmbH, Germany). A vertically polarised Helium-Neon laser was the light source ($\lambda=632.8$ nm). Measurement were done over a range of scattering wave vectors ($q=4\pi n/\lambda \cdot \sin(\theta/2)$, with n the refractive index of the solvent and θ the angle of observation) between 2.5×10^6 and 2.7×10^7 m⁻¹.

Dynamic light scattering. The Siegert equation: $g_2(t)=1+\beta \cdot g_1^2(t)$, where β is the spatial coherence factor, was used to determine the electric field autocorrelation function, $g_1(t)$, from the measured normalized autocorrelation function of the scattered light intensity, $g_2(t)$.³⁹ The relaxation time (τ) distributions, $A(\tau)$, were extracted from $g_1(t)$ using the REPES routine³⁹:

$$g_1(t) = \int A(\tau) \exp(-t/\tau) d\tau \quad (1)$$

The calculated average relaxation rate was q^2 -dependent indicating cooperative diffusion of the solute and the diffusion coefficient was calculated as $D_c = \langle \tau^{-1} \rangle / q^2$. In dilute solution interaction between the solute is negligible so that the z-average hydrodynamic radius of the solute can be calculated from the diffusion coefficient using the Stokes-Einstein equation:

$$R_h = \frac{kT}{6\pi\eta D_c} \quad (2)$$

with k Boltzmann's constant, T the absolute temperature and η the viscosity of the solvent.

Static light scattering. The Rayleigh ratio, R_θ , was calculated as:

$$R_\theta = \frac{I_{\text{solution}}(\theta) - I_{\text{solvent}}(\theta)}{I_{\text{toluene}}(\theta)} \left(\frac{n_{\text{solvent}}}{n_{\text{toluene}}} \right)^2 R_{\text{toluene}} \quad (3)$$

where I_{solution} , I_{solvent} , and I_{toluene} are the average intensities scattered, respectively, by the solution, the solvent, and the reference (toluene). The Rayleigh ratio of the reference is $R_{\text{toluene}} = 1.35 \times 10^{-5} \text{ cm}^{-1}$ and the refractive index of the reference and the solvent (water) are respectively $n_{\text{toluene}} = 1.496$ and $n_{\text{solvent}} = 1.333$.

The apparent molar mass (M_{app}) of the solute was calculated from the Rayleigh ratio of the solution as:

$$R_\theta = K \cdot C \cdot M_{\text{app}} \cdot S(q) \quad (4)$$

where $S(q)$ is the structure factor and K a constant:

$$K = \frac{4\pi^2 n_{\text{solvent}}^2}{\lambda^4 N_a} \left(\frac{\partial n}{\partial C} \right)^2 \quad (5)$$

Here $\partial n / \partial C$ is the specific refractive index increment of the solute and N_a is Avogadro's number. $S(q)$ was close to unity over the whole q -range measured. Light scattering experiments on the diblock copolymers were performed at a total polymer concentration of 2 g/L at which interactions could be neglected³⁷ so that M_{app} could be considered equal to the true weight average molar mass (M_w) of the scatterers.

The total aggregation number (N_T) was calculated by dividing M_w by the weight average molecular weight of the polymer chains.

3. Sample Preparation. Each sample was prepared independently using the following procedure. First, the polymer was dissolved in demineralized water (Millipore) with the right amount of sodium hydroxide to ionize ~90% of the acrylic acid units ($\alpha = [AA^-] / ([AA^-] + [AAH]) \sim 0.9$). The system was homogenized by stirring during one day. The ionization degree (α) was then gradually decreased using freshly prepared D-glucono- δ -lactone (GDL) which slowly hydrolysed into gluconic acid ($pK_a \sim 3.4$). GDL was fully hydrolyzed after 24 hours leading to steady-state. For $\alpha > 0.4$, the acid-base reaction between gluconic acid and the AA units of the polymers is complete so that the amount of GDL required to reach a target value of α could be calculated straightforwardly. For $\alpha < 0.4$, it is necessary to take into account that GDL is not a strong acid as explained in the supporting information of ref⁴⁰.

Mixtures were prepared at $\alpha \sim 0.9-1$ and α was subsequently decreased using GDL, unless specified otherwise. As is shown in section 1 of the supporting information, the characteristics of the mixtures of diblocks determined by light scattering were the same no matter whether

the solutions of polymers were mixed at $\alpha = 0.9$ before decreasing α or were mixed once the targeted value of α had been reached. Since the relationship between the pH and α did not depend significantly on x within the range investigated,¹⁵ α was the same for both polymers in the mixtures.

4. *Dynamic mechanical measurements.* Oscillatory shear measurements were done in the linear response regime as a function of the frequency using controlled-stress rheometers equipped with cone-plate geometries: ARG2 (TA Instrument, angle = $4^\circ - 2^\circ - 1^\circ$, diameter 20 - 60 mm) and MCR301 (Anton-Paar, angle = $2^\circ - 1^\circ$, diameter = 25 - 50 mm). The geometry was covered with silicon oil in order to prevent water evaporation. The temperature was controlled with a Peltier system. GDL was added to the solution just before loading the samples onto the rheometer and the measurements were done after steady state had been reached, see refs^{9,40} for details.

III. Results and Discussion

1. Diblock copolymers

Self-assembly of pure and mixed diblock copolymers (DH x) with different amounts of acrylic acid (AA) units within the hydrophobic block ($x = 40, 50$ and 60%) was investigated by light scattering in aqueous medium at 0.1 M and 0.5 M NaCl. The self-assembly of pure DH40 and DH60 aqueous solutions at 0.1 M NaCl was already reported,³⁷ as well as that of pure DH50 aqueous solutions at 0.1 M and 0.5 M NaCl.^{10, 37, 41} The dependence of the total aggregation number (N_T) on the ionization degree (α) for DH x in the presence of 0.5 M NaCl is shown in fig. 1 and was found to be qualitatively similar to that already reported at 0.1 M NaCl.³⁷ At $\alpha=1$ the measured weight average molar masses were close to that of the unimers ($M_w=1.9 \times 10^4$ g/mol) implying that the polymers were not associated ($N_T=1$). Decreasing the ionization degree (α) caused an increase of N_T due to self-assembly of the diblocks into star-like polymeric micelles. In the case of DH40 and DH50, the increase of N_T with decreasing α stagnated at approximately the same N_T value, indicating that at low α the aggregation number of the micelles (N_T) is limited by the corona. The limiting value of N_T was not yet reached for DH60 at $\alpha=0.2$.

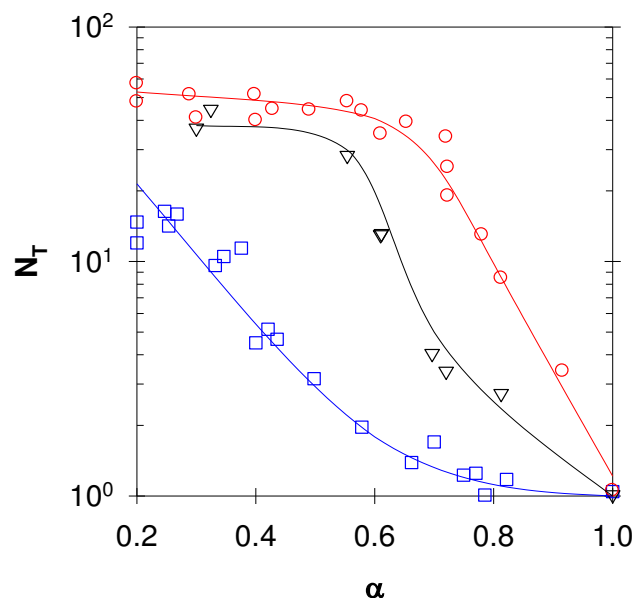


Figure 1. Evolution of the total aggregation number (N_T) as a function of the ionization degree for DH40 (\circ), DH50 (∇), and DH60 (\square) at $[\text{NaCl}] = 0.5 \text{ mol/L}$. The solid lines are guides to the eye. The results for DH50 were taken from refs.^{37, 41}

Figure 2a shows the dependence of N_T on the weight fraction of DH40 (F_{40}) in mixed solutions of DH40 and DH60 at $[\text{Na}^+] = 0.5 \text{ mol/L}$ and at three values of α equal to 0.20, 0.40 and 0.77. For each value of α , the experimental N_T was compared to the calculated values assuming that DH40 and DH60 do not co-micellize: $N_T = (1-F_{40}) \cdot N_{\text{DH60}} + F_{40} \cdot N_{\text{DH40}}$, where N_{DH60} and N_{DH40} correspond, respectively, to the aggregation numbers of pure DH60 and DH40 solutions, see Figure 1. At $\alpha=0.77$, pure DH60 does not associate, whereas pure DH40 forms micelles with $N_T \approx 12$. In this case, the calculated values of N_T correspond to the measured values indicating that co-micellization did not occur in the mixtures at any value of F_{40} . At $\alpha=0.40$ and 0.20 both pure DH40 and pure DH60 formed micelles, and N_T of the mixtures was clearly different from the calculated values for non-interacting chains, which points to co-micellization. N_T was systematically larger at $\alpha=0.2$ than at $\alpha=0.4$, but the dependence on F_{40} was qualitatively the same. The average hydrodynamic radius obtained from DLS for the mixtures shows the same dependence on F_{40} , see section 2 of the supporting information.

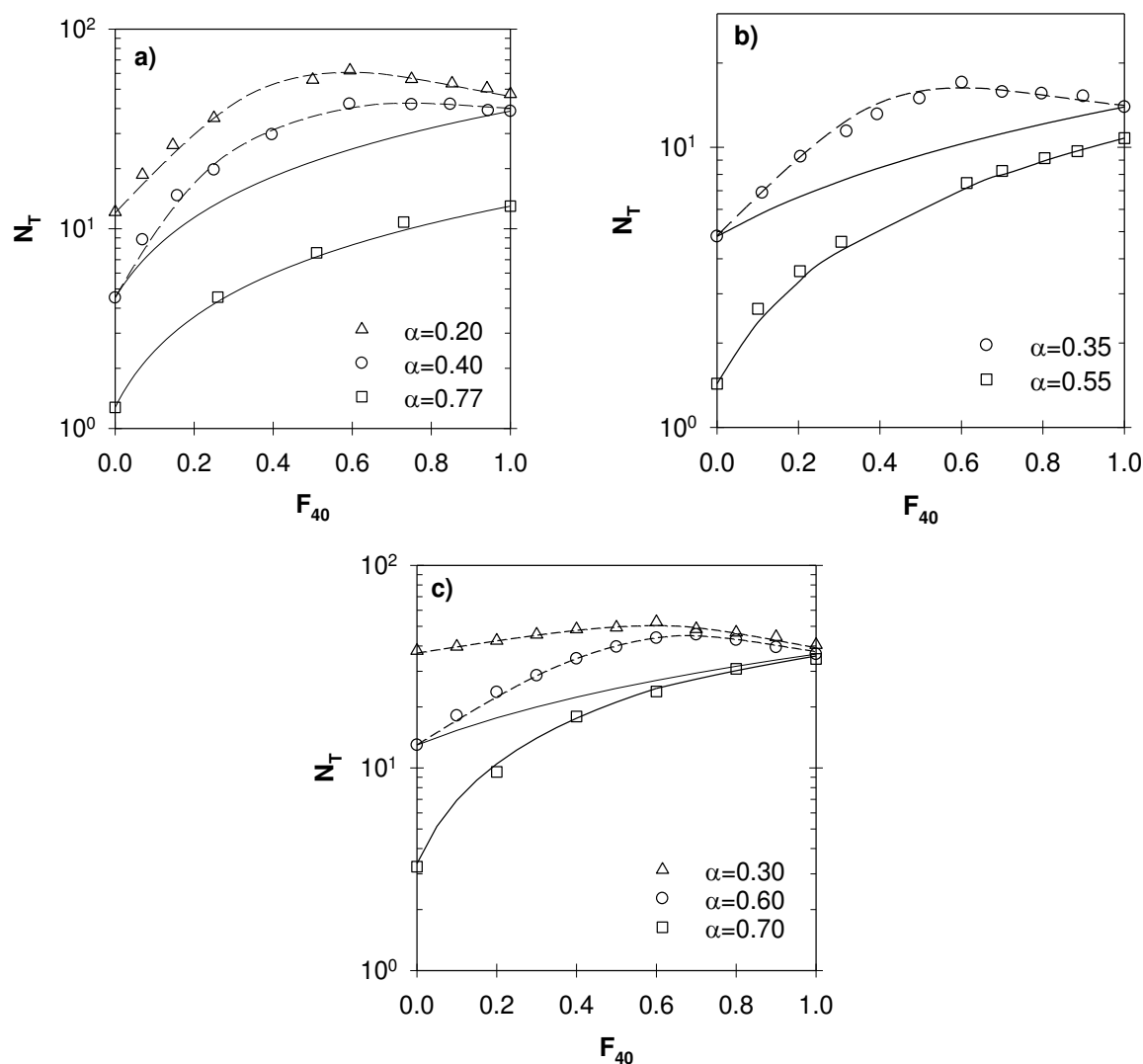


Figure 2. Evolution of the total aggregation number (N_T) as a function of the weight fraction of DH40 (F_{40}) in solutions of DH40 and DH60 at $[Na^+] = 0.5$ mol/L (a) or at $[Na^+] = 0.1$ mol/L (b) and solutions of DH40 and DH50 at $[Na^+] = 0.5$ mol/L (c). Different ionization degrees were investigated as indicated in the figures. The values for mixtures in the absence of co-micellization are shown for a number of systems by the solid lines.

These experiments indicate that co-micellization of DH40 and DH60 chains occurs at 0.5 M Na^+ if, and only if, both DH40 and DH60 self-assemble. This was also the case for mixtures of DH40 and DH60 at $[Na^+] = 0.1$ mol/L and for DH40 and DH50 at $[Na^+] = 0.5$ mol/L, see Figures 2b and 2c.

It was shown recently that mixtures of diblocks with a similar architecture as DHx, but consisting of a pure poly(dimethylaminoethyl methacrylate) (PDMAEMA) hydrophilic block connected to a random block of DMAEMA and diethylaminoethylmethacrylate (DEAEMA) units, also formed mixed polymeric micelles.¹³ A remarkable difference is, however, that for

the latter system, the aggregation number of the mixed micelles was lower than the average of the two individual micelles, whereas for the present system N_T of the mixed micelles was larger. Furthermore, mixed micelles of PDMAEMA-*b*-P(DMAEMA-*co*-DEAEMA) were formed even if one of the diblocks did not form micelles by itself.

2. Triblock copolymers

As was mentioned in the introduction, self-assembly in aqueous solutions of THx leads to the formation of networks above a critical concentration and below a given ionization degree which depend on x .^{9, 14} The terminal relaxation time (τ) of the transient networks was found to increase sharply with decreasing α and/or x until it becomes incommensurably long and the systems behave as permanently cross-linked hydrogels.¹⁴ In the following we will first discuss mixtures that did not co-assemble and then mixtures that formed hybrid hydrophobic cores.

2.1. Non hybridized mixtures of TH40 and TH60. The frequency dependence of the storage (G') and loss (G'') shear moduli was measured for mixtures of TH40 and TH60 with different weight fractions of TH40 (F_{40}) at conditions where no hybridization occurred for the diblocks, viz. at $\alpha=0.65$ and $C=30$ g/L. The results obtained at different temperatures could be superimposed using horizontal and vertical shift factors leading to a master curve as was already shown elsewhere for pure THx solutions^{9, 14}, see fig. 3a. The frequency dependence of G' and G'' is typical for viscoelastic liquids with a broad distribution of relaxation times. The temperature dependence of the relaxation times was controlled by an activation energy that was independent of F_{40} and close to that reported earlier for pristine THx solutions ($E_a \approx 120$ kJ/mol), see section 3 of the supporting information. Master curves obtained at different F_{40} with $T_{ref}=20$ °C and $F_{40,ref}=1$ could themselves be superimposed, see Figure 3b, which means that the width of the relaxation time distribution did not depend significantly on F_{40} .

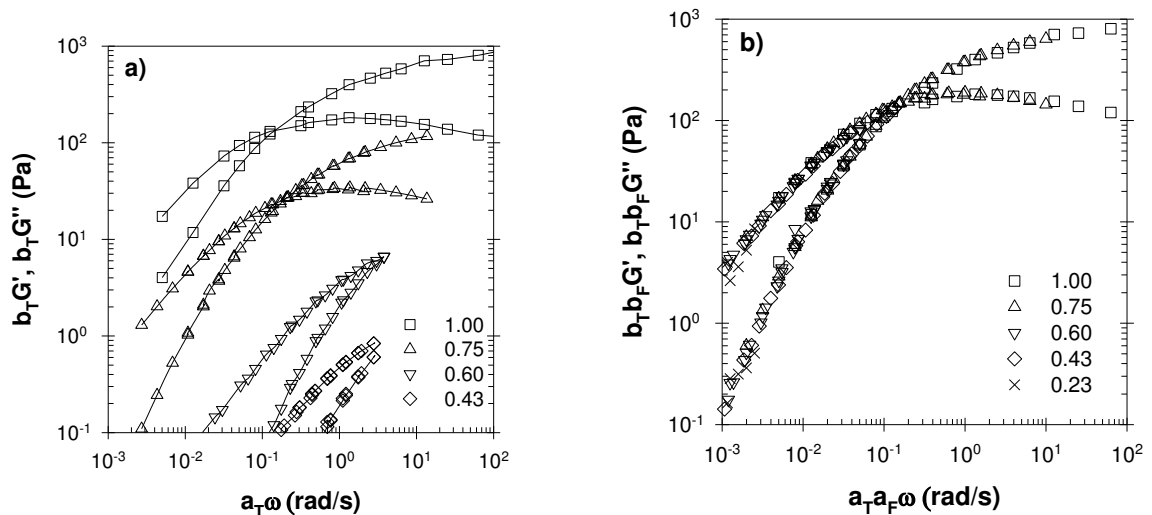


Figure 3. (a) Master curves obtained by frequency-temperature superposition of the shear moduli at $T_{\text{ref}}=20$ °C for mixtures of TH40 and TH60 with different F_{40} as indicated in the figure at $C=30$ g/L and $\alpha=0.65$ without added salt. For clarity, not all data points are shown. (b) Master curve obtained by superposition of the data shown in figure 3a using $F_{40}=1$ as the reference.

The relaxation time (τ) defined as the inverse of the angular frequency at which $G'=G''$ is plotted as a function of F_{40} in Figure 4a. τ decreased initially weakly with decreasing F_{40} down to $F_{40} = 0.6$ followed by a sharp decrease at lower values of F_{40} . The relaxation time could no longer be determined for $F_{40} < 0.4$ where viscous liquids were obtained. In order to distinguish the effect of replacing TH40 by TH60 in the mixtures from the mere effect of diluting TH40, the values of the relaxation time were compared with those obtained for pure TH40 solutions at the same TH40 concentrations as in the mixtures. The relaxation time and also the viscosity, see Figure 4b, were the same with and without TH60. The implication is that TH60 does not have a significant influence on the behavior of TH40 at $\alpha=0.65$, in agreement with the fact that no co-micellization of DH40 and DH60 was observed at the same conditions.

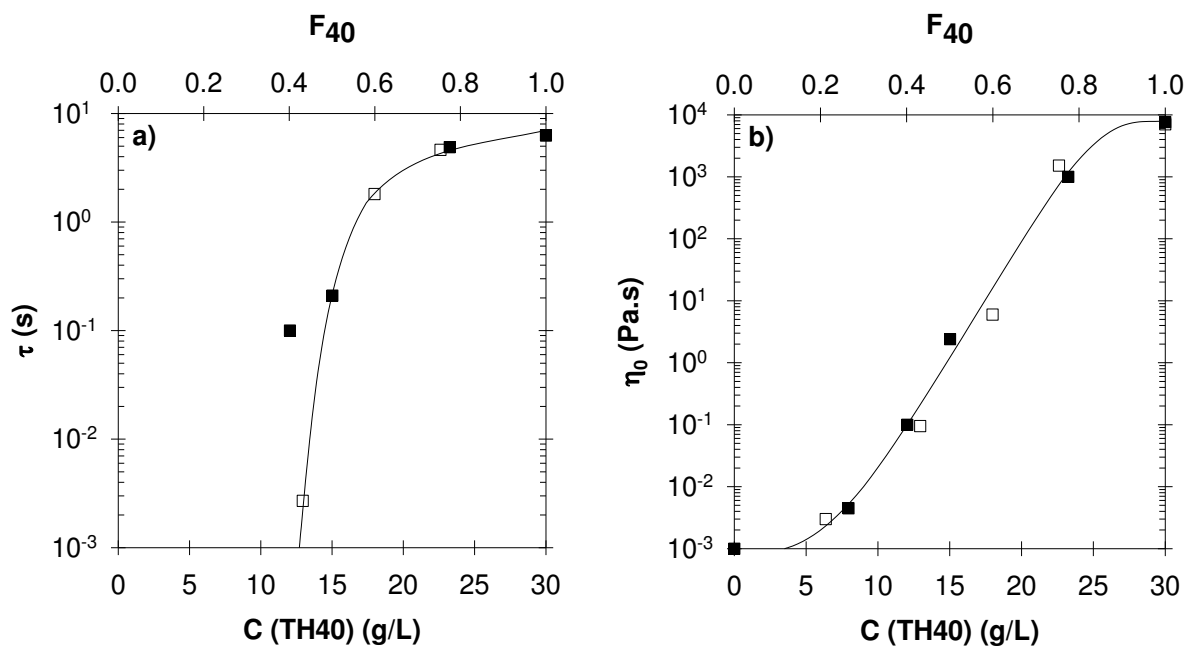


Figure 4. Dependence of the relaxation time (a) and the viscosity (b) as a function of the TH40 concentration (bottom axis) or F_{40} (top axis) for mixtures of TH60 and TH40 at $\alpha = 0.65$, $C = 30$ g/L and $T = 20$ °C without added salt. The results for the mixtures (open symbols) are compared with those for pure TH40 solutions (closed symbols). The solid lines are guides to the eye.

2.2 Hybridized mixtures of TH40 and TH60. TH40/TH60 mixtures were also studied at $\alpha = 0.2$ where DH40 and DH60 co-micellized. Figure 5 shows master curves of the storage modulus obtained by temperature-frequency superposition for mixtures at different compositions at a total polymer concentration of $C = 30$ g/L. The temperature dependence was controlled by an activation energy that was within the experimental error the same as for pure THx solutions. For $F_{40} \geq 0.43$, frozen networks were formed with a weakly frequency dependent storage modulus at low frequencies that increased sharply with increasing F_{40} . Mixtures with $F_{40} \leq 0.33$ formed viscoelastic networks with a terminal relaxation time that increased with increasing F_{40} . The relaxation time distribution also appears to broaden with increasing F_{40} .

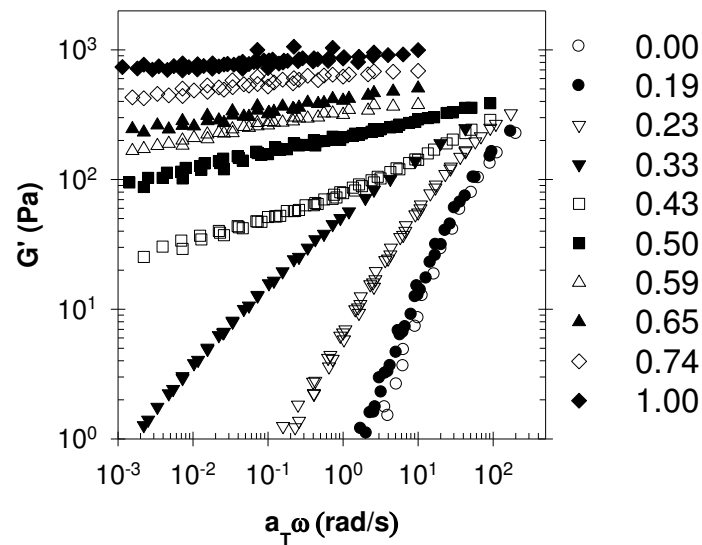


Figure 5. Master curves obtained by frequency-temperature superposition of the storage shear modulus at $T_{\text{ref}}=20$ °C for mixtures of TH60 and TH40 with different fractions of TH40 indicated in the figure at $C=30$ g/L and $\alpha=0.2$ without added salt. For clarity, not all data points are shown.

As previously reported,¹⁴ pure TH40 solutions at $\alpha = 0.2$ formed frozen networks ($\tau > 10^7$ s) above the percolation concentration $C_p = 5$ g/L, which corresponds to $F_{40}=0.16$ for the mixtures at $C = 30$ g/L. The elastic modulus of the frozen network increased with increasing polymer concentration. Pure TH60 solutions at $\alpha = 0.2$ formed viscoelastic liquids with a terminal relaxation time that decreased with decreasing concentration close to the percolation concentration. It is clear that the behavior of the mixtures cannot be understood as the response of independent interpenetrated TH40 and TH60 networks. Considering that mixed micelles were formed in mixtures of DH40 and DH60 at $\alpha = 0.2$, it is likely that the mixtures of TH40 and TH60 at $\alpha=0.2$ formed a single network of mixed micellar cores bridged by both TH40 and TH60 chains.

If it had been the case that neither the percolation concentration of TH40 nor its relaxation time were affected by mixing with TH60, the amount of frozen TH40 bridges would have been sufficient to allow the formation of a system spanning hybrid network for $F_{40} \geq 0.16$ ($C_{\text{TH40}} = 5$ g/L) and an elastic solid would have been observed at these conditions. However, the signature of an elastic gel was only observed for $F_{40} > 0.43$. It follows that either the percolation concentration of TH40 increased to 10-13 g/L ($F_{40} = 0.33-0.43$) and/or its relaxation time decreased in the presence of TH60. It was not possible to exclude either

scenario on the basis of the present experimental results. Nevertheless, for $F_{40} > 0.43$, the absence of a terminal relaxation time in the frequency range investigated is a clear indication that TH40 chains eventually percolated the hybrid network with an immeasurably long terminal relaxation time.

A relaxation process was observed at high frequencies for the relatively weak frozen network at $F_{40} = 0.43$ that can be attributed to the exchange of the TH60 bridges in the hybrid network. This relaxation process was much slower than for pure TH60, indicating that the exchange time of TH60 was increased by the presence of TH40 in the micellar cores. For $F_{40} < 0.43$, the increase of τ with increasing F_{40} can therefore be explained by the slow down of TH60 exchange by the presence of an increasing amount of TH40 in the cores.

Replacement of TH40 chains by TH60 chains at the same polymer concentration does not modify the total number of chains that constitute the fully formed network. Therefore, the elastic modulus at very high frequencies is not expected to depend on F_{40} .

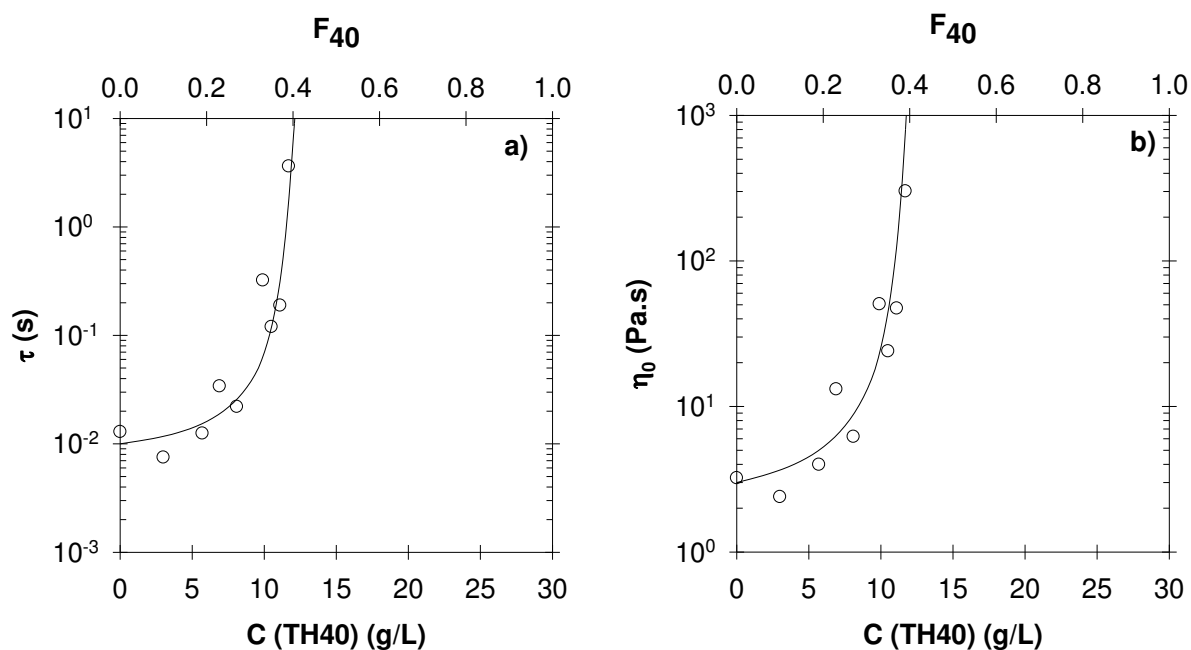


Figure 6. Evolution of the terminal relaxation time (a) and the viscosity (b) as a function of the TH40 concentration (bottom axis) or F_{40} (top axis) for mixtures of TH40 and TH60 at $\alpha=0.2$, $C=30$ g/L and $T=20$ °C without added salt. The solid lines are guides to the eye.

2.3 Hybridizing mixtures of TH40 and TH50. So far we have studied mixtures at conditions where one of the components did not self-assemble or where one of the pure components was kinetically frozen. A third type of mixture is formed when both components form transient networks. We have studied the dynamic mechanical properties of this type of system by

mixing TH40 and TH50 at $\alpha=0.60$ and $C=30$ g/L as a function of the fraction of TH40 in the mixture. At this ionization degree DH40 and DH50 co-micellized and both TH40 and TH50 had measurable relaxation times.¹⁴ Master curves of the frequency dependence of G' could be obtained by temperature-frequency superposition, see Figure 7, showing viscoelastic behavior for all compositions. In section 4 of the supporting information the frequency dependence of both G' and G'' is shown. The temperature dependence of τ was controlled by an activation energy that was the same as for pure THx solutions. The width of the relaxation time distribution appears broader for intermediate values of F_{40} .

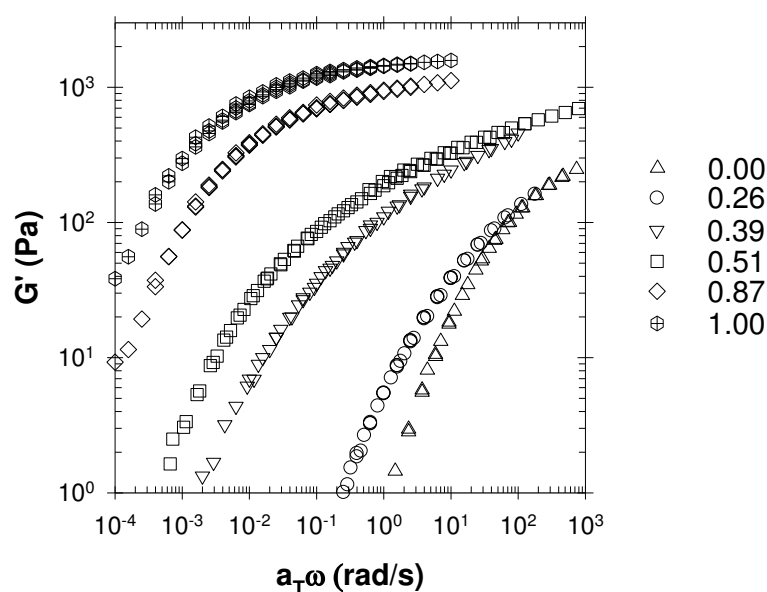


Figure 7. Master curves obtained by frequency-temperature superposition of the shear moduli at $T_{ref}=20$ °C for mixtures of TH40 and different fractions of TH40 indicated in the figure at $C=30$ g/L and $\alpha=0.60$ without added salt. For clarity, not all data points are shown.

The dynamic mechanical properties of these mixtures can be understood by assuming that the networks are formed by mixed micelles. η_0 and τ are plotted as a function of F_{40} in Figure 8. With increasing F_{40} , τ increased sharply between $F_{40}=0.3$ and 0.4 and more weakly at larger F_{40} . The sharp increase of τ and η_0 in the mixtures occurred at a TH40 concentration close to the percolation concentration of pure TH40 solutions, see Figure 4 and ref.¹⁴. Most likely, the sharp increase of τ at $F_{40} = 0.3-0.4$ is caused by percolation of micelles bridged by TH40 chains.

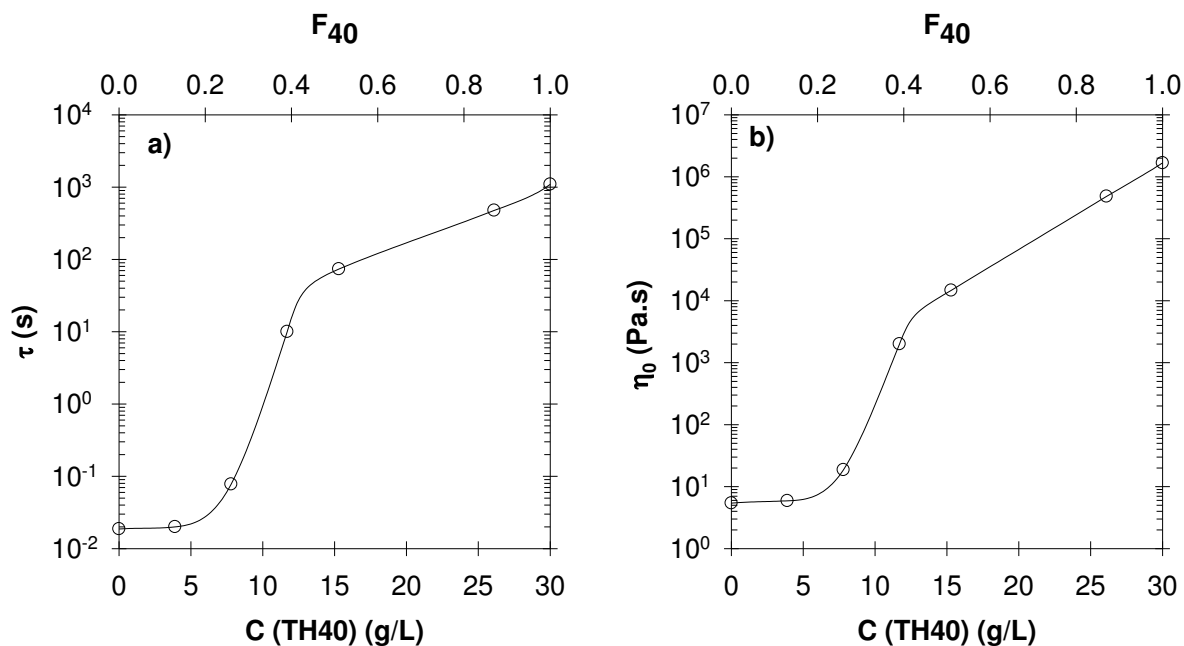


Figure 8. Terminal relaxation time (a) and viscosity (b) as a function of the TH40 concentration (bottom axis) or F_{40} (top axis) at $C=30$ g/L, $\alpha = 0.60$ and $T=20$ °C without added salt. The solid lines are guides to the eye.

The broader relaxation time distribution at intermediate values of F_{40} suggests that the stress relaxation involved dynamic exchange of both TH50 and TH40. However, we cannot distinguish two distinct relaxation processes corresponding to the exchange of B-blocks from TH50 and TH40, as was reported for mixtures of neutral triblock copolymers.^{3, 36} We speculate that the exchange time of B blocks of each polymer was affected by the presence of B blocks of the other polymer, i.e. the faster escape of TH50 B blocks was slowed down by the presence of TH40 blocks and vice versa. Since the relaxation time distribution of the pure system was already rather broad, this mutual influence in the mixture may have led to the observed monomodal broad relaxation time distribution.

The strong mutual influence on the exchange rate is most probably caused by the polyelectrolyte nature of the self-assembling blocks. It was shown elsewhere¹⁴ that the exchange dynamics of THx are mainly controlled by the fraction of charged units within the hydrophobic blocks. The latter depends both on the fraction of AA units in the B block (x) within these blocks and on the pH, which affects their ionization degree. Mixing two polymer solutions at the same pH did not influence the pH. However, the average AA/ n BA ratio changed as a function of F_{40} in the hybrid hydrophobic cores, which probably affected the way charges were expressed within the core because the local dielectric constant changed.¹⁵ Note also that mixing amphiphilic copolymers with surfactants was already observed to

CHAPTER 5: ARTICLE 2

increase the exchange rate.⁴²⁻⁴⁴ In mixtures of TH40 with TH50 or TH60, the more dynamic triblock may play the same role as a surfactant by transforming the frozen TH40 network into a dynamic network.

TH40 and TH50 chains do not differ so strongly in their AA content within the hydrophobic blocks, but nevertheless mixing them resulted in an important broadening of the relaxation time distribution. This explains why stress relaxation even of networks formed by pure THx with small composition dispersity was characterized by rather broad relaxation time distributions. The implication is that a very precise control of the composition of the hydrophobic blocks is required if a narrow relaxation time distribution is aimed for. On the contrary, formulation by mixing THx with different x leads to a very broad relaxation distribution, but allows easy control of the viscosity at a given pH.

IV. Conclusions

Hydrophobic blocks of DHx and THx assemble into micellar cores below a critical ionization degree that depends on the content of AA units in these blocks. In mixtures of copolymers with different values of x, mixed micellar cores are formed only when both copolymers self-assemble in pure solutions, that is if α is below the critical value for both polymers. Hybrid networks have rheological properties controlled by the relaxation of both types of triblock copolymers, allowing control of the viscosity over a broad range at a given pH by simple formulation, see Figure 6 and 8.

For hybrid networks the exchange rate of the B blocks was influenced by the presence of the other type of B block in the micellar core. The mutual influence was strong enough to render a frozen network of TH40 dynamic by adding rapidly exchanging TH60 chains. For TH40/TH50 mixtures the mutual influence resulted in a system with a monomodal broad relaxation time distribution with a terminal relaxation time that increased with increasing fraction of TH40 for a given pH and polymer concentration.

ASSOCIATED CONTENT

Details on the influence of the preparation pathway, the evolution of the hydrodynamic radius and the triblock mixtures are available on supporting information.

REFERENCES

1. Mai, Y.; Eisenberg, A. Self-assembly of block copolymers. *Chem. Soc. Rev.* **2012**, 41, (18), 5969-5985.
2. Chassenieux, C.; Nicolai, T.; Benyahia, L. Rheology of associative polymer solutions. *Curr. Opin. Colloid Interface Sci.* **2011**, 16, (1), 18-26.
3. Annable, T.; Buscall, R.; Ettelaie, R.; Whittlestone, D. The rheology of solutions of associating polymers: Comparison of experimental behavior with transient network theory. *J. Rheol.* **1993**, 37, (4), 695-726.
4. Wever, D. A. Z.; Picchioni, F.; Broekhuis, A. A. Polymers for enhanced oil recovery: A paradigm for structure-property relationship in aqueous solution. *Prog. Polym. Sci.* **2011**, 36, (11), 1558-1628.
5. Raffa, P.; Wever, D. A. Z.; Picchioni, F.; Broekhuis, A. A. Polymeric Surfactants: Synthesis, Properties, and Links to Applications. *Chem. Rev.* **2015**, 115, (16), 8504-8563.
6. Bakshi, M. S.; Sachar, S.; Yoshimura, T.; Esumi, K. Association behavior of poly(ethylene oxide)-poly(propylene oxide)-poly(ethylene oxide) block copolymers with cationic surfactants in aqueous solution. *J. Colloid Interface Sci.* **2004**, 278, (1), 224-233.
7. Nicolai, T.; Colombani, O.; Chassenieux, C. Dynamic polymeric micelles versus frozen nanoparticles formed by block copolymers. *Soft Matter* **2010**, 6, (14), 3111-3118.
8. Halperin, A.; Alexander, S. Polymeric micelles: their relaxation kinetics. *Macromolecules* **1989**, 22, (5), 2403-2412.
9. Charbonneau, C.; Chassenieux, C.; Colombani, O.; Nicolai, T. Controlling the Dynamics of Self-Assembled Triblock Copolymer Networks via the pH. *Macromolecules* **2011**, 44, (11), 4487-4495.
10. Lejeune, E.; Chassenieux, C.; Colombani, O., pH Induced Desaggregation Of Highly Hydrophilic Amphiphilic Diblock Copolymers. In *Trends in Colloid and Interface Science Xxiv*, Starov, V.; Prochazka, K., Eds. 2011; Vol. 138, pp 7-16.
11. Bendejacq, D. D.; Ponsinet, V.; Joanicot, M. Chemically tuned amphiphilic diblock copolymers dispersed in water: From colloids to soluble macromolecules. *Langmuir* **2005**, 21, (5), 1712-1718.
12. Borisova, O.; Billon, L.; Zaremski, M.; Grassl, B.; Bakaeva, Z.; Lapp, A.; Stepanek, P.; Borisov, O. pH-triggered reversible sol-gel transition in aqueous solutions of amphiphilic gradient copolymers. *Soft Matter* **2011**, 7, (22), 10824-10833.

CHAPTER 5: ARTICLE 2

13. Wright, D. B.; Patterson, J. P.; Pitto-Barry, A.; Cotanda, P.; Chassenieux, C.; Colombani, O.; O'Reilly, R. K. Tuning the aggregation behavior of pH-responsive micelles by copolymerization. *Polym. Chem.* **2015**, (6), 2761-2768.

14. Shedge, A.; Colombani, O.; Nicolai, T.; Chassenieux, C. Charge Dependent Dynamics of Transient Networks and Hydrogels Formed by Self-Assembled pH-Sensitive Triblock Copolyelectrolytes. *Macromolecules* **2013**, 47, (7), 2439-2444.

15. Colombani, O.; Lejeune, E.; Charbonneau, C.; Chassenieux, C.; Nicolai, T. Ionization Of Amphiphilic Acidic Block Copolymers. *J. Phys. Chem. B* **2012**, 116, (25), 7560-7565.

16. Konak, C.; Helmstedt, M. Comicellization of Chemically Identical Diblock Copolymers with Different Molecular Parameters of the Constituent Blocks in a Selective Solvent. *Macromolecules* **2001**, 34, (17), 6131-6133.

17. Konak, C.; Helmstedt, M. Comicellization of diblock and triblock copolymers in selective solvents. *Macromolecules* **2003**, 36, (12), 4603-4608.

18. Huang, X.; Xiao, Y.; Lang, M. Self-assembly of pH-sensitive mixed micelles based on linear and star copolymers for drug delivery. *J. Colloid Interface Sci.* **2011**, 364, (1), 92-99.

19. Van Butsele, K.; Sibret, P.; Fustin, C. A.; Gohy, J. F.; Passirani, C.; Benoit, J. P.; Jérôme, R.; Jérôme, C. Synthesis and pH-dependent micellization of diblock copolymer mixtures. *J. Colloid Interface Sci.* **2009**, 329, (2), 235-243.

20. Groger, S.; Geschke, D.; Karger, J.; Stallmach, F.; Konak, C. Co-micellization investigated by pulsed field gradient-NMR spectroscopy. *Macromol. Rapid Commun.* **2004**, 25, (10), 1015-1018.

21. Lo, C.-L.; Lin, S.-J.; Tsai, H.-C.; Chan, W.-H.; Tsai, C.-H.; Cheng, C.-H. D.; Hsiue, G.-H. Mixed micelle systems formed from critical micelle concentration and temperature-sensitive diblock copolymers for doxorubicin delivery. *Biomaterials* **2009**, 30, (23-24), 3961-3970.

22. Yin, H.; Lee, E. S.; Kim, D.; Lee, K. H.; Oh, K. T.; Bae, Y. H. Physicochemical characteristics of pH-sensitive poly(l-Histidine)-b-poly(ethylene glycol)/poly(l-Lactide)-b-poly(ethylene glycol) mixed micelles. *J. Controlled Release* **2008**, 126, (2), 130-138.

23. Chang, C.; Wei, H.; Li, Q.; Yang, B.; Chen, N.; Zhou, J.-P.; Zhang, X.-Z.; Zhuo, R.-X. Construction of mixed micelle with cross-linked core and dual responsive shells. *Polym. Chem.* **2011**, 2, (4), 923-930.

24. Kellarakis, A.; Havredaki, V.; Yuan, X.-F.; Yang, Y.-W.; Booth, C. Mixed micelles of block copolymers of ethylene oxide and 1,2-butyl

lene oxide. Solutions and gels of triblock BEB plus diblock EB copolymers studied by light scattering and rheology. *J. Mater. Chem.* **2003**, 13, (11), 2779-2784.

25. Yu, L.; Zhang, Z.; Zhang, H.; Ding, J. Mixing a Sol and a Precipitate of Block Copolymers with Different Block Ratios Leads to an Injectable Hydrogel. *Biomacromolecules* **2009**, 10, (6), 1547-1553.

26. Kotsuchibashi, Y.; Ebara, M.; Yamamoto, K.; Aoyagi, T. Tunable stimuli-responsive self-assembly system that forms and stabilizes nanoparticles by simple mixing and heating/cooling of selected block copolymers. *Polym. Chem.* **2011**, 2, (6), 1362-1367.

27. Liu, T.; Qian, Y.; Hu, X.; Ge, Z.; Liu, S. Mixed polymeric micelles as multifunctional scaffold for combined magnetic resonance imaging contrast enhancement and targeted chemotherapeutic drug delivery. *J. Mater. Chem.* **2012**, 22, (11), 5020-5030.

28. Wu, H.; Zhu, L.; Torchilin, V. P. pH-sensitive poly(histidine)-PEG/DSPE-PEG copolymer micelles for cytosolic drug delivery. *Biomaterials* **2013**, 34, (4), 1213-1222.

29. Tian, M.; Qin, A.; Ramireddy, C.; Webber, S. E.; Munk, P.; Tuzar, Z.; Prochazka, K. Hybridization of block copolymer micelles. *Langmuir* **1993**, 9, (7), 1741-1748.

30. Honda, C.; Yamamoto, K.; Nose, T. Comicellization of binary mixtures of block copolymers with different block lengths in a selective solvent. *Polymer* **1996**, 37, (10), 1975-1984.

31. Esselink, F. J.; Dormidontova, E. E.; Hadziioannou, G. Redistribution of Block Copolymer Chains between Mixed Micelles in Solution. *Macromolecules* **1998**, 31, (15), 4873-4878.

32. Stepanek, M.; Podhajecka, K.; Tesarova, E.; Prochazka, K.; Tuzar, Z.; Brown, W. Hybrid Polymeric Micelles with Hydrophobic Cores and Mixed Polyelectrolyte/Nonelectrolyte Shells in Aqueous Media. 1. Preparation and Basic Characterization. *Langmuir* **2001**, 17, (14), 4240-4244.

33. Zhang, W.; Shi, L.; An, Y.; Gao, L.; He, B. Unimacromolucule Exchange between Bimodal Micelles Self-Assembled by Polystyrene-block-Poly(acrylic acid) and Polystyrene-block-Poly(amino propylene-glycol methacrylate) in Water. *J. Phys. Chem. B* **2004**, 108, (1), 200-204.

34. Wright, D. B.; Patterson, J. P.; Gianneschi, N. C.; Chassenieux, C.; Colombani, O.; O'Reilly, R. K. Blending block copolymer micelles in solution; obstacles of blending. *Polym. Chem.* **2016**.

35. Wright, D. B.; Patterson, J. P.; Pitto-Barry, A.; Lu, A.; Kirby, N.; Gianneschi, N. C.; Chassenieux, C.; Colombani, O.; O'Reilly, R. K. The Copolymer Blending Method: A New

CHAPTER 5: ARTICLE 2

Approach for Targeted Assembly of Micellar Nanoparticles. *Macromolecules* **2015**, 48, (18), 6516-6522.

36. Rufier, C.; Collet, A.; Viguier, M.; Oberdisse, J.; Mora, S. Asymmetric End-Capped Poly(ethylene oxide). Synthesis and Rheological Behavior in Aqueous Solution. *Macromolecules* **2008**, 41, (15), 5854-5862.

37. Lauber, L.; Chassenieux, C.; Nicolai, T.; Colombani, O. Highlighting the Role of the Random Associating Block in the Self-Assembly of Amphiphilic Block-Random Copolymers. *Macromolecules* **2015**, 48, (20), 7613-7619.

38. Lejeune, E.; Drechsler, M.; Jestin, J.; Muller, A. H. E.; Chassenieux, C.; Colombani, O. Amphiphilic Diblock Copolymers with a Moderately Hydrophobic Block: Toward Dynamic Micelles. *Macromolecules* **2010**, 43, (6), 2667-2671.

39. Berne, B.; Pecora, R., *Dynamic Light Scattering: With Applications to Chemistry, Biology, and Physics*. John Wiley Sons, Inc.: 1976.

40. Klymenko, A.; Nicolai, T.; Benyahia, L.; Chassenieux, C.; Colombani, O.; Nicol, E. Multiresponsive Hydrogels Formed by Interpenetrated Self-Assembled Polymer Networks. *Macromolecules* **2014**, 47, (23), 8386-8393.

41. Charbonneau, C.; Lima, M. M. D.; Chassenieux, C.; Colombani, O.; Nicolai, T. Structure of pH sensitive self-assembled amphiphilic di- and triblock copolyelectrolytes: micelles, aggregates and transient networks. *Phys. Chem. Chem. Phys.* **2013**, 15, (11), 3955-3964.

42. Creutz, S.; van Stam, J.; De Schryver, F. C.; Jerome, R. Dynamics of poly((dimethylamino)alkyl methacrylate-block-sodium methacrylate) micelles. Influence of hydrophobicity and molecular architecture on the exchange rate of copolymer molecules. *Macromolecules* **1998**, 31, (3), 681-689.

43. Van Stam, J.; Creutz, S.; De Schryver, F. C.; Jérôme, R. Tuning of the Exchange Dynamics of Unimers between Block Copolymer Micelles with Temperature, Cosolvents, and Cosurfactants. *Macromolecules* **2000**, 33, (17), 6388-6395.

44. Okay, O., Self-Healing Hydrogels Formed via Hydrophobic Interactions. In *Supramolecular Polymer Networks and Gels*, Seiffert, S., Ed. Springer International Publishing: Cham, 2015; pp 101-142.

Supporting information of article 2

pH-Controlled Rheological Properties of Mixed Amphiphilic Triblock Copolymers

Lionel Lauber, Olivier Colombani, Taco Nicolai and Christophe Chassenieux*

1. Influence of the preparation pathway on the characteristics of the DH40/DH60 mixtures

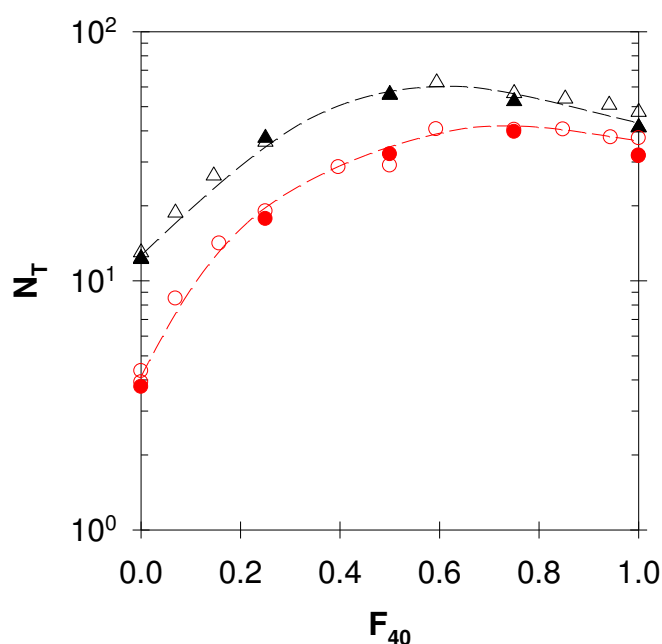


Figure S1. Total aggregation number (N_T) at $\alpha=0.2$ (Δ) and $\alpha=0.4$ (\circ) as a function of the fraction of DH40 in mixed micelle solutions of DH40/DH60, $[\text{Na}^+]=0.5$ mol/L and $C=2$ g/L for two different pathways of preparation. Open symbols: polymer solutions mixed at $\alpha=0.9$, followed by addition and hydrolysis of D-glucono- δ -lactone to reach the target α value. Closed symbols: polymer solutions prepared separately at the target α values using GDL, followed by mixing after the target α value has been reached.

2. Evolution of the hydrodynamic radius as a function of F_{40} for the mixtures of diblock copolymers

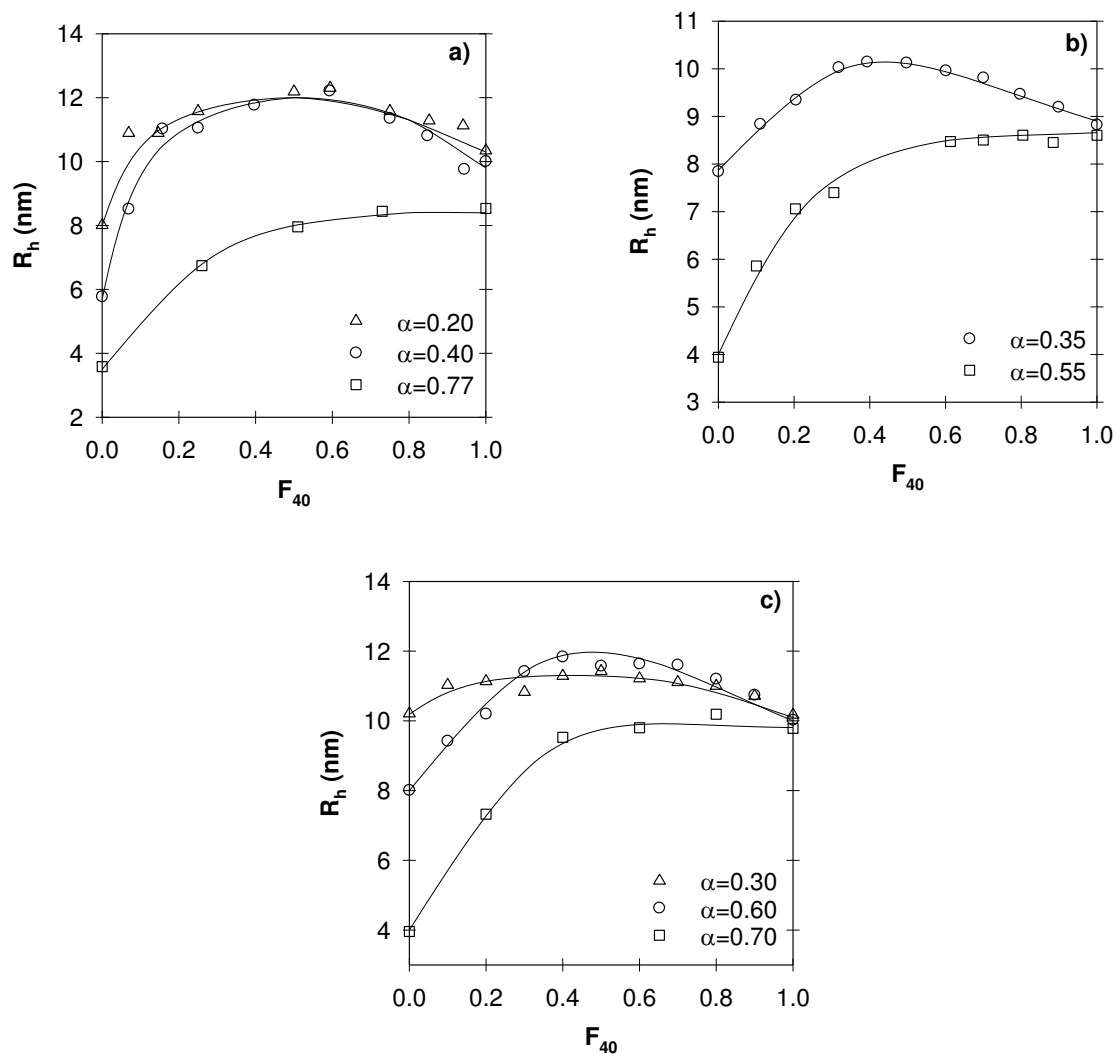


Figure S2. Evolution of R_h as a function of the weight fraction of DH40 (F_{40}) in aqueous solutions of DH40 and DH60 at $[Na^+] = 0.5$ mol/L (a) DH40 and DH60 at $[Na^+] = 0.1$ mol/L (b) and DH40 and DH50 at $[Na^+] = 0.5$ mol/L (c), $C = 2$ g/L for different ionization degrees. The solid lines are guides to the eye.

3. Mixture of non hybridizing TH40/TH60 triblock copolymers

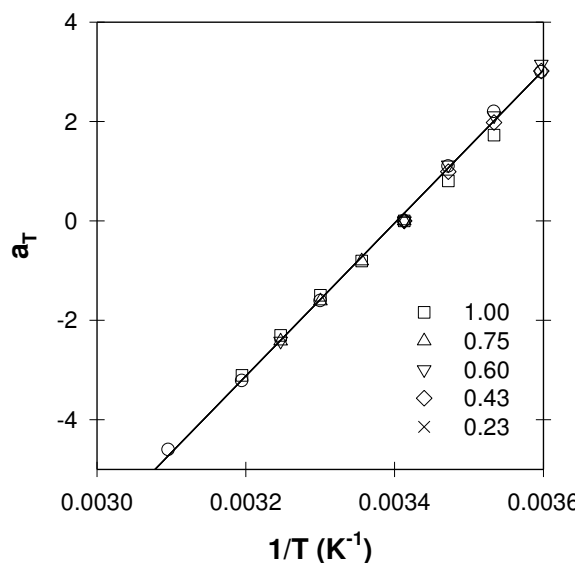


Figure S3. Arrhenius representation of the temperature dependence of the shift factors normalized by the value at 20°C for mixtures of TH40/TH60 at different fractions of TH40 at $C=30$ g/L and $\alpha=0.65$ without added salt. The symbol keys are the same as in fig. 3.

4. Mixture of hybridizing TH40/TH50 triblock copolymers

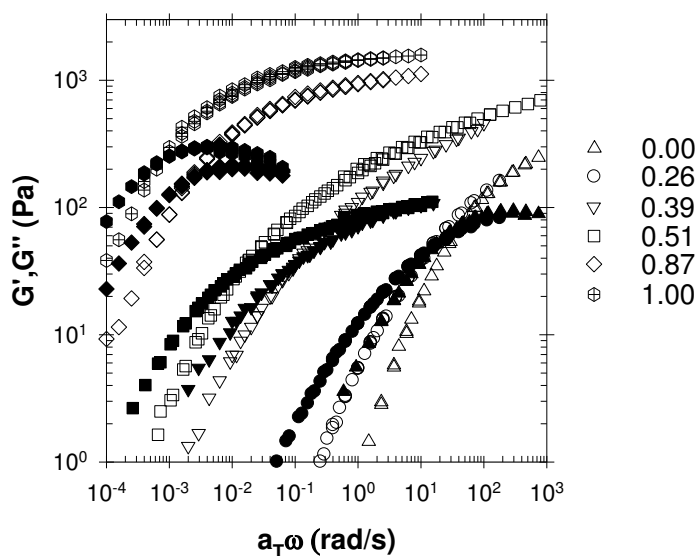


Figure S4. Master curves obtained by frequency-temperature superposition of the shear moduli at $T_{ref}=20$ °C for mixtures of TH40 and different fractions of TH40 indicated in the figure at $C=30$ g/L and $\alpha=0.65$ without added salt. For clarity, not all data points are shown.

CHAPTER 6: ARTICLE 3

CHAPTER 6 : ARTICLE 3

**pH-Responsive Transient Networks Formed By Amphiphilic
Graft Copolymers**

Lionel Lauber, Jérémy Depoorter, Taco Nicolai, Christophe Chassenieux and Olivier
Colombani*

LUNAM Université, Université du Maine, IMMM-UMR CNRS 6283, Equipe Polymères,
Colloïdes et Interfaces, av. O. Messiaen, 72085 Le Mans cedex 9, France

AUTHOR EMAIL ADDRESS: christophe.chassenieux@univ-lemans.fr

CHAPTER 6: ARTICLE 3

ABSTRACT: Graft copolymers consisting of a polydisperse poly(acrylic acid) (PAA) backbone and monodisperse random grafts of *n*-butyl acrylate and acrylic acid, P(*n*BA_{50%}-*stat*-AA_{50%})₁₀₀ were synthesized by free radical polymerization of the backbone followed by ATRP polymerization of the grafts via a grafting from approach. The rheological properties of their aqueous solutions were measured by oscillatory shear measurements at different temperatures, pH and concentrations. All graft copolymers formed transient networks above their percolation concentrations with pH-dependent relaxation times. These results implied that incorporation of hydrophilic AA units within the hydrophobic grafts allowed controlling their exchange dynamics in a pH-dependent way, leading to visco-elastic fluids with a pH-tunable terminal relaxation time. Provided that the grafting density remained low, the rheological properties of the graft copolymers were very similar to those of model BAB triblock copolymers consisting of a PAA central block and P(*n*BA_{50%}-*stat*-AA_{50%})₁₀₀ lateral blocks.

KEYWORDS: hydrogels, self-assembly, graft copolymer, rheology, transient network

I. Introduction

By association of their solvophobic block(s), amphiphilic block copolymers self-assemble in selective solvents.¹ When the copolymers consist of at least two solvophobic blocks, their self-assembly may result in the formation of a 3D network with useful rheological properties.^{2,3} The self-assembly of BAB triblock copolymers with solvophobic B-blocks has been studied extensively because they are well-defined model systems. In water BAB triblock copolymers self-assemble in dilute solution into flower-like micelles consisting of a core formed by associated B blocks surrounded by a corona of hydrophilic A blocks. At higher concentrations the copolymers form bridges between the micelles and above a critical concentration (C_p) the bridged micelles percolate and form a system spanning network. As a consequence, the viscosity increases sharply, but does not diverge if the lifetime of the bridges is finite.⁴⁻⁸

In recent years, we have studied in detail a particular type of BAB triblock copolymers in aqueous solution for which the lifetime of the bridges and therefore the rheology could be finely tuned by the pH.^{9,10} The hydrophilic A block consisted of poly(acrylic acid) (PAA) and the hydrophobic B blocks consisted of random copolymers of acrylic acid and *n*butyl acrylate: $P(nBA_{1-x}\text{-stat-AA}_x)_{100}\text{-}b\text{-PAA}_{200}\text{-}b\text{-P}(nBA_{1-x}\text{-stat-AA}_x)_{100}$.^{9,10} It was shown that the pH-range over which the dynamics of the self-assembled network varied could be shifted by varying the composition of the B-blocks.¹⁰

However, polymers with relatively high molecular weight bearing many associative groups, also called multi stickers², are easier to obtain than their triblock homologues and offer interesting rheological properties relevant for applications in coatings¹¹ and enhanced oil recovery¹² for example. Therefore, it is of interest to investigate if the approach to control the dynamics by the pH that was successful for triblock copolymers can be extended to copolymers containing more associative groups.

Most multi-sticker polymers that have been investigated so far are hydrophobically modified polymers (HMP) consisting of a hydrophilic backbone grafted with hydrophobic stickers. Most of the literature on HMP deals with poly(acrylamide) (PAM)¹³⁻²¹ or poly(acrylic acid) (PAA)^{22,23} hydrophilic backbones bearing alkyl chains (6 to 18 carbons). An increase in alkyl chain length or in grafting density leads to an increase of viscosity, but when it is too high the polymer precipitates. Therefore, the size and the amount of the grafts are usually chosen so as optimize the desired rheological properties while maintaining good solubility.

In the field of pH-sensitive systems, hydrophobically modified alkali-swelling emulsion polymers (HASE) are interesting and already used at industrial scale for good performance and easy synthesis. HASE are comb-like polymers usually made of a polyelectrolyte poly(ethyl acrylate-*co*-methacrylic acid) backbone with poly(ethylene oxide)-alkyl grafts.²⁴⁻²⁸ In alkaline medium, HASE form networks due to the hydrophobic grafts and the visco-elastic properties of the network are controlled by the size of the alkyl chains.²⁵

Temperature-responsive networks received many attentions two decades ago. They have been obtained by grafting a hydrophilic backbone, usually PAA or poly(acrylamide) (PAM) with temperature sensitive grafts such as poly(N-isopropylacrylamide) (PNIPAM) or poly(propylene oxide).^{23, 29-35} However, to the best of our knowledge graft copolymers for which the dynamics can be finely tuned by the pH was not reported in the literature.

Here we report on an investigation of graft copolymers analogous to the $P(nBA_{1-x}\text{-stat-AA}_x)_{100}\text{-}b\text{-PAA}_{200}\text{-}b\text{-}P(nBA_{1-x}\text{-stat-AA}_x)_{100}$ triblocks mentioned above. Instead of two terminal B-blocks attached to the central A block several B blocks were grafted to the PAA backbone at random positions; $PAA\text{-}g\text{-}P(nBA\text{-stat-AA})$. The dynamic mechanical properties in water of graft polymers with 3 different grafting densities as a function of the pH will be compared with those of the equivalent triblock copolymers.

II. Materials and methods.

1. Potentiometric Titration. An automatic titrator (TIM 856, Radiometer Analytical) controlled by the TitrMaster 85 software was used to run potentiometric titration at room temperature according to the procedure published in ref.³⁶ 30 mL of an aqueous polymer solution at an overall AA concentration $[AA] = 0.043$ mol/L, 0.047 mol/L NaOH and 0.1 M NaCl was titrated with HCl (1 M) at a rate of 0.1 mL/min.

The total amount of titrable AA units and the evolution of the pH of the solution as a function of the ionization degree of the polymer $\alpha = [AA^-]/([AAH] + [AA^-])$ were determined from the raw titration data, where $[AA^-]$ and $[AAH]$ are the concentrations of charged and protonated AA units, respectively. It was verified that all acrylic acid units within the graft copolymers could be ionized no matter whether they were situated in the backbone or in the grafts.

2. Sample Preparation. Stock solutions were prepared by dissolving the polymers in demineralized water (Millipore) with the required amount of NaOH to reach an ionization degree $\alpha \sim 0.9\text{-}1$ while stirring overnight. For the final solutions, freshly prepared solutions of

D-glucono- δ -lactone (GDL) were used to decrease α in-situ as previously reported.¹⁰ Solutions were prepared at least 24 hours prior to measurements to ensure full hydrolysis of GDL into gluconic acid.^{37, 38} The ionization degrees were corrected to take into account the incomplete acid-base reaction between gluconic acid and the polymer, as explained in details in the supporting information of ref.³⁸

3. *Oscillatory shear measurements.* Oscillatory shear measurements were performed using controlled-stress rheometers equipped with cone-plate geometries: ARG2 (angles = 4° - 2° - 1°, diameters 20 - 60 mm) and MCR301 (angles = 2° - 1°, diameters = 25 - 50 mm). Silicon oil was used to protect the samples against water evaporation. A Peltier system controlled the temperature and the measurements were conducted in the linear response regime. Solutions were loaded onto the rheometers just after the addition of GDL.

III. Results.

1. Synthesis of the graft copolymers

PAA₅₀₀-g-[P(*n*BA_{50%}-*stat*-AA_{50%})₁₀₀]_x graft copolymers with different grafting densities (*x*) were synthesized in four steps as shown in Figure 1. First, 2-(2-bromoisobutyryloxy)ethyl acrylate (BIEA) was obtained by reaction of 2-hydroxyethyl acrylate (HEA) with α -bromoisobutyryl bromide. Second, BIEA was copolymerized with *tert*-butyl acrylate (*t*BA) by free radical polymerization to synthesize a P(*t*BA-*stat*-BIEA) copolymer. Third, the graft copolymer, P*t*BA-g-[P(*n*BA_{50%}-*stat*-*t*BA_{50%})₁₀₀]_x, was obtained by a grafting-from method using P(*t*BA-*stat*-BIEA) as multifunctional ATRP macroinitiator to initiate the copolymerization of *t*BA and *n*-butyl acrylate (*n*BA) by atom transfer radical polymerisation (ATRP). The graft copolymer precursor was acidolysed to produce the final graft copolymer PAA₅₀₀-g-[P(*n*BA_{50%}-*stat*-AA_{50%})₁₀₀]_x. The backbone dispersities were always lower than 2.9 and the graft copolymers dispersities were equal to 2.5.

Three graft copolymers were produced consisting of a PAA backbone with number average polymerisation degree around 500 and 2, 7 or 30 grafts per chain noted as G2H50, G7H50 and G30H50, respectively. The grafts had a number average degree of polymerization of 100 and contained 50 %mol of AA units. More details of the synthesis are given in section 1 of the supporting information.

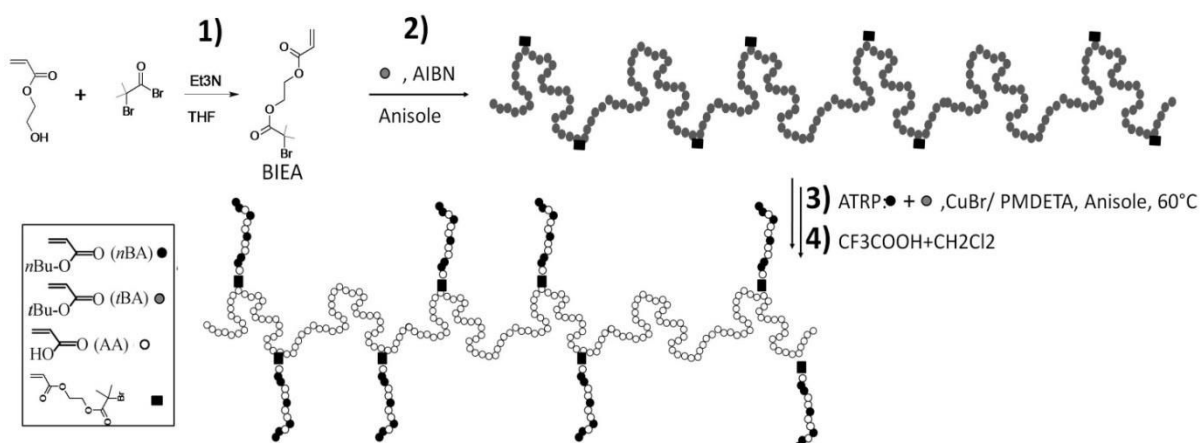


Figure 1. Schematic representation of the four steps of the synthesis of $\text{PAA-g-[P}(n\text{BA}_{50\%}\text{-stat-AA}_{50\%})_{100}]_x$: (1) synthesis of the functional monomer BIEA, (2) synthesis of the $\text{P}(t\text{BA-stat-BIEA})$ backbone by free radical polymerization (3) synthesis of the $\text{P}t\text{BA-g-[P}(n\text{BA}_{50\%}\text{-stat-tBA}_{50\%})_{100}]_x$ copolymer precursor by grafting from using atom transfer radical polymerization (ATRP), and (4) acidolysis of the $t\text{BA}$ units into AA.

2. pH dependence of the charge density

Figure 2a shows the ionization degree (α) of the 3 graft copolymers as a function of the pH. The dependence is close for G2H50 and G7H50, but for G30H50 the increase of α with increasing pH starts at a higher value. Following the method described elsewhere for the equivalent triblock copolymers,^{10, 36} the ionization degree of the hydrophobic blocks (α_{MH}) and of the PAA backbone was determined as a function of the overall ionization degree (α), see Figure 2b. Figure 2b shows that the relationship between α_{MH} and α depends strongly on the grafting density. For a given α , the ionization degree of the grafts decreases with increasing graft density, which is a consequence of the relative increase of AA units in the grafts if the grafting density is increased. The fraction of AA units in the hydrophobic blocks is close for TH50 and G7H50, which explains why the relationship between α_{MH} and α is close for these two polymers.

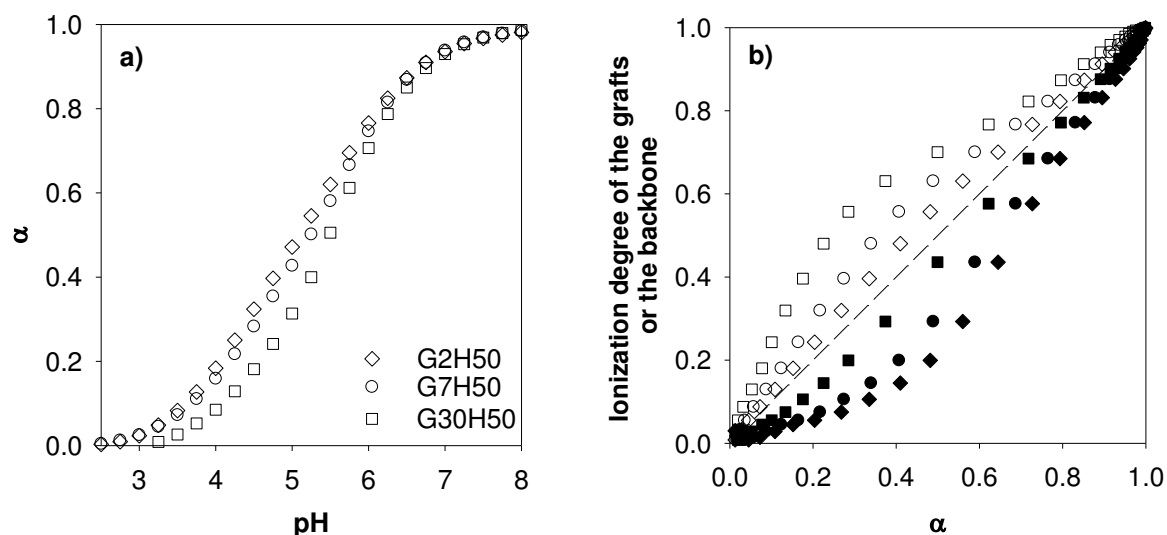


Figure 2. (a) Degree of ionization of the AA units as a function of the pH for G2H50, G7H50 and G30H50. (b) Degree of ionization of the PAA backbone (open symbols) and of the grafts (closed symbols) as a function of the overall degree of ionization (α) for G2H50 (\diamond), G7H50 (\circ) and G30H50 (\square).³⁶

3. Viscosity

Figure 3a shows the evolution of the viscosity at different α as a function of the concentration at $T=20$ °C for G7H50. The viscosity increased steeply with increasing polymer concentration above the percolation concentration (C_p), which increased with α . The viscosity at $C \gg C_p$ remained finite for all α except $\alpha=0.17$ where it became immeasurably high, implying that at higher α the network formed by self-assembly of the graft copolymers was transient. The increase of the viscosity was less steep at higher α . Similar measurements were done for G2H50 and G30H50, see section 2 and 3 of the supporting information.

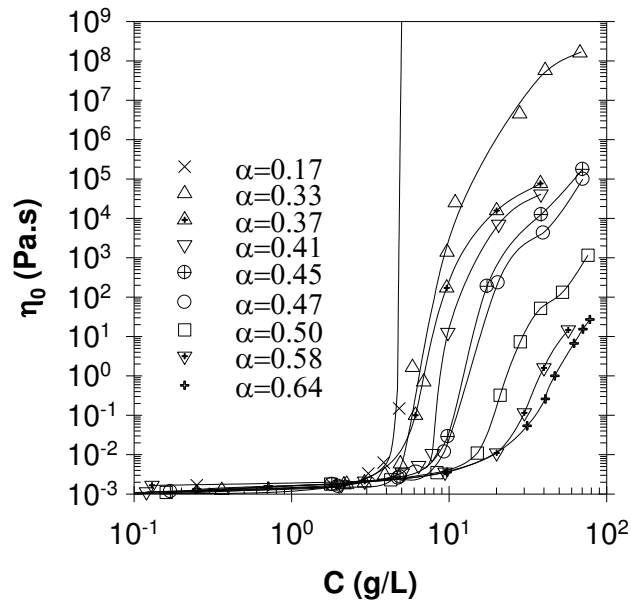


Figure 3. Dependence of the zero shear viscosity (η_0) of G7H50 as a function of the concentration at different ionization degrees as indicated in the figure. The solid lines are guides to the eye.

In Figure 4 the evolution of C_p taken as the concentration at which $\eta_0=0.1$ Pa.s. is plotted as a function of α for the three copolymers. At low ionization degrees, C_p was about 5 g/L for G7H50, 10 g/L for G2H50 and 25 g/L for G30H50. For all 3 polymers C_p increased with increasing α up to 50 g/L at $\alpha=0.65$.

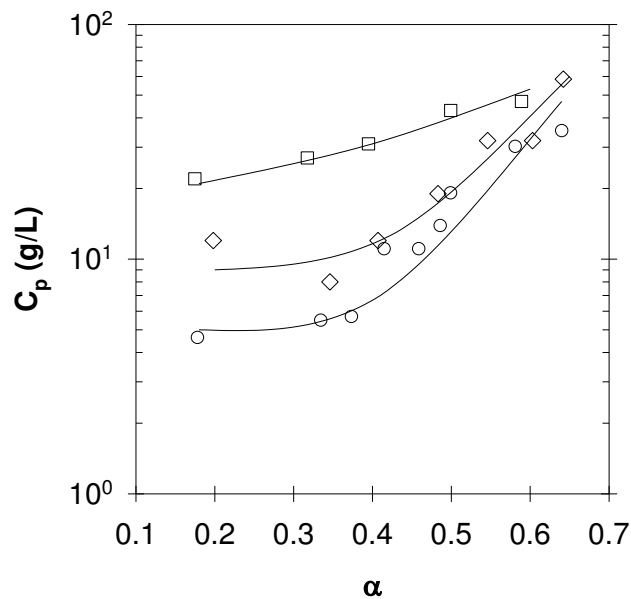


Figure 4. Dependence of the percolation concentration on the degree of ionization for G2H50 (\diamond), G7H50 (\circ) and G30H50 (\square). The solid lines are guides to the eye.

4. Shear modulus

The storage (G') and loss (G'') shear moduli were determined as a function of the radial oscillation frequency (ω) at different temperatures and master curves could be obtained by frequency-temperature superposition as was shown elsewhere for the equivalent triblock copolymers, see ref.⁹ and section 4 of the supplementary information. For all three graft copolymers the frequency shift factors had an Arrhenius temperature dependence characterized by an activation energy $E_a \approx 120$ kJ/mol. As an example Figure 5a shows the master curves for G7H50 at $C=40$ g/L at different α between 0.45 and 0.65. The observed frequency dependence of the shear moduli is characteristic for viscoelastic fluids. Results obtained at different α could be superimposed using horizontal and vertical shifts and a master curve was obtained with $\alpha_{\text{ref}} = 0.45$ (see Figure 5b). Similar results were obtained at other polymer concentrations.

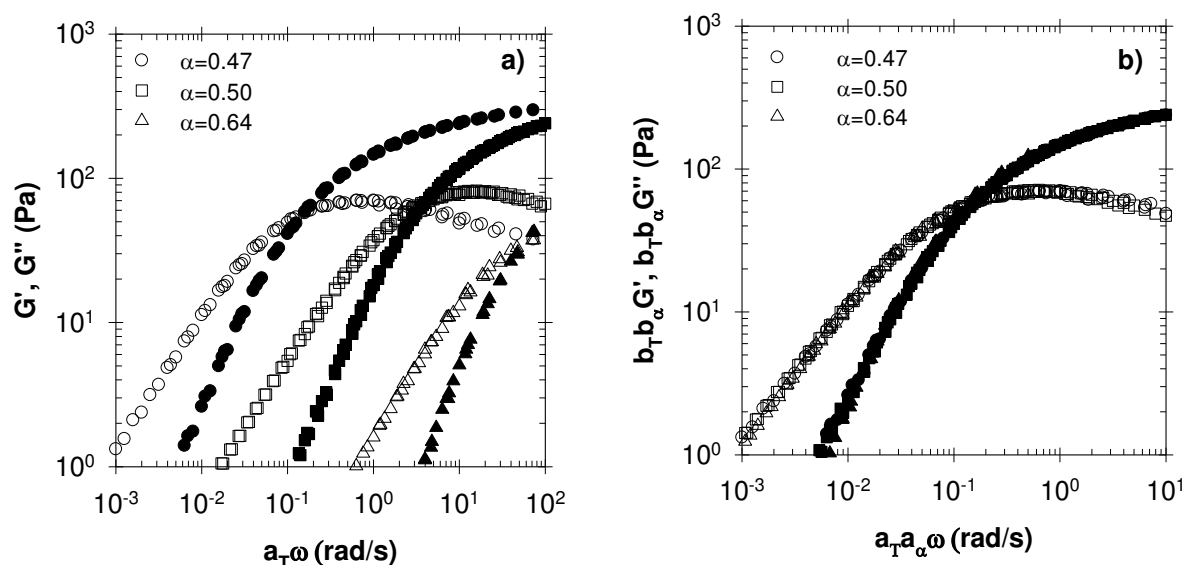


Figure 5. (a) Frequency dependence of the storage (open symbols) and loss (filled symbols) shear moduli of G7H50 at different α for $C = 40$ g/L and $T_{\text{ref}} = 20$ °C. (b) Same data as in (a) after frequency- α superposition with $\alpha_{\text{ref}}=0.45$.

The relaxation time (τ) defined as the inverse of the angular frequency (ω) at which $G'=G''$ is shown as a function of the concentration in Figure 6a. τ increased with increasing concentration, but the dependence was weak at high concentrations. For a given polymer

concentration, τ increased strongly with decreasing α with values varying over seven decades within the investigated α -range. In Figure 6b the elastic modulus (G_e) defined as G' at $\omega\tau=10^2$ is plotted as a function of the polymer concentration. G_e increased with the concentration, but the effect of α was small except close to the percolation threshold.

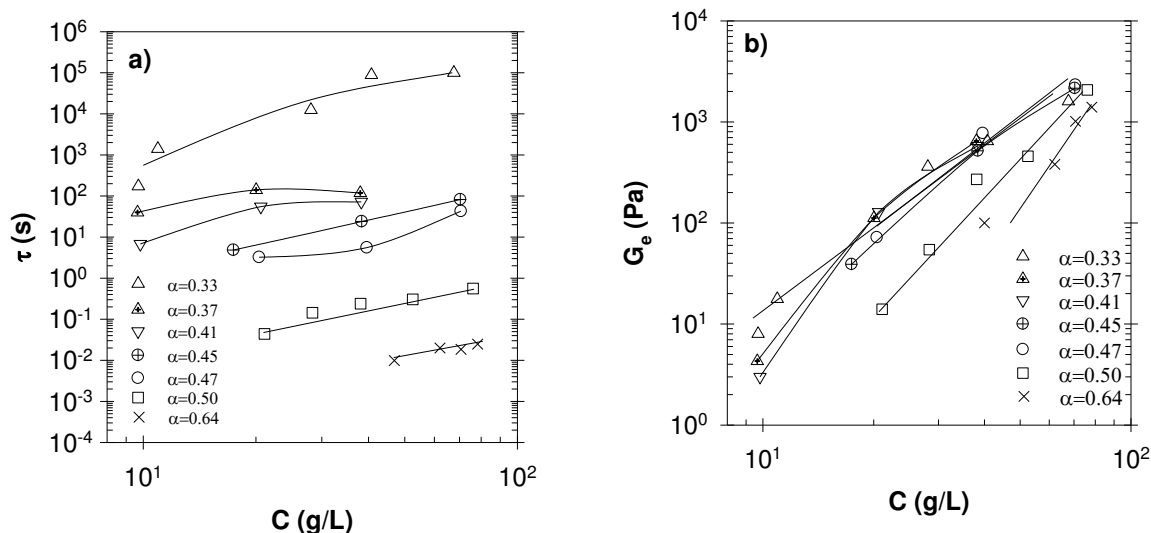


Figure 6. Concentration dependence of the relaxation time (a) and the elastic modulus (b) for G7H50 at different ionization degrees. The solid lines are guides to the eye.

The same measurements were done for G2H50 and G30H50. The shape of the master curves obtained by temperature-frequency and α -frequency superposition, was the same for all three graft copolymer, see section 5 of the supporting information.

Figure 6 shows that for G7H50 the relaxation time depended little on the concentration and that the elastic modulus depended little on α except close to the percolation threshold. Therefore we compare the dependence of τ on α (Figure 7a) and the dependence of G_{el} on C (Figure 7b) for systems that were not close to the percolation threshold. The relaxation time increases steeply with decreasing α for G2H50 and G7H50, but occurs at larger α for G2H50. The increase of τ with decreasing α is much weaker for G30H50 and occurs at lower α . There is a large spread of the values τ at a given α as was also found for dynamic networks formed by the equivalent triblock copolymers.^{9, 10}

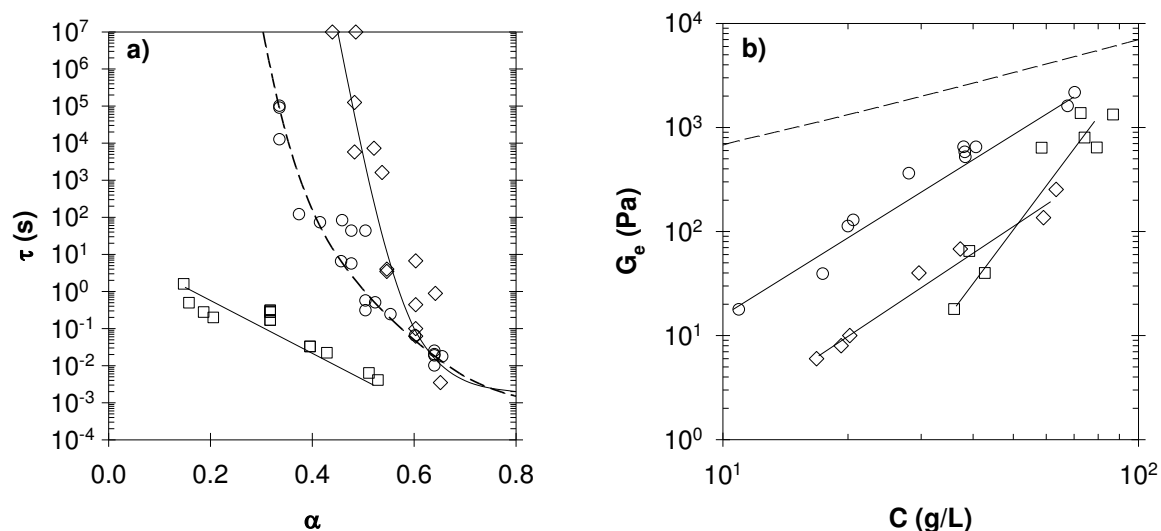


Figure 7. (a) Dependence of the relaxation time on the ionization degree at $C \gg C_p$ for G2H50 (\diamond), G7H50 (\circ) and G30H50 (\square) (b) Dependence of the elastic modulus on the polymer concentration at small α for G2H50, G7H50 and G30H50. Solid lines are guides to the eye. The dashed line indicates the results obtained for TH50.

As expected, the elastic modulus increased with increasing concentration for all copolymers. G_{el} was significantly larger for G7H50 than for G2H50 over the whole concentration range covered in the experiment. For G30H50, G_{el} started to increase at higher polymer concentrations and reached values intermediate between G2H50 and G7H50 at the highest concentrations.

IV Discussion

The dynamic mechanical behaviour of the graft copolymers is qualitatively similar to that of the equivalent BAB triblock copolymer (TH50): $P(nBA_{50\%}\text{-stat-AA}_{50\%})_{100}\text{-}b\text{-PAA}_{200}\text{-}b\text{-}P(nBA_{50\%}\text{-stat-AA}_{50\%})_{100}$ reported in refs ^{9, 10, 39}, with B blocks that were the same as the grafts. Master curves for TH50 formed by temperature-frequency and α -frequency superpositions had the same shape as for the graft copolymers and the temperature dependence of the relaxation time was characterized by the same activation energy. This suggests that stress relaxation is for all polymers controlled by the escape of a hydrophobic block from the micellar core, which is corroborated by the observation that the dependence of τ on α was within the experimental error same for TH50 and G7H50 for which the charge density of the hydrophobic blocks (α_{MH}) was by chance the same for a given α , see dashed lines in Figure 2b and Figure 7a.

If the relaxation time is fully determined by the escape of a graft from the micellar core, it is to be expected that it is determined by the fraction of charged units in the grafts (f), which in turn depends on α_{MH} . Figure 8, compares the relaxation time of the 3 graft copolymers as a function of f . In this representation the relaxation times of G2H50 and G7H50 were indeed closer, though still significantly different. However, the relaxation time of G30H50 was much smaller for a given f . We speculate that the escape time of the hydrophobic blocks is influenced by the length of PAA chain sections between grafts, which are on average very short (16 units) for G30H50.

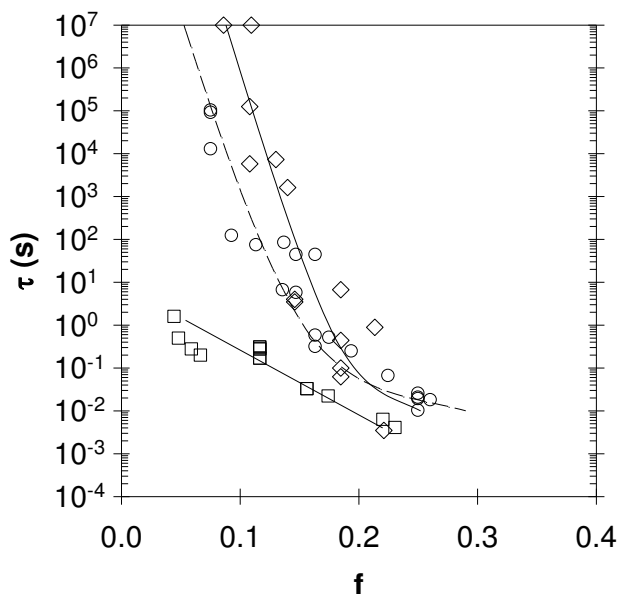


Figure 8. Evolution of the relaxation time of the transient networks as a function of the fraction of charged units within the grafts of G2H50 (◇), G7H50 (○) and G30H50 (□). The solid lines are guides to the eye.

The high frequency elastic modulus of the networks is determined by the concentration of elastically active bridges $G_e = \nu RT$ with ν the molar concentration of elastically active chains, T the absolute temperature and R the gas constant. For the triblock copolymers each polymer can make a single bridge and it was found that most of the polymers were elastically active for $C \gg C_p$.⁹ For graft copolymers with x grafts per chain, each polymer can in principle form on average $x-1$ elastically active bridges. It follows that for ideal networks G_e should increase with increasing grafting density: $G_e = 23.C$, $1.4 \times 10^2.C$ and $6.6 \times 10^2.C$ for G2H50, G7H50 and G30H50, respectively. The experimentally observed moduli were much smaller implying that the networks were far from ideal even for C larger than $10 \times C_p$. We suggest that for the densely grafted polymers many inelastic loops are formed instead of elastic bridges, because

the average length of the PAA chain sections between grafts is shorter. For G2H50, G_e is smaller than for ideal networks, because a significant fraction of the polymers contains a single graft and therefore cannot form elastic bridges. The elastic moduli of G7H50 happen to be close to those of TH50 for $C \gg C_p$, see Figure 7b, due to a fortuitous compensation of the higher fraction of loops by the higher concentration of PAA chains sections between the hydrophobic blocks.

The percolation concentration of the graft polymers was independent of α for $\alpha < 0.4$ where it was about 5 g/L, 10 g/L and 25 g/L for G7H50, G2H50 and G30H50, respectively. In the same range of α , C_p of TH50 increased from 4 to 10 g/L.^{9, 10} The decrease of C_p with increasing grafting density may be explained by the higher concentration of grafts for a given polymer concentration. However, if the grafting density is too high C_p increases again. In dilute solution more densely grafted polymers are collapsed into denser particles for which the overlap concentration is lower. We speculate that the minimum value of C_p at intermediate x is caused by the antagonistic effects increasing of graft concentration and increasing intra molecular association with increasing x .

IV. Conclusions

The dynamic mechanical behavior of aqueous solutions of pH sensitive graft copolymers with a hydrophilic backbone and hydrophobic grafts was qualitatively similar to that of the equivalent BAB triblock copolymers with hydrophobic B blocks with the same composition. For all systems dynamic networks were formed by self-assembly of the hydrophobic blocks, whether terminal or grafted, into micellar cores bridged by the hydrophilic chains. Above a critical percolation concentration the terminal relaxation time of applied mechanical stress increased strongly with decreasing ionization degree and therefore decreasing pH. As a consequence, the viscosity of the systems could be modulated over many orders of magnitude by varying the pH.

The relaxation time was to a large extent determined by the charge density of the hydrophobic blocks, but decreased with decreasing length of the PAA chain sections between the grafts. The elastic modulus of the transient networks was determined by the concentration of elastically active bridges. It was higher for polymers with intermediate graft density ($x=7$) than for polymers with smaller ($x=2$) or higher ($x=30$) average graft density. The percolation concentration was lowest for intermediate graft density. The optimum grafting density is a compromise between the increase of the density of hydrophobic grafts, which allows

CHAPTER 6: ARTICLE 3

formation of more bridges, and the increase of intra over inter molecular association (loops vs bridges).

The strategy to obtain dynamic pH-sensitive self-assembled networks by inserting hydrophilic pH sensitive units within the hydrophobic blocks that was developed for triblock copolymers can be successfully applied to graft copolymers.

ASSOCIATED CONTENT

Details on the synthesis, the construction of the master curves, the viscoelastic properties are available in Supporting Information. This material is available free of charge via the Internet at <http://pubs.acs.org>.

REFERENCES

1. Mai, Y.; Eisenberg, A. Self-assembly of block copolymers. *Chem. Soc. Rev.* **2012**, 41, (18), 5969-5985.
2. Chassenieux, C.; Nicolai, T.; Benyahia, L. Rheology of associative polymer solutions. *Curr. Opin. Colloid Interface Sci.* **2011**, 16, (1), 18-26.
3. Chassenieux, C.; Tsitsilianis, C. Recent trends in pH/thermo-responsive self-assembling hydrogels: from polyions to peptide-based polymeric gelators. *Soft Matter* **2016**, 12, (5), 1344-1359.
4. Serero, Y.; Aznar, R.; Porte, G.; Berret, J. F.; Calvet, D.; Collet, A.; Viguiier, M. Associating polymers: From "flowers" to transient networks. *Phys. Rev. Lett.* **1998**, 81, (25), 5584-5587.
5. Bossard, F.; Aubry, T.; Gotzamanis, G.; Tsitsilianis, C. pH-Tunable rheological properties of a telechelic cationic polyelectrolyte reversible hydrogel. *Soft Matter* **2006**, 2, (6), 510-516.
6. Bossard, F.; Sfika, V.; Tsitsilianis, C. Rheological properties of physical gel formed by triblock polyampholyte in salt-free aqueous solutions. *Macromolecules* **2004**, 37, (10), 3899-3904.
7. Bossard, F.; Tsitsilianis, C.; Yannopoulos, S. N.; Petekidis, G.; Sfika, V. A novel thermo-thickening phenomenon exhibited by a triblock polyampholyte in aqueous salt-free solutions. *Macromolecules* **2005**, 38, (7), 2883-2888.
8. Tam, K. C.; Jenkins, R. D.; Winnik, M. A.; Bassett, D. R. A structural model of hydrophobically modified urethane-ethoxylate (HEUR) associative polymers in shear flows. *Macromolecules* **1998**, 31, (13), 4149-4159.
9. Charbonneau, C.; Chassenieux, C.; Colombani, O.; Nicolai, T. Controlling the Dynamics of Self-Assembled Triblock Copolymer Networks via the pH. *Macromolecules* **2011**, 44, (11), 4487-4495.
10. Shedge, A.; Colombani, O.; Nicolai, T.; Chassenieux, C. Charge Dependent Dynamics of Transient Networks and Hydrogels Formed by Self-Assembled pH-Sensitive Triblock Copolyelectrolytes. *Macromolecules* **2013**, 47, (7), 2439-2444.
11. Raffa, P.; Wever, D. A. Z.; Picchioni, F.; Broekhuis, A. A. Polymeric Surfactants: Synthesis, Properties, and Links to Applications. *Chem. Rev.* **2015**, 115, (16), 8504-8563.
12. Wever, D. A. Z.; Picchioni, F.; Broekhuis, A. A. Polymers for enhanced oil recovery: A paradigm for structure-property relationship in aqueous solution. *Prog. Polym. Sci.* **2011**, 36, (11), 1558-1628.

CHAPTER 6: ARTICLE 3

13. Zhu, Z.; Jian, O.; Paillet, S.; Desbrières, J.; Grassl, B. Hydrophobically modified associating polyacrylamide (HAPAM) synthesized by micellar copolymerization at high monomer concentration. *Eur. Polym. J.* **2007**, 43, (3), 824-834.
14. Yang, Q.; Song, C.; Chen, Q.; Zhang, P.; Wang, P. Synthesis and aqueous solution properties of hydrophobically modified anionic acrylamide copolymers. *J. Polym. Sci., Part B: Polym. Phys.* **2008**, 46, (22), 2465-2474.
15. Regalado, E. J. n.; Selb, J.; Candau, F. o. Viscoelastic Behavior of Semidilute Solutions of Multisticker Polymer Chains. *Macromolecules* **1999**, 32, (25), 8580-8588.
16. Kujawa, P.; Audibert-Hayet, A.; Selb, J.; Candau, F. o. Effect of Ionic Strength on the Rheological Properties of Multisticker Associative Polyelectrolytes. *Macromolecules* **2006**, 39, (1), 384-392.
17. Feng, Y.; Billon, L.; Grassl, B.; Bastiat, G.; Borisov, O.; François, J. Hydrophobically associating polyacrylamides and their partially hydrolyzed derivatives prepared by post-modification. 2. Properties of non-hydrolyzed polymers in pure water and brine. *Polymer* **2005**, 46, (22), 9283-9295.
18. Cram, S. L.; Brown, H. R.; Spinks, G. M.; Hourdet, D.; Creton, C. Hydrophobically Modified Dimethylacrylamide Synthesis and Rheological Behavior. *Macromolecules* **2005**, 38, (7), 2981-2989.
19. Caputo, M. R.; Selb, J.; Candau, F. Effect of temperature on the viscoelastic behaviour of entangled solutions of multisticker associating polyacrylamides. *Polymer* **2004**, 45, (1), 231-240.
20. Castelletto, V.; Hamley, I. W.; Xue, W.; Sommer, C.; Pedersen, J. S.; Olmsted, P. D. Rheological and structural characterization of hydrophobically modified polyacrylamide solutions in the semidilute regime. *Macromolecules* **2004**, 37, (4), 1492-1501.
21. Hourdet, D.; Ducouret, G.; Varghese, S.; Badiger, M. V.; Wadgaonkar, P. P. Thermodynamic behavior of hydrophobically modified polyacrylamide containing random distribution of hydrophobes: Experimental and theoretical investigations. *Polymer* **2013**, 54, (11), 2676-2689.
22. Riemer, S.; Prévost, S.; Dzionara, M.; Appavou, M.-S.; Schweins, R.; Gradzielski, M. Aggregation behaviour of hydrophobically modified polyacrylate: Variation of alkyl chain length. *Polymer* **2015**, 70, 194-206.
23. Hourdet, D.; Gadgil, J.; Podhajecka, K.; Badiger, M. V.; Brûlet, A.; Wadgaonkar, P. P. Thermoreversible Behavior of Associating Polymer Solutions: Thermo thinning versus Thermo thickening. *Macromolecules* **2005**, 38, (20), 8512-8521.

24. English, R. J.; Laurer, J. H.; Spontak, R. J.; Khan, S. A. Hydrophobically Modified Associative Polymer Solutions: Rheology and Microstructure in the Presence of Nonionic Surfactants. *Ind. Eng. Chem. Res.* **2002**, 41, (25), 6425-6435.
25. English, R. J.; Raghavan, S. R.; Jenkins, R. D.; Khan, S. A. Associative polymers bearing n-alkyl hydrophobes: Rheological evidence for microgel-like behavior. *J. Rheol.* **1999**, 43, (5), 1175-1194.
26. Tam, K. C.; Ng, W. K.; Jenkins, R. D. Relaxation behavior of hydrophobically modified polyelectrolyte solution under various deformations. *Polymer* **2005**, 46, (12), 4052-4059.
27. Tam, K. C.; Ng, W. K.; Jenkins, R. D. Rheological properties of hydrophobically modified polyelectrolyte systems: Concentration effects. *J. Appl. Polym. Sci.* **2006**, 102, (6), 5166-5173.
28. Tam, K. C.; Ng, W. K.; Jenkins, R. D. Further studies on the rheological properties of hydrophobically modified polyelectrolyte systems: effect of varying degree of ethoxylation. *Polym. Int.* **2007**, 56, (4), 569-575.
29. Iatridi, Z.; Bokias, G. Temperature-Sensitive Water-Soluble Hybrid Organic/Inorganic Nanoparticles Formed through Complexation of Cu²⁺ Ions with Poly(sodium acrylate)-g-poly(N-isopropylacrylamide) Comb-Type Copolymers in Aqueous Solution. *Langmuir* **2009**, 25, (13), 7695-7703.
30. Durand, A.; Hourdet, D. Synthesis and thermoassociative properties in aqueous solution of graft copolymers containing poly(N-isopropylacrylamide) side chains. *Polymer* **1999**, 40, (17), 4941-4951.
31. Durand, A.; Hourdet, D. Thermoassociative graft copolymers based on poly(N-isopropylacrylamide): effect of added co-solutes on the rheological behaviour. *Polymer* **2000**, 41, (2), 545-557.
32. Bromberg, L. Self-Assembly in Aqueous Solutions of Polyether-Modified Poly(acrylic acid). *Langmuir* **1998**, 14, (20), 5806-5812.
33. Hourdet, D.; Lalloret, F.; Audebert, R. REVERSIBLE THERMOTHICKENING OF AQUEOUS POLYMER-SOLUTIONS. *Polymer* **1994**, 35, (12), 2624-2630.
34. Petit, L.; Karakasyan, C.; Pantoustier, N. g.; Hourdet, D. Synthesis of graft polyacrylamide with responsive self-assembling properties in aqueous media. *Polymer* **2007**, 48, (24), 7098-7112.

CHAPTER 6: ARTICLE 3

35. Gouveia, L. M.; Grassl, B.; Müller, A. J. Synthesis and rheological properties of hydrophobically modified polyacrylamides with lateral chains of poly(propylene oxide) oligomers. *J. Colloid Interface Sci.* **2009**, 333, (1), 152-163.
36. Colombani, O.; Lejeune, E.; Charbonneau, C.; Chassenieux, C.; Nicolai, T. Ionization Of Amphiphilic Acidic Block Copolymers. *J. Phys. Chem. B* **2012**, 116, (25), 7560-7565.
37. Charbonneau, C.; Chassenieux, C.; Colombani, O.; Nicolai, T. Progressive Freezing-in of the Junctions in Self-Assembled Triblock Copolymer Hydrogels during Aging. *Macromolecules* **2012**, 45, (2), 1025-1030.
38. Klymenko, A.; Nicolai, T.; Benyahia, L.; Chassenieux, C.; Colombani, O.; Nicol, E. Multiresponsive Hydrogels Formed by Interpenetrated Self-Assembled Polymer Networks. *Macromolecules* **2014**, 47, (23), 8386-8393.
39. Charbonneau, C.; Lima, M. M. D.; Chassenieux, C.; Colombani, O.; Nicolai, T. Structure of pH sensitive self-assembled amphiphilic di- and triblock copolyelectrolytes: micelles, aggregates and transient networks. *Phys. Chem. Chem. Phys.* **2013**, 15, (11), 3955-3964.

Supporting information of article 3

Supporting information

pH-Responsive Transient Networks Formed By Amphiphilic Graft Copolymers

Lionel Lauber, Jérémy Depoorter, , Taco Nicolai, Christophe Chassenieux* and Olivier

Colombani

1) Three step synthesis of the graft copolymers GxH50

a. Chemical characterization

Materials. 2-hydroxyethyl acrylate (HEA, 96% Aldrich) was purified by liquid-liquid extraction: once with water (1:3 v/v), ten times with cyclohexane (99% Fisher, 3:1 v/v), twice with NaCl solution (200g/L, 1:3 v/v) and once with diethyl ether (99% Aldrich, 3:1 v/v). *n*-butyl acrylate (*n*BA) and *tert*-butyl acrylate (*t*BA) (Acros, 99%) were stirred overnight with hydroquinone (Prolabo) on calcium hydride (Acros, 93%) and distilled under vacuum. N,N'-azobisisobutyronitrile (AIBN, 98%, Merck Chemical) was recrystallized from 95% methanol (99.99%, Fisher Chemical) before use. N,N,N',N',N''-Pentamethyldiethylenetriamine (PMDETA, Acros, 99%), copper(II) bromide (CuBr₂, Acros, 99%), copper bromide (CuBr, Acros, 98%), chloroform (Aldrich, 99.8%), methanol (Aldrich, 99%), trifluoroacetic acid (CF₃COOH, Acros, 99%), 4-methoxyphenol (99 %, Aldrich), tetrahydrofuran (99.9% Aldrich), triethylamine (99% Fisher), toluene (99% Fisher), dichloromethane (99%, Fischer Chemical) and pentane (99%, Sigma-Aldrich) were used as received.

Size exclusion chromatography (SEC) was done with a system consisting of a guard column (5 μm, 50 mm × 7.5 mm) connected to a PLgel Mixed-D column (5 μm, 300 mm × 7.5 mm) and a PLgel "individual pore size" column (5 μm, 50 mm × 7.5 mm). Online light scattering (miniDAWN TREOS from Wyatt) and refractive index (RID10A from Shimadzu) were used for detection. The samples were analyzed in THF at room temperature using a flow rate of 1 mL.min⁻¹ with a Prominence HPLC system from Shimadzu. After filtration through a 0.2 μm pore size membrane, the polymers were injected at a concentration of 5 mg mL⁻¹ in THF. The average molar masses were calculated from the light scattering detector, using a specific

CHAPTER 6: ARTICLE 3

refractive index increment $dn/dc = 0.057 \text{ mL/g}$ that was determined from the integrated refractive index (RI)-signal knowing the polymer concentration.

^1H NMR spectra were recorded in CDCl_3 at $20 \text{ }^\circ\text{C}$ on a Brüker AC400 (400 MHz) spectrometer.

b. Synthesis of the functional monomer.

For the synthesis of the functional monomer, 2-(2-bromoisobutyryloxy)ethyl acrylate (BIEA), 2-hydroxyethyl acrylate (5.52 g, 4.75×10^{-2} mol), triethylamine (5.29 g, 5.23×10^{-2} mol), 4-methoxyphenol (5.9 mg, 4.75×10^{-4} mol), and dry THF (52 g) were mixed in a double-neck flask at $0 \text{ }^\circ\text{C}$. A dropping funnel containing α -bromoisobutyryl bromide (19.8 g, 8.61×10^{-2} mol) and dry THF (20 g) was adjusted on the double-neck flask. A septum was placed on the other neck. The dropping funnel was gently opened to add dropwise, at $0 \text{ }^\circ\text{C}$ under stirring, the α -bromoisobutyryl bromide solution to the 2-hydroxyethyl acrylate solution. The mixture was let reacting for 22 hours. The solution was filtered on a Büchner to remove the insoluble triethylammonium bromide salt and THF was evaporated under reduced pressure ($T=40^\circ\text{C}$). An orange liquid was recovered.

To remove impurities, the liquid was diluted in CHCl_3 (40 mL) and extracted five times with a saturated solution of NaHCO_3 (87g/L) to hydrolyze and neutralize the excess of α -bromoisobutyryl bromide, then twice with salted water (25 mL at 200 g/L) and once with water (10 mL). Finally, the organic phase was dried with MgSO_4 and CHCl_3 was removed by rotary evaporation (40°C), yielding 11.2 g (yield of 95%) of an orange liquid. Despite our efforts impurities remained in the products, as illustrated by the double peaks at $\delta=1.9$ ppm in ^1H NMR, see Figure S1. We do believe that it comes from side reactions between HEA and BIBB since hydrolysed BIBB should be totally removed after these purifications. Since the next step involves copolymerisation and precipitation, it is believed that this side product should not affect the reaction and will be removed with the polymer precipitation.

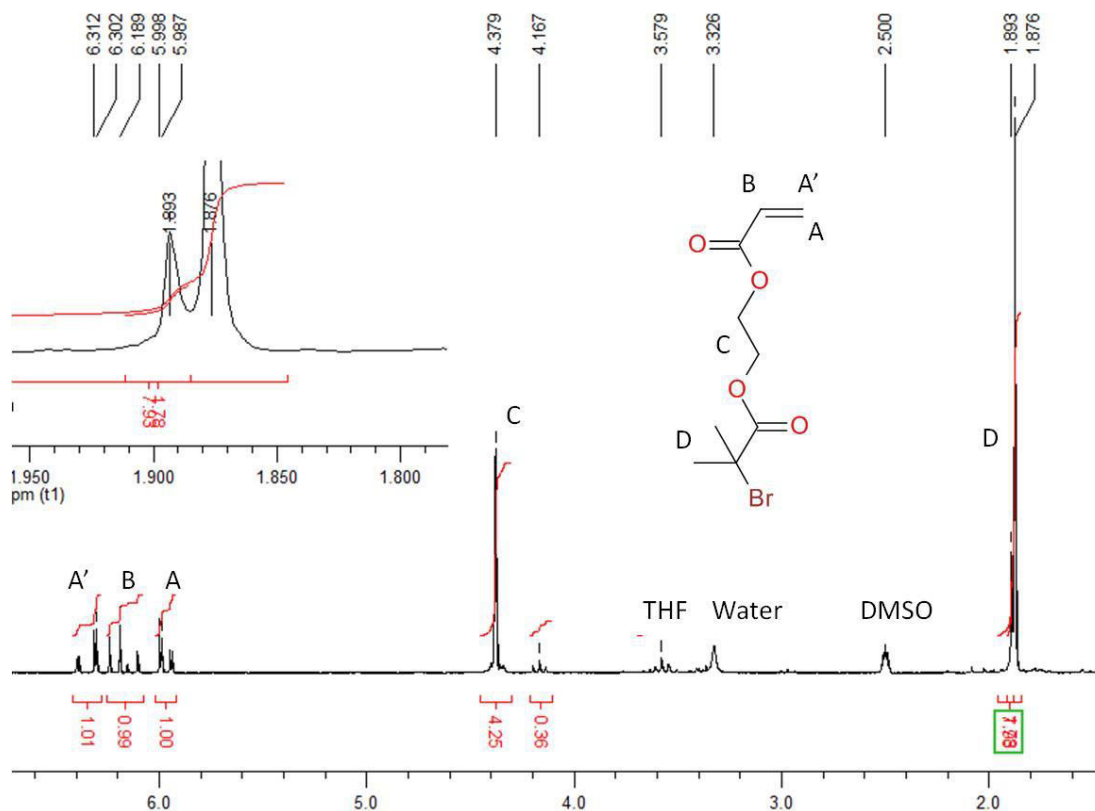


Figure S1. 200MHz ^1H NMR of the 2-(2-bromoisobutyryl)ethyl acrylate after purification in DMSO. δ (ppm) = 1.9 (s, 2H BIEA+impuritiy, H-d) ; δ (ppm) = 4.4 (m, 4H BIEA+impuritiy, H-c) ; δ (ppm) = 6.0 (dd, 1H BIEA, H-a) ; δ (ppm) = 6.2 (dd, 1H BIEA, H-b) ; δ (ppm) = 6.4 (dd, 1H BIEA, H-a).

c. Synthesis of the backbone.

Here, the synthesis of the backbone of G7H50 is detailed. The others backbones were prepared by adjusting the functional monomer to *t*BA ratio.

For the backbone synthesis, *tert*-butyl acrylate (39 g, 3.05×10^{-1} mol), BIEA (1.04 g, 3.9×10^{-3} mol), anisole (4.56 g, 4.2×10^{-2} mol), toluene (119 g) and azobisisobutyronitrile (9.2×10^{-2} g, 5.6×10^{-4} mol) were introduced in a 250 mL round-bottom flask. The flask was closed with a screw cap equipped with a septum, degassed by argon bubbling for 30 min and dipped in an oil bath at 60 °C. The mixture was let reacting for 24 hours. The reaction was stopped by cooling the flask to 0 °C. The polymer was precipitated twice in methanol/water (90/10 vol/vol), yielding a white powder. ^1H NMR in CDCl_3 was performed on the final polymer to confirm its composition, see Figure S2. Size exclusion chromatography (SEC) in THF yielded the number (M_n) and weight (M_w) average molar masses and the dispersity, see Figure S7a. For the three backbones, M_n was around 6.0×10^4 g/mol with $\text{Đ} \sim 2.7$.

CHAPTER 6: ARTICLE 3

The ^1H NMR gave a molar BIEA/*t*BA ratio of 1.48% assuming no impurity in agreement with the theoretical value of 1.44%, see Table S1.

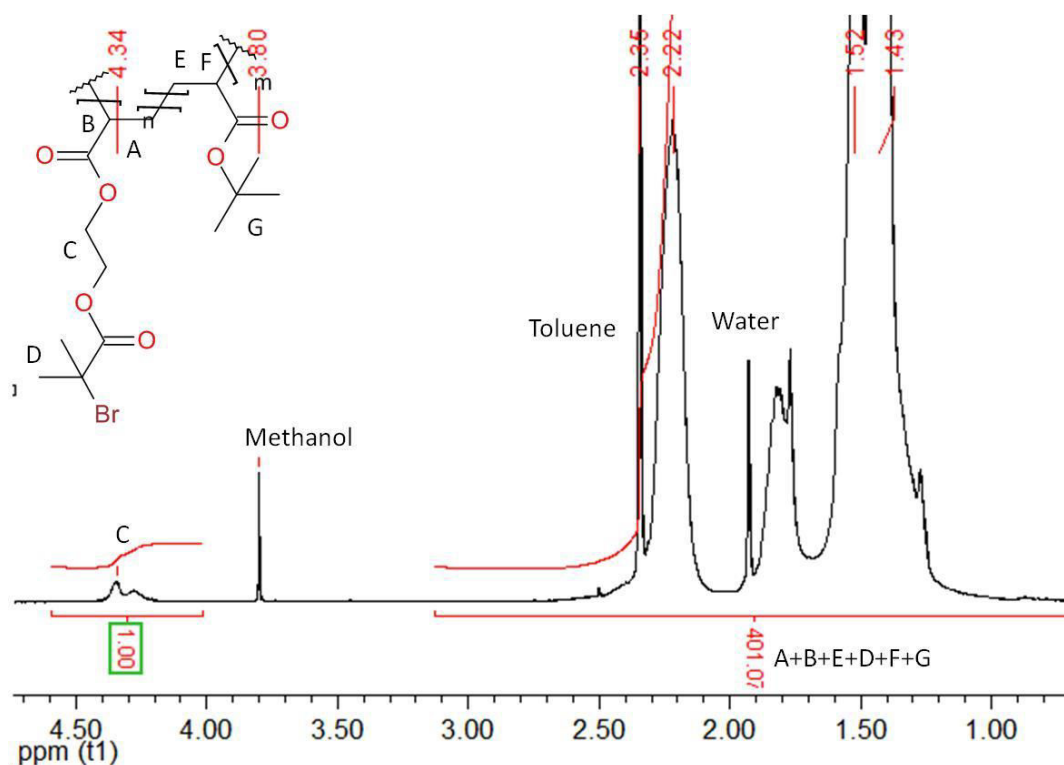


Figure S2. 200MHz ^1H NMR of the polymer backbone of G7H50 in CDCl_3 after purification. δ (ppm) = 1.4-2.5 (m, 21H, H-a-b-d-e-f-g) ; δ (ppm) = 3.7 (s, 4H BIEA, H-c).

d. Synthesis of the graft copolymer precursor.

Here, the synthesis of the graft copolymer precursor of G7H50 is detailed. The others graft copolymers precursors were prepared by adjusting the polymer to monomers ratio.

For the graft copolymer $\text{P}(t\text{BA})_{500}\text{-g-}[\text{P}(n\text{BA}_{0.5}\text{-stat-}t\text{BA}_{0.5})_{100}]_7$, *tert*-butyl acrylate (41.2 g, 3.22×10^{-1} mol), *n*-butyl acrylate (41.3 g, 3.23×10^{-1} mol), Cu(II)Br_2 (0.038 g, 1.7×10^{-4} mol) and $\text{P}(t\text{BA-}stat\text{-BIEA})$ (32.8 g, 1.44% BIEA) were introduced in a 500 mL round-bottom flask. PMDETA (0.62 g, 3.58×10^{-3} mol) and anisole (9.2 g) were introduced in a 50 mL vial. The flask and the vial were closed with screw caps equipped with a septum, and degassed by argon bubbling for 2 hours (a long degassing time was selected because of the viscosity of the polymer solution) and 10 min respectively. CuBr (0.479 g, 3.34×10^{-3} mol) was introduced in the 500 mL round-bottom flask under a counter-flux of argon and the solution was degassed again after that. The molar ratios are as follows $[\text{tBA}+n\text{BA}]:[\text{active Br in } \text{P}(t\text{BA-}stat\text{-BIEA})]:[\text{CuBr}]:[\text{PMDETA}] = 200:1:1:1.05$. The PMDETA solution was finally transferred in

the flask under argon using a double-tipped needle. A few drops of the solution were taken as sample t_0 , and the flask was dipped in an oil bath at 60 °C. Kinetics were followed by gas chromatography using anisole as internal standard, see Figure S6. $\ln([M]_0/[M])$ evolved linearly with time for G7H50 and G30H50, whereas it was linear versus $t^{2/3}$ for G2H50. Conversion of both t BA and n BA were equal throughout the reaction meaning that statistical grafts were formed as previously observed.^{1,2}

The reaction was stopped at 50% conversion. The copper was removed by three liquid-liquid extractions with EDTA solution (1% (w/w) EDTA, 2:1 $\text{NaHCO}_3/\text{EDTA}$ and 20% (w/w) NaCl) since purification by flash column chromatography on SiO_2 was not possible due to the viscosity of the polymer solution. Thereafter, the solution was washed three times with water. The polymer was precipitated twice in methanol/water (90/10 vol/vol), yielding a white powder. Size exclusion chromatography (SEC) in THF yielded the number (M_n) and weight (M_w) average molar masses and the dispersity, see Figure S7b and Table S1. The n BA/ t BA ratio was measured by ^1H NMR in CDCl_3 and compared to the expected values, see Table S2 and Figure S3.

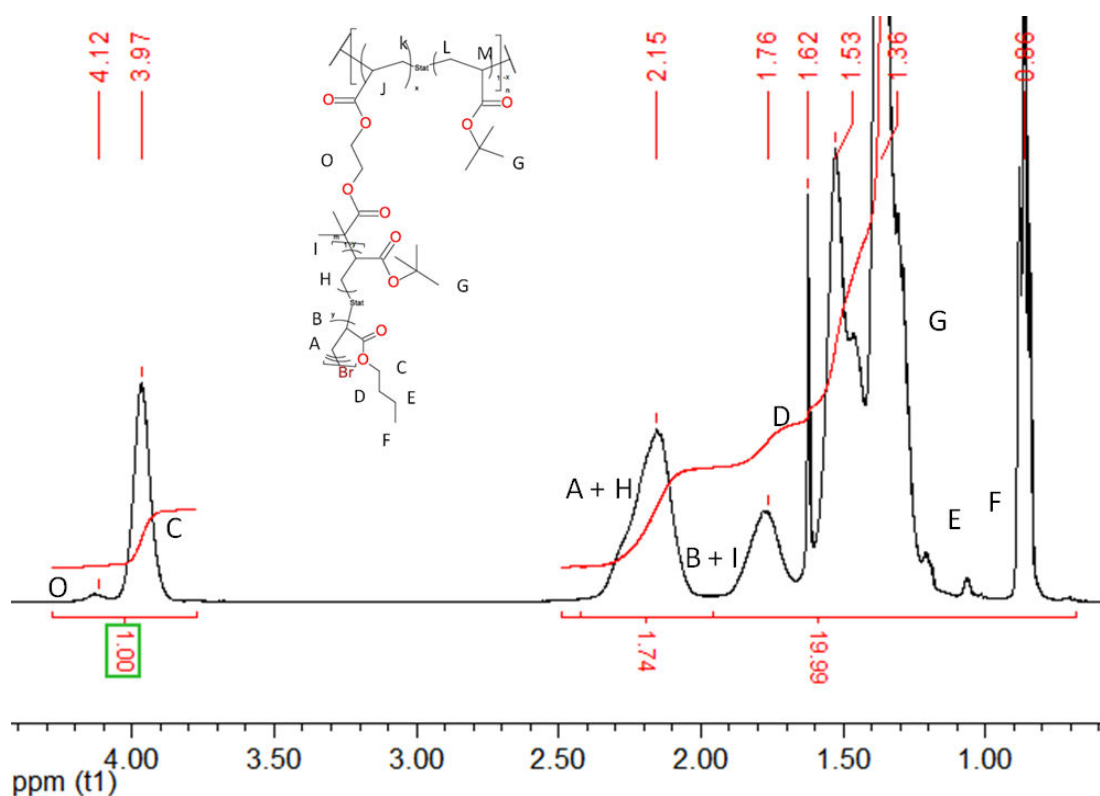


Figure S3. 200MHz ^1H NMR of the G7H50 graft copolymer precursor (unacidolyzed) in CDCl_3 after purification. δ (ppm) = 0.96 (t, 3H, n BA, H-f) ; δ (ppm) = 1.2-1.5 (m, 13H, n BA+ t BA, H-d+e+g) ; δ (ppm) = 1.78 (s, 2H, n BA+ t BA, H-b+i) ; δ (ppm) = 2.15 (s, 4H, n BA+ t BA, H-a+h); δ (ppm) = 3.97 (s, 2H, n BA, H-c).

e. Acidolysis.

The polymer was dissolved in dichloromethane ($C \sim 150$ g/L) and stirred at room temperature for at least 24 h with 5 equivalent of trifluoroacetic acid (CF_3COOH) relative to the amount of *t*BA units, as previously reported.¹⁻³ The polymer was finally precipitated twice in pentane. The *n*BA/AA ratio was measured by 1H NMR, see Table S2. ^{13}C NMR revealed the absence of significant quantities of residual CF_3COOH (data not shown) and complete acidolysis of the *t*BA units into AA ones as already reported.

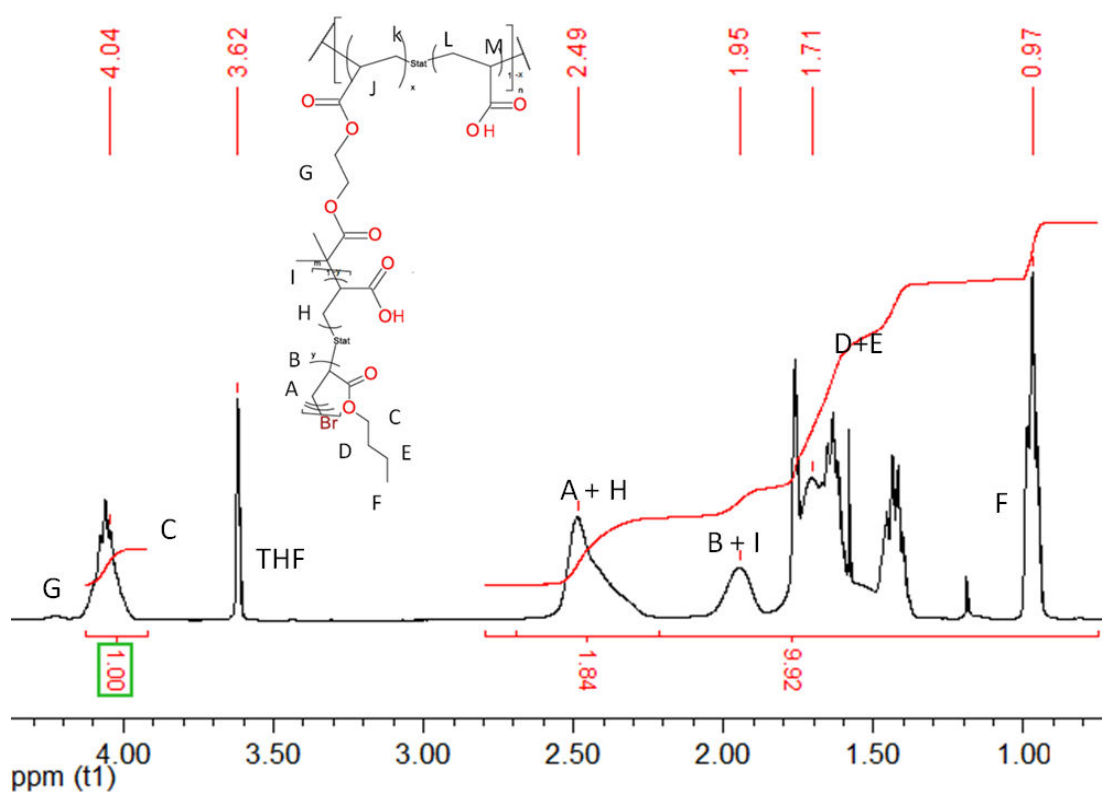


Figure S4. 200MHz 1H NMR of the G7H50 graft copolymer in $THF-D_8$ after purification. δ (ppm) = 0.97 (t, 3H, *n*BA, H-f) ; δ (ppm) = 1.2-1.8 (m, 11H, *n*BA, H-d+e) ; δ (ppm) = 1.95 (s, 2H, *n*BA+*t*BA, H-b+i) ; δ (ppm) = 2.49 (s, 4H, *n*BA+AA, H-a+h) ; δ (ppm) = 4.04 (s, 2H, *n*BA, H-c).

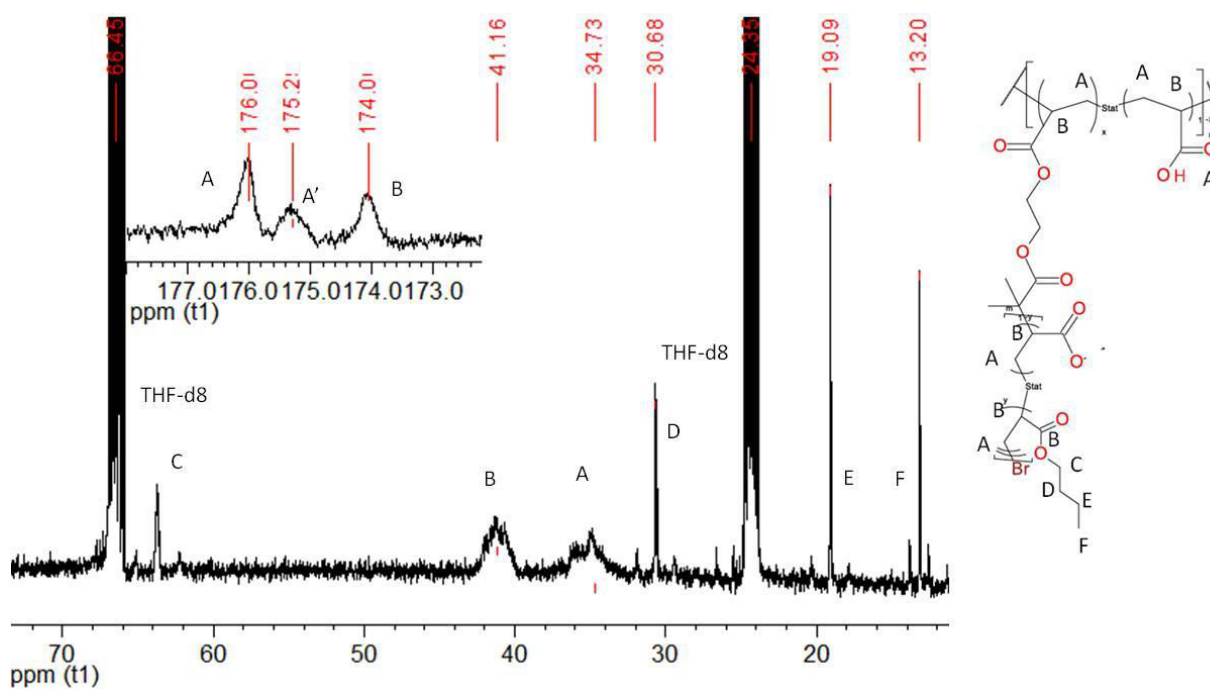


Figure S5. 50MHz ^{13}C NMR of the G7H50 graft copolymer after purification in THF-D₈. δ (ppm) = 176 (C-a, AA) ; δ (ppm) = 175 (C-a', AA); δ (ppm) = 174 (C-b, *n*BA); δ (ppm) = 66.4 (C-c, *n*BA); δ (ppm) = 41 (C-d, *n*BA+AA); δ (ppm) = 24 (C-a-b, *n*BA+AA); δ (ppm) = 19 (C-e, *n*BA); δ (ppm) = 13 (C-f, *n*BA).

Table S1. Characteristics of the G_xH50 copolymers synthesized.

Name	Backbone		Graft copolymer		
	% BIEA (mol/mol) th.	% BIEA (mol/mol) NMR ^1H	$M_{n,SEC}$ (g/mol)	\bar{D}	M_n (g/mol) ^a
G2H50	0.54	0.55	1.1×10^5	2.5	5.6×10^4
G7H50	1.44	1.48	1.7×10^5	2.5	8.6×10^4
G30H50	5.81	5.96	5.2×10^5	2.5	3.4×10^5

^a Theoretical M_n calculated assuming 100% acidolysis of the *t*BA units into AA ones.

Table S2. *t*BA/*n*BA and AA/*n*BA ratios of the GxH50 copolymers synthesized.

Name	% <i>t</i> BA (th.)	% <i>t</i> BA (exp.)	% AA (th.)	% AA (exp.)
G2H50	85.0	85.2	85.0	83.4
G7H50	71.0	71.4	71.0	72.8
G30H50	58.0	57.6	58.0	56.1

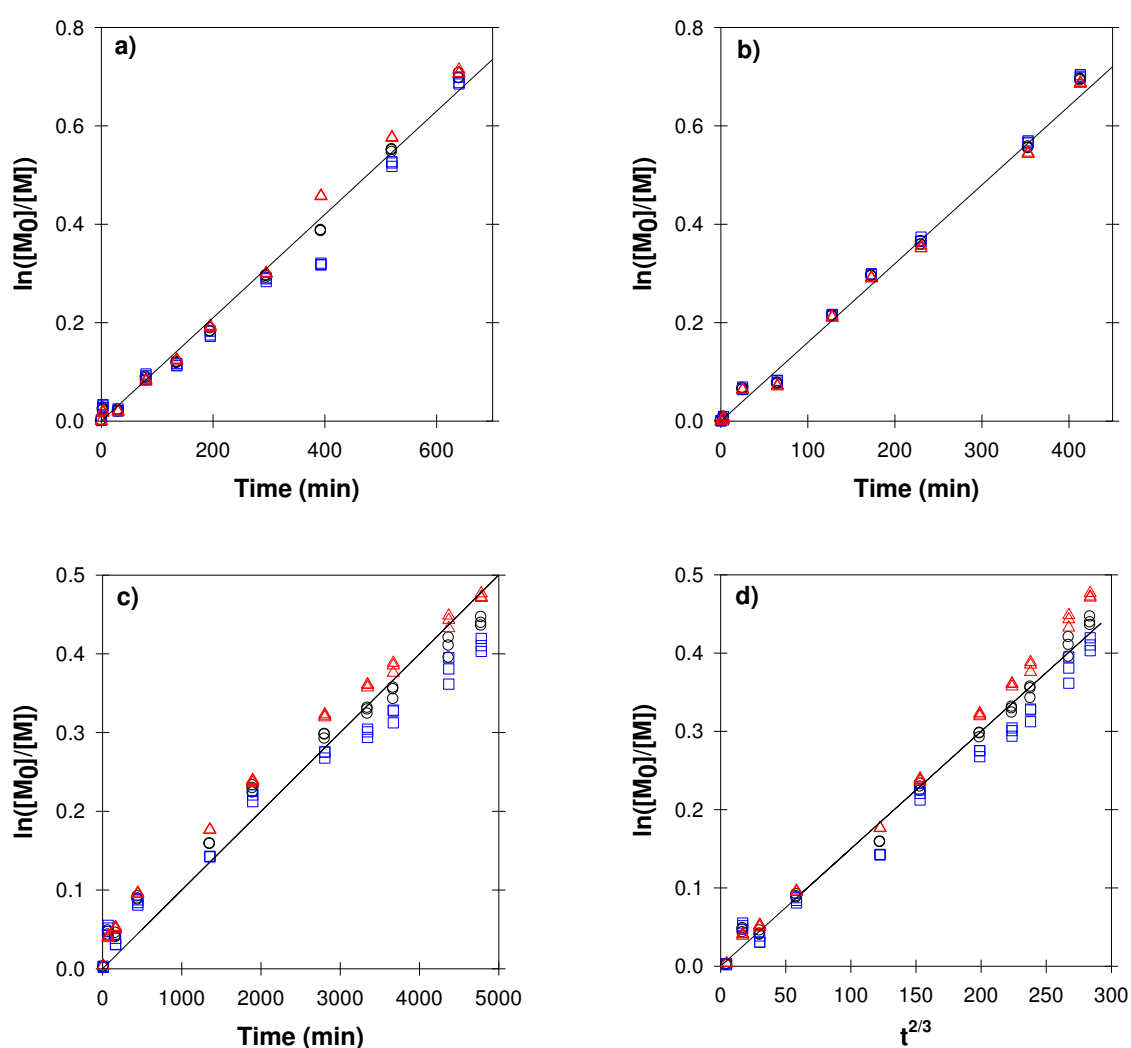


Figure S6. Kinetics of the polymerisation for the synthesis of the $P(nBA_{50\%}\text{-stat-}tBA_{50\%})_{100}$ grafts from the *Pt*BA functional backbones (step 3 in Figure 1 of the manuscript) with $[tBA+nBA]:[P(tBA\text{-stat-BIEA})]:[CuBr]:[PMDETA]$ ratios of 200:1:1:1.05 for G7H50 (a), 200:1:1:1.05 for G30H50 (b) and 245:1:1:1.05 for G2H50 (c+d). The monomer consumption of *t*BA (Δ), *n*BA (\square) and total (\circ) were measured by gas chromatography.⁴

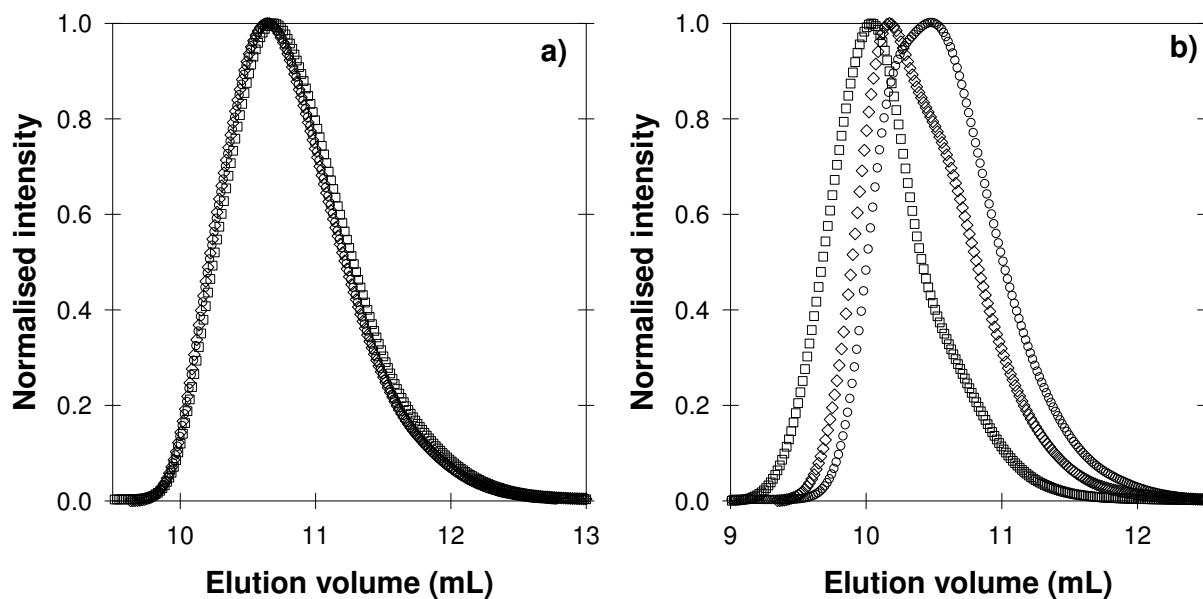
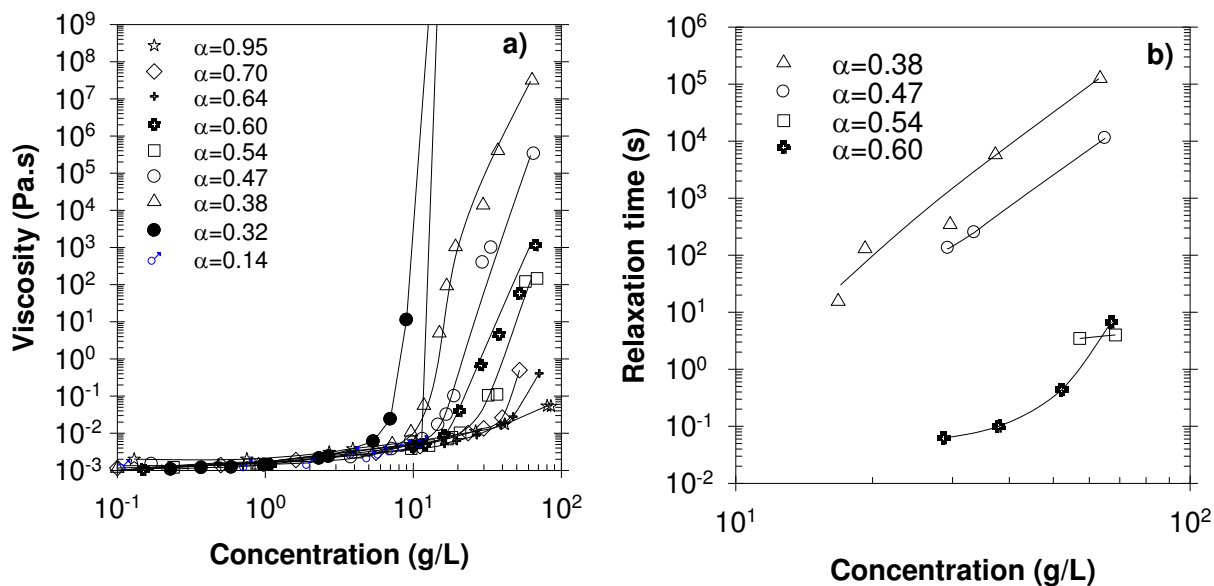


Figure S7. Size exclusion chromatograms for the backbones of G2H50 (◇), G7H50 (○) and G30H50 (□) (a) for the unacidolyzed graft copolymers G2H50 (◇), G7H50 (○) and G30H50 (□) (b). The light scattering detector was used.

2) Viscoelastic properties of G2H50



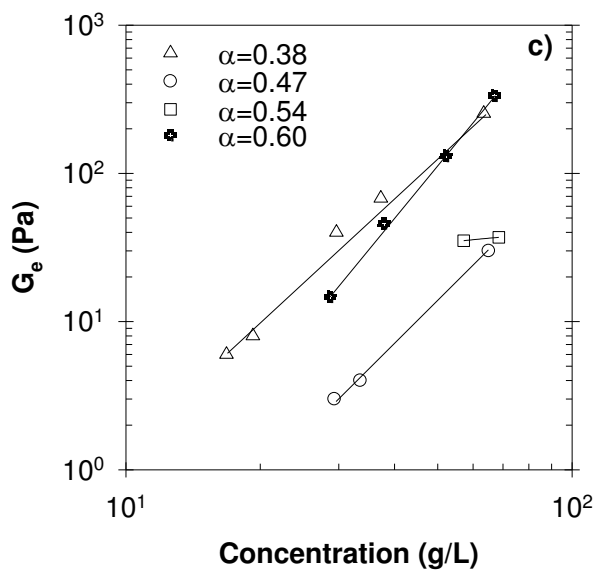
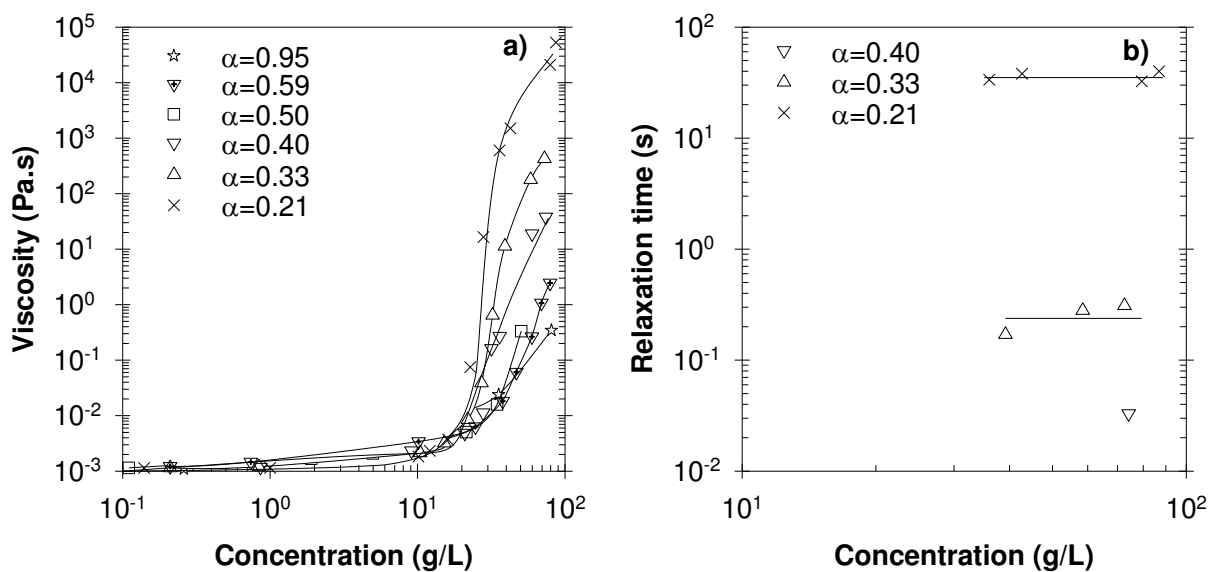


Figure S8. (a) viscosity (b) relaxation time and (c) elastic moduli as a function of the concentration for G2H50 at different ionization degrees. The solid lines are guides to the eye.

3) Viscoelastic properties of G30H50



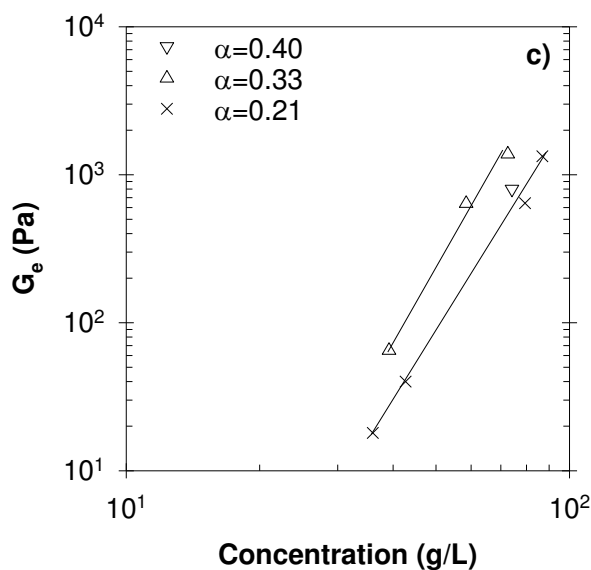


Figure S9. (a) viscosity (b) relaxation time and (c) elastic moduli as function of the concentration for G30H50 at different ionization degree. The solid lines are guides to the eye.

4) Example of frequency-temperature superposition at $T_{ref}=20^{\circ}\text{C}$

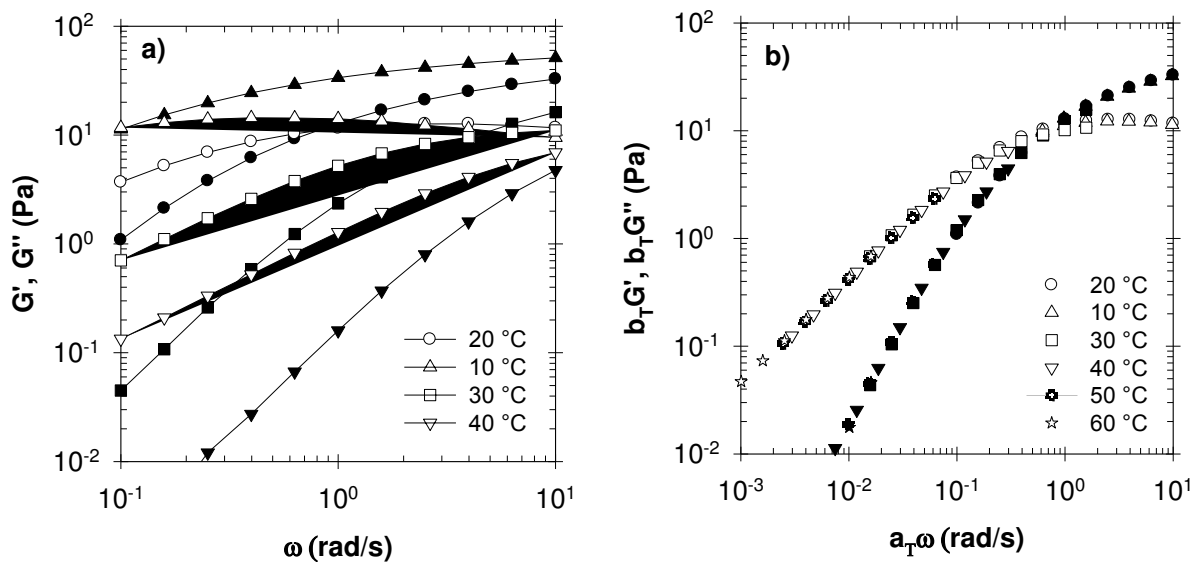


Figure S10. (a) Frequency dependence of the storage (open symbols) and loss (filled symbols) shear moduli of G2H50 at different temperatures for $C = 20\text{ g/L}$ and $\alpha = 0.60$. (b) Same data as in (a) after frequency-temperature superposition at $T_{ref} = 20^{\circ}\text{C}$.

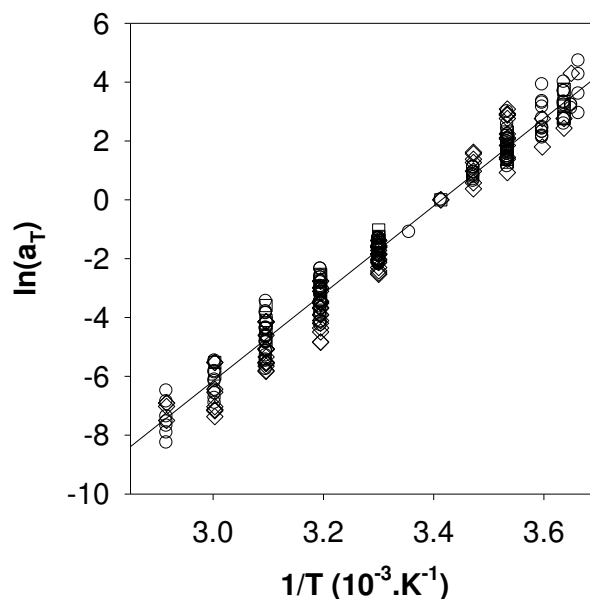


Figure S11. Arrhenius representation of the temperature dependence of the vertical shift factor at several ionization degrees and concentrations for G2H50 (\diamond), G7H50 (\circ) and G30H50 (\square). The solid line represents $E_a = 120$ kJ/mol.

5) Master curves of G2H50, G7H50, G30H50 and TH50

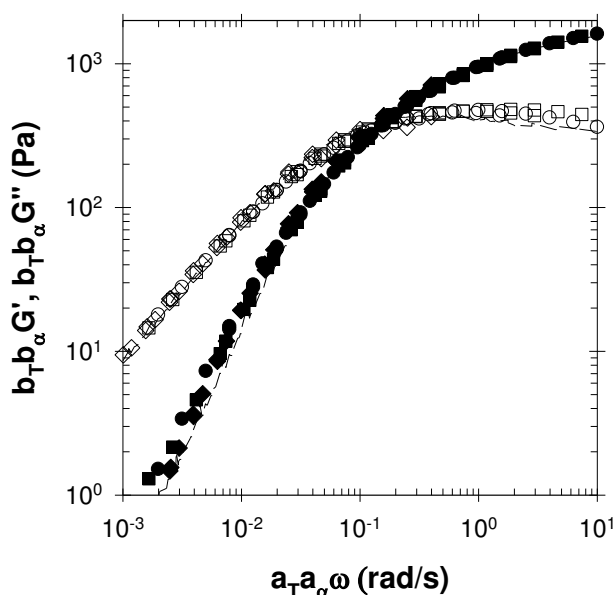


Figure S12. Comparison of master curves of the elastic modulus (open symbols) and the loss modulus (closed symbols) obtained for G2H50 (\diamond), G7H50 (\circ) and G30H50 (\square). The master curves were obtained by combining frequency–temperature and frequency– α superposition

with $\alpha_{\text{ref}}=0.60$ for G2H50, $\alpha_{\text{ref}}=0.45$ for G7H50 and $\alpha_{\text{ref}}=0.21$ for G30H50 at $T_{\text{ref}}=20^{\circ}\text{C}$. The dashed lines represent TH50.

REFERENCES

1. Lejeune, E.; Drechsler, M.; Jestin, J.; Muller, A. H. E.; Chassenieux, C.; Colombani, O. Amphiphilic Diblock Copolymers with a Moderately Hydrophobic Block: Toward Dynamic Micelles. *Macromolecules* **2010**, 43, (6), 2667-2671.
2. Shedge, A.; Colombani, O.; Nicolai, T.; Chassenieux, C. Charge Dependent Dynamics of Transient Networks and Hydrogels Formed by Self-Assembled pH-Sensitive Triblock Copolyelectrolytes. *Macromolecules* **2013**, 47, (7), 2439-2444.
3. Charbonneau, C.; Chassenieux, C.; Colombani, O.; Nicolai, T. Controlling the Dynamics of Self-Assembled Triblock Copolymer Networks via the pH. *Macromolecules* **2011**, 44, (11), 4487-4495.
4. Colombani, O.; Langelier, O. I.; Martwong, E.; Castignolles, P. Polymerization Kinetics: Monitoring Monomer Conversion Using an Internal Standard and the Key Role of Sample t0. *J. Chem. Educ.* **2011**, 88, (1), 116-121.

CHAPTER 7: ARTICLE 4

CHAPTER 7 : ARTICLE 4

**pH and thermo-responsive self-assembly of cationic triblock
copolymers with controlled dynamics**

*Lionel Lauber, Julien Santarelli, O. Boyron, Christophe Chassenieux, Olivier Colombani**,

Taco Nicolai

LUNAM Université, Université du Maine, IMMM-UMR CNRS 6283, Equipe Polymères,

Colloïdes et Interfaces, av. O. Messiaen, 72085 Le Mans cedex 9, France

AUTHOR EMAIL ADDRESS: olivier.colombani@univ-lemans.fr

CHAPTER 7: ARTICLE 4

ABSTRACT: Transient hydrogels formed by BAB triblock copolymers were investigated consisting of a hydrophilic poly(dimethylaminoethyl methacrylate) (P(DMAEMA)) A block and amphiphilic B blocks composed of randomly distributed DMAEMA and *n*-butyl methacrylate (*n*BMA) units. Oscillatory shear measurements revealed formation of dynamic networks with terminal relaxation times that can be controlled by tuning the content or ionization degree (α) of the DMAEMA units or the temperature up till 50°C. Above 50°C irreversible aggregation was observed.

KEYWORDS: hydrogels, exchange dynamics, triblock copolymers, rheology, thermo-sensitive, pH-sensitive, DMAEMA

I. Introduction

When dissolved in a selective solvent for the A block at a sufficiently high concentration, BAB triblock copolymers form system spanning networks consisting of hydrophobic cores of the B blocks connected via bridging A blocks.¹ The rheological properties of these networks depend to a large extent on the lifetime of the bridges i.e. the dynamic exchange of the B blocks between the hydrophobic cores.^{2, 3} Amphiphilic copolymers are however usually in a frozen state in aqueous medium, so that the exchange of B blocks between the hydrophobic cores is immeasurably slow⁴ and permanently cross-linked hydrogels are obtained.⁵

Stimuli-responsive systems are obtained if the B blocks can switch between hydrophilic and hydrophobic upon application of a stimulus. Such polymers generally display on/off behavior between that of a hydrogel when the B blocks are hydrophobic and a low viscosity liquid when the B blocks are hydrophilic.^{4, 6, 7}

It was recently shown for BAB triblock copolymers based on a poly(acrylic acid) (PAA) hydrophilic A block and hydrophobic B blocks consisting of randomly distributed *n*-butyl acrylate (*n*BA) and AA units, that the incorporation of hydrophilic AA units within the B blocks resulted in dynamic rather than frozen networks.⁸⁻¹⁰ Moreover, the pH-sensitive character of the AA units allowed control of the exchange dynamics over more than 10 decades by changing the pH,^{8, 9} the AA content⁹ or by formulation.¹⁰ In this manner, the rheological properties of the system could be reversibly modified to a large extent.

So far this methodology to control the dynamics of self-assembled triblock copolymers has not yet been tested quantitatively for other types of polymers. However, qualitative observations suggest that this strategy may be universally applicable. In particular, Billon et al. showed that at 20°C BAB triblock copolymers consisting of a PAA hydrophilic A block connected to gradient B blocks of styrene and AA units formed pH-sensitive hydrogels that were dynamic above pH~7.1 and frozen at low pH.¹¹ Moreover, the self-assembly in water of amphiphilic BA diblock copolymers became sensitive to pH after incorporation of AA¹²⁻¹⁶ or dimethylaminoethyl methacrylate (DMAEMA)¹⁷ units within their hydrophobic blocks. For diblock copolymers, the temperature^{11, 16, 18} and the microstructure (statistical vs. gradient distribution of the units within the B blocks)^{11, 16, 19} strongly affected the reversibility of the self-assembly.

In order to assess the generality of this strategy consisting of incorporating hydrophilic units inside hydrophobic blocks to induce dynamic exchange, and in particular for cationic polymers, triblock copolymers made of a poly(dimethylaminoethyl methacrylate) central

block and statistical copolymers containing dimethylaminoethyl methacrylate (DMAEMA) and *n*-butyl methacrylate (*n*BMA) as end blocks (THxc) were synthesized. An additional interest of DMAEMA is that it is not only pH-sensitive, but also temperature-sensitive,²⁰⁻²⁷ which has been used to form hydrogels above a Lower Critical Solution Temperature (LCST).²⁰⁻²³ The synthesis of the polymers was done by Radical Addition Fragmentation Transfer (RAFT) polymerization. The rheological properties, and hence the exchange dynamics were studied in aqueous solutions as a function of the ionization degree of the DMAEMA units and of the temperature.

II. Materials and methods.

1. Polymer characteristics. Diblock copolymers made of DMAEMA and *n*BMA were previously synthesized in our research group using ATRP.¹⁷ However, it was found that reinitiation of the P(DMAEMA)-Br macroinitiator for the synthesis of the second B block was only partial. Therefore, RAFT polymerization was preferred here.^{28, 29} Triblock copolymers made of dimethylaminoethyl methacrylate (DMAEMA) and *n*-butyl methacrylate (*n*BMA) were synthesized in three steps by RAFT polymerization as briefly shown in Figure 1 and described in detail in section 1 of the supporting information. Their chemical structure is $P(nBMA_{1-x}\text{-stat-DMAEMA}_x)_{100}\text{-}b\text{-}P(\text{DMAEMA})_{200}\text{-}b\text{-}P(nBMA_{1-x}\text{-stat-DMAEMA}_x)_{100}$, corresponding to a P(DMAEMA) central hydrophilic block with a number average degree of polymerization (DP_n) of 200 and lateral blocks with $DP_n=100$ made of x mol% of DMAEMA and $(1-x)$ mol% of *n*BMA randomly distributed. Two triblock copolymers were synthesized with either $x=50$ (TH50c) or $x=70$ %mol (TH70c). The polymers had rather narrow dispersities as shown by Size Exclusion Chromatography (SEC), see Table 1.

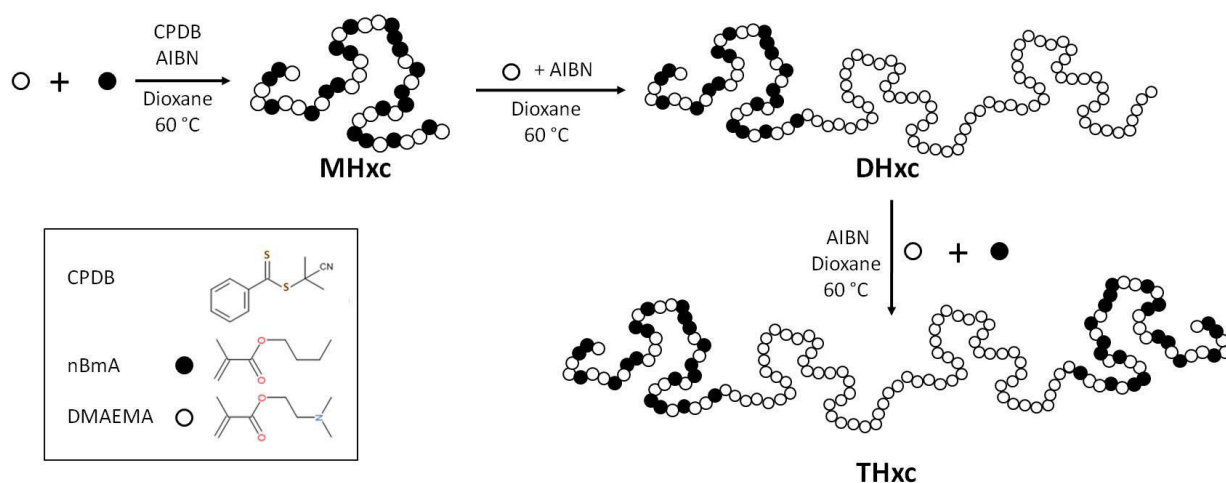


Figure 1. Schematic representation of the three-step synthesis of the THxc triblock copolymers by Reversible Addition–Fragmentation chain-Transfer (RAFT) polymerization. *x* stands for the molar ratio of DMAEMA units within the hydrophobic lateral blocks and is equal to 50 or 70 %mol.

Table 1. Characteristics of the synthesized copolymers (see Figure 1 for the corresponding chemical structures). The molecular weights ($M_{n,SEC}$) are calculated by calibration with poly(methyl methacrylate) standards. ^a The molecular weights ($M_{n,th}$) expected at ~50% of monomers conversion, see supporting information for details. ^b DHxc has a hydrophilic block twice as long as that of the anionic DHx^{12, 13} or similar diblock copolymer made in our research group¹⁷.

Name	% DMAEMA theoretical	% DMAEMA NMR	$M_{n,th}$ (g/mol) ^a	$M_{n,SEC}$ (g/mol)	\bar{D}
MH50c	50	50	1.5×10^4	1.7×10^4	1.2
MH70c	70	70	1.5×10^4	9.5×10^3	1.2
DH50c ^b	83	84	4.7×10^4	3.4×10^4	1.2
DH70c ^b	89	90	4.7×10^4	2.3×10^4	1.2
TH50c	76	76	6.1×10^4	4.3×10^4	1.4
TH70c	85	85	6.2×10^4	3.7×10^4	1.3

2. *Potentiometric Titration.* Potentiometric titration of the copolymers was done at room temperature with an automatic titrator (TIM 856, Radiometer Analytical) controlled by the TitraMaster 85 software, utilizing the procedure described in ref.³⁰ For each sample, 30 mL of polymer solution were prepared by addition of 1.1 equiv of HCl (1M) and water to the polymer powder to reach an overall DMAEMA concentration [DMAEMA]=0.043 mol/L. The NaCl concentration in the polymer solutions was adjusted to 0.5M by incorporation of the right amount of a NaCl stock solution (4M). Back-titrations with NaOH (1M) at a rate of NaOH addition of 0.1 mL/min were done to determine the total amount of titrable DMAEMA

CHAPTER 7: ARTICLE 4

units and the ionization degree $\alpha = [\text{DMAEMA}^+]/([\text{DMAEMA}] + [\text{DMAEMA}^+])$ as a function of the pH, with $[\text{DMAEMA}^+]$ and $[\text{DMAEMA}]$ the concentrations of the charged and uncharged DMAEMA units, respectively. The fraction of charged units in the hydrophobic blocks was calculated as follows: $f = [\text{DMAEMA}^+]_{\text{MHxc}}/([\text{DMAEMA}^+] + [\text{DMAEMA}] + [n\text{BMA}])_{\text{MHxc}} = x \cdot \alpha_{\text{MHxc}}$.⁹ The ionization degree of MH70c was computed from the data for TH70c and P(DMAEMA) assuming that the effect of covalent connection between the blocks on the ionization was negligible as was verified earlier for a different type of triblock copolymer.⁹

3. *Sample Preparation.* Direct dissolution of these triblock copolymers at the desired α by addition of the required amount of HCl was only possible for a range of α , typically $\alpha \geq 0.7$ for TH50c and $\alpha \geq 0.05$ for TH70c. For TH50c, below these values, the polymer powder hydrated, but did not form a homogeneous gel. Aqueous polymer solutions were therefore prepared by dissolving the copolymers in demineralized water (Millipore) containing the required amount of HCl to reach an ionization degree α_0 between 0.9 and 1. HCl was used in stoichiometric quantities with respect to the amount of DMAEMA units to be ionized ($[\text{DMAEMA}^+] = [\text{HCl}]$). Dissolution was done under stirring for at least 24 hours at room temperature. Transparent, slightly pink, homogeneous liquids were obtained. The Cl⁻ concentration was kept constant at 0.5 mol/L by adding the desired amount of a NaCl stock solution (4M). The molar concentration of Cl⁻ in the system, $[\text{Cl}^-]$, is the sum of the amount of HCl added to reach α_0 and the amount of added NaCl:

$$[\text{Cl}^-] = \frac{x_{\text{DMAEMA}} C \cdot \alpha_0}{x_{\text{DMAEMA}} M_{\text{DMAEMA}} + x_{n\text{BMA}} M_{n\text{BMA}}} + [\text{NaCl}]$$

where C is the weight concentration of polymer, α_0 is the initial ionization degree, x_{DMAEMA} and $x_{n\text{BMA}}$ are the overall molar fractions of each monomer within the triblock and $M_{\text{DMAEMA}} = 157 \text{ g}\cdot\text{mol}^{-1}$ and $M_{n\text{BMA}} = 142 \text{ g}\cdot\text{mol}^{-1}$ are the molar masses of DMAEMA and $n\text{BMA}$ units, respectively.

Measurements were done at high ionic strength in order to screen electrostatic interactions. However, the transition from low viscous liquid to highly viscous fluids discussed here as a function of α was also visually observed without salt (data not shown).

To obtain the desired ionization degree, the required amount of NaOH was added. Dilute NaOH solutions, typically between 0.01 and 0.1 mol/L, had to be used and the addition had to be done under vigorous stirring in order to limit the formation of heterogeneities.

Nevertheless, homogeneous and transparent solutions were obtained only for $\alpha > 0.60$. At lower degrees of ionization, the solutions were macroscopically heterogeneous.

4. Oscillatory shear measurements. Oscillatory shear measurements were performed using controlled-stress rheometers equipped with cone-plate geometries: ARG2 (angle = $4^\circ - 2^\circ - 1^\circ$, diameter 20 - 60 mm) and MCR301 (angle = $2^\circ - 1^\circ$, diameter = 25 - 50 mm). Silicon oil was used during measurements to cover the samples and limit water evaporation. A Peltier system controlled the temperature and the measurements were conducted in the linear response regime.

III. Results and Discussion.

This section is divided into two parts. In part A, results obtained at 20°C are discussed, starting with those on the cationic triblock copolymer containing 50%mol of DMAEMA units within the hydrophobic end blocks (TH50c). Then the effect of the DMAEMA content is shown by comparing TH50c with TH70c. Finally, results obtained with the cationic triblock copolymers based on DMAEMA and *n*BMA are compared with those obtained with anionic triblock copolymers based on AA and *n*BA units (TH50) described in the literature.⁸ In part B, the effect of the temperature on the behaviour of TH50c and TH70c is discussed.

A. Rheological properties at 20°C

1. Viscosity of TH50c at 20°C

Figure 2a shows the evolution of the viscosity of TH50c as a function of the ionization degree at several polymer concentrations (*C*). For $C > 20\text{g/L}$, the viscosity increased steeply when α is decreased below a characteristic value. By interpolation, the zero shear viscosity (η_0) could be determined as a function of the polymer concentration for a given degree of ionization. η_0 increased sharply above a critical concentration when a percolating network was formed as was already reported in ref.⁸ for TH50. Figure 2b, shows the dependence of the viscosity as a function of the polymer concentration normalized by the percolation concentration (C_p). The sharp increase of the viscosity at C_p is expected for transient networks made by self-assembly of BAB triblock copolymers. It is important to note that the lowest ionization degree investigated was around 0.60 and that at lower α homogeneous samples could not be obtained.

Between $\alpha=0.60$ and 0.70 , $C_p \approx 20$ g/L and independent of α , but for $\alpha > 0.70$, C_p increased with increasing α to $C_p=85$ g/L at $\alpha=0.80$. For TH70c, C_p was between 50-80 g/L for all α .

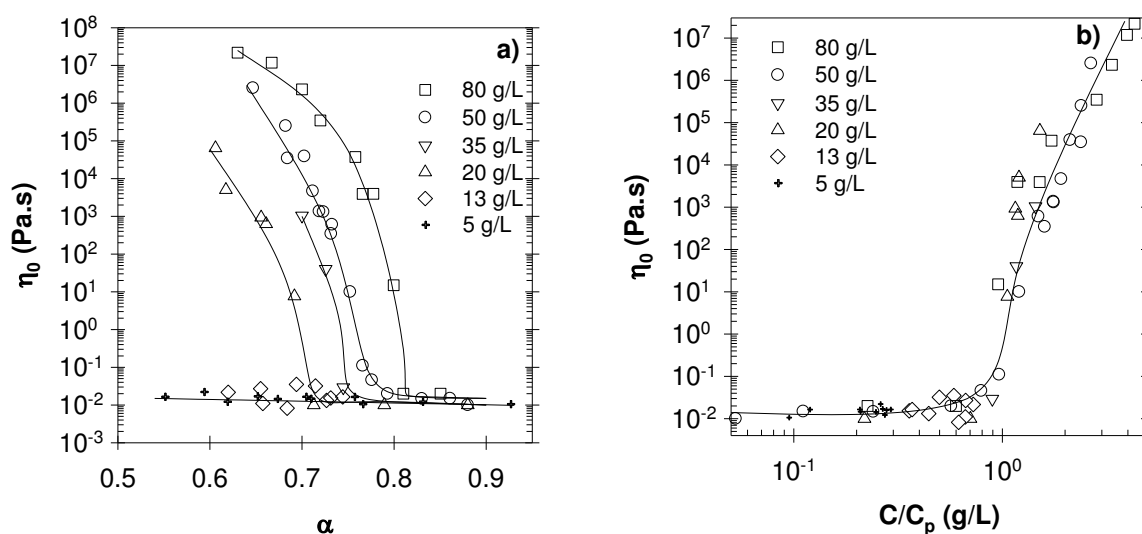


Figure 2. (a) The dependence of the viscosity on the ionization degree (α) for TH50c at different concentrations ($T=20^\circ\text{C}$). The solid lines are guides to the eye. (b) Same data as in figure 2a as a function of the polymer concentration normalized by the percolation concentration .

2. Viscoelastic properties of TH50c and TH70c

The radial frequency (ω) dependence of the elastic (G') and loss (G'') moduli at different ionization degrees between 0.68 and 0.71 are shown in Figure 3a for TH50c at $C=50$ g/L. By vertical and horizontal shifting, a master curve was obtained at $\alpha_{\text{ref}}=0.68$ over a broad range of frequencies, see Figure 3b. The frequency dependence of the master curve is characteristic for viscoelastic liquids at all ionization degrees with a liquid like behaviour at low frequencies and a solid-like behaviour at high frequencies.

We define the terminal relaxation time (τ) as the inverse of the radial frequency at which $G'=G''$ and the elastic modulus of the network (G_{el}) as the value of G' at $\omega=100/\tau$. Interestingly, the master curve of TH70c at $C=80$ g/L superimposed with the one of TH50c at larger α_{ref} . The implication is that the relaxation process of the transient networks was the same even though the amount of hydrophilic units inside the hydrophobic blocks was different.

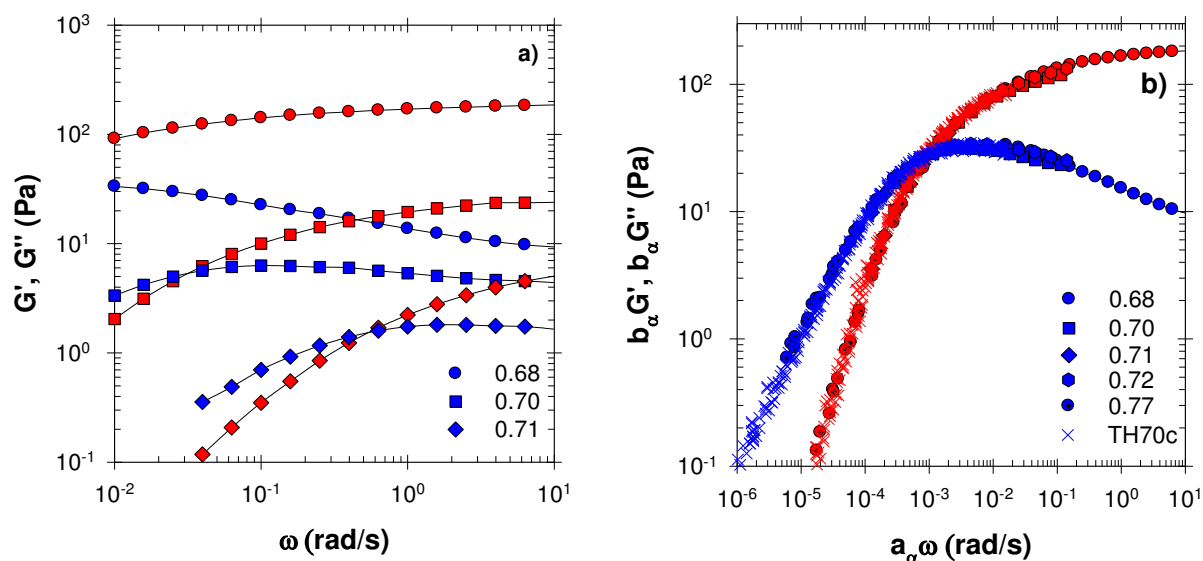


Figure 3. (a) Frequency dependence of the storage (red) and loss (blue) shear moduli at different ionization degrees for TH50c at $C = 50$ g/L ($T=20^\circ\text{C}$). (b) Master curves obtained by superposition of the results shown in fig. 3a using horizontal and vertical shifts, with $\alpha_{\text{ref}}=0.68$. For comparison the master curve obtained for TH70c at $C = 80$ g/L with $\alpha_{\text{ref}}=0.29$ is also shown.

Figure 4 shows the dependence of G_{el} on α at several concentrations for TH50c and at $C=80$ g/L for TH70c. We note that for TH70c homogeneous solutions could be formed down to $\alpha=0.1$. For all systems G_{el} increased with decreasing α and for a given ionization degree, G_{el} increased with increasing polymer concentration. Increasing the concentration or decreasing α led to a network with less defects.^{3, 8} At the highest polymer concentration ($C=80$ g/L) the measured G_{el} was close to the value expected for an ideal rubber elastic network for which all chains are elastically active, i.e; $G_{\text{el}}=CRT/M_n=2 \times 10^3$ Pa.³¹

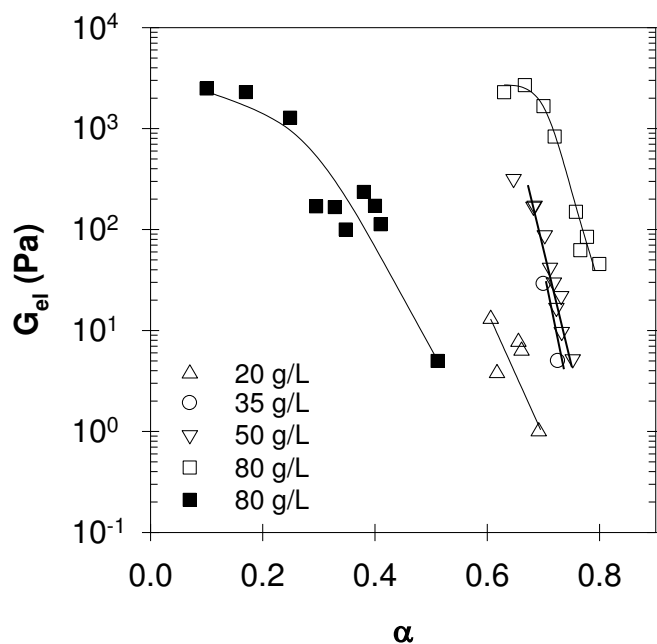


Figure 4. Evolution of the elastic modulus as a function of the ionization degree (α) for TH50c at different concentrations (open symbols) and TH70c at 80 g/L (closed symbols) ($T=20^\circ\text{C}$). The solid lines are guides to the eye.

The dependence of the relaxation time on α is shown in Figure 5 for TH50c at several concentrations and for TH70c at $C=80$ g/L. τ increased sharply with decreasing α , but did not vary significantly with the polymer concentration for TH50c for $\alpha < 0.72$ and $C > 35$ g/L. At these conditions, τ corresponds to the average extraction time of a hydrophobic block from the micellar core.³

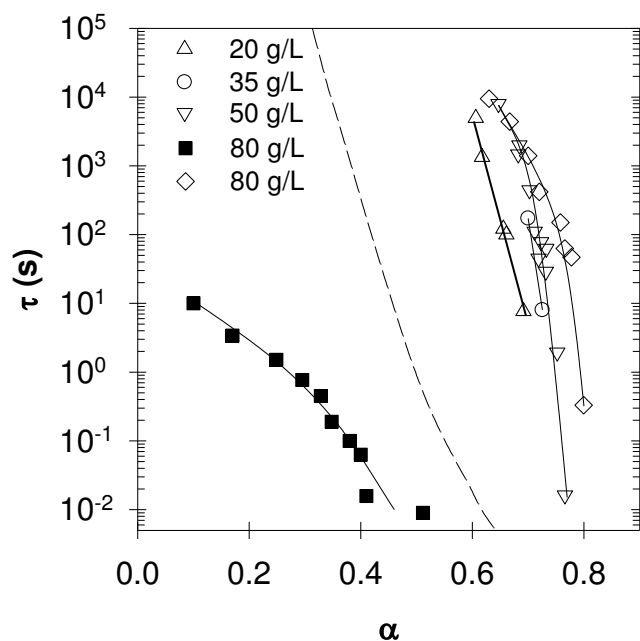


Figure 5. Dependence of the relaxation time on the ionization degree for TH50c (open symbols) and TH70c (closed symbols) at different concentrations ($T=20^{\circ}\text{C}$). The solid lines are guides to the eye. The dashed line represents the data for TH50 at high polymer concentrations.^{8,9}

The dependence of the elastic modulus and the relaxation time on α followed the same trends for TH70c at $C=80\text{g/L}$ as for TH50c, see Figures 4 and 5, but the increase of the relaxation time with decreasing α was much more progressive for TH70c than for TH50c and occurred at larger α . As might be expected, increasing the amount of hydrophilic DMAEMA units within the hydrophobic blocks leads to a decrease of the relaxation time for a given α .

3. DMAEMA and AA-based triblock copolymers: similarities and differences

The behaviour observed for the cationic triblock copolymers THxc studied here was qualitatively similar to that previously reported for the anionic triblock copolymers THx,^{8,9} with the same general chemical structure but with different monomer units: $P(n\text{BA}_{1-x}\text{-stat-AA}_x)_{100}\text{-}b\text{-PAA}_{200}\text{-}b\text{-P}(n\text{BA}_{1-x}\text{-stat-AA}_x)_{100}$. Both types of polymers transformed from low viscous liquids to visco-elastic fluids and finally to gels upon decreasing α due to the formation of transient networks with increasing relaxation times. Moreover, the transition occurred for both types within different α -windows and more or less abruptly depending on the content of hydrophilic units within the hydrophobic blocks : x . The master curves of the frequency dependency of G' and G'' obtained for THx and THxc could be superimposed, see Figure 6, implying that, qualitatively, the relaxation mechanism did not depend on α , x , the polydispersity or the chemical nature of the hydrophilic (and hydrophobic) monomer units.

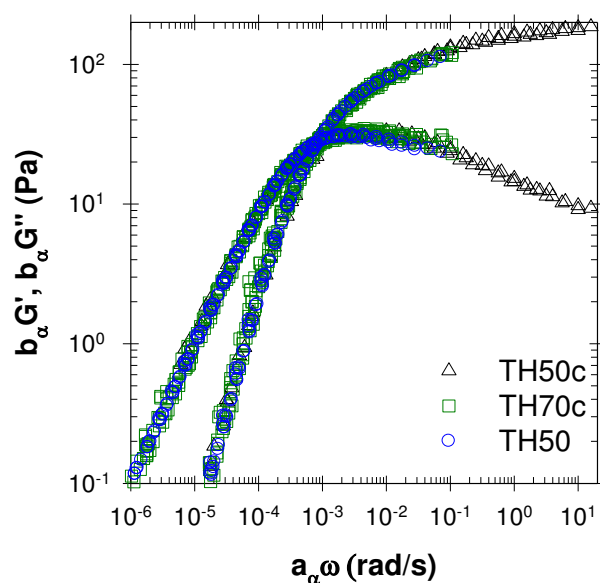


Figure 6. Comparison of master curves of TH50c (Δ), TH70c (\square) and TH50 (\circ) obtained after frequency- α superposition, $\alpha_{\text{ref}}=0.68$ for TH50c, $\alpha_{\text{ref}}=0.29$ for TH70c and $\alpha_{\text{ref}}=0.48$ for TH50. The data for TH50 were extracted from ref.⁸

From a quantitative point of view, noteworthy differences were observed between the cationic DMAEMA-based THxc copolymers and the anionic AA-based THx copolymers. Most importantly, as DMAEMA units are basic the ionization degree of THxc increased with decreasing pH from $\alpha < 0.1$ at pH 8.5 to $\alpha > 0.9$ at pH 6, see Figure 7, whereas the ionization degree of THx increased with increasing pH as AA units are acidic.³⁰ This is particularly relevant for applications where it may be required to form gels or more viscous solutions either by increasing or by decreasing the pH.

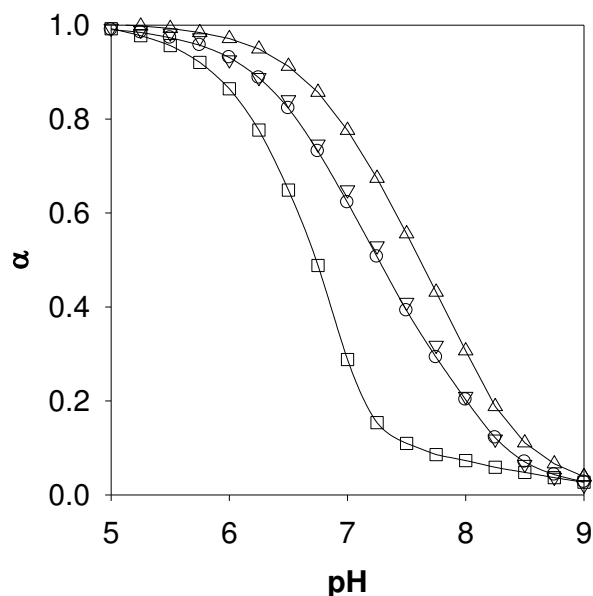


Figure 7. Degree of ionization of DMAEMA units as a function of the pH for MH50c (□), TH50c (○), TH70c (▽), P(DMAEMA) (Δ).

The dependence of the relaxation time on α was much more abrupt for TH50c than for TH50 although both polymers contained the same proportion of hydrophilic units and had the same degrees of polymerization (Figure 5). It was found for THx that the dependence of τ on α could to a large extent be explained by the dependence of the fraction of charged units within the hydrophobic blocks (f) on α .⁹

Titration experiments analogous to those reported for THx,^{9, 30} allowed us to calculate the ionization degree of the hydrophobic blocks of TH50c and TH70c as a function of α , see Figure 8. The ionization degree of the DMAEMA units within the hydrophobic blocks was always smaller than α due to the increased difficulty to create charges within a hydrophobic environment.³⁶ This effect was particularly strong for TH50c and led to a steep increase of f between $\alpha = 0.6$ and $\alpha = 0.8$, which explains the strong variation of the relaxation time for TH50c in this α -range.

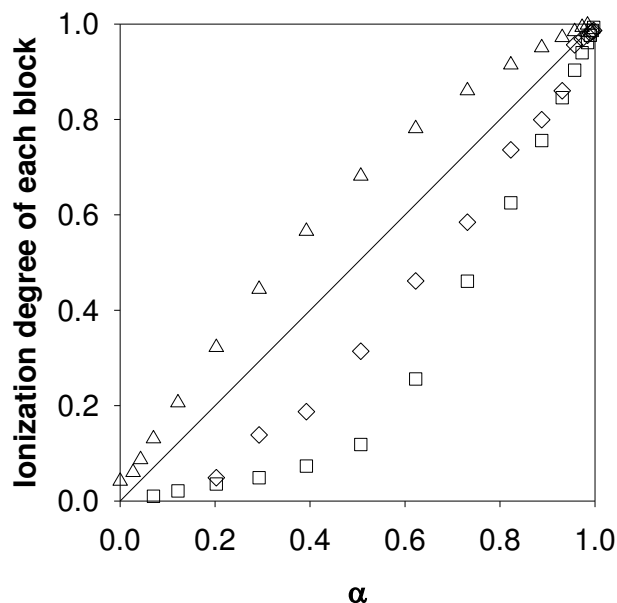


Figure 8. Degree of ionization of the P(DMAEMA) block (Δ), MH70c (\diamond), MH50c (\square) as a function of the overall ionization degree of the triblock copolymer TH50c and TH70c.

In Figure 9 the relaxation times are plotted as a function of f for TH50c at different concentrations and for TH70c at 80 g/L. The comparison shows that for the same f relaxation is much faster for TH70c. The reason is that the hydrophobic character of the B blocks depends not only on f , but also on the chemical nature of the units. *n*BMA units are much more hydrophobic than uncharged DMAEMA units, which explains why TH50c, which contains more *n*BMA units, relaxes more slowly at the same value of f . A similar dependence of the relaxation time on x at constant f was found for THx.⁹

For comparison the results obtained for TH50, TH40 and TH60 at high concentrations are also indicated in Figure 9.^{8,9} For a given value of f , relaxation was much faster for TH50c than TH50. Since the polymerization degree of the B blocks of TH50c and TH50 are very close, the difference could be due to different hydrophobicity and/or different mobility of the hydrophobic blocks.

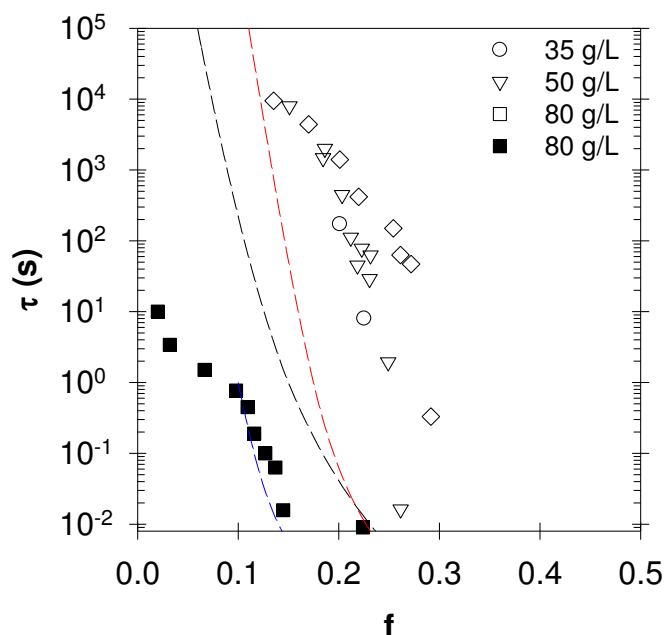


Figure 9. Same data as in Figure 5 represented as a function of the fraction of charged units (f), the dashed lines represent the results for anionic triblock copolymers TH50 (black), TH40 (red) and TH60 (blue).^{8,9}

To summarize, incorporation of hydrophilic units inside the hydrophobic blocks appears to be a generally applicable method to obtain amphiphilic self-assembling copolymers with tunable dynamics of exchange both for cationic and anionic triblock copolymers. However, the required amount of hydrophilic units that needs to be incorporated in order to be able to tune the relaxation time with the pH depends on the chemical nature of the polymers.

B. Effect of temperature

At $T > 50^\circ\text{C}$, some systems slowly evolved with time and formed gels at higher concentrations that persisted after cooling. For example, TH50c at $\alpha = 0.80$ and $C = 50 \text{ g/L}$ was liquid at 20°C , became a gel at $60\text{--}65^\circ\text{C}$ and remained gelled after cooling to 20°C for at least 90 days, see Figure S5 of the supporting information. The origin of this irreversible heat-induced gelation is unclear. It was shown that DMAEMA homopolymers does not hydrolyze their DMAEMA units into AA units at conditions studied^{32,33}

To assess whether chemical cross-linking occurred during heating, the aggregation number (N_{ag}) of assemblies formed by a TH50c solution at $C = 2 \text{ g/L}$ and $\alpha = 0.57$ was determined by light scattering at 20°C before heating and after heating at 80°C during 1 hour. Before

CHAPTER 7: ARTICLE 4

heating, N_{ag} was around 5. After heating, N_{agg} increased to 8. However, when α was increased to 1 these aggregates fell apart and when α was set back to 0.59 N_{ag} was again around 5. The reversal of the aggregation upon increasing α showed that strong chemical cross-linking did not occur. Sui et al. studied a graft copolymer made of poly(ethylene oxide) backbone and P(DMAEMA) grafts with high content of P(DMAEMA).³⁴ They showed that aqueous solutions of this polymer had a pH-dependent LCST and the viscosity at 20°C was the same before and after heating up to 60°C. The origin of this irreversible process is therefore still unclear but cannot be attributed to chemical reactions.

In the following, we focus on systems at $T < 50^\circ\text{C}$ since the rheological properties of these solutions did not evolve with time and were always reversible.

The dependence of G_{el} on α at 50°C is shown in Figure S6 of the supporting information for solutions of TH50c and TH70c at different concentrations. Similarly to anionic systems, THx,⁸ G_{el} increased upon heating for TH50c and TH70c and the increase was more important close to the percolation concentration.

For TH70c, τ increased with increasing temperature for all ionization degrees, but for TH50c, τ either increased with increasing temperature at low α or decreased at high α , see Figure S7 of the supporting information. As a consequence TH50c exhibits either a thermothinning or a thermothickening behavior depending on α and C as shown in Figure S8 of the supporting information.

Interestingly, the effect of the temperature on τ appeared to be determined by f independent of the polymer concentration or composition, see Figure 10. For $f > 0.2$, τ decreased with increasing temperature, while for $f < 0.2$ it increased. The temperature dependence of THxc is clearly very different from that of THx for which τ systematically decreased with increasing temperature and was characterized by an activation energy of ~ 120 kJ/mol that was independent of α and C .⁹

The original temperature dependence of THxc is most likely caused by the sensitivity of DMAEMA to the temperature. PDMAEMA is well-known to have a pH-dependent LCST that increases with decreasing pH from 45°C at pH=10 to 80°C at pH=7.²⁴ It follows that PDMAEMA is more sensitive to the temperature when α is smaller. The LCST was also observed to decrease when DMAEMA was statistically copolymerized with hydrophobic monomers.^{23, 35, 36} We speculate that the increase of the associative interactions between

DMAEMA segments with increasing temperature reduces the energy barrier. This effect increases with decreasing f and dominates the temperature dependence for $f < 0.2$.

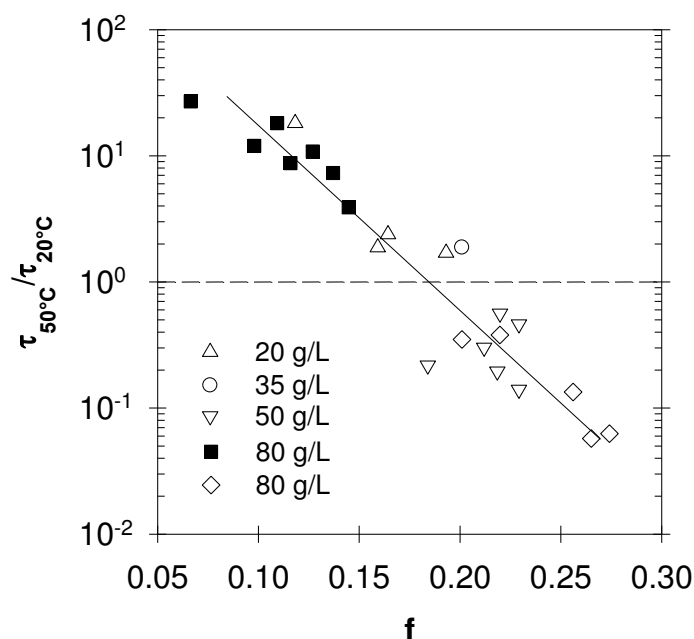


Figure 10. Dependence of the relaxation time at 50°C normalized by the value at 20°C as a function of the fraction of charged units in the B blocks (f) for TH50c at different concentrations (open symbols) and for TH70c at $C=80\text{g/L}$ (closed symbol). The solid line is a guide to the eye.

IV. Conclusions

Cationic triblock copolymers consisting of a hydrophilic P(DMAEMA) central block connected to two lateral blocks containing randomly distributed hydrophobic $n\text{BMA}$ units and hydrophilic DMAEMA units were synthesized by RAFT copolymerization. It was observed that these triblock copolymers formed system spanning networks in aqueous solution above a critical percolation concentration. The relaxation time of the transient networks was directly correlated to the exchange time of the hydrophobic blocks between the hydrophobic cores and could be varied by varying the ionization degree and the proportion of DMAEMA units in the B blocks. In the light of results previously obtained for AA-based amphiphilic triblock copolymers,^{8,9} the study presented here suggests that incorporating hydrophilic units within the hydrophobic block of amphiphilic copolymers is a generally applicable method to obtain dynamic self-assembled structures. The basic character of the DMAEMA units allows the reversible formation of hydrogels with increasing pH, whereas for the triblocks based on

CHAPTER 7: ARTICLE 4

acidic AA units hydrogels were formed with decreasing pH. Finally, the thermosensitivity of the DMAEMA units resulted in a complex effect of the temperature on the self-assembly. Provided that the content of charged DMAEMA units within the hydrophobic blocks was less than 0.2, the exchange dynamics slowed down with increasing the temperature, which resulted in thermo-thickening. However, for $T > 50^{\circ}\text{C}$ irreversible aggregation and gelation was observed.

ASSOCIATED CONTENT

Details on polymer synthesis and behaviour under heating are available in Supporting Information. This material is available free of charge via the Internet at <http://pubs.acs.org>.

REFERENCES

1. Mai, Y.; Eisenberg, A. Self-assembly of block copolymers. *Chem. Soc. Rev.* **2012**, 41, (18), 5969-5985.
2. Chassenieux, C.; Nicolai, T.; Benyahia, L. Rheology of associative polymer solutions. *Curr. Opin. Colloid Interface Sci.* **2011**, 16, (1), 18-26.
3. Annable, T.; Buscall, R.; Ettelaie, R.; Whittlestone, D. The rheology of solutions of associating polymers: Comparison of experimental behavior with transient network theory. *J. Rheol.* **1993**, 37, (4), 695-726.
4. Nicolai, T.; Colombani, O.; Chassenieux, C. Dynamic polymeric micelles versus frozen nanoparticles formed by block copolymers. *Soft Matter* **2010**, 6, (14), 3111-3118.
5. Tsitsilianis, C.; Iliopoulos, I. Viscoelastic properties of physical gels formed by associative telechelic polyelectrolytes in aqueous media. *Macromolecules* **2002**, 35, (9), 3662-3667.
6. Tsitsilianis, C.; Iliopoulos, I.; Ducouret, G. An associative polyelectrolyte end-capped with short polystyrene chains. Synthesis and rheological behavior. *Macromolecules* **2000**, 33, (8), 2936-2943.
7. Tsitsilianis, C.; Katsampas, I.; Sfika, V. ABC heterotelechelic associative polyelectrolytes. Rheological behavior in aqueous media. *Macromolecules* **2000**, 33, (24), 9054-9059.
8. Charbonneau, C.; Chassenieux, C.; Colombani, O.; Nicolai, T. Controlling the Dynamics of Self-Assembled Triblock Copolymer Networks via the pH. *Macromolecules* **2011**, 44, (11), 4487-4495.
9. Shedge, A.; Colombani, O.; Nicolai, T.; Chassenieux, C. Charge Dependent Dynamics of Transient Networks and Hydrogels Formed by Self-Assembled pH-Sensitive Triblock Copolyelectrolytes. *Macromolecules* **2013**, 47, (7), 2439-2444.
10. Lauber, L.; Chassenieux, C.; Nicolai, T.; Colombani, O., pH-Controlled Rheological Properties of Mixed Amphiphilic Triblock Copolymers. 2016.
11. Borisova, O.; Billon, L.; Zaremski, M.; Grassl, B.; Bakaeva, Z.; Lapp, A.; Stepanek, P.; Borisov, O. pH-triggered reversible sol-gel transition in aqueous solutions of amphiphilic gradient copolymers. *Soft Matter* **2011**, 7, (22), 10824-10833.
12. Lauber, L.; Chassenieux, C.; Nicolai, T.; Colombani, O. Highlighting the Role of the Random Associating Block in the Self-Assembly of Amphiphilic Block-Random Copolymers. *Macromolecules* **2015**, 48, (20), 7613-7619.

CHAPTER 7: ARTICLE 4

13. Lejeune, E.; Chassenieux, C.; Colombani, O., pH Induced Desaggregation Of Highly Hydrophilic Amphiphilic Diblock Copolymers. In *Trends in Colloid and Interface Science Xxiv*, Starov, V.; Prochazka, K., Eds. 2011; Vol. 138, pp 7-16.
14. Bendejacq, D. D.; Ponsinet, V.; Joanicot, M. Chemically tuned amphiphilic diblock copolymers dispersed in water: From colloids to soluble macromolecules. *Langmuir* **2005**, *21*, (5), 1712-1718.
15. Laruelle, G.; Francois, J.; Billon, L. Self-assembly in water of poly(acrylic acid)-based diblock copolymers synthesized by nitroxide-mediated polymerization. *Macromol. Rapid Commun.* **2004**, *25*, (21), 1839-1844.
16. Borisova, O.; Billon, L.; Zaremski, M.; Grassl, B.; Bakaeva, Z.; Lapp, A.; Stepanek, P.; Borisov, O. Synthesis and pH- and salinity-controlled self-assembly of novel amphiphilic block-gradient copolymers of styrene and acrylic acid. *Soft Matter* **2012**, *8*, (29), 7649-7659.
17. Dutertre, F.; Boyron, O.; Charleux, B.; Chassenieux, C.; Colombani, O. Transforming Frozen Self-Assemblies of Amphiphilic Block Copolymers Into Dynamic pH-Sensitive Micelles. *Macromol. Rapid Commun.* **2012**, *33*, (9), 753-759.
18. Wright, D. B.; Patterson, J. P.; Gianneschi, N. C.; Chassenieux, C.; Colombani, O.; O'Reilly, R. K. Blending block copolymer micelles in solution; obstacles of blending. *Polym. Chem.* **2016**.
19. Zhang, X.; Boisson, F.; Colombani, O.; Chassenieux, C.; Charleux, B. Synthesis of Amphiphilic Poly(acrylic acid)-b-poly(n-butyl acrylate-co-acrylic acid) Block Copolymers with Various Microstructures via RAFT Polymerization in Water/Ethanol Heterogeneous Media. *Macromolecules* **2014**, *47*, (1), 51-60.
20. Henn, D. M.; Wright, R. A. E.; Woodcock, J. W.; Hu, B.; Zhao, B. Tertiary-Amine-Containing Thermo- and pH-Sensitive Hydrophilic ABA Triblock Copolymers: Effect of Different Tertiary Amines on Thermally Induced Sol-Gel Transitions. *Langmuir* **2014**, *30*, (9), 2541-2550.
21. Peng, Z. P.; Li, G. Z.; Liu, X. X.; Tong, Z. Synthesis, pH- and temperature-induced micellization and gelation of doubly hydrophilic triblock copolymer of poly(N,N-dimethylamino-2-ethylmethacrylate)-b-poly(ethylene glycol)-b-poly(N,N-dimethylamino-2-ethylmethacrylate) in aqueous solutions. *Journal of Polymer Science Part a-Polymer Chemistry* **2008**, *46*, (17), 5869-5878.
22. Sui, K. Y.; Zhao, X.; Wu, Z. M.; Xia, Y. Z.; Liang, H. C.; Li, Y. J. Synthesis, Rapid Responsive Thickening, and Self-Assembly of Brush Copolymer Poly(ethylene oxide)-graft-

- Poly(N,N-dimethylaminoethyl methacrylate) in Aqueous Solutions. *Langmuir* **2012**, 28, (1), 153-160.
23. Zheng, J. Y.; Tan, M. J.; Thoniyot, P.; Loh, X. J. Unusual thermogelling behaviour of poly[2-(dimethylamino)ethyl methacrylate] (PDMAEMA)-based polymers polymerized in bulk. *Rsc Advances* **2015**, 5, (76), 62314-62318.
24. Plamper, F. A.; Ruppel, M.; Schmalz, A.; Borisov, O.; Ballauff, M.; Müller, A. H. E. Tuning the Thermoresponsive Properties of Weak Polyelectrolytes: Aqueous Solutions of Star-Shaped and Linear Poly(N,N-dimethylaminoethyl Methacrylate). *Macromolecules* **2007**, 40, (23), 8361-8366.
25. Tang, X. D.; Liang, X. C.; Gao, L. C.; Fan, X. H.; Zhou, Q. F. Water-Soluble Triply-Responsive Homopolymers of N,N-Dimethylaminoethyl methacrylate with a Terminal Azobenzene Moiety. *Journal of Polymer Science Part a-Polymer Chemistry* **2010**, 48, (12), 2564-2570.
26. Xu, W.; Choi, I.; Plamper, F. A.; Synatschke, C. V.; Müller, A. H. E.; Melnichenko, Y. B.; Tsukruk, V. V. Thermo-Induced Limited Aggregation of Responsive Star Polyelectrolytes. *Macromolecules* **2014**, 47, (6), 2112-2121.
27. Plamper, F. A.; Schmalz, A.; Ballauff, M.; Müller, A. H. E. Tuning the thermoresponsiveness of weak polyelectrolytes by pH and light: Lower and upper critical-solution temperature of Poly(N,N-dimethylaminoethyl methacrylate). *J. Am. Chem. Soc.* **2007**, 129, (47), 14538-+.
28. Sahnoun, M.; Charreyre, M.-T.; Veron, L.; Delair, T.; D'Agosto, F. Synthetic and characterization aspects of dimethylaminoethyl methacrylate reversible addition fragmentation chain transfer (RAFT) polymerization. *J. Polym. Sci., Part A: Polym. Chem.* **2005**, 43, (16), 3551-3565.
29. Wright, D. B.; Patterson, J. P.; Pitto-Barry, A.; Cotanda, P.; Chassenieux, C.; Colombani, O.; O'Reilly, R. K. Tuning the aggregation behavior of pH-responsive micelles by copolymerization. *Polym. Chem.* **2015**, (6), 2761-2768.
30. Colombani, O.; Lejeune, E.; Charbonneau, C.; Chassenieux, C.; Nicolai, T. Ionization Of Amphiphilic Acidic Block Copolymers. *J. Phys. Chem. B* **2012**, 116, (25), 7560-7565.
31. Green, M. S.; Tobolsky, A. V. A New Approach to the Theory of Relaxing Polymeric Media. *J. Chem. Phys.* **1946**, 14, (2), 80-92.
32. van de Wetering, P.; Zuidam, N. J.; van Steenberg, M. J.; van der Houwen, O. A. G. J.; Underberg, W. J. M.; Hennink, W. E. A Mechanistic Study of the Hydrolytic Stability of Poly(2-(dimethylamino)ethyl methacrylate). *Macromolecules* **1998**, 31, (23), 8063-8068.

CHAPTER 7: ARTICLE 4

33. Cotanda, P.; Wright, D. B.; Tyler, M.; O'Reilly, R. K. A comparative study of the stimuli-responsive properties of DMAEA and DMAEMA containing polymers. *Journal of Polymer Science Part a-Polymer Chemistry* **2013**, 51, (16), 3333-3338.
34. Sui, K.; Zhao, X.; Wu, Z.; Xia, Y.; Liang, H.; Li, Y. Synthesis, Rapid Responsive Thickening, and Self-Assembly of Brush Copolymer Poly(ethylene oxide)-graft-Poly(N,N-dimethylaminoethyl methacrylate) in Aqueous Solutions. *Langmuir* **2011**, 28, (1), 153-160.
35. Liu, F.; Urban, M. W. Dual Temperature and pH Responsiveness of Poly(2-(N,N-dimethylamino)ethyl methacrylate-co-n-butyl acrylate) Colloidal Dispersions and Their Films. *Macromolecules* **2008**, 41, (17), 6531-6539.
36. Zhang, C.; Maric, M. Synthesis of Stimuli-responsive, Water-soluble Poly[2-(dimethylamino)ethyl methacrylate/styrene] Statistical Copolymers by Nitroxide Mediated Polymerization. *Polymers* **2011**, 3, (3), 1398-1422.

Supporting information of article 4

pH and thermo-responsive self-assembly of cationic triblock copolymers with controlled dynamics

Lionel Lauber, Julien Santarelli, O. Boyron, Christophe Chassenieux, Olivier Colombani*,

Taco Nicolai

1) Synthesis of the triblock copolymers

The BAB triblock copolymer TH70c consisting of a central PDMAEMA₂₀₀ A block and two statistical P(*n*BMA_{1-x}-*stat*-DMAEMA_x)₁₀₀ B blocks with x equal to 70%mol was synthesized by RAFT¹ according to the detailed procedure described below. TH50c, with x = 50%mol, was synthesized according to the same procedure simply adapting the ratio of comonomers for the synthesis of the lateral blocks.

i. Materials and Chemical Characterization

Materials. 2-dimethylaminoethyl methacrylate (98%, Sigma-Aldrich) and *n*-butyl methacrylate (99%, Sigma-Aldrich) were dried over CaH₂ and distilled under vacuum before use. N,N-azobisisobutyronitrile (AIBN, 98%, Merck Chemical) was recrystallized from 95% methanol (99.99%, Fisher Chemical) before use. 1,4-dioxane (99%, Merck), 2-cyano-2-propyl benzodithioate (CPDB, 97%, Sigma-Aldrich), dichloromethane (99%, Fischer Chemical) and pentane (99%, Sigma-Aldrich) were used as received.

Size exclusion chromatography (SEC) was performed using a EcoSEC semi-micro CPG Tosoh system equipped with a 3 PSS GRAM (10 μm, 300 x 7,5mm) column with DMF with 0.01M of LiBr as eluent (flow rate = 0.8 mL/min), at 60°C, and using refractometry for detection (Shodex RI 71 refractometer, Showa Denko). The number-average molecular weight (M_n) and dispersity (M_w/M_n) were determined using poly(methyl methacrylate) standards for calibration ranging from 580 to 3 x10⁶ g/mol. It should be noted that this conventional calibration of SEC yields apparent values of M_n , M_w , and dispersity (M_w/M_n). The molecular weights of the final polymers were calculated from the conversion assuming that termination and transfer reactions were negligible.

CHAPTER 7: ARTICLE 4

^1H NMR spectra were recorded in CDCl_3 at 20 °C on a Brüker AC400 (400 MHz) spectrometer.

ii. First block: $\text{P}(n\text{BMA}_{0.3}\text{-stat-DMAEMA}_{0.7})_{100}$ (MHxc)

For the first block $\text{P}(n\text{BMA}_{0.3}\text{-stat-DMAEMA}_{0.7})_{100}$, *n*-butyl methacrylate (3.31 g, 2.33×10^{-2} mol), dimethylaminoethyl methacrylate (8.52 g, 5.42×10^{-2} mol), azobisisobutyronitrile (AIBN, 2.16×10^{-2} g, 1.31×10^{-4} mol), cumyl dithiobenzoate (CDTB, 0.10 g, 3.77×10^{-4} mol) and dioxane (14.5 g) were introduced in a 500 mL round-bottom flask. The flask was closed with a screw cap equipped with a septum, and degassed by argon bubbling for 20 min. The molar ratios were as follows $[\text{nBMA}+\text{DMAEMA}]:[\text{CDTB}]:[\text{AIBN}] = 205:1:0.35$.

A few drops of the solution were taken as sample t_0 , and the flask was dipped in an oil bath at 70 °C. To follow the kinetics, samples were withdrawn throughout the reaction. The conversion was determined by ^1H NMR² revealing that both monomers polymerized at the same speed resulting in a statistical distribution of the monomer units, see Figure S2. The reaction was stopped at 49 % conversion by cooling the flask to 0 °C and injecting air. The polymer was purified by two precipitations in pentane, yielding a dark pink powder (3.93g, yield of the precipitation = 65%). Size exclusion chromatography (SEC) was performed on the final polymer to determine the number (M_n) and weight (M_w) average molar masses as well as their dispersity, see Figure S5b and Table 1. ^1H NMR demonstrated that the DMAEMA/*n*BMA ratio was the same as in the initial monomer feed, see Table 1. The polymer characteristics are summarized in Table 1.

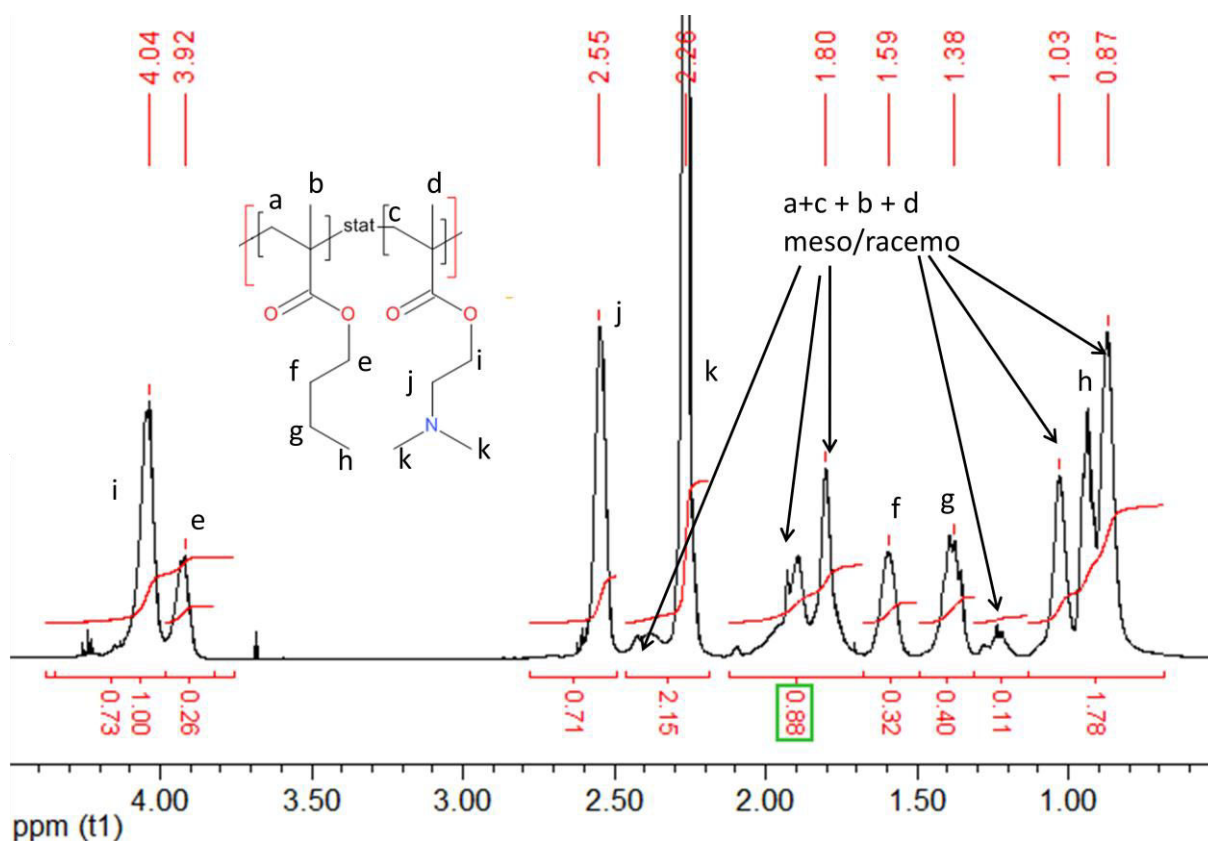


Figure S1. ^1H NMR of MH70c after purification in CDCl_3 . δ (ppm) = 4.04 (t, 2H, H-i) ; δ (ppm) = 3.92 (t, 2H, H-e) ; δ (ppm) = 2.55 (m, 2H, H-j) ; δ (ppm) = 2.26 (s, 6H, H-k) ; δ (ppm) = 1.59 (m, 2H, H-f) ; δ (ppm) = 1.38 (m, 2H, H-g) ; δ (ppm) = 0.93 (t, 3H, H-h) ; δ (ppm) = 2.40+1.93+1.80+1.30+1.03+0.87 (m, 6H, H-a+c+b+d).

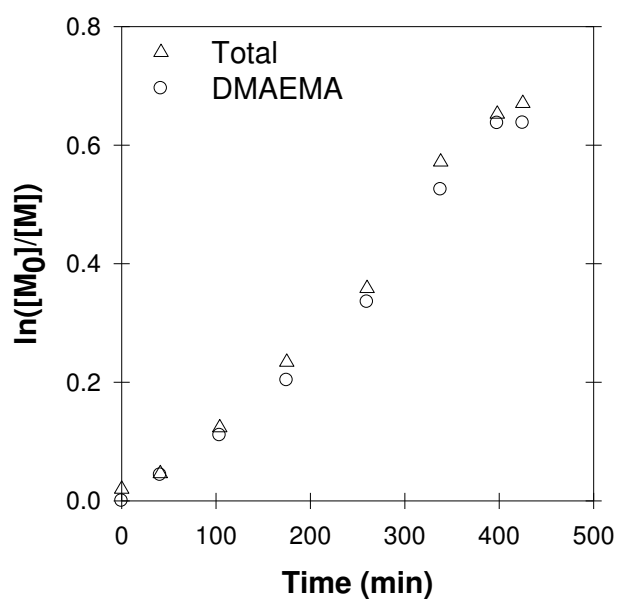


Figure S2. Kinetics of the polymerisation for the synthesis of MH70c. The monomer consumption of total (Δ), DMAEMA (\circ) were measured by ^1H NMR.

iii. Diblock: P(*n*BMA_{0.3}-*stat*-DMAEMA_{0.7})₁₀₀-*b*-P(DMAEMA)₂₀₀ (DHxc)

For the diblock copolymer P(*n*BMA_{0.3}-*stat*-DMAEMA_{0.7})₁₀₀-*b*-P(DMAEMA)₂₀₀ a similar procedure was used with the following amounts of reagents: dimethylaminoethyl methacrylate (15.3 g, 9.73 x10⁻² mol), azobisisobutyronitrile (1.4 x10⁻² g, 8.77 x10⁻⁵ mol), P(*n*BMA_{0.3}-*stat*-DMAEMA_{0.7})₁₀₀ (3.72 g, 2.44 x10⁻⁴ mol) and dioxane (9.31 g). The molar ratios were as follows [DMAEMA] : [P(*n*BMA_{0.3}-*stat*-DMAEMA_{0.7})₁₀₀] : [AIBN] = 399 : 1 : 0.36. The reaction was stopped at 49% conversion and the polymer was recovered by two precipitations in pentane which gave 8.1 g of a pink powder (yield of the precipitation = 71%). The same analyses as for the first block were achieved see Figure S3, Figure S5b and Table 1.

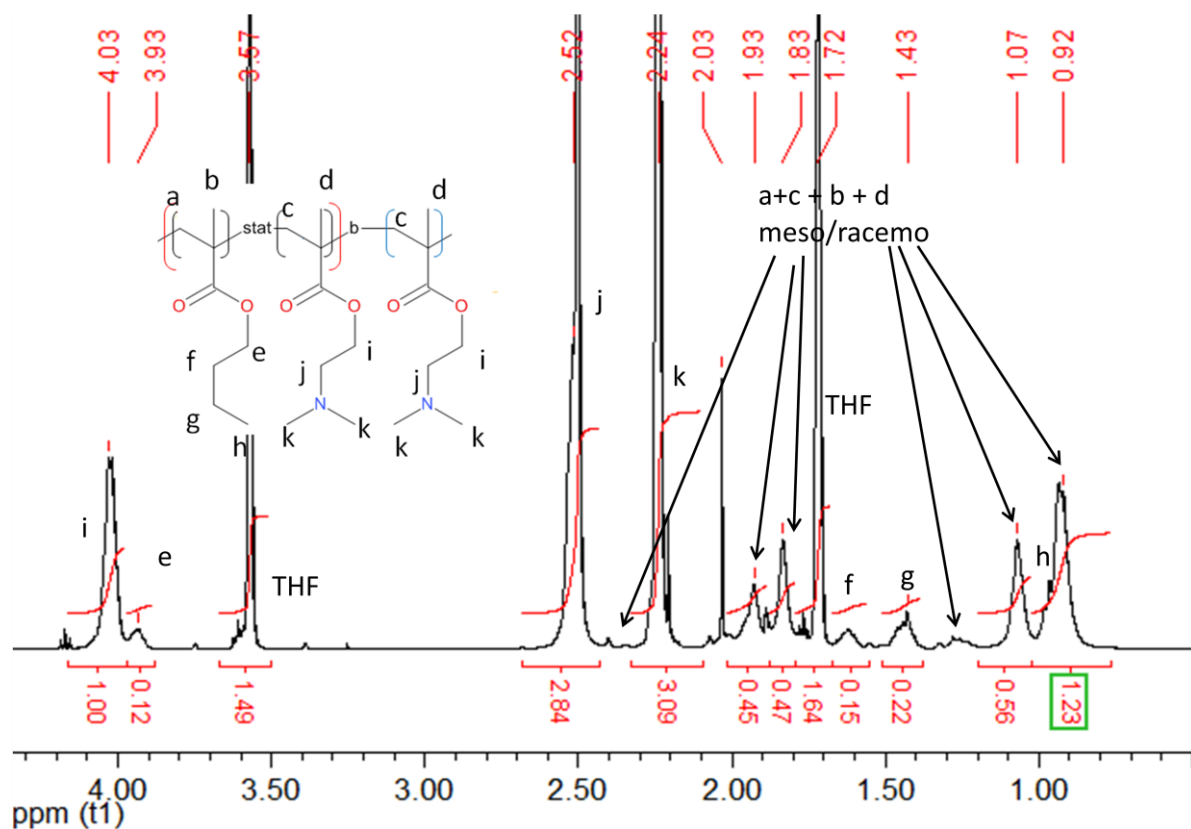


Figure S3. ¹H NMR of DH70c after purification in THF-D₈. δ (ppm) = 4.03 (t, 2H, H-i) ; δ (ppm) = 3.93 (t, 2H, H-e) ; δ (ppm) = 2.52 (m, 2H, H-j) ; δ (ppm) = 2.24 (s, 6H, H-k) ; δ (ppm) = 1.62 (m, 2H, H-f); δ (ppm) = 1.43 (m, 2H, H-g); δ (ppm) = 0.93 (t, 3H, H-h); δ (ppm) = 2.40+1.93+1.80+1.30+1.03+0.87 (m, 6H, H-a+c+b+d).

iv. Triblock: $P(nBMA_{0.3}\text{-}stat\text{-}DMAEMA_{0.7})_{100}\text{-}b\text{-}P(DMAEMA)_{200}\text{-}b\text{-}P(nBMA_{0.3}\text{-}stat\text{-}DMAEMA_{0.7})_{100}$ (THxc)

For the triblock copolymer $P(nBMA_{0.3}\text{-}stat\text{-}DMAEMA_{0.7})_{100}\text{-}b\text{-}P(DMAEMA)_{200}\text{-}b\text{-}P(nBMA_{0.3}\text{-}stat\text{-}DMAEMA_{0.7})_{100}$, a similar procedure was used with the following amounts of reagents: *n*-butyl methacrylate (1.48 g, 1.04×10^{-2} mol), dimethylaminoethyl methacrylate (3.91 g, 2.49×10^{-2} mol), azobisisobutyronitrile (9.20×10^{-3} g, 5.60×10^{-5} mol), $P(nBMA_{0.3}\text{-}stat\text{-}DMAEMA_{0.7})_{100}\text{-}b\text{-}P(DMAEMA)_{200}$ (7.96 g, 1.70×10^{-4} mol) and dioxane (6.62 g). The molar ratios were as follows $[nBMA+DMAEMA]:[P(nBMA_{0.3}\text{-}stat\text{-}DMAEMA_{0.7})_{100}\text{-}b\text{-}P(DMAEMA)_{200}]:[AIBN] = 207:1:0.33$.

The reaction was stopped at 50% conversion resulting in 9.3 g of a pink powder (yield of the precipitation = 88%) after two precipitations in pentane. The same analyses as for the first block were achieved see Figure S4, Figure S5b and Table 1. It is interesting to remark that the M_n ratio between the theoretical and experimental values were different for the triblock copolymers than for the diblocks and monoblocks.

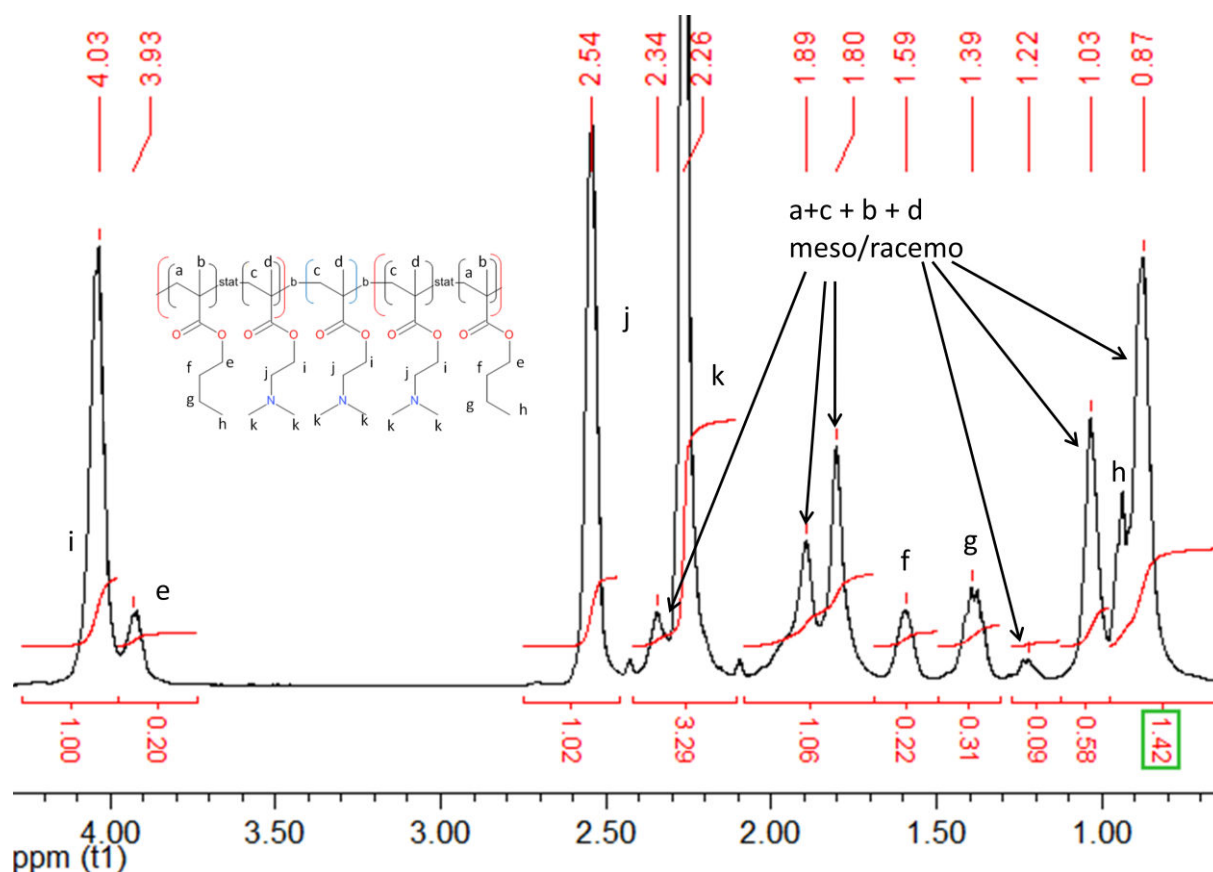


Figure S4. 1H NMR of TH70c after purification in $CDCl_3$. δ (ppm) = 4.03 (t, 2H, H-i) ; δ (ppm) = 3.93 (t, 2H, H-e) ; δ (ppm) = 2.54 (m, 2H, H-j) ; δ (ppm) = 2.26 (s, 6H, H-k) ; δ

(ppm) = 1.59 (m, 2H, H-f) ; δ (ppm) = 1.39 (m, 2H, H-g) ; δ (ppm) = 0.90 (t, 3H, H-h); δ (ppm) = 2.40+1.93+1.80+1.30+1.03+0.87 (m, 6H, H-a+c+b+d).

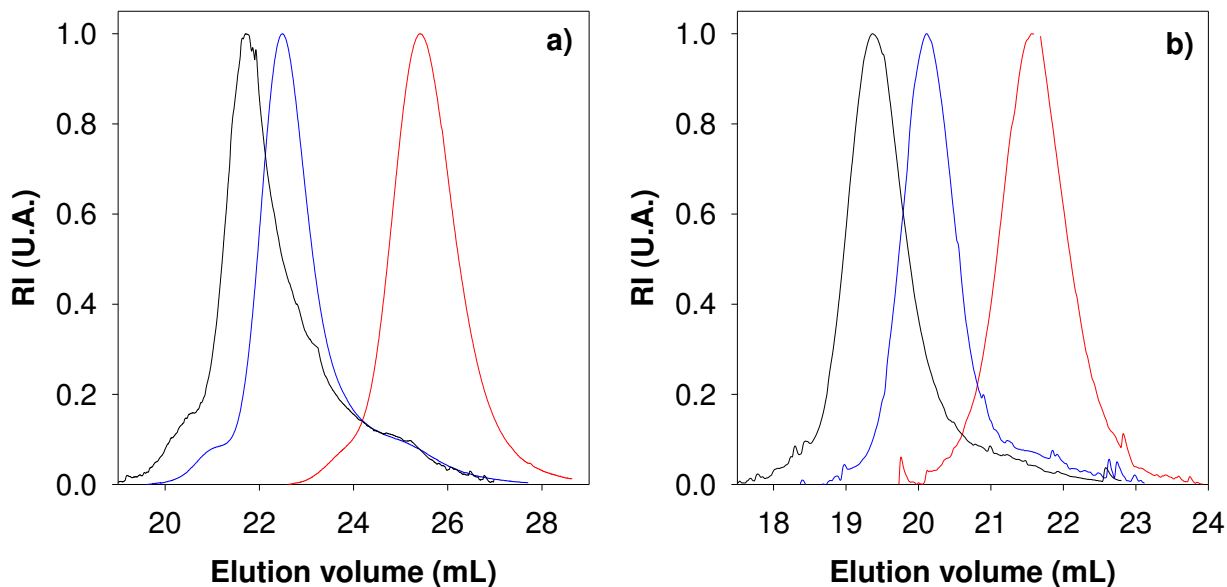


Figure S5. Size exclusion chromatograms of the first block MHxc (red), diblock DHxc (blue) and triblock THxc (black) of TH50c (a) and TH70c (b) in DMF with 0.01 M LiBr at 60°C.

2) Effect of the temperature on TH50c and TH70c solutions

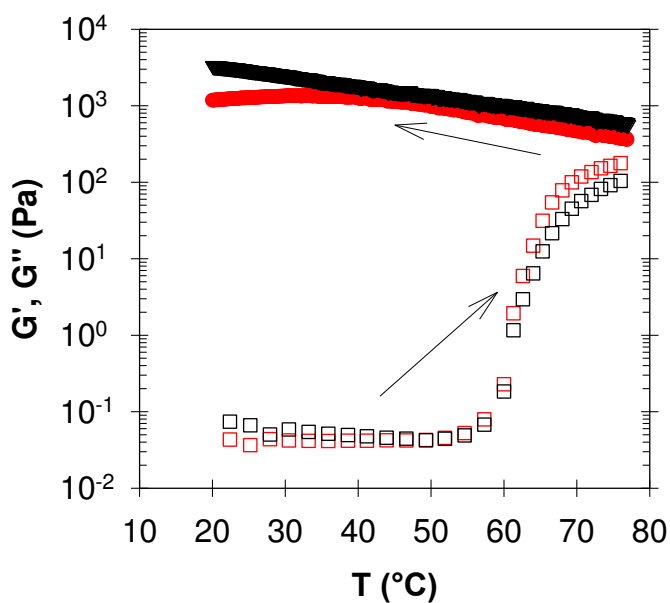


Figure S6. Evolution of the elastic (red) and loss (black) moduli as a function of the temperature for TH50c at $\omega=1$ rad/s, $\alpha=0.8$, $C=50$ g/L without added salt. The arrows represent the evolution of the temperature.

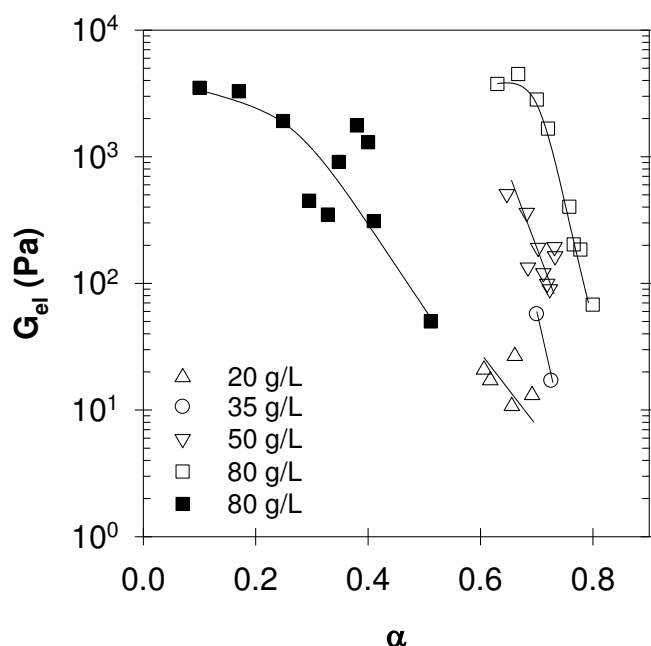
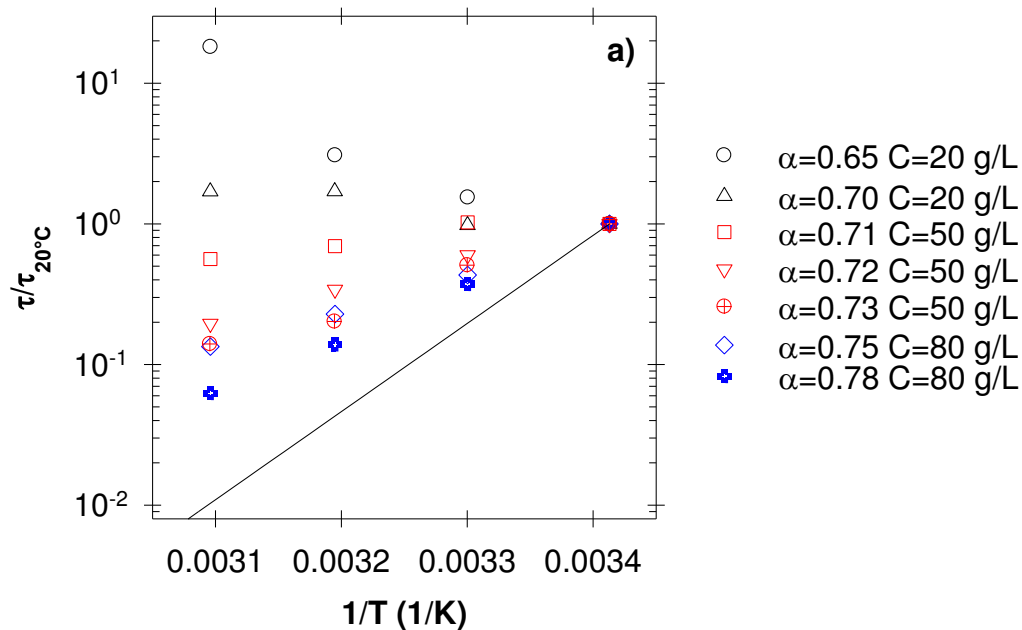


Figure S7. Evolution of the elastic modulus as a function of the ionization degree (α) for TH50c at different concentrations (open symbols) and TH70c at 80 g/L (closed symbols) ($T=50^\circ\text{C}$). The solid lines are guides to the eye.



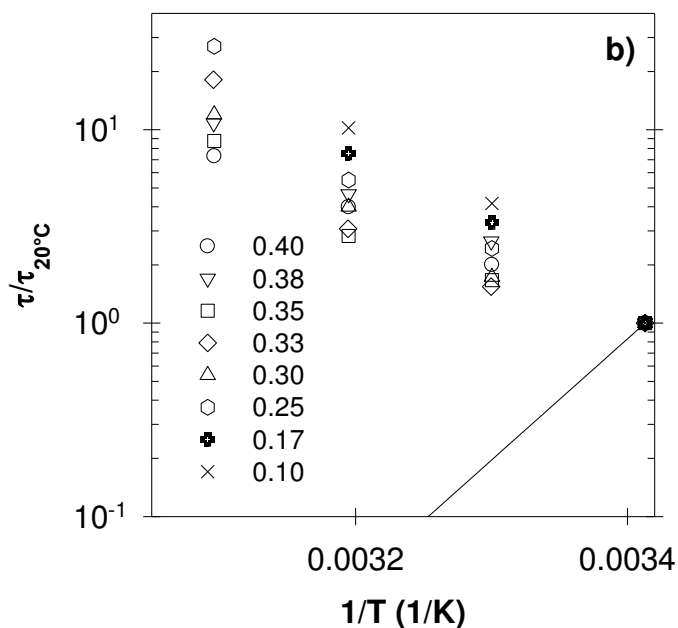


Figure S8. Evolution of the relaxation time normalized by its original value at 20°C as a function of $1/T$ at different ionization degrees and concentrations for TH50c (a) and TH70c (b). The solid lines represent an activation energy of 120 kJ/mol, typical for THx.³

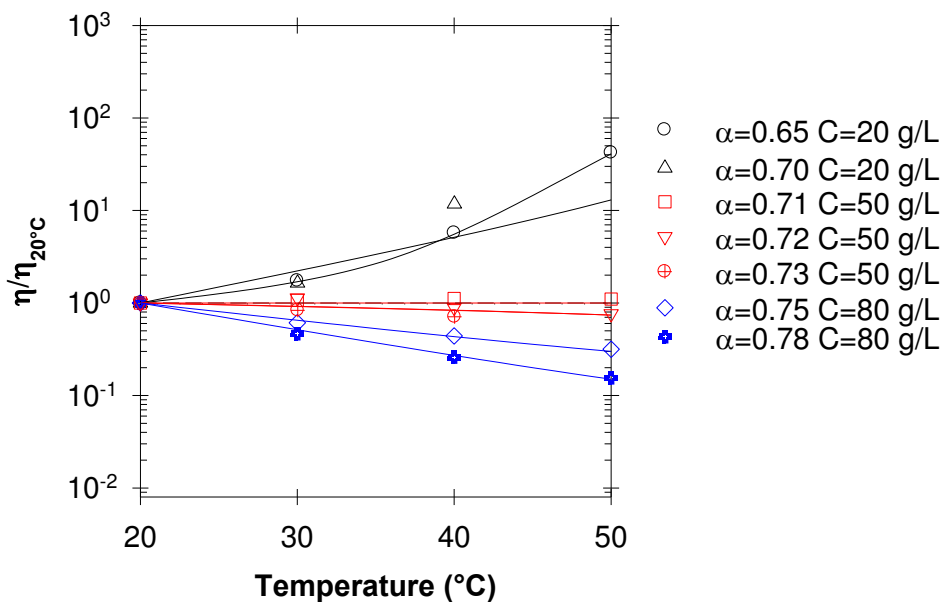


Figure S9. Evolution of the viscosity normalized by its original value at 20°C as a function of the temperature at different ionization degrees and concentrations for TH50c. The solid lines are guides to the eye.

REFERENCES

1. Moad, G.; Rizzardo, E.; Thang, S. H. Living radical polymerization by the RAFT process. *Aust. J. Chem.* **2005**, 58, (6), 379-410.
2. Dutertre, F.; Boyron, O.; Charleux, B.; Chassenieux, C.; Colombani, O. Transforming Frozen Self-Assemblies of Amphiphilic Block Copolymers Into Dynamic pH-Sensitive Micelles. *Macromol. Rapid Commun.* **2012**, 33, (9), 753-759.
3. Shedge, A.; Colombani, O.; Nicolai, T.; Chassenieux, C. Charge Dependent Dynamics of Transient Networks and Hydrogels Formed by Self-Assembled pH-Sensitive Triblock Copolyelectrolytes. *Macromolecules* **2013**, 47, (7), 2439-2444.

CHAPTER 8 : APPENDIX 1

In this work and in the literature, random copolymers were used as hydrophobic blocks to tune the exchange dynamics of block copolymers.^{1, 2} However, the impact of the comonomers' repartition has not been investigated yet.³ In the literature interesting sol-gel transitions were obtained after heating above the glass transition triblock copolymers made of a hydrophilic poly(acrylic acid) central block and two gradient copolymers made of styrene and acrylic acid as hydrophobic blocks: $P(S\text{-}grad\text{-}AA)\text{-}b\text{-}PAA\text{-}b\text{-}P(S\text{-}grad\text{-}AA)$.⁴⁻⁶ However, to date no comparison between triblock copolymers having statistical and gradient repartition of the monomers units was undertaken.

This appendix shows the results for three copolymers with poly(acrylic acid) as the hydrophilic central block and gradient copolymers end blocks containing x acrylic acid (AA) and $(1-x)$ *n*-butyl acrylate (*n*BA) units, hereafter called $TH_gx = P(nBA_{1-x}\text{-}grad\text{-}AA_x)_{50}\text{-}b\text{-}PAA_{110}\text{-}b\text{-}P(nBA_{1-x}\text{-}grad\text{-}AA_x)_{50}$, illustrated in Figure 8.2. The length of these polymers was around half that of their statistical homologues: $TH_x = P(nBA_{1-x}\text{-}stat\text{-}AA_x)_{100}\text{-}b\text{-}PAA_{200}\text{-}b\text{-}P(nBA_{1-x}\text{-}stat\text{-}AA_x)_{100}$. However, the comparison remains interesting as a preliminary study.

I. Synthesis and titration of the gradient triblock copolymers

I.1. Synthesis of the gradient triblock copolymers

Three triblock copolymers were synthesized by nitroxide-mediated radical copolymerization (NMP) of acrylic acid (AA) and *n*-butyl acrylate (*n*BA) by L. Billon and E. Deniau-Lejeune (UMR5254). The synthesis strategy was adapted from previously published studies.^{4, 5} The nitroxide control agents used were SG1 (N-tert-butyl-N-[1-diethylphosphono-(2,2-dimethylpropyl)]nitroxide) and its difunctional equivalents DIAMS.

The reactivity ratios of AA and *n*BA were around 3.2 and 4.5 respectively using the Fineman-Ross method. The evolution of the instantaneous fraction of AA and *n*BA units along the chain of a similar diblock copolymer, $PAA_{100}\text{-}b\text{-}P(nBA_{0.5}\text{-}stat\text{-}AA_{0.5})_{100}$, were deduced from kinetic studies using ¹H NMR as shown in Figure 8.1. The data for the triblock copolymers are missing as yet, but are expected to be similar. The gradient strength of hydrophobic units was smooth, especially since it was almost a statistical copolymer at the end. From these kinetic data, it was concluded that the gradient blocks were rich in AA units close to the central PAA block and rich in *n*BA units at the extremities.

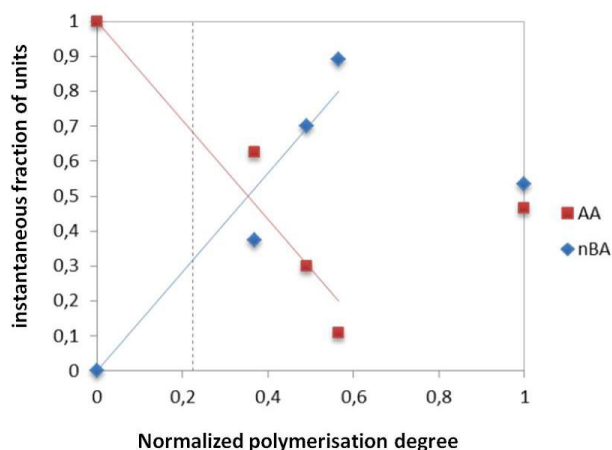


Figure 8.1. Evolution of the instantaneous fraction of AA and nBA units along the chain of a PAA₁₀₀-*b*-P(nBA_{0.5}-stat-AA_{0.5})₁₀₀ diblock copolymer. The normalized polymerization degree is length of the block normalized by its final length.

The triblock copolymers obtained are schematically represented in Figure 8.2.

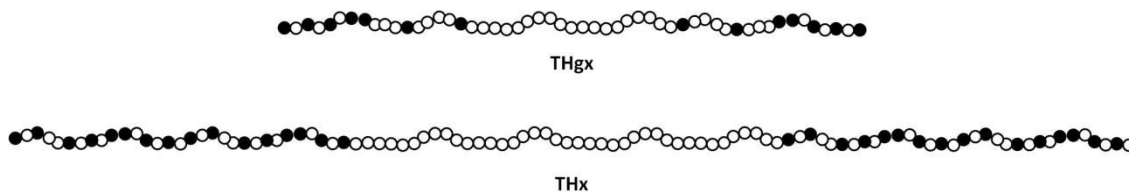


Figure 8.2. Schematic representation of the triblock copolymers THgx and THx.

The structure of the three triblock copolymers was determined by ¹H NMR. Results are summarized in Table 8-1, whereas details on the NMR spectra are available in Figure 8.3. The structures can be approximated as follows: P(nBA_{1-x}-grad-AA_x)₅₀-*b*-PAA₁₁₀-*b*-P(nBA_{1-x}-grad-AA_x)₅₀, x standing for the percentage of acrylic acid in the hydrophobic blocks (40, 50 and 60%), thereafter called THgx. It is important to remark that the dispersities were rather high, Đ ≥ 1.8.

Table 8-1. Main characteristic of the triblock copolymers. ^a Monomer conversion determined by ¹H NMR.

Name	DP (PAA) ^a	DP (P(<i>n</i> BA- <i>grad</i> -AA))	M _n (g.mol ⁻¹) (SEC visco)	Đ	%AA in the copolymers ^a	%AA in the hydrophobic blocks ^a
THg50	96	56	2.0 x 10 ⁴	1.8	0,73	50
THg40	99	60	2.2 x 10 ⁴	1.9	0,66	38
THg60	126	41	1.7 x 10 ⁴	2.4	0,87	67

^a The amount of AA units were obtained by ¹H NMR.

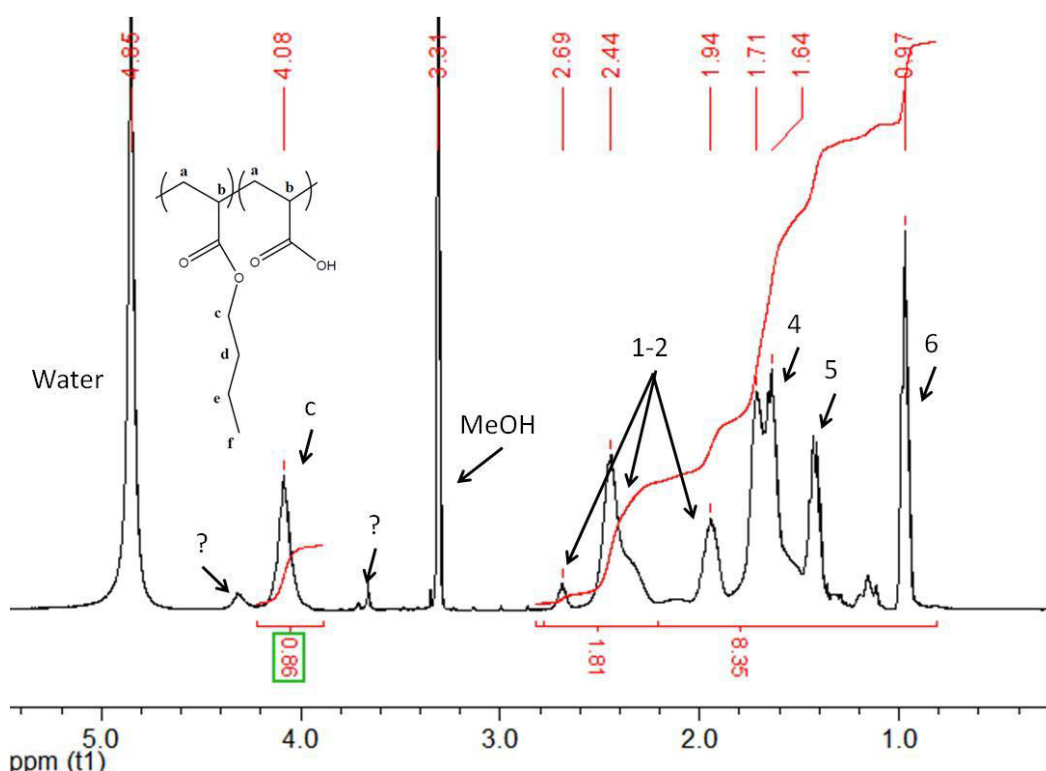


Figure 8.3. ¹H NMR spectra of the triblock copolymer THg50 in MeOD. δ (ppm) = 4.92 (water) δ (ppm) = 4.10 (t, 2H *n*BA), δ (ppm) = 3.17 (MeOH), δ (ppm) = 2.3 (m, 1H AA et 1H *n*BA), δ (ppm) = 1.90 (m, 2H AA et 2H *n*BA), δ (ppm) = 1.75 (m, 2H *n*BA), δ (ppm) = 1.40 (m, 2H *n*BA), δ (ppm) = 0.98 (t, 3H *n*BA).

I.2. Titration of the gradient triblock copolymers

First, the microstructure was probed by titration experiments. As was emphasized by Colombani et al. ⁷ it is harder to ionize AA units in statistical copolymers containing hydrophobic *n*BA units, P(*n*BA-*stat*-AA), than in a homopolymer of P(AA).

As demonstrated by Zhang *et al.*³, when the gradient structure is particularly pronounced the titration curves of the gradient copolymer are similar to the ones for the diblock copolymers i.e. the same as an homoPAA, and different from that of the statistical copolymers.

In Figure 8.4, the evolution of the ionisation degree as function of pH is similar for the three THgx and very close to that of the triblock TH50. No strong difference can be seen between gradient and statistical copolymers implying that THgx does not exhibit gradients as strong as those obtained by Zhang *et al.* Considering that a gradient does exist in the THgx according to the kinetics of the polymerization, the titration experiments do not seem to be able to distinguish a perfectly statistical microstructure (TH50) from a moderate gradient (THgx).

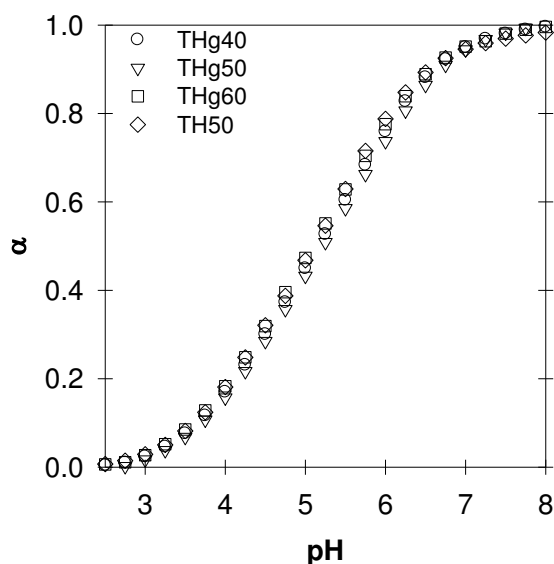


Figure 8.4. Evolution of the ionization degree as function of pH for the three gradient copolymers and TH50 at $[Na^+]=0.5\text{ M}$, $[AA]=0.043\text{ M}$ and an HCl (1M) addition speed of 0.1 mL/min.

II. Self-association of THgx

To understand the self-association of THgx, light scattering experiments were conducted in aqueous medium at different concentrations and at $\alpha=1$. As already observed for similar systems, a slow mode originating from the presence of spurious aggregates appeared in dynamic light scattering.⁸ Since it represented a very small amount of the polymer it was neglected. The refractive index increment was taken from similar copolymers with a statistical repartition of the monomers in the hydrophobic blocks.⁹ In Figure 8.5, the evolution of the apparent molar mass and hydrodynamic radius as a function of the polymer concentration indicated that at 2 g/L the repulsive interactions can be neglected so that the measured

apparent molecular weight and hydrodynamic radius corresponded to the true molecular weight of the scatterers. Surprisingly, the molar mass of both THg50 and THg60 at $\alpha=1$ were twice smaller than the expected values for the unimers. Such results could come from an important error bar in the dispersity or the dn/dc . On the contrary, THg40 seemed associated even at $\alpha=1$ with an aggregation number around 3. The evolution of the hydrodynamic radius was equivalent and indicates that both THg50 and THg60 were unassociated at $\alpha=1$.

More information could have been obtained from a study at different ionization degrees,⁸ but for this preliminary study we focused on the investigation of the rheological properties of the solutions.

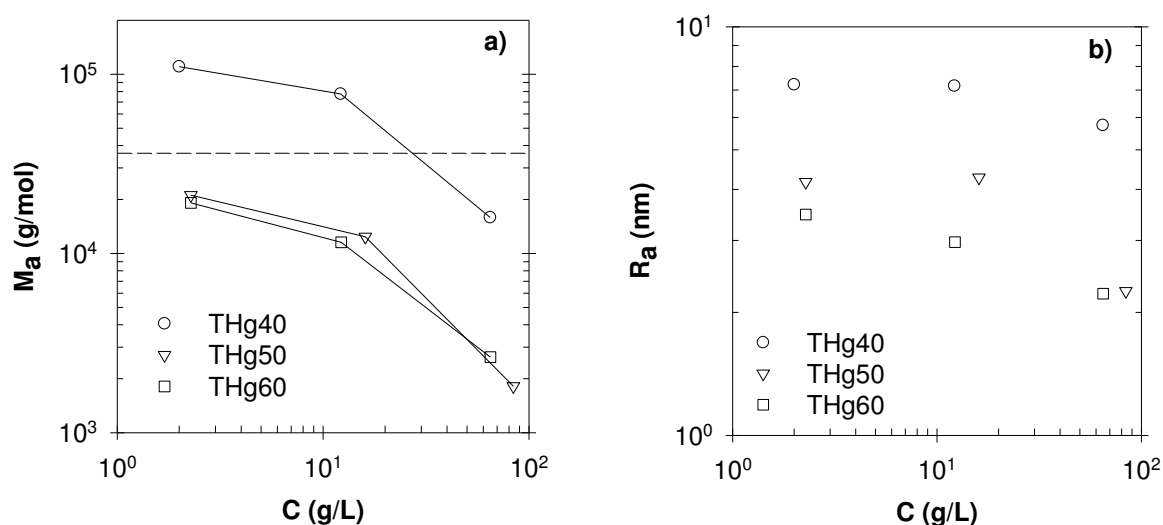


Figure 8.5. Apparent molar mass M_a (a) and hydrodynamic radius (b) as a function of the polymer concentration for the three gradient triblocks at $[Na^+]=0.5 M$, $\alpha=1$ and different concentrations. Open symbols correspond to the measurements, whereas the dashed line corresponds to the expected values of the unimers.

III. Rheological properties

The solutions were prepared as described in the materials and methods section, p.54.

Solutions at different ionization degrees of the three triblock copolymers were prepared at $C=60-80$ g/L. Only THg50 percolated, THg40 and THg60 did not percolate even at $\alpha\sim 0$ and $C=70$ g/L.

This high percolation concentration for THg50 was most probably due to the size of the copolymer that was twice as small as that of the statistical triblock homologue TH50. The absence of percolation of THg60 at the conditions investigated was not surprising. Indeed, it

CHAPTER 8: APPENDIX 1

was observed for the $\text{TH}_x = \text{P}(n\text{BA}_{1-x}\text{-stat-AA}_x)_{100}\text{-}b\text{-PAA}_{200}\text{-}b\text{-P}(n\text{BA}_{1-x}\text{-stat-AA}_x)_{100}$ series, that the percolation concentration increased with increasing x and, here, even THg50 only percolated at high concentrations due to its small size.² This is reinforced by the shortness of the hydrophobic blocks of THg60 compared to the ones of the two other gradient copolymers, see Table 8-1. It is harder to understand the absence of percolation for THg40 since THg50 percolated. We speculate that the absence of percolation of THg40 may be due to the fact that this polymer formed frozen aggregates and could not rearrange into a network with increasing concentration. This speculation is supported by the fact that THg40 was already aggregated at $\alpha = 1$ as explained in section II.

In the following we will, focus on THg50 and its rheological properties. However, since the percolation concentrations were high it was difficult from a practical point of view to reach polymer concentrations far from the percolation concentration ($C_p > 60$ g/L). Therefore, the networks studied have many defects and it was not sure that the relaxation time was fully related to the exchange time of the hydrophobic blocks from the micellar cores. It would be interesting to compare these results with a study at several concentrations on a gradient triblock copolymer of the same size as TH50.

By doing vertical and horizontal shifts, a unique master curve for THg50 was obtained by superimposing data from different ionization degrees and temperatures as shown in Figure 8.6. The activation energy derived from frequency-temperature superposition was close to 120 kJ/mol for all α . At low frequencies liquid-like behaviour was observed with $G' \sim \omega^2$ and $G'' \sim \omega^1$ and a solid-like behaviour was reached at high frequencies with the storage modulus almost independent of ω . The relaxation time distribution was extremely broad and different from TH50. This high dispersity led to some uncertainty in the determination of the relaxation time.

The very broad relaxation time distribution has three possible origins. First, the experiments were conducted close to the percolation concentration where the amount of defects in the network is larger, causing an increase of the dispersity of the relaxation phenomenon.¹ Second, it was previously shown that the relaxation time of the networks critically depends on the amount of AA units within the hydrophobic blocks.² As a consequence, increasing the dispersity of the polymers in terms of chemical composition of the hydrophobic blocks leads to a higher dispersity in terms of relaxation times as shown in this thesis for mixtures of THx copolymers with different %AA in the hydrophobic blocks. The rather high dispersity of the

THgx triblock copolymers studied here ($\mathcal{D} = 1.8\text{-}2.4$) implies a dispersity in length and most probably also in composition, which could very well explain the broad relaxation time distribution. Finally, the gradient structure may also cause broadening of the distribution of relaxation times. Further studies using longer and less disperse polymers will be required to conclude.

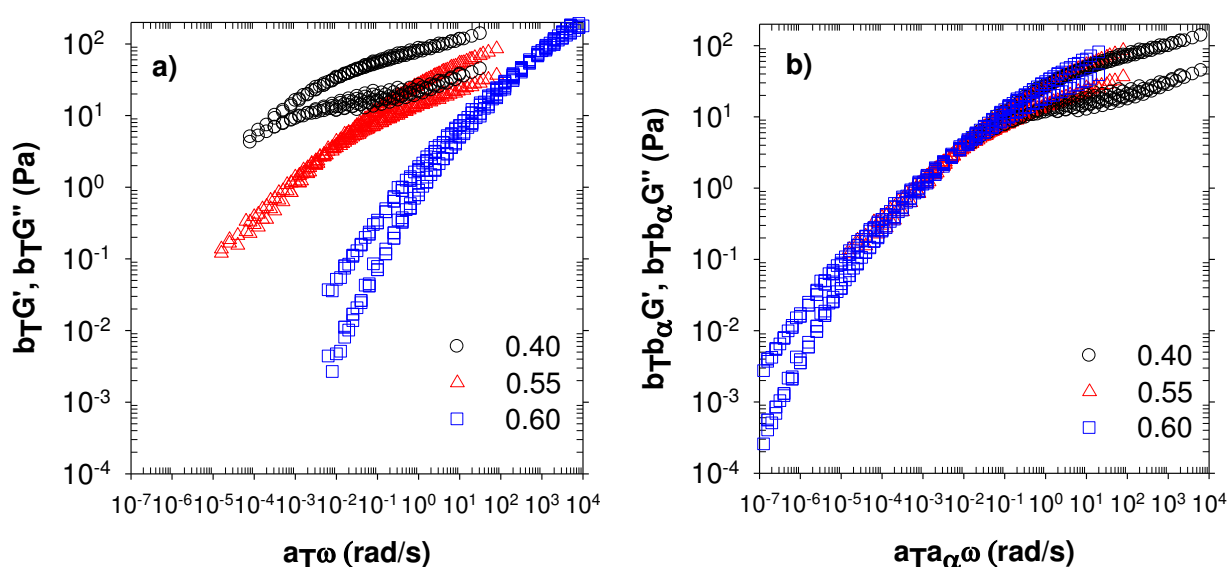


Figure 8.6. (a) Frequency dependence of the storage and loss shear moduli at different ionization degrees for THg50 after temperature-frequency superposition at $T_{ref}=20^\circ\text{C}$ (b) Master curves of master curves at several temperatures and ionization degrees for THg50. $T=20^\circ\text{C}$, $\alpha_{ref}=0.55$, $C=60\text{-}80$ g/L without salt.

The relaxation time is plotted as a function of the ionisation degree in Figure 8.7. The relaxation time increased when the ionisation degree decreased, by 7 orders of magnitude. The dependence of the relaxation time on α was qualitatively the same as for TH50 but quantitatively different. The relaxation time was systematically larger for THg50 than for TH50 at the same ionization degree. This was unexpected considering the THg50 solutions were studied close to the percolation concentration and consisted of shorter polymers than TH50 solutions. The relaxation time is lower close to the percolation concentration due to the existence of superbridges and shorter hydrophobic blocks have shorter exchange times.¹⁰ Therefore the larger relaxation times for THg50 compared to TH50 are caused by is caused by the difference in structure.

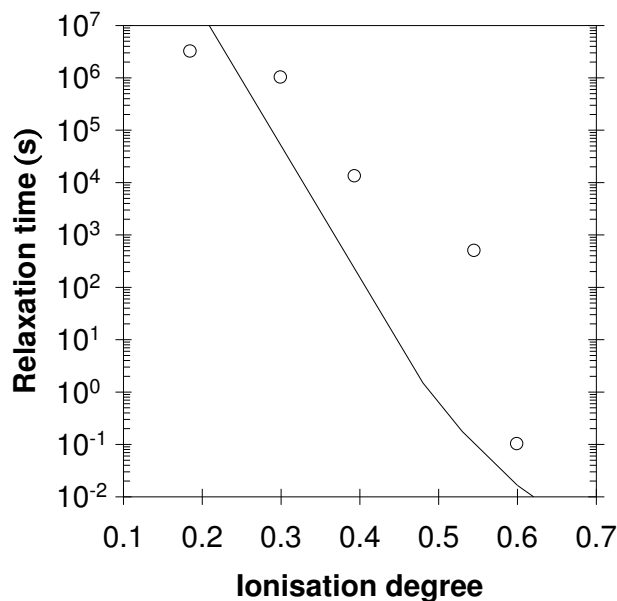


Figure 8.7. Evolution of the relaxation time as a function of the ionisation degree for THg50. The solid line represents the trends for TH50 at $C \gg C_p$.¹

IV. Conclusion

Three BAB triblock copolymers made of an hydrophilic poly(acrylic acid) central A block and gradient copolymers made of *n*-butyl acrylate and acrylic acid as hydrophobic lateral B blocks were investigated. The amount of AA varied from 40 to 60%, the dispersity was above 1.8, the triblocks were twice as small as previously studied triblock copolymers with a statistical distribution of the *n*BA and AA units within the B blocks and the gradient strength of hydrophobic units was small.

Only THg50 formed viscoelastic fluids, THg40 and THg60 did not percolate. We speculate that the percolation concentration is extremely high for THg60 and that THg40 did not percolate because it was in a frozen state.

Rheological properties of THg50 demonstrated a pH-dependent relaxation time as for statistical TH50. Interestingly, THg50 exhibited a much higher dispersity of relaxation times than TH50. The dispersity of the polymers, their gradient profile or the high percolation concentration could explain this result. In addition, THg50 had a larger relaxation time than TH50 for the same ionization degree, suggesting that the structure of the polymers is important.

These preliminary results did reveal differences between triblock copolymers consisting of statistical or gradient association blocks. However triblock copolymers having the same length and dispersity as the previously studied TH50 would be required to elucidate the effect of the structure quantitatively.

V. References

1. Charbonneau, C.; Chassenieux, C.; Colombani, O.; Nicolai, T. *Macromolecules* **2011**, *44*, (11), 4487-4495.
2. Shedge, A.; Colombani, O.; Nicolai, T.; Chassenieux, C. *Macromolecules* **2013**, *47*, (7), 2439-2444.
3. Zhang, X.; Boisson, F.; Colombani, O.; Chassenieux, C.; Charleux, B. *Macromolecules* **2014**, *47*, (1), 51-60.
4. Borisova, O.; Billon, L.; Zaremski, M.; Grassl, B.; Bakaeva, Z.; Lapp, A.; Stepanek, P.; Borisov, O. *Soft Matter* **2012**, *8*, (29), 7649-7659.
5. Borisova, O.; Billon, L.; Zaremski, M.; Grassl, B.; Bakaeva, Z.; Lapp, A.; Stepanek, P.; Borisov, O. *Soft Matter* **2011**, *7*, (22), 10824-10833.
6. Laruelle, G.; Francois, J.; Billon, L. *Macromol. Rapid Commun.* **2004**, *25*, (21), 1839-1844.
7. Colombani, O.; Lejeune, E.; Charbonneau, C.; Chassenieux, C.; Nicolai, T. *J. Phys. Chem. B* **2012**, *116*, (25), 7560-7565.
8. Charbonneau, C.; Lima, M. M. D.; Chassenieux, C.; Colombani, O.; Nicolai, T. *Phys. Chem. Chem. Phys.* **2013**, *15*, (11), 3955-3964.
9. Lauber, L.; Chassenieux, C.; Nicolai, T.; Colombani, O. *Macromolecules* **2015**, *48*, (20), 7613-7619.
10. Halperin, A.; Alexander, S. *Macromolecules* **1989**, *22*, (5), 2403-2412.

CHAPTER 9 : APPENDIX 2

Static and dynamic light scattering experiments were conducted on the three graft copolymers $\text{PAA}_{500}\text{-}g\text{-}[\text{P}(n\text{BA}_{0.5}\text{-}stat\text{-AA}_{0.5})_{100}]_y$ with $y=2, 7$ and 30 for G2H50, G7H50 and G30H50. The aim of this study was to determine whether the unassociated polymers had a coil or a rod shape. A rod-like shape may be expected for polymers with high grafting density such as G30H50.

All solutions were measured at an ionization degree of one at which there were not associated. Interactions between the polymers were negligible for $C \leq 1$ g/L (data not shown). The systems were explored at two different salt concentrations, 0.05 and 0.5 M. Concentration fluctuations characterized by dynamic light scattering showed monomodal relaxation time distributions in all cases, see Figure 9.1.

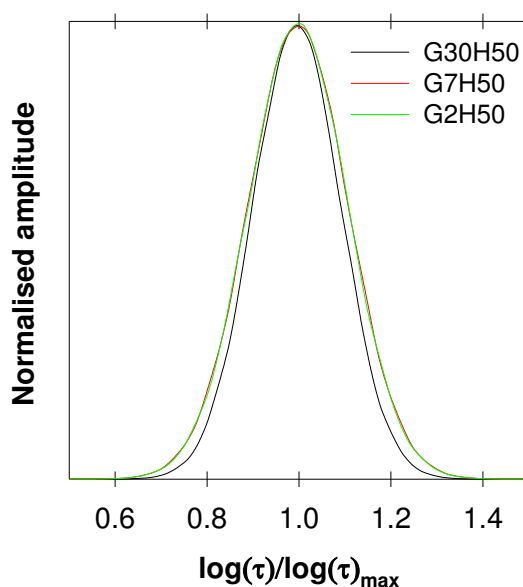


Figure 9.1. Distributions of relaxation times obtained by dynamic light scattering for solutions of graft copolymers at $C = 1$ g/L, $\theta = 90^\circ$, $\alpha = 1$ and $[\text{Na}^+] = 0.5$ M.

The main characteristics of the graft copolymers are summarized in Table 9-1. M_w and R_h were similar for G2H50 and G7H50, whereas the values for G30H50 were larger. Interestingly, the R_g of G2H50 and G30H50 was similar and larger than R_g of G7H50.

For monodisperse particles, the ratio R_g/R_h can be used as an indicator of the shape of polymers in solution for instance for sphere $R_g/R_h = 0.77$ and for random-coil polymer R_g/R_h

CHAPTER 9: APPENDIX 2

=1.54. In our case, the dispersities were high, as shown by the \mathcal{D} values, which precludes drawing conclusion from the value of the R_g/R_h about the shape of the particles.

The only conclusion that can be drawn from these analysis is that the polydispersity is so high that it is impossible to determine the shape of the self-assemblies by scattering techniques.

Table 9-1. Main characteristics of the graft copolymers solutions at $C=1$ g/L, $\alpha=1$ and two salt concentrations.^a measured in dynamic light scattering.

Name	[Na ⁺] (M)	M _{app} (g/mol)	R _h (nm)	R _g (nm)	R _g /R _h	\mathcal{D}^a
G2H50	0.05	2.2 x10 ⁵	12	54	4.5	2.0
G7H50		2.7 x10 ⁵	13	45	3.5	1.5
G30H50		4.3 x10 ⁵	16	55	3.4	1.7
G2H50	0.50	1.6 x10 ⁵	9	37	4.1	2.4
G7H50		1.9 x10 ⁵	10	21	2.1	1.5
G30H50		6.0 x10 ⁵	14	39	2.8	1.9

Thèse de Doctorat

Lionel Lauber

Contrôle des propriétés rhéologiques d'hydrogels formés par auto-assemblage de copolymères amphiphiles, à blocs et greffés, anioniques ou cationiques

Control of the rheological properties of hydrogels made by self-association of amphiphilic copolymers, blocks and grafts, anionics or cationics

Résumé

L'objectif de ce travail était de contrôler les propriétés rhéologiques de solutions aqueuses de copolymères amphiphiles. Dans l'eau, ces copolymères s'auto-associent et leurs propriétés peuvent être contrôlées en partie par leur dynamique d'échange. Il avait précédemment été montré que cette dynamique pouvait être contrôlée par le pH et la quantité d'unités acide acrylique dans des triblocs BAB (TH_x) où le bloc A est du poly(acide acrylique) (PAA) et les blocs B sont des copolymères statistiques (MH_x) d'acrylate de *n*-butyle (*n*BA) et d'acide acrylique (AA).

Tout d'abord, l'étude de l'auto-association en solution des blocs B seuls (MH_x) a montré un lien fort entre leur agrégation et celle des diblocs de type BA (DH_x). Cette agrégation est contrôlée par la quantité de charge des blocs B.

Par la suite, des mélanges de triblocs (BAB) TH_x contenant différentes proportions (*x*) d'unités AA ont permis la formation de réseaux hybrides dont les propriétés rhéologiques sont maîtrisées par formulation plutôt que via la chimie.

Des propriétés rhéologiques similaires aux triblocs BAB (TH_x) ont été obtenues avec des copolymères greffés possédant un squelette hydrophile PAA et des greffons B. Leurs propriétés rhéologiques sont principalement contrôlées par la structure chimique des blocs B, mais aussi par le taux de greffage. Ces copolymères greffés devraient être plus simples à obtenir à l'échelle industrielle que des triblocs.

Pour finir, l'approche consistant à incorporer des unités hydrophiles dans les blocs hydrophobes de copolymères amphiphiles pour en contrôler la dynamique d'échange a été appliquée avec succès à des copolymères à base de méthacrylate de diméthylaminoéthyle et de méthacrylate de *n*-butyle. Leurs propriétés rhéologiques peuvent être contrôlées à nouveau par le pH, mais dans une gamme différente des polymères à base d'acide acrylique, et aussi dans une certaine mesure par la température.

Mots clés

Rhéologie, auto-association, hydrogel, copolymère amphiphile, diffusion de la lumière, thermosensible, acide acrylique, DMAEMA

Abstract

The aim of this work was to control the rheological properties of aqueous solutions of amphiphilic copolymers. In water, these copolymers self-assemble and part of their properties can be controlled by their dynamic of exchange. As previously reported, the exchange dynamics can be controlled by the pH and the acrylic acid (AA) content for BAB triblock copolymers (TH_x) consisting of a poly(acrylic acid) (PAA) A block and two statistical B blocks (MH_x) of *n*-butyl acrylate (*n*BA) and AA.

First, the study of the self-association of B blocks (MH_x) alone showed a strong relationship between their aggregation and the one of BA diblocks (DH_x). This aggregation was mainly controlled by the amount of charges within the B blocks.

Then, mixtures of BAB triblocks (TH_x) with different contents of AA units, *x*, formed hybrid networks the rheological properties of which were controlled by formulation rather than chemistry.

Similar rheological properties were obtained using graft copolymers consisting of a PAA hydrophilic backbone and B grafts. Their rheological properties were mainly controlled by the chemical structure of the B grafts and by the grafting density. Such graft copolymers should be easier to produce at an industrial scale than triblock copolymers.

To finish, the strategy consisting of incorporating hydrophilic units inside the hydrophobic blocks of amphiphilic copolymers to control their exchange dynamics was successfully applied to copolymers made of dimethylaminoethyl methacrylate and *n*-butyl methacrylate. Their rheological properties were controlled by the pH on a different pH-range than the AA based polymers, and, to some extent, by the temperature.

Key Words

Rheology, self-assembly, hydrogels, amphiphilic copolymers, light scattering, thermo-sensitive, acrylic acid, DMAEMA